

Morphological description and mitochondrial DNA-based phylogenetic placement of a new species of *Callistoctopus* Taki, 1964 (Cephalopoda, Octopodidae) from the southeast waters of China

Xiaodong Zheng^{1,2}, Chenxi Xu^{1,2}, Jiahua Li^{1,2}

1 Institute of Evolution and Marine Biodiversity, Ocean University of China, Qingdao, 266003, China **2** Key Laboratory of Mariculture, Ocean University of China, Qingdao, 266003, China

Corresponding author: Xiaodong Zheng (xdzheng@ouc.edu.cn)

Academic editor: Pavel Stoev | Received 8 May 2022 | Accepted 10 August 2022 | Published 12 September 2022

<https://zoobank.org/18A5CC36-D9F4-488A-AB4D-E7C30179839A>

Citation: Zheng X, Xu C, Li J (2022) Morphological description and mitochondrial DNA-based phylogenetic placement of a new species of *Callistoctopus* Taki, 1964 (Cephalopoda, Octopodidae) from the southeast waters of China. ZooKeys 1121: 1–15. <https://doi.org/10.3897/zookeys.1121.86264>

Abstract

In this study, we described a new species of octopus and named it *Callistoctopus xiaohongxu* **sp. nov.** based on nine specimens captured in the waters of southeast China. *Callistoctopus xiaohongxu* **sp. nov.** is a small to moderate-sized octopus. The most characteristic and defining morphological features are the reddish-orange to reddish-brown skin, gills with 8 or 9 lamellae per demibranch, \wedge/\wedge -shaped funnel organ, and small suckers. Fragments obtained from the mitochondrial cytochrome c oxidase subunit I (COI) gene of nine specimens were 593 bp in length, and the genetic distance among the specimens of *C. xiaohongxu* **sp. nov.** and the other 16 octopods ranged from 11.13 to 21.09%. Topologies resulting from ML and BI analyses of the COI gene showed a highly supported monophyletic clade (bootstrap value [BS] = 94%, posterior probability [PP] = 100%) containing all the specimens identified as *C. xiaohongxu* **sp. nov.**

Keywords

Callistoctopus xiaohongxu sp. nov., COI gene, new species, octopus, taxonomy

Introduction

Among the cephalopods, 134 species have been recorded in the China Seas (Li 1983; Dong 1988; Zheng et al. 1999; Lu et al. 2012). Due to the influence of three strong warm currents – the Kuroshio Current (KC), the South China Sea Current (SCSC), and the Taiwan Current (TC) – water temperatures of the East China Sea and South China Sea range between 14–16 °C in coastal areas even during winter (Liu 2013), providing ideal environmental conditions to generate abundant marine biodiversity, as well as cephalopods.

Species in the genus *Callistoctopus* were previously treated as the “*Octopus macropus* group”, from which Norman (1993) separated four new species. The current taxonomy of species in this genus is mainly based on morphological features, while there are still very limited molecular data. In Chinese waters, only two species *Callistoctopus ornatus* (Gould, 1852) and *C. luteus* (Sasaki, 1929), have been recorded so far (Lu et al. 2012; Norman et al. 2014).

In this paper, we described one new species of *Callistoctopus*, which was called ‘xiaohongxu’ in Chinese for its smooth skin and reddish-brown colour, from the south-east China Sea area. The newly discovered species has been mistakenly identified and sold in fish markets of Dongshan Island in Zhangzhou, Fujian Province, as juveniles of ‘*Octopus*’ *minor* (Sasaki, 1920). However, based on the obvious differences in the size of the adult animals, gill lamellae number, and the funnel organ shape, we can readily distinguish this new species from ‘*O.*’ *minor* externally. Here we present a full morphological description and genetic analyses of the new species of octopod.

Materials and methods

Specimen collection

Samples were collected from Dongshan Seafood Market Pier (23°25'12"N, 117°51'0"E) in Zhangzhou, Fujian Province, China. The type specimens are deposited in the Specimen Room, Fisheries College, Ocean University of China (OUC), Qingdao, China. All specimens were attributed to mature or immature stages based on the absence or presence of spermatophores in males, and ovary fullness or egg development in females.

Morphological feature analyses

All specimens were measured after being fixed according to Roper and Voss (1983) and indices were calculated on the basis of Huffard and Hochberg (2005). Abbreviations: **TL** – total length; **ML** – mantle length; **WF** – web formula (web sectors ordered from deepest to shallowest); **GC** – gill count (number of gill lamellae per outer demi-branch, excluding the terminal lamella); **SC** – number of suckers on normal arms; **MWI** – mantle width index (mantle width/ML×100).; **HWI** – head width index (head

width/mantle width \times 100); **WDI** – the web depth index (deepest web length/longest arm \times 100); **ALI** – arm length index (arm length/ML \times 100); **AWI** – arm width index (arm width/ML \times 100); **SDI** – sucker diameter index (sucker diameter/ML \times 100); **FLI** – funnel length index (funnel length/ML \times 100); **FFLI** – free funnel length index (free funnel length/funnel length \times 100); **PAI** – pallial aperture index (pallial aperture/mantle width \times 100); **LLI** – ligula length index (ligula length/hectocotylyzed arm length \times 100); **CaLI** – calamus length index (calamus length/ligula length \times 100); **HAMI** – hectocotylyzed arm mantle index (hectocotylyzed arm length/ML \times 100); **OAI** – opposite arm index (hectocotylyzed arm length/normal third arm length \times 100); **HASC** – number of suckers on hectocotylyzed arm of male; **SpC** – spermatophore count; **SpL** – spermatophore length; **SpW** – spermatophore width; **EgC** – egg count; **EgL** – egg length; **EgW** – egg width. All measurements are in millimeters and weights in grams.

The beaks and radulae were removed from the buccal mass. Then beaks were cleaned and stored in 75% ethanol. Seven beak morphological indices, upper hood length (**UHL**), upper crest length (**UCL**), upper rostrum length (**URL**), upper rostrum width (**URW**), lower hood length (**LHL**), lower crest length (**LCL**), and lower rostrum width (**LRW**), were measured to the nearest 0.01 mm by Vernier caliper (Clarke, 1986). Five ratios were calculated as follows: UHL/UCL, URW/UCL, URL/UHL, LHL/LCL, and LRW/LCL. The radulae were cleaned with 10% NaOH, air-dried, coated with gold, and then scanned using a VEGA3 scanning electron microscope. Funnel organ and anal flaps were stained with methylene blue.

DNA extraction and sequencing

Before fixation with formalin and alcohol, about 100 mg of muscle tissue was cut from the mantle inside all chilled specimens. Total genomic DNA was extracted using a CTAB (hexadecyltrimethylammonium bromide) method (Winnepenninckx 1993). DNA was dissolved in TE buffer (10 mM Tris-HCl, 1 mM EDTA, pH 8.0) and stored at -30°C . Regions of mitochondrial cytochrome c oxidase subunit I (COI) fragments were amplified using primers referenced to *Octopus conispadiceus* Sasaki, 1917 by Ma et al. (2016). These sequences were amplified by PCR with the following conditions: 94°C (3 min), 34 cycles of 94°C (45 s), 50°C (1 min), 72°C (1 min), and a final extension of 72°C (5 min).

Molecular analyses

The COI sequences of the other 17 species were downloaded from GenBank (Table 1). *Vampyroteuthis infernalis* Chun, 1903 was used as an outgroup in all analyses. ModelFinder (Kalyaanamoorthy et al. 2017) was used to select the best-fit model using the BIC criterion. Maximum likelihood phylogenies were inferred using IQ-TREE (Nguyen et al. 2015) under the GTR+I+G4+F model for 1000 ultrafast (Minh et al. 2013) bootstraps, as well as the Shimodaira-Hasegawa-like approximate likelihood-ratio test (Guindon et al. 2010). Bayesian inference phylogenies were inferred using MrBayes 3.2.6 (Ronquist

Table 1. GenBank accession numbers for species analysed in this study.

Species	GenBank numbers	References
<i>Amphioctopus aegina</i>	NC_029702	Zhang et al. (2017)
<i>Amphioctopus fangxiao</i>	HQ846126	Dai et al. (2012)
<i>Amphioctopus neglectus</i>	MH899749	Tang et al. (2019)
<i>Amphioctopus rex</i>	MF447874	Tang et al. (2019)
<i>Callistoctopus ornatus</i>	HM104257	Strugnell et al. (2014)
<i>Callistoctopus asilosomatis</i>	AB430525	Kaneko et al. (2011)
<i>Callistoctopus luteus</i>	NC_039848	Unpublished
<i>Callistoctopus macropus</i>	MN933634	Lima et al. (2020)
<i>Callistoctopus xiaohongxu</i>	OP135961-OP135969	This study
<i>Cistopus chinensis</i>	KF017606	Cheng et al. (2013)
<i>Cistopus taiwanicus</i>	NC_023257	Cheng et al. (2013)
<i>Octopus vulgaris</i>	KU525762	Amor et al. (2017)
<i>Octopus bimaculatus</i>	NC_028547	Dominguez-Contreras et al. (2016)
<i>Octopus conispadiceus</i>	KJ789854	Ma et al. (2016)
<i>Octopus cyanea</i>	NC_039847	Unpublished
<i>Octopus minor</i>	HQ638215	Cheng et al. (2012)
<i>Octopus sinensis</i>	MT712046	Li et al. (2021)
<i>Vampyroteuthis infernalis</i>	NC_009689	Yokobori et al. (2007)

et al. 2012) under GTR+I+G4+F model (4 parallel runs, 1 000 000 generations) as well, in which the initial 25% of sampled data were discarded as burn-in. And COI sequences of new species have been deposited in GenBank under accession numbers OP135961-OP135969. Pairwise comparisons of the distances based on COI gene were also calculated by MEGA X under the Kimura 2-parameter model (Kumar et al. 2018).

Results

Taxonomy

Order Octopoda Leach, 1818

Family Octopodidae d'Orbigny, 1840

Genus *Callistoctopus* Taki, 1964

Type species. *Callistoctopus ornatus* (Gould, 1852).

Callistoctopus xiaohongxu sp. nov.

<https://zoobank.org/C4E08679-59A2-47AF-AA85-D19D1F78415B>

Figs 1–4

Type material. *Holotype*: OUC-201808200301, mature ♂, 45.5 mm ML, Dongshan Seafood Market Pier, Zhangzhou, Fujian, China, 20 August 2018, coll. *Paratypes*: OUC-201812050301, mature ♂, 49.5 mm ML, Dongshan Seafood Market Pier,

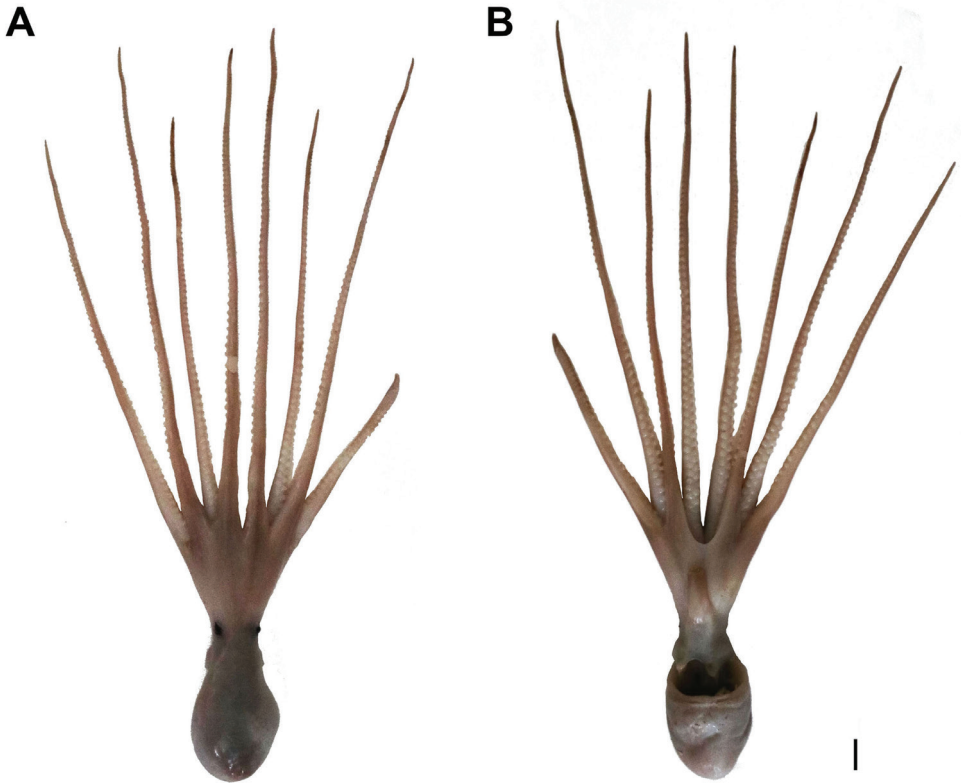


Figure 1. *Callistoctopus xiaohongxu* sp. nov., holotype, male, 45.5 mm ML (OUC-201808200301) **A** photograph of dorsal view **B** photograph of ventral view. Scale bars: 10 mm (**A, B**).

Zhangzhou, Fujian, China, 5 December 2018, coll. OUC-201812050302, mature ♂, 53.2 mm ML, Dongshan Seafood Market Pier, Zhangzhou, Fujian, China, 5 December 2018, coll. OUC-201812050303, mature ♂, 56.3 mm ML, Dongshan Seafood Market Pier, Zhangzhou, Fujian, China, 5 December 2018, coll. OUC-201806080302, immature ♀, 50.7 mm ML, Dongshan Seafood Market Pier, Zhangzhou, Fujian, China, 8 June 2018, coll. OUC-201812050305, mature ♀, 51.7 mm ML, Dongshan Seafood Market Pier, Zhangzhou, Fujian, China, 5 December 2018, coll. OUC-201812050306, mature ♀, 83.3 mm ML, Dongshan Seafood Market Pier, Zhangzhou, Fujian, China, 5 December 2018, coll.

Other material. OUC-201812050304, mature ♂, 63.2 mm ML, Dongshan Seafood Market Pier, Zhangzhou, Fujian, China, 5 December 2018, coll. OUC-201806080301, immature ♀, 41.7 mm ML, Dongshan Seafood Market Pier, Zhangzhou, Fujian, China, 8 June, 2018, coll.

Diagnosis. Small to moderate size (ML 41.7–83.3 mm). Colour of skin reddish-orange to reddish-brown, no papillae or patch. One or two lines of black chromatophores on the lateral margins of arms under the skin (Fig. 2A). Head narrow (HWI 23.0–39.1). Arms of moderate length (ALI 154.9–336.3), thin (AWI 8.7–18.0). Web deep (WDI 15.7–22.9). Suckers small (SDI 5.0–6.9) and biserial. Enlarged suckers

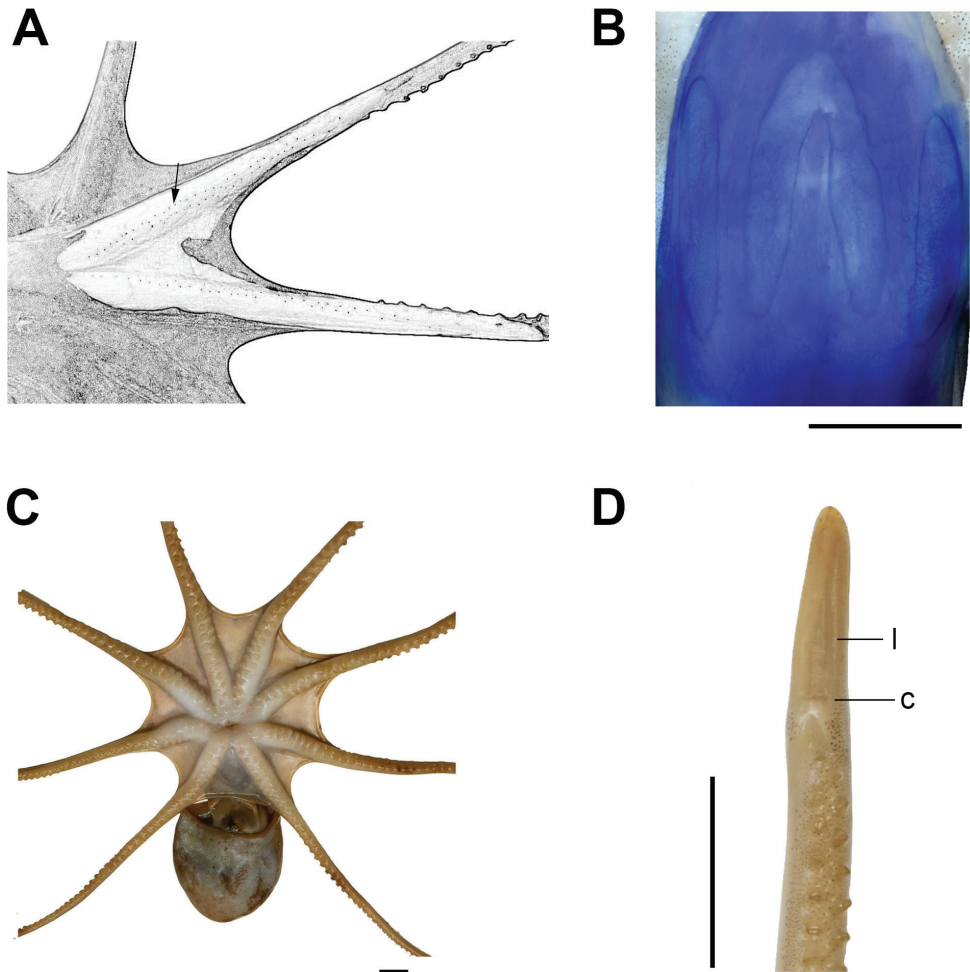


Figure 2. *Callistoctopus xiaohongxu* sp. nov. **A** proximal portion of arms 1–3 (left side), male, 49.5 mm ML (OUC-201812050301) **B** funnel organ, male, 53.2 mm ML (OUC-201812050302) **C** oral view of basal portion of arms, male, 63.2 mm ML (OUC-201812050304) **D** distal portion of hectocotylus, male, 63.2 mm ML (OUC-201812050304). Abbreviations: c, calamus; l, ligula. Scale bars: 10 mm (**B, C, D**).

absent. Funnel organ \wedge /-shaped, long (FLI 51.0–68.5). Gills with 8–9 lamellae per demibranch. Ligula moderate size (LLI 7.0–11.6) with groove.

Description. Measurements and indices of nine specimens are presented in Table 2. Small to moderate-size species (ML 41.7–83.3 mm), total length (TL) 195.7–382.1 mm, body weight up to 39.2 g. Skin smooth, one or two lines of black chromatophores on the lateral margins of arms under the skin (Fig. 2A). Mantle slightly ovoid to elongate, muscular. Head width narrower than mantle width (HWI 23.0–39.1). Stylets absent. Funnel long (FLI 51.0–68.5), free funnel length around 24–46% funnel length (FFLI 23.9–46.0), funnel organ \wedge /-shaped (Fig. 2B). Outer limbs

Table 2. Measurements (mm) and indices for *Callistoctopus xiaohongxu* sp. nov. Abbreviation: D, damaged.

Name	OUC- 201808200301	OUC- 201812050301	OUC- 201812050302	OUC- 201812050303	OUC- 201812050304	OUC- 201806080301	OUC- 201806080302	OUC- 201812050305	OUC- 201812050306
Status	Holotype	Paratype	Paratype	Paratype			Paratype	Paratype	Paratype
Sex	♂	♂	♂	♂	♂	♀	♀	♀	♀
Maturity	mature	mature	mature	mature	mature	immature	immature	mature	mature
TL	212.7	216.3	212.1	258.6	283.9	195.7	208.6	234.8	382.1
TW(g)	30.6	24.5	37.3	28.8	23.4	17.6	16.1	25.1	39.2
ML	45.5	49.5	53.2	56.3	63.2	41.7	50.7	51.7	83.3
MWI	72.5	69.7	65.6	66.2	65.0	64.5	60.5	77.4	46.2
HWI	35.2	29.1	23.9	30.7	27.2	30.0	27.6	39.1	23.0
PAI	120.9	116.6	111.5	116.5	103.2	149.6	111.0	125.0	98.3
FLI	63.1	65.1	66.2	67.1	53.2	61.4	57.8	68.5	51.0
FFLI	46.0	35.1	23.9	26.2	25.9	40.6	32.4	34.2	33.6
WDI	17.0	17.3	22.9	15.7	18.3	19.8	20.0	16.9	16.2
AL1I	333.8	331.9	237.2	322.7	196.7	D	285.4	324.8	294.5
AL2I	336.3	276.0	241.2	302.1	304.1	322.5	251.1	313.5	154.9
AL3I	291.9	273.1	231.8	220.1	220.4	294.5	226.8	272.7	293.0
AL4I	296.7	259.2	193.2	265.2	229.9	299.0	211.8	281.8	237.1
AWI	15.2	13.8	14.3	13.2	11.6	14.5	18.0	16.2	8.7
LLI	7.0	11.6	9.8	9.6	10.4	–	–	–	–
CaLI	31.6	26.3	28.2	30.9	31.1	–	–	–	–
HAMI	184.2	160.8	162.4	182.8	155.5	–	–	–	–
OAI	63.1	58.9	70.1	81.8	70.6	–	–	–	–
SDI	6.9	6.5	5.7	6.6	6.5	5.4	5.0	5.9	5.4
HASC	79	82	83	83	70	–	–	–	–
SC	157	191	171	198	195	191	163	178	177
GC	8	9	8	9	8	8	8	8	8
SpC	–	6	8	–	4	–	–	–	–
SpL	–	37.8	58.1	–	79.1	–	–	–	–
SpW	–	1.4	1.5	–	1.6	–	–	–	–
EgC	–	–	–	–	–	–	–	64	67
EgL	–	–	–	–	–	–	–	14.0	14.5
EgW	–	–	–	–	–	–	–	4.3	3.3
UHL/UCL	–	0.31	0.28	0.28	0.29	–	–	0.32	0.28
URW/UCL	–	0.18	0.13	0.17	0.15	–	–	0.16	0.12
URL/UHL	–	0.33	0.28	0.38	0.23	–	–	0.27	0.23
LHL/LCL	–	0.38	0.39	0.40	0.45	–	–	0.34	0.36
LRW/LCL	–	0.33	0.32	0.41	0.36	–	–	0.26	0.30

slightly shorter than medial limbs. Arms moderate length (ALI 154.9–336.3), slender (AWI 8.7–18.0), dorsal arms always longest (arm formula of most specimens belongs to $1 > 2 > 4 > 3$). Suckers in two rows (Fig. 2C), small (SDI 5.0–6.9). In larger animals, 157–198 suckers on each normal arm, and the first or second arm has the most suckers. Enlarged suckers absent. Webs deep (WDI 15.7–22.9), typical web formula $A > B > C > D > E$. The third right arm of mature males hectocotylized, length approximately 60–80% of the opposite arm (Fig. 2D). Ligula of moderate size, robust and cylindrical with deep groove. LLI ranges from 7.0–11.6 of arm length. Calamus of

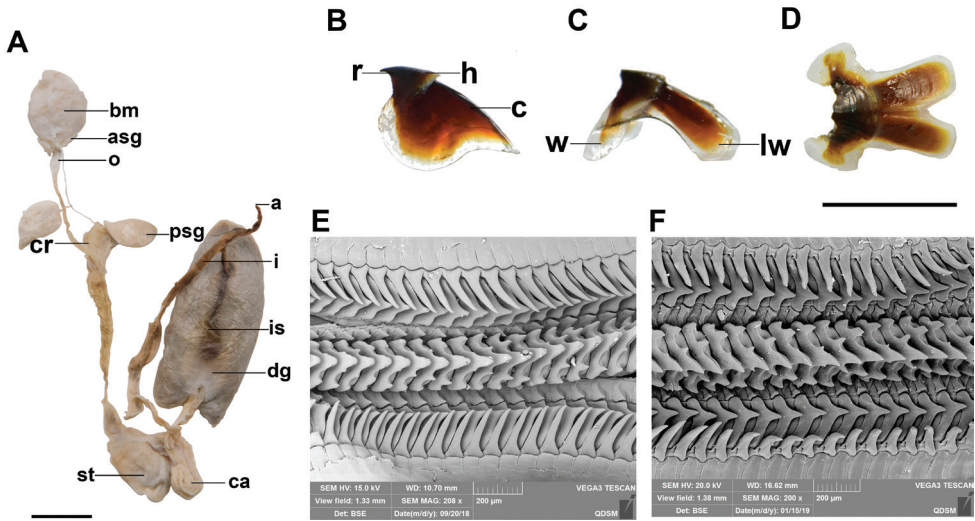


Figure 3. *Callistoctopus xiaohongxu* sp. nov. **A** digestive system, female, 83.3 mm ML (OUC-201812050306) **B** upper beak, lateral view, female, 50.7 mm ML (OUC-201806080302) **C** lower beak, lateral view, female, 50.7 mm ML (OUC-201806080302) **D** lower beak, ventral view, female, 50.7 mm ML (OUC-201806080302) **E, F** scanning electron micrograph of radulae, male, 53.2 mm ML (OUC-201812050302). Abbreviations: a, anus; asg, anterior salivary gland; bm, buccal mass; c, crest; ca, caecum; cr, crop; dg, digestive gland; h, hood; i, intestine; is, ink sac; lw, lateral wing; o, oesophagus; psg, posterior salivary gland; r, rostrum; st, stomach; w, wing. Scale bars: 10 mm (**A–D**); 200 µm (**E, F**).

moderate size, around 25–30% of ligula length (CaLI 26.3–31.6). Hectocotylied arm with 70–83 suckers. Gills with 8–9 lamellae per demibranch.

Digestive tract (Fig. 3A). Anterior salivary glands small, approximately one-third length of buccal mass. Posterior salivary glands triangular and smaller than buccal mass. Oesophagus long. Spiral caecum with one whorl. Intestine long. Digestive gland well developed, brown. Ink sac present, embedded in the digestive gland and attached to the intestine posteriorly. Ink sac opening into the anus. Anal flaps small.

Upper beak (Fig. 3B) with short rostrum, narrow hood, and slightly curved crest. Ratios of upper beak measurements 0.28–0.32 for UHL/UCL, 0.12–0.18 for URW/UCL, and 0.23–0.38 for URL/UHL. Lower beak (Fig. 3C, D) with a blunt rostrum, narrow hood, moderately broad wings and flared lateral walls separated in posterior, posterior notch deep. Radula (Fig. 3E, F) with 7 teeth and 2 marginal plates per transverse row. Ratios of lower beak measurements 0.34–0.45 for LHL/LCL and 0.26–0.41 for LRW/LCL. Rhachidian tooth with 1–2 lateral cusps on each side; first lateral teeth small, sharp; second lateral teeth broad-based triangular, larger than first, sharp; marginal teeth long, curved, sharply pointed, longer than second lateral teeth; marginal plates flat.

Male reproductive tract (Fig. 4A). In mature males, the terminal organ inverse 6-shaped. Spermatophore storage sac long. Accessory gland curved, longer than

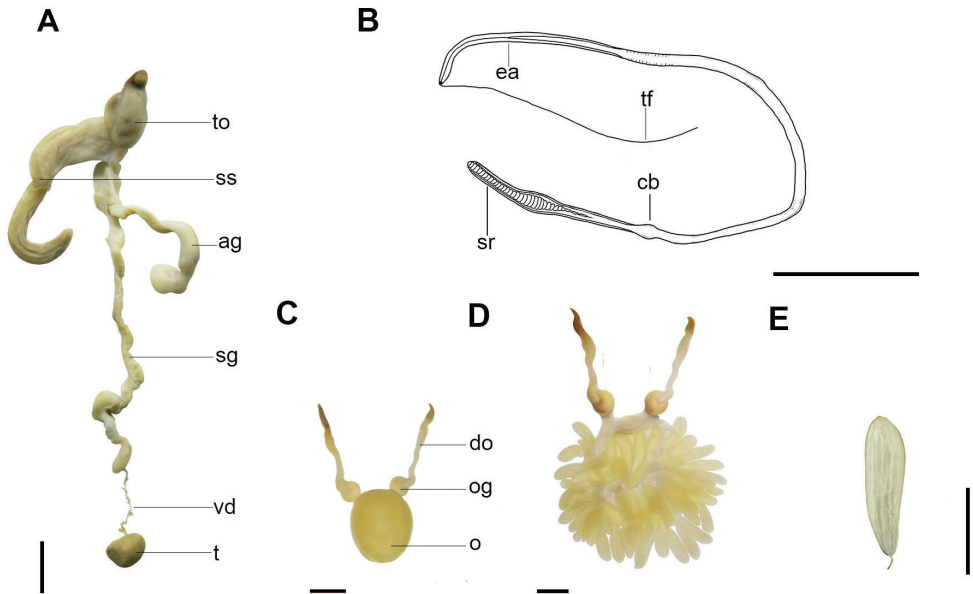


Figure 4. *Callistoctopus xiaohongxu* sp. nov. **A** reproductive system of male, 56.3 mm ML (OUC-201812050303) **B** spermatophore, male, 56.3 mm ML (OUC-201812050303) **C** reproductive system of female, 51.7 mm ML (OUC-201812050305) **D** egg cluster, female, 51.7 mm ML (OUC-201812050305) **E** single egg female, 51.7 mm ML (OUC-201812050305). Abbreviations: ag, accessory gland; cb, cement body; do, distal oviduct; ea, ejaculatory apparatus; o, ovary; og, oviducal gland; sg, spermatophore gland; sr, sperm reservoir; ss, spermatophore storage sac; t, testis; tf, terminal filament; to, terminal organ; vd, vas deferens. Scale bars: 10 mm.

spermatophore storage sac. Spermatophore gland long. Vas deferens very short, narrow. Testis roundish, small. Spermatophores (Fig. 4B) of moderate size, average length 60 mm, approximately 75% ML, narrow (average 1.5 mm in width); approximately 4–8 spermatophores in storage sac.

Female reproductive tract (Fig. 4C–E). Ovary large, round in mature females. Two distal oviducts long. Two oviducal glands wider than distal oviducts. Mature females with approximately 65 large eggs (average 14.3 mm in length).

Integument (Fig. 5A). Colour of live animal reddish-orange. Animal turning white when stressed or post mortem. In live animals, a linear structure appears on the tissue connecting two adjacent arms, forming a net-like structure (Fig. 5B). Arm chromatophores under the skin distinct.

Etymology. The name ‘*xiaohongxu*’, which refers to its small body size and reddish body colour, is the phonetic translation of the local Chinese name of this species in Zhangzhou, where specimens were collected.

Distribution. According to fishermen in Zhangzhou, this species is distributed in the East China Sea and the South China Sea, mainly in Quanzhou, Fujian Province to Shanwei, Guangdong Province.

Table 3. Pairwise comparison of the genetic distances among Octopodidae species based on the COI gene. Abbreviations: *A. a.*, *Amphioctopus aegina*; *A. f.*, *Amphioctopus fangsiao*; *A. n.*, *Amphioctopus neglectus*; *A. r.*, *Amphioctopus rex*; *Ca. a.*, *Callistoctopus aspilosomatis*; *Ca. l.*, *Callistoctopus luteus*; *Ca. m.*, *Callistoctopus macropus*; *Ca. o.*, *Callistoctopus ornatus*; *Ca. x.*, *Callistoctopus xiaohongxu*; *Ci. c.*, *Cistopus chinensis*; *Ci. t.*, *Cistopus taiwanicus*; *O. b.*, *Octopus bimaculatus*; *O. co.*, *Octopus conispadiceus*; *O. cy.*, *Octopus cyanea*; ‘*O.*’ *m.*, ‘*Octopus*’ *minor*; *O. s.*, *Octopus sinensis*; and *O. v.*, *Octopus vulgaris*.

	<i>A. a.</i>	<i>A. f.</i>	<i>A. n.</i>	<i>A. r.</i>	<i>Ca. a.</i>	<i>Ca. l.</i>	<i>Ca. m.</i>	<i>Ca. o.</i>	<i>Ca. x.</i>	<i>Ci. c.</i>	<i>Ci. t.</i>	<i>O. b.</i>	<i>O. co.</i>	<i>O. cy.</i>	‘ <i>O.</i> ’ <i>m.</i>	<i>O. s.</i>
<i>A. a.</i>	–															
<i>A. f.</i>	14.29	–														
<i>A. n.</i>	12.43	16.36	–													
<i>A. r.</i>	11.78	16.56	11.03	–												
<i>Ca. a.</i>	20.32	20.34	22.76	21.09	–											
<i>Ca. l.</i>	20.10	19.02	20.18	19.50	14.54	–										
<i>Ca. m.</i>	19.62	20.57	21.27	20.37	12.22	15.12	–									
<i>Ca. o.</i>	21.03	20.38	19.63	21.13	10.95	15.40	5.01	–								
<i>Ca. x.</i>	18.51	19.40	20.29	18.63	14.04	15.54	12.18	11.97	–							
<i>Ci. c.</i>	18.26	18.81	20.97	19.47	21.40	20.55	19.70	20.22	17.76	–						
<i>Ci. t.</i>	16.45	19.01	16.93	18.05	19.87	21.11	18.49	17.58	19.08	13.11	–					
<i>O. b.</i>	18.05	14.74	20.21	20.68	20.40	19.27	19.96	20.50	17.40	16.28	19.04	–				
<i>O. co.</i>	20.09	19.22	18.73	20.36	16.94	17.68	19.02	17.39	16.63	20.87	20.34	21.17	–			
<i>O. cy.</i>	14.95	16.74	17.47	18.61	17.19	17.65	17.83	17.16	15.33	17.17	16.24	15.00	18.05	–		
‘ <i>O.</i> ’ <i>m.</i>	19.87	19.44	23.52	22.04	13.50	14.17	10.77	11.43	11.13	18.28	20.60	19.21	19.01	17.59	–	
<i>O. s.</i>	14.30	17.90	17.47	18.37	21.07	20.44	20.35	20.36	20.72	17.68	17.93	15.27	20.36	16.99	20.81	–
<i>O. v.</i>	14.37	17.51	17.23	18.29	21.51	21.04	20.14	20.15	21.09	18.87	18.60	15.21	20.69	18.30	20.69	2.97

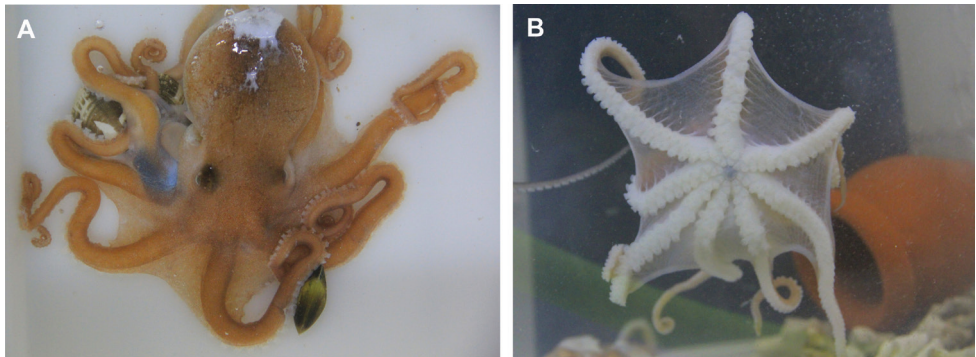


Figure 5. *Callistoctopus xiaohongxu* sp. nov. **A** live specimen **B** net-like structure on web.

Molecular analyses. Phylogenetic analyses were performed based on the fragments of the COI gene using Maximum likelihood (ML) and Bayesian inference (BI) methods. Fragments 593 bp in length were obtained from the mitochondrial COI gene of nine specimens. Both ML and BI trees showed a similar topology (Fig. 6) with a highly supported monophyletic clade (bootstrap value [BS] = 94%, posterior probability [PP] = 100%) containing all nine specimens identified as *Callistoctopus xiaohongxu* sp. nov. *C. xiaohongxu* sp. nov. belonged to the clade of ‘*O.*’ *minor* and other four species of *Callistoctopus* with [BS] = 82% and [PP] = 89%, respectively. Moreover, the COI gene analyses suggested that species of the genus *Octopus* used

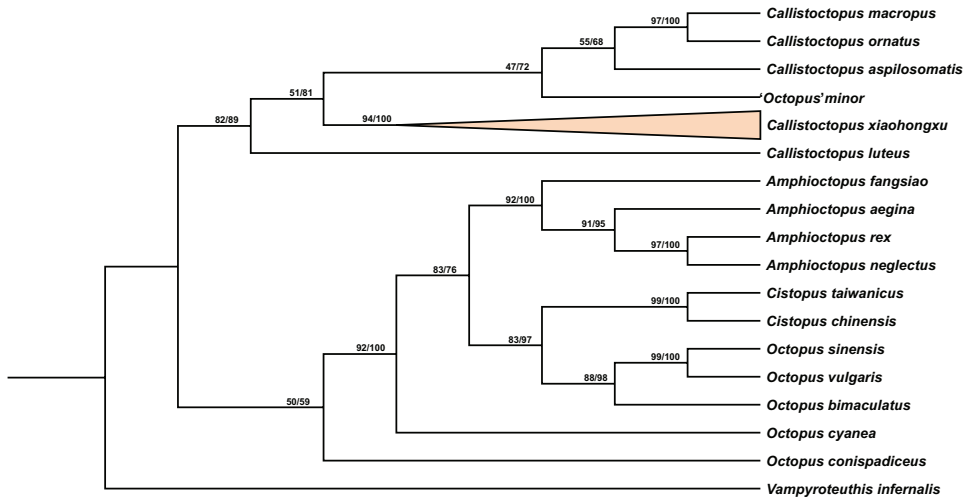


Figure 6. Phylogenetic trees derived from Maximum likelihood (ML) and Bayesian inference (BI) methods based on the *COI* gene. Numbers at each node are bootstrap (left) for ML and posterior probability (right) for BI analyses, respectively.

in this study were not clustered into one clade. Additionally, the genetic distance of *C. xiaohongxu* sp. nov. and the other 16 Octopodidae species ranged from 11.13 to 21.09% (Table 3).

Discussion

As mentioned previously, *Callistoctopus xiaohongxu* sp. nov. has been mistakenly identified and sold in fish markets as the juveniles of '*O. minor*', because they are similar in having smooth skin and reddish-brown colour in chilled specimens. However, *C. xiaohongxu* sp. nov. and '*O. minor*' can be readily distinguished by the morphological characteristics compared in Table 4. *Callistoctopus xiaohongxu* sp. nov. has:

1. no spots on mantle surfaces ('*O. minor*' has light yellow spots);
2. a \wedge -shaped funnel organ (the funnel organ shape of '*O. minor*' is VV-shaped);
3. gills with 8 or 9 lamellae per demibranch (10–12 lamellae per demibranch in '*O. minor*');
4. no enlarged suckers in mature males ('*O. minor*' has enlarged suckers);
5. cylindrical ligula with groove (spoon-like with a wide hollow groove in '*O. minor*').

Callistoctopus xiaohongxu sp. nov. is also distinct from other species of *Callistoctopus* (Table 4). Compared to the key morphological characters, *C. xiaohongxu* sp. nov. has no spot on the skin (vs other *Callistoctopus* species that have white spots or bars on the mantle, head, and arms), fewer gill lamellae (gill lamellae 8–9 vs 10–14 in *Callistoctopus*

Table 4. Comparison of key morphological characters between *Callistoctopus xiaohongxu* sp. nov., *Callistoctopus* species, and '*Octopus*' *minor* Sasaki, 1920.

Item	<i>Callistoctopus xiaohongxu</i> sp. nov.	<i>Callistoctopus</i> species	' <i>Octopus</i> ' <i>minor</i> Sasaki, 1920
Data source	this study	Norman et al. 2014	Norman et al. 2014
Colour	reddish-orange to reddish-brown, no spot	Typically, red-brown to red, white spots or bars on mantle, head and arms	red-brown, light yellow spots on mantle surface
Sculpture	smooth	smooth or with scattered low papillae	smooth
GC	8–9	10–14	10–12
Funnel organ	\ / \ /-shaped	W, UU or VV-shaped	V V-shaped
WDI	15.7 to 22.9	around 7 to 28	deepest around 10
ALI	154.9–336.3	300–800	400–500
OAI	58.9–81.8	around 40–95	around 50
Enlarged suckers	absent	absent	present
Ligula	cylindrical with groove, LLI 7.0–11.6	cylindrical with deep groove, LLI around 1.5–9	spoon-like with wide hollow groove, LLI around 18–23

species), funnel organ \ / \ /-shaped (vs W, UU or VV-shaped in other species), and relatively shorter arms (ALI 154.9–336.3 vs 300–800 in the other *Callistoctopus* species).

Judging from the K2P genetic distance (Table 3), *C. xiaohongxu* sp. nov. can be separated from the other 16 species of Octopodidae by genetic distances ranging from 11.13 to 21.09%. According to the phylogenetic tree (Fig. 6), *C. xiaohongxu* sp. nov. has a close relationship to '*O. minor*' and four species of *Callistoctopus* with [BS] = 82% and [PP] = 89%. However, the taxonomic status of '*O. minor*' is unresolved, and it is placed in the genus *Octopus* provisionally. Besides, the very limited suite of molecular data suggested that genetic relationships among species of the genus *Callistoctopus* need further studies. Still, for the accurate phylogenetic status of '*O. minor*', more research would be required to establish the relationships among species of *Octopus* and *Callistoctopus*.

Octopus is one of the most species-rich cephalopod genera but was considered a 'catch-all' genus by Guzik et al. (2005). It is not monophyletic in its current composition and needs revision and robust phylogenetic analyses (Strugnell et al. 2005; Dai et al. 2012; Amor et al. 2015; Ritschard et al. 2019; Tang et al. 2020). In our study, species in *Octopus* were not clustered into one clade. Accordingly, our study supports the polyphyly of the genus *Octopus*.

We are planning to analyse the mitochondrial genome of *C. xiaohongxu* sp. nov. in the future. Better taxon sampling would facilitate a better understanding of octopod phylogeny as well as a better substantiated generic assignment of *C. xiaohongxu* sp. nov.

Acknowledgements

We would like to thank Dr Hong Zhong, Ms Feige Sunxie for collecting specimens, and Pongthong Itsaret for helping to take a few photos of the new species. We are also grateful to Prof ChungCheng Lu for the valuable advice for improving the manuscript. This study was supported by the National Natural Science Foundation of China (No.31672257, 32170536).

References

- Amor MD, Laptikhovsky V, Norman MD, Strugnell JM (2015) Genetic evidence extends the known distribution of *Octopus insularis* to the mid-Atlantic islands Ascension and St Helena. *Journal of the Marine Biological Association of the United Kingdom* 97(4): 753–758. <https://doi.org/10.1017/S0025315415000958>
- Amor MD, Norman MD, Roura A, Leite TS, Gleadow IG, Reid A, Perales-Raya C, Lu CC, Silvey CJ, Vidal EAG, Hochberg FG, Zheng X, Strugnell JM (2017) Morphological assessment of the *Octopus vulgaris* species complex evaluated in light of molecular-based phylogenetic inferences. *Zoologica Scripta* 46(3): 275–288. <https://doi.org/10.1111/zsc.12207>
- Cheng R, Zheng X, Lin X, Yang J, Li Q (2012) Determination of the complete mitochondrial DNA sequence of *Octopus minor*. *Molecular Biology Reports* 39(4): 3461–3470. <https://doi.org/10.1007/s11033-011-1118-2>
- Cheng R, Zheng X, Ma Y, Li Q (2013) The complete mitochondrial genomes of two octopods *Cistopus chinensis* and *Cistopus taiwanicus*: Revealing the phylogenetic position of the genus *Cistopus* within the Order Octopoda. *PLoS ONE* 8(12): e84216. <https://doi.org/10.1371/journal.pone.0084216>
- Clarke MR (1986) *A handbook for the identification of cephalopod beaks*. Clarendon Press, Oxford, 273 pp.
- Dai L, Zheng X, Kong L, Li Q (2012) DNA barcoding analysis of Coleoidea (Mollusca: Cephalopoda) from Chinese waters. *Molecular Ecology Resources* 12(3): 437–447. <https://doi.org/10.1111/j.1755-0998.2012.03118.x>
- Dominguez-Contreras JF, Munguia-Vega A, Ceballos-Vazquez BP, Garcia-Rodriguez FJ, Arellano-Martinez M (2016) The complete mitochondrial genome of *Octopus bimaculatus* Verrill, 1883 from the Gulf of California. *Mitochondrial DNA Part A* 27(6): 4584–4585. <https://doi.org/10.3109/19401736.2015.1101575>
- Dong Z (1988) *Chinese fauna, Mollusca, Cephalopods*. Science Press, Beijing, 206 pp.
- Guindon S, Dufayard J-F, Lefort V, Anisimova M, Hordijk W, Gascuel O (2010) New algorithms and methods to estimate maximum-likelihood phylogenies: Assessing the performance of PhyML 3.0. *Systematic Biology* 59(3): 307–321. <https://doi.org/10.1093/sysbio/syq010>
- Guzik MT, Norman MD, Crozier RH (2005) Molecular phylogeny of the benthic shallow-water octopuses (Cephalopoda: Octopodinae). *Molecular Phylogenetics and Evolution* 37(1): 235–248. <https://doi.org/10.1016/j.ympev.2005.05.009>
- Huffard CL, Hochberg FG (2005) Description of a new species of the genus *Amphioctopus* (Mollusca: Octopodidae) from the Hawaiian Islands. *Molluscan Research* 25: 113–128.
- Kalyaanamoorthy S, Bui Quang M, Wong TKF, von Haeseler A, Jermiin LS (2017) ModelFinder: Fast model selection for accurate phylogenetic estimates. *Nature Methods* 14(6): 587–589. <https://doi.org/10.1038/nmeth.4285>
- Kaneko N, Kubodera T, Dinh T, Iguchis A (2011) Taxonomic study of shallow-water octopuses (Cephalopoda: Octopodidae) in Japan and adjacent waters using mitochondrial genes with perspectives on octopus DNA barcoding. *Malacologia* 54(1–2): 97–108. <https://doi.org/10.4002/040.054.0102>

- Kumar S, Stecher G, Li M, Knyaz C, Tamura K (2018) MEGA X: Molecular evolutionary genetics analysis across computing platforms. *Molecular Biology and Evolution* 35(6): 1547–1549. <https://doi.org/10.1093/molbev/msy096>
- Li F (1983) Studies on the cephalopod fauna of the Taiwan Strait. *Journal of oceanography in Taiwan Strait* 2: 103–109.
- Li F, Liu Y, Qin B, Bian L, Ge J, Chang Q, Liu H, Chen S (2021) Sequence and phylogenetic analysis of the mitochondrial genome for the East Asian common octopus, *Octopus sinensis* (Octopodidae: Octopoda). *Mitochondrial DNA Part B* 6(8): 2120–2122. <https://doi.org/10.1080/23802359.2021.1944360>
- Lima FD, Strugnell JM, Leite TS, Lima SM (2020) A biogeographic framework of octopod species diversification: The role of the Isthmus of Panama. *PeerJ* 8: e8691. <https://doi.org/10.7717/peerj.8691>
- Liu JY (2013) Status of marine biodiversity of the China seas. *PLoS ONE* 8(1): e50719. <https://doi.org/10.1371/journal.pone.0050719>
- Lu CC, Zheng X, Lin X (2012) Diversity of Cephalopoda from the waters of the Chinese mainland and Taiwan. In: Lin M, Wang C (Eds) *Proceedings of the 1st Taiwan symposium of marine biodiversity studies*. Ocean Press, Beijing, 76–87.
- Ma Y, Zheng X, Cheng R, Li Q (2016) The complete mitochondrial genome of *Octopus conispadiceus* (Sasaki, 1917) (Cephalopoda: Octopodidae). *Mitochondrial DNA Part A* 27: 1058–1059. <https://doi.org/10.3109/19401736.2014.928866>
- Minh BQ, Nguyen MAT, von Haeseler A (2013) Ultrafast approximation for phylogenetic bootstrap. *Molecular Biology and Evolution* 30(5): 1188–1195. <https://doi.org/10.1093/molbev/mst024>
- Nguyen L-T, Schmidt HA, von Haeseler A, Minh BQ (2015) IQ-TREE: A fast and effective stochastic algorithm for estimating maximum-likelihood phylogenies. *Molecular Biology and Evolution* 32(1): 268–274. <https://doi.org/10.1093/molbev/msu300>
- Norman MD (1993) Four new octopus species of the *Octopus macropus* group (Cephalopoda: Octopodidae) from the Great Barrier Reef, Australia. *Memoirs of the Museum of Victoria* 53(2): 267–308. <https://doi.org/10.24199/j.mmv.1992.53.13>
- Norman MD, Finn JK, Hochberg FG (2014) Family Octopodidae. In: Jereb P, Roper CFE, Norman MD, Finn JK (Eds) *Cephalopods of the world. An annotated and illustrated catalogue of cephalopod species known to date. Vol. 3. Octopods and Vampire Squids. FAO Species Catalogue for Fishery Purposes, No. 4, FAO, Rome, 40–201.*
- Ritschard EA, Guerrero-Kommritz J, Sanchez JA (2019) First molecular approach to the octopus fauna from the southern Caribbean. *PeerJ* 7: e7300. <https://doi.org/10.7717/peerj.7300>
- Ronquist F, Teslenko M, van der Mark P, Ayres DL, Darling A, Höhna S, Larget B, Liu L, Suchard MA, Huelsenbeck JP (2012) MrBayes 3.2: Efficient Bayesian phylogenetic inference and model choice across a large model space. *Systematic Biology* 61(3): 539–542. <https://doi.org/10.1093/sysbio/sys029>
- Roper CFE, Voss GL (1983) Guidelines for taxonomic descriptions of cephalopod species. *Memoirs of the National Museum of Victoria* 44: 48–63. <https://doi.org/10.24199/j.mmv.1983.44.03>

- Strugnell JM, Norman MD, Jackson J, Drummond AJ, Cooper A (2005) Molecular phylogeny of coleoid cephalopods (Mollusca: Cephalopoda) using a multigene approach; the effect of data partitioning on resolving phylogenies in a Bayesian framework. *Molecular Phylogenetics and Evolution* 37(2): 426–441. <https://doi.org/10.1016/j.ympev.2005.03.020>
- Strugnell JM, Norman MD, Vecchione M, Guzik M, Allcock AL (2014) The ink sac clouds octopod evolutionary history. *Hydrobiologia* 725(1): 215–235. <https://doi.org/10.1007/s10750-013-1517-6>
- Tang Y, Zheng X, Zhong H, Li Q (2019) Phylogenetics and comparative analysis of the mitochondrial genomes of three violet-ringed octopuses. *Zoologica Scripta* 48(4): 482–493. <https://doi.org/10.1111/zsc.12359>
- Tang Y, Zheng X, Liu H, Sunxie F (2020) Population genetics and comparative mitogenomic analyses reveal cryptic diversity of *Amphioctopus neglectus* (Cephalopoda: Octopodidae). *Genomics* 112(6): 3893–3902. <https://doi.org/10.1016/j.ygeno.2020.06.036>
- Winnepenninckx B (1993) Extraction of high molecular weight DNA from molluscs. *Trends in Genetics* 9(12): 407–407. [https://doi.org/10.1016/0168-9525\(93\)90102-N](https://doi.org/10.1016/0168-9525(93)90102-N)
- Yokobori S, Lindsay DJ, Yoshida M, Tsuchiya K, Yamagishi A, Maruyama T, Oshima T (2007) Mitochondrial genome structure and evolution in the living fossil vampire squid, *Vampyroteuthis infernalis*, and extant cephalopods. *Molecular Phylogenetics and Evolution* 44(2): 898–910. <https://doi.org/10.1016/j.ympev.2007.05.009>
- Zhang X, Zheng X, Ma Y, Li Q (2017) Complete mitochondrial genome and phylogenetic relationship analyses of *Amphioctopus aegina* (Gray, 1849) (Cephalopoda: Octopodidae). *Mitochondrial DNA Part A* 28(1): 17–18. <https://doi.org/10.3109/19401736.2015.1106522>
- Zheng Y, Ling J, Yan L, Zhou J, Shen J (1999) Cephalopod resources and rational utilization in East China Sea. *Journal of Fishery Sciences of China* 6: 52–56.

Ecdyonurus aurasius sp. nov. (Insecta, Ephemeroptera, Heptageniidae, Ecdyonurinae), a new micro-endemic mayfly species from Aurès Mountains (north-eastern Algeria)

Besma M. Dambri¹, Nadhira Benhadji², Laurent Vuataz^{3,4}, Michel Sartori^{3,4}

1 Department of Ecology and Environment, Faculty of Natural and Life Sciences, University of Batna 2, 05078 Fesdis, Batna, Algeria **2** Department of Hydrobiology, Institute of Biology, University of Szczecin, Felczaka street 3 c, 71- 412 Szczecin, Poland **3** Musée cantonal de zoologie, Palais de Rumine, Place de la Riponne 6, 1014 Lausanne, Switzerland **4** Department of Ecology and Evolution, Biophore, University of Lausanne, 1015 Lausanne, Switzerland

Corresponding author: Michel Sartori (michel.sartori@vd.ch)

Academic editor: Lyndall Pereira-da-Conceicao | Received 28 June 2022 | Accepted 10 August 2022 | Published 12 September 2022

<https://zoobank.org/B4DF8A3A-9306-488B-B5F0-786456E709FA>

Citation: Dambri BM, Benhadji N, Vuataz L, Sartori M (2022) *Ecdyonurus aurasius* sp. nov. (Insecta, Ephemeroptera, Heptageniidae, Ecdyonurinae), a new micro-endemic mayfly species from Aurès Mountains (north-eastern Algeria). ZooKeys 1121: 17–37. <https://doi.org/10.3897/zookeys.1121.89613>

Abstract

Ecdyonurus aurasius sp. nov., a micro-endemic species reported from several streams within the Aurès Mountains (north-eastern Algeria), is described and illustrated at nymphal, subimaginal and imaginal stages of both sexes. Critical morphological diagnostic characters distinguishing the new species are presented, together with molecular affinities as well as notes on the biology and distribution of the species.

Keywords

Belezma National Park, COI, mayflies, new species, North Africa, taxonomy

Introduction

The genus *Ecdyonurus* Eaton, 1868 belongs to the Ecdyonurinae Ulmer, 1920, a subfamily with rather challenging and controversial taxonomy as genera delineation and phylogeny are still partially unsolved or in process (Kluge 2004; Wang and McCafferty 2004; Bauernfeind

and Soldán 2012; Yanai et al. 2017). The identification key to genera proposed by Webb and McCafferty (2008) displayed 14 genera in the world; among them, four genera *Ecdyonurus*, *Electrogena* Zurwerra & Tomka, 1985, *Afronurus* Lestage, 1924 and *Paracinygmula* Bajkova, 1975 (sub. nom. *Nixe* Flowers, 1980; see Sartori 2014 for discussion) possess Palearctic species. The first three are the most diversified with 61, 45 and 64 species respectively worldwide (Barber-James et al. 2013; Yanai et al. 2017). Recently, the new genus *Anapos* Yanai & Sartori, 2017 was created to accommodate two Mediterranean species.

In Africa, only three Ecdyonurinae genera are present: *Ecdyonurus* is restricted to North Africa, whereas *Afronurus* and *Notonurus* Crass, 1947 are found in the Afro-tropical region (Webb and McCafferty 2008; Vuataz et al. 2013).

Bauernfeind and Soldán (2012) proposed to split the West Palearctic species of the genus *Ecdyonurus* into two subgenera: *Ecdyonurus* (25 species) and *Helvetoraeticus* Bauernfeind & Soldán, 2012 (15 species), according to the arrangement of setae on the superlingua, the number of bristles on the ventral side of the labrum and the number of comb-shaped bristles on the maxilla in nymphs, as well as the shape of the apical sclerite of the male genitalia.

Currently, four taxa of this genus are reported from North Africa (Thomas 1998). Two of them are well-known species with a clear status: *Ecdyonurus rothschildi* Navás, 1929 and *Ecdyonurus ifranensis* Vitte & Thomas, 1988, whereas one remains doubtful: *Ecdyonurus venosus* var. *constantinicus* Lestage, 1925, and the presence of *Ecdyonurus venosus* (Fabricius, 1793) mentioned by Gauthier (1928) is still unconfirmed. All of them belong to the subgenus *Ecdyonurus*.

Navás (1929) described *Ecdyonurus rothschildi* from an oasis in Biskra Province, north-eastern Algeria, based on a male imago. The species was redescribed by Thomas and Dakki (1979) which gave a detailed account of the adult morphology and related it to the *E. aurantiacus* (Burmeister, 1839) species group. Later, Soldán and Gagneur (1985), proposed the first description of the nymph and an identification key to separate *E. rothschildi*, *E. dispar* (Curtis, 1834) and *E. aurantiacus* nymphs. The species is now known from all Maghreb countries and is one of the most widespread species (Boumaiza and Thomas 1995; Zrelli et al. 2016; Bouhala et al. 2020). Vitte and Thomas (1988) described *Ecdyonurus ifranensis* at nymphal and adult stages from the Middle Atlas; the species has later been found in other areas of Morocco (El Alami et al. 2022).

The present study aims to examine *Ecdyonurus* populations from the Aurès region (Algeria). We collected and reared fresh material at all stages. After critical observations and comparison with other *Ecdyonurus* species, we have clearly distinguished a new Algerian endemic species.

Materials and methods

The material was collected by the first author between February 2020 and November 2021 from six localities from the Aurès region; the sampling sites are located in the Belezma National Park (BNP) and the Western Aurès Massif (Fig. 1). The region is

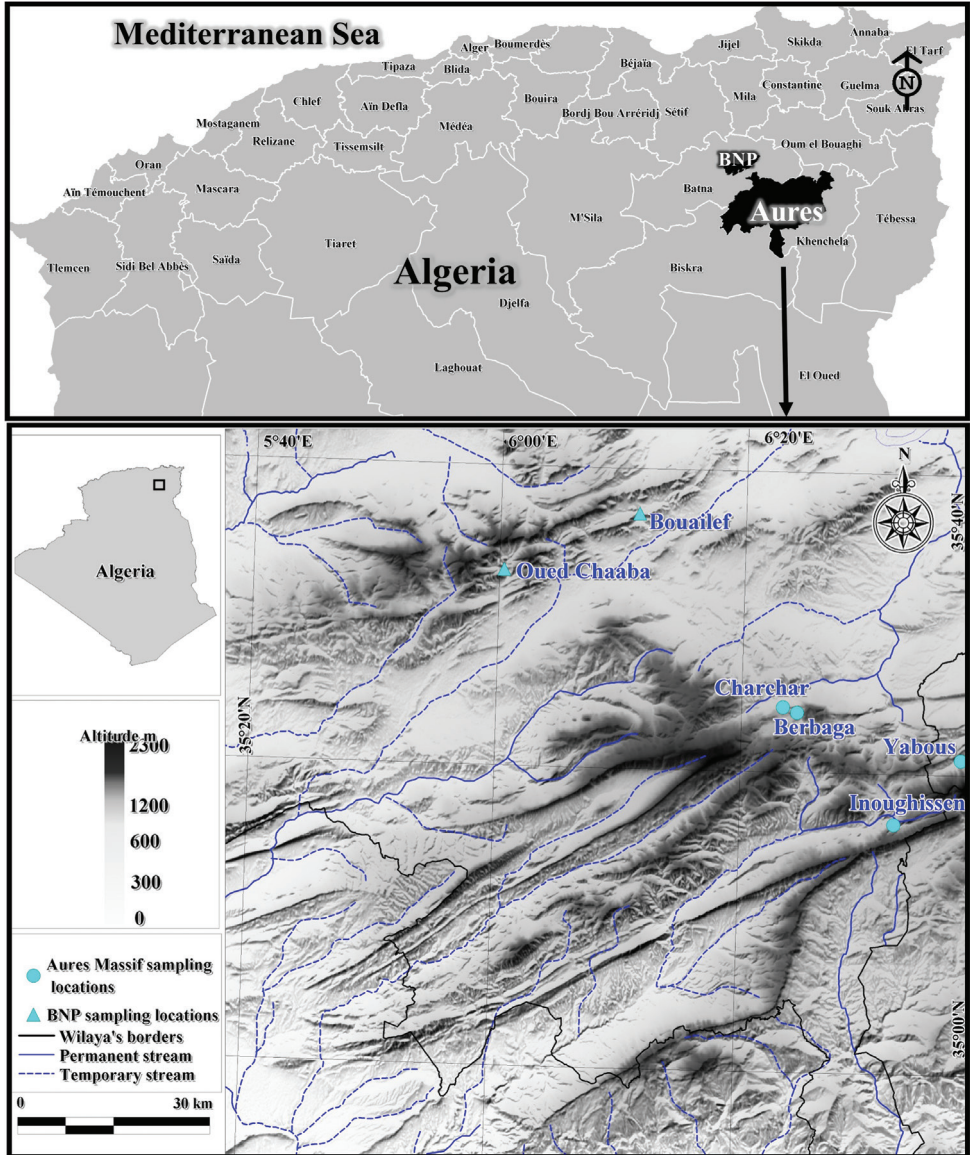


Figure 1. Map of the sampling sites.

characterized by a semi-arid climate with cold winters and very hot and dry summers. Sampling was performed using a standard benthic net using the kick-sampling method. Imagos and subimagos were obtained by rearing mature nymphs from the Charchar, Yabous and Berbaga sites. All specimens were preserved in 96% ethanol in the field and stored in the laboratory at 4 °C.

The physical and chemical parameters of the water was measured in situ for each sampling site using a multi-probe. The following variables were measured: average

water depth, bed width, current velocity with a FLOWATCH flowmeter; conductivity, water temperature and pH using an Adwa AD32 tester and a HANNA HI1271 pH electrode; while dissolved oxygen was recorded using a Lutron PDO-519 Dissolved Oxygen Meter.

Morphological analysis

Morphological characteristics for the description of the new species were used according to Hrivniak et al. (2018). Pictures of habitus were made using a Canon EOS 6D camera and the Visionary Digital Passport imaging system (formerly available and distributed by Dun Inc., Virginia), and processed with Adobe Photoshop Lightroom ver. 4.4. and Helicon Focus ver. 5.3. Four nymphs were dissected in Cellosolve (2-Ethoxyethanol) with subsequent embedding in Euparal medium and mounting on slides. Microscopic pictures were taken using an Olympus BX51 microscope coupled with an Olympus SC50 camera; pictures were enhanced with the stacking software Olympus Stream Basic ver. 2.3.2. and Adobe Photoshop ver. 21.2.2.

Molecular analysis

Five specimens belonging to the new species as well as five specimens of *Ecdyonurus rothschildi* were used for DNA extraction to get a 658 bp fragment of the mitochondrial cytochrome oxidase I gene (COI) (see Table 1). DNA extraction, PCR amplification, sequencing and alignment construction were performed according to Benhadji et al. (2020) or Martynov et al. (2022). One sequence of *E. rothschildi* was retrieved from GenBank, as well as two sequences of *E. aurantiacus* and two of *E. dispar*. Three *Electrogena* sequences were chosen as the outgroup. We estimated the evolutionary divergence within and between our new species and the other *Ecdyonurus* species using the COI genetic distances. Both pairwise distance between all sequences and mean distance between and within species were calculated in MegaX (Kumar et al. 2018; Stecher et al. 2020) under the Kimura 2-parameter (K80) substitution model (Kimura 1980). We then applied the recently developed species delimitation method ASAP (Assemble Species by Automatic Partitioning; Puillandre et al. 2021) to our COI data set using the graphical web-interface available at <https://bioinfo.mnhn.fr/abi/public/asap/asapweb.html>. This distance-based method is similar to the popular ABGD (Automatic Barcode Gap Discovery; Puillandre et al. 2012) approach but has the advantage of providing a score (i.e. asap-score) that indicates the most likely species delimitation. Pairwise genetic distances were computed under the K80 model, and all other settings were set to default. Because ASAP outputs produced two partitions with equal asap-scores, we favored the partition with the smallest p-value.

Finally, we conducted a Bayesian inference gene tree reconstruction in MrBayes ver. 3.2.7a (Ronquist et al. 2012), using the best evolutionary model (GTR + Γ + I)

Table 1. Sequenced specimens of *E. aurasius* sp. nov. and *Ecdyonurus rothschildi* with collection data and nomenclature of sequences used in the molecular study.

Species	Specimen catalogue number	Stage	Locality	GPS coordinates	Date	GenBank ID	GenSeq Nomenclature
<i>Ecdyonurus aurasius</i> sp. nov.	GBIFCH 01119302	Male imago	Algeria, Wilaya de Batna, Berbag	35°24'01"N, 6°24'31"E	5.xi.2021	ON920531	genseq-2 COI
<i>Ecdyonurus aurasius</i> sp. nov.	GBIFCH 01119304	Male imago	Algeria, Wilaya de Batna, Charchar	35°24'22"N, 6°23'21"E	17.x.2021	ON920532	genseq-2 COI
<i>Ecdyonurus aurasius</i> sp. nov.	GBIFCH 00673191	Nymph	Algeria, Wilaya de Batna, Charchar	35°24'22"N, 6°23'21"E	23.vi.2019	ON920533	genseq-2 COI
<i>Ecdyonurus aurasius</i> sp. nov.	GBIFCH 00673192	Nymph	Algeria, Wilaya de Batna, Charchar	35°24'22"N, 6°23'21"E	23.vi.2019	ON920534	genseq-2 COI
<i>Ecdyonurus aurasius</i> sp. nov.	GBIFCH 00673193	Male imago	Algeria, Wilaya de Batna, Charchar	35°24'22"N, 6°23'21"E	23.vi.2019	ON920535	genseq-2 COI
<i>Ecdyonurus rothschildi</i>	GBIFCH 00763579	Nymph	Algeria, oued Cherf, Dbabcha	36°13'00"N, 7°19'05"E	18.x.2019	ON920536	genseq-4 COI
<i>Ecdyonurus rothschildi</i>	GBIFCH 00763578	Nymph	Algeria, oued Bougous, Oum Ali	36°37'53"N, 8°18'54"E	23.i.2019	ON920537	genseq-4 COI
<i>Ecdyonurus rothschildi</i>	GBIFCH 01116263	Nymph	Morocco, Draa, Mgoune downstream	31°20.07'N, 6°10.82'W	22.x.2021	ON920538	genseq-4 COI
<i>Ecdyonurus rothschildi</i>	EC-CH0	Nymph	Algeria, Tafna, Chouly 0	34°47'20"N, 1°13'07"W	19.xii.2015	ON920529	genseq-4 COI
<i>Ecdyonurus rothschildi</i>	EC-CH1	Nymph	Algeria, Tafna, Chouly 1	34°49'15"N, 1°10'55"W	19.xii.2015	ON920530	genseq-4 COI
<i>Ecdyonurus rothschildi</i>		Nymph	Tunisia		vii.2009	HG935040	genseq-4 COI

selected in JModelTest ver. 2.1.10 (Darriba et al. 2012) following the second-order Akaike information criterion (AICc). We used five substitution scheme and six gamma categories, with all other parameters set to default. To accommodate different substitution rates among COI codon positions, we analyzed our data set in two partitions, one with first and second codon positions and one with third positions (1 + 2, 3). Two independent analyses of four MCMC chains run for one million generations with trees sampled every 1000 generations were implemented, and 100 000 generations were discarded as a burnin after visually verifying run stationarity and convergence in Tracer ver. 1.7.2 (Rambaut et al. 2018). The consensus tree was visualized and edited in iTOL 6 (Letunic and Bork 2021).

Material is deposited in the following institutions:

- FEEL-UB2** Functional Ecology and Environmental Laboratory, University Batna 2, Algeria;
IB-US Institute of Biology, University of Szczecin, Poland;
MZL Museum of zoology, Lausanne, Switzerland.

Results

Molecular analysis

The COI ingroup data set was 100% complete (no missing data) and included 25% of parsimony informative sites. The COI gene tree grouped the five sequences of *Ecdyonurus aurasius* sp. nov. into a well-supported monophyletic clade, and was supported as a distinct species in the ASAP analysis (Fig. 2). The K80 mean genetic distance within the five *Ecdyonurus aurasius* sp. nov. COI sequences was 0.14%. As expected, all other included species were also recovered as distinct species with high node supports. The K80 mean genetic distance between *Ecdyonurus aurasius* sp. nov. and the other three species of *Ecdyonurus* ranged from 7.6% (mean distance to *E. rothschildi*) to 20.1% (mean distance to *E. aurantiacus*), with a minimum distance of 7.1% between GBIFCH01119302 / GBIFCH00673192 and EC-CH0 sequences.

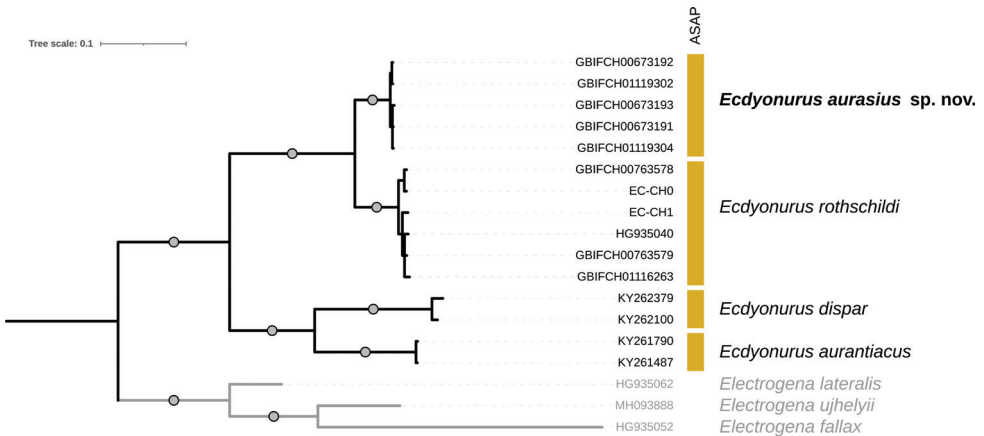


Figure 2. Bayesian majority-rule consensus tree reconstructed from the COI data set. Tips labelled with GBIF and EC-CH codes indicate newly sequenced specimens, other codes correspond to previously published GenBank sequences. Vertical boxes indicate species delimitation hypotheses according to the ASAP analysis. The outgroups are represented in grey. Circles on branches indicate Bayesian posterior probabilities > 0.95.

Morphological analysis

Heptageniidae Neddham, 1901

Ecdyonurinae Ulmer, 1920

Ecdyonurus aurasius Dambri, Benhadji & Sartori sp. nov.

<https://zoobank.org/0A552D79-3329-4CCA-9724-D01492F82D7B>

Material. Holotype. ALGERIA • male imago in ethanol, with its corresponding nymphal and subimaginal exuviae, Wilaya de Batna, Charchar, 35°24'22"N, 6°23'21"E, 1340 m. a.s.l., 09 Nov. 2021, B. Dambri coll. (GBIFCH01128855) [MZL] • **Paratypes.** 1 male

imago, with its nymphal and subimaginal exuviae (GBIFCH01128846), 1 female imago, with its nymphal and subimaginal exuviae (GBIFCH01128858), [MZL]; 6 female imagos [IB-US], same data as holotype; 1 male imago, 1 male subimago [IB-US], 2 female imagos, 7 male subimagos [FEEL-UB2], 06 Nov. 2021; 1 male imago [IB-US], 1 male imago [FEEL-UB2], 20 Oct. 2021; 1 male imago, with its nymphal and subimaginal exuviae (GBIFCH01119304), 1 female imago, with its nymphal and subimaginal exuviae (GBIFCH01128861) [MZL], 17 Oct. 2021; 1 female imago with its subimaginal exuvia, 1 female subimago (GBIFCH01128849) [MZL], 15 Oct. 2021; 1 female subimago, 1 male subimago [IB-US], 1 male subimago (GBIFCH01128853) [MZL], 2 nymphs [FEEL-UB2], 10 Oct. 2021; 3 nymphs [IB-US], 2 nymphs (GBIFCH01128857), 1 nymph on slide (GBIFCH01119301) [MZL], 09 Oct. 2021; 7 nymphs [IB-US], 15 nymphs [FEEL-UB2], 18 Jun. 2020; 15 nymphs [IB-US], 18 nymphs [FEEL-UB2], 5 nymphs (GBIFCH01128850) [MZL], 3 Mar. 2020; same locality, B. Dambri coll; 10 nymphs (GBIFCH00832138), 2 nymphs on slide (GBIFCH00673191-GBIFCH00673192), 1 male imago (GBIFCH00673193), 1 male imago, 1 female imago, 2 female subimagos (GBIFCH00832125), 23 Jun. 2019, same locality, L. Kechemir coll. et leg. [MZL]

Other paratypes. ALGERIA • Wilaya de Batna, Berbag, 35°24'01"N, 6°24'31"E, 1445 m. a.s.l., 1 male imago, with its nymphal and subimaginal exuviae (GBIFCH01119302), 1 female subimago with its nymphal exuvia (GBIFCH01128848) [MZL], 5 Nov. 2021; 1 male imago (GBIFCH01128852), 2 nymphs (GBIFCH01128847), 1 nymph on slide (GBIFCH01119303) [MZL], 13 nymphs [IB-US], 5 nymphs [FEEL-UB2], 4 Nov. 2021; 1 male imago [IB-US], 12 nymphs [FEEL-UB2], 30 Nov. 2020; 1 nymph [IB-US], 16 nymphs [FEEL-UB2], 03 May 2020; 1 male imago [IB-US], 10 nymphs [FEEL-UB2], 02 Mar. 2020, B. Dambri coll. ALGERIA • Wilaya de Khenchela, Yabous, 35°21'11"N, 6°38'35"E, 1420 m. a.s.l., 2 female imagos [IB-US], 2 female subimagos, 3 nymphs [FEEL-UB2], 22 Oct. 2021; 1 female subimago [IB-US], 2 nymphs [FEEL-UB2], 1 female imago with its subimaginal exuvia, 1 female subimago (GBIFCH01128854) [MZL], 13-14 Oct. 2021; 1 male imago with its subimaginal exuvia GBIFCH01128851), 1 female imago with is subimaginal exuvia (GBIFCH01128845) [MZL], 12 Oct. 2021; 5 nymphs [IB-US], 1 female imago, 2 male subimagos, 6 nymphs [FEEL-UB2], 09 Oct. 2021; 4 nymphs [IB-US], 2 nymphs [FEEL-UB2], 1 nymph (GBIFCH01128859) [MZL], 20 Jul. 2020; 2 nymphs [IB-US], 19 nymphs [FEEL-UB2], 1 nymph (GBIFCH01128856) [MZL], 02 Jun. 2020; 1 female subimago with its nymphal exuvia [IB-US], 8 nymphs [FEEL-UB2], 09 May 2020; 1 female subimago [IB-US], 15 nymphs [FEEL-UB2], 08 Mar. 2020; 1 female subimago with its nymphal exuvia [IB-US], 3 nymphs [FEEL-UB2], 23 Feb. 2020, B. Dambri coll. ALGERIA • Wilaya de Batna, Inoughissen, 35°16'42"N, 6°32'34"E, 1670 m. a.s.l., 1 nymph (GBIFCH01128863) [MZL], 07 Jul. 2020; 1 nymph (GBIFCH01128865) [MZL], 18 Apr. 2020, B. Dambri coll.

Other material. ALGERIA • Wilaya de Batna, oued Chaâba, 35°33'03"N, 6°00'22"E, 1262 m. a.s.l., 1 nymph [IB-US], 17 Jun. 2020; 3 nymphs [IB-US], 10 nymphs [FEEL-UB2], 1 nymph (GBIFCH01128860) [MZL], 20 Apr. 2020, B. Dambri coll. ALGERIA • Wilaya de Batna, Bouailef, 35°37'01"N, 6°11'17"E, 1060 m, 1 nymph [IB-US], 08 Mar. 2020, B. Dambri coll.

Etymology. Aurès mountains were coined by the Berber people as Awras, meaning tawny; translated by the Romans as *Aurasius mons*; *aurasius* is a noun in apposition.

Description. Male imago Size: body length: 9.0–9.8 mm; forewing length 9.1–10.9 mm; cerci broken. General body color distinctly brown to reddish-brown (Fig. 3A).

Head. Light brown, clypeal plate with blackish maculations; eyes grayish blue separated by a distance equal to the diameter of the frontal ocellus; a brownish lateral stripe present at one third of the ventral side; ocelli apically whitish-yellow, dark brown basally; antennae with scapus medium brown, flagellum grayish brown.

Thorax. Pronotum medium brown; mesonotum dorsally dark brown; ventrally with basisternum and furcasternum also dark brown, laterally with spiracles and pleura yellowish-brown. **Wings.** Forewings hyaline, C, Sc and R₁ longitudinal veins medium brown with transverse veins fringed with brown; first transversal vein in the costal field surrounded by a dark brown maculation; others longitudinal veins dark brown, as transversal veins; pterostigmatic area milky, with 15–20 medium brown, simple and forked cross veins. Hind wings same color as forewings. **Legs.** Fore legs markedly darker than middle and hind ones, brown to reddish-brown; fore femora only slightly darker than tibiae and tarsi; fore legs 8.25–9.4 mm; femur:tibia:tarsi proportion: femur 2.11–2.54 mm; tibia 2.46–2.68 mm; tarsal segments 2.68–4.18 mm; T1 = 0.66–0.73 mm; T2 = 0.99–1.08 mm; T3 = 0.87–1.06 mm; T4 = 0.67–0.77 mm; T5 = 0.49–0.54 mm; gradation of tarsal segments: 2 > 3 > 4 > 1 > 5. Middle and hind legs yellowish-brown; dorsal face of femora washed with gray; distal part of femora and proximal part of tibiae dark brown; tarsi darker than tibiae; middle legs 5.16–5.49 mm; femur:tibia:tarsi proportions: femur 2.39–2.49 mm; tibia 1.87–1.91 mm; tarsal segments 0.9–1.09 mm; hind legs 4.97–5.71 mm; femur:tibia:tarsi proportions: femur 2.53–2.82 mm; tibia 1.65–1.93 mm; tarsal segments 0.79–0.96 mm.

Abdomen. General color brown to rusty tawny. Terga light tawny to rusty tawny. Tergum I dark brown, terga II–VII reddish-brown with two median pairs of light markings, proximal pair elongated and slightly divergent, distal pair subparallel to body axis (Fig. 4A). Segments II–VIII with rusty-brown lateral stripes stretching from anterior to posterior margin of the segment (Fig. 3A) and connected dorso-posteriorly (Fig. 4A); terga VII–X slightly darker than other ones; tergum X reddish-brown, yellowish-brown posteriorly. Abdominal sterna yellowish to light brown, with two pairs of light markings, the proximal pair elongated, and divergent, distal pair rounded (Fig. 4B). Sterna VIII–IX darker. Nervous ganglia well visible and tinted with purple on sterna II–VII. Cerci brown, with joints of segments blackish.

Genitalia. Styli plate medium brown, lighter in the middle, strongly convex, with two small bumps near gonostyli base; first segment of gonostyli dark brown, second and third lighter (Fig. 4D). Penis lobes yellowish-brown to brown moderately expanded laterally, outer margin rather quadratic (Fig. 4D, E). Basal and lateral sclerites brown, darker than apical sclerite (Fig. 4E). Lateral sclerite rather quadratic slightly larger on inner side; apical sclerite with few medium sized teeth on inner margin (Fig. 5A); basal sclerite outer margin smooth, without teeth. Titillators straight, yellowish-brown, darker on outer margin, with two spines on the dorsal face.

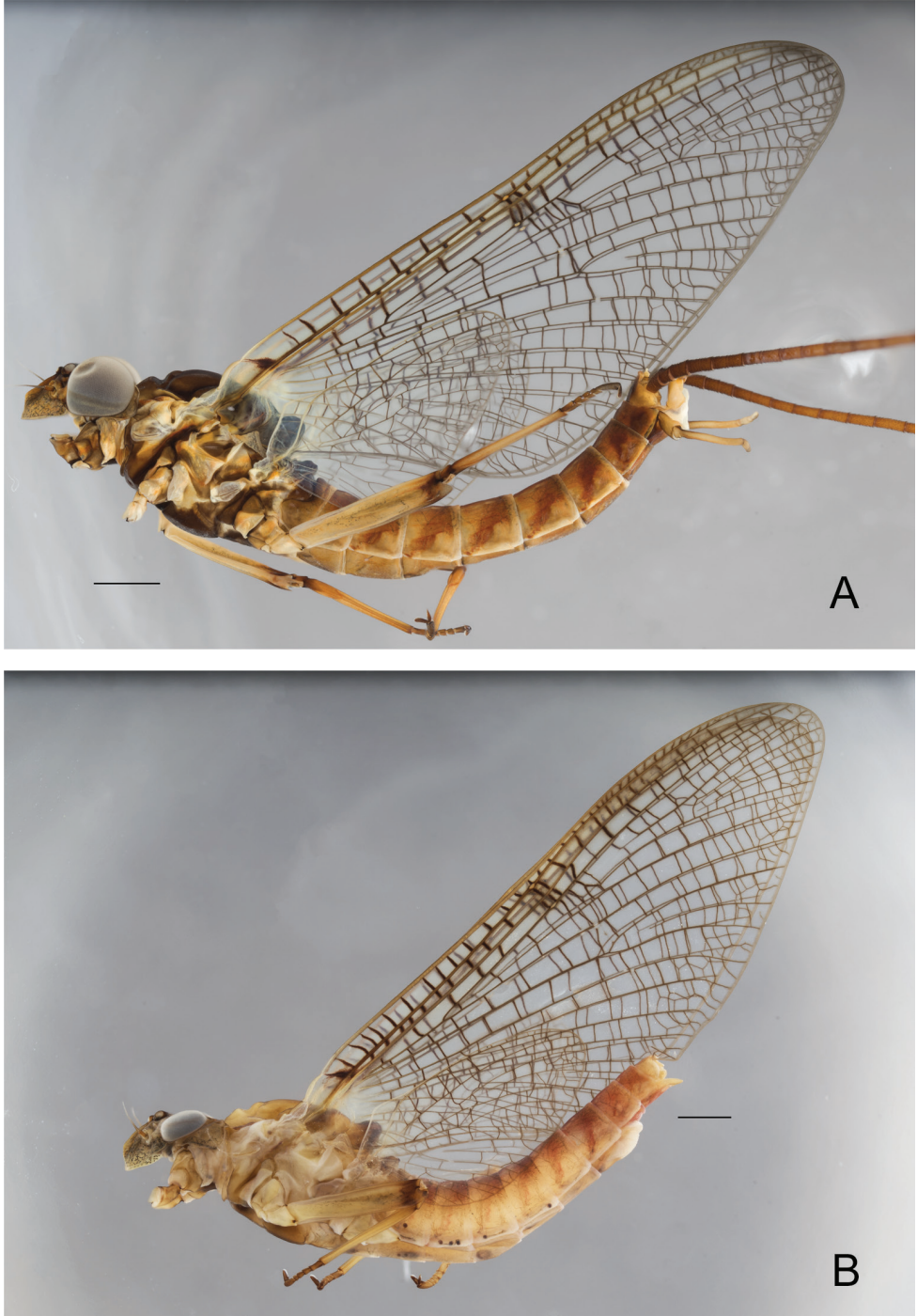


Figure 3. *Ecdyonurus aurasius* sp. nov., adults in lateral view **A** male **B** female. Scale bar: 1 mm.

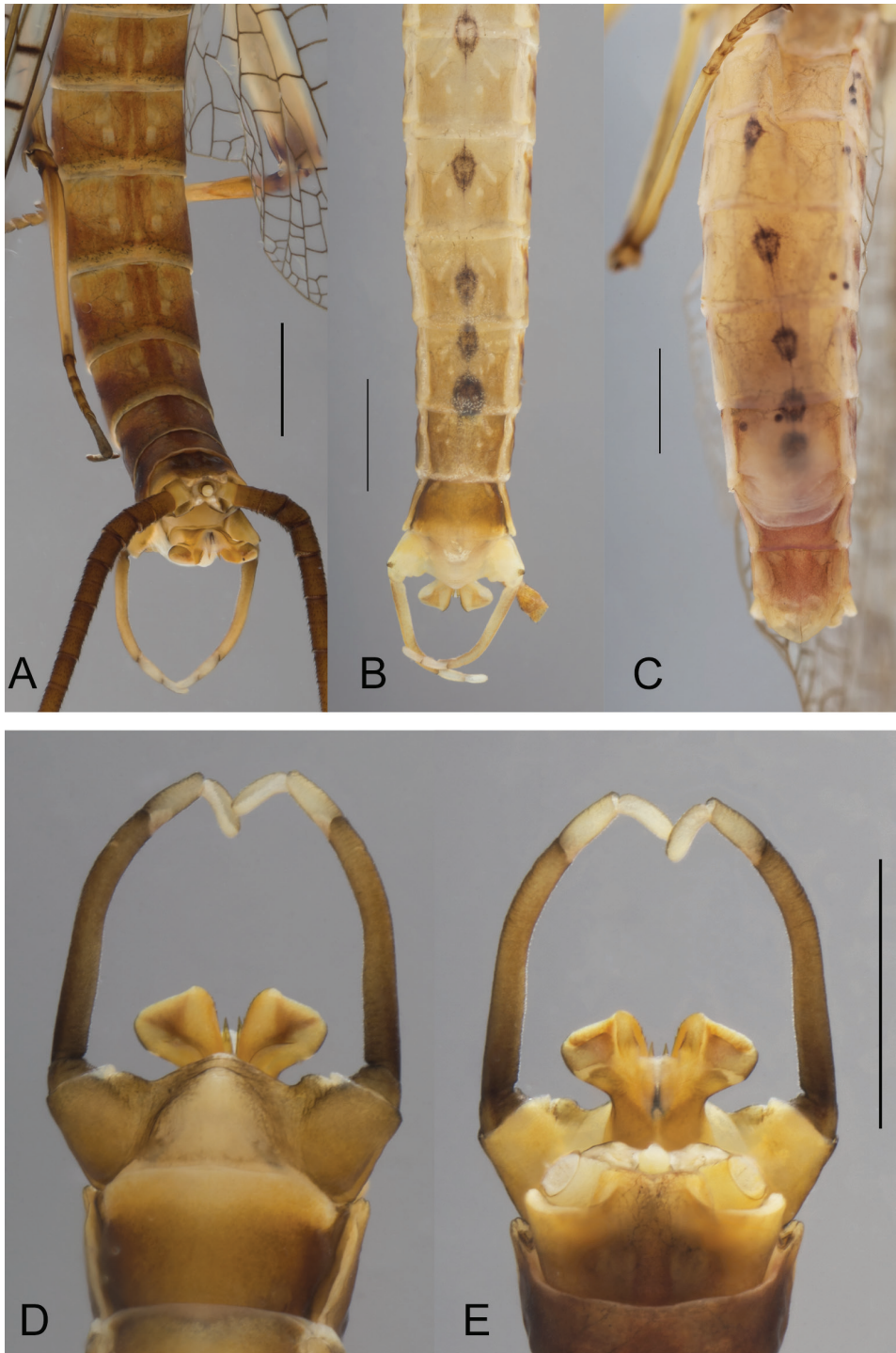


Figure 4. *Ecdyonurus aurasius* sp. nov., abdomen of adults **A** male in dorsal view **B** male in ventral view **C** female in ventral view **D** male genitalia in ventral view **E** male genitalia in dorsal view. Scale bar: 1 mm.

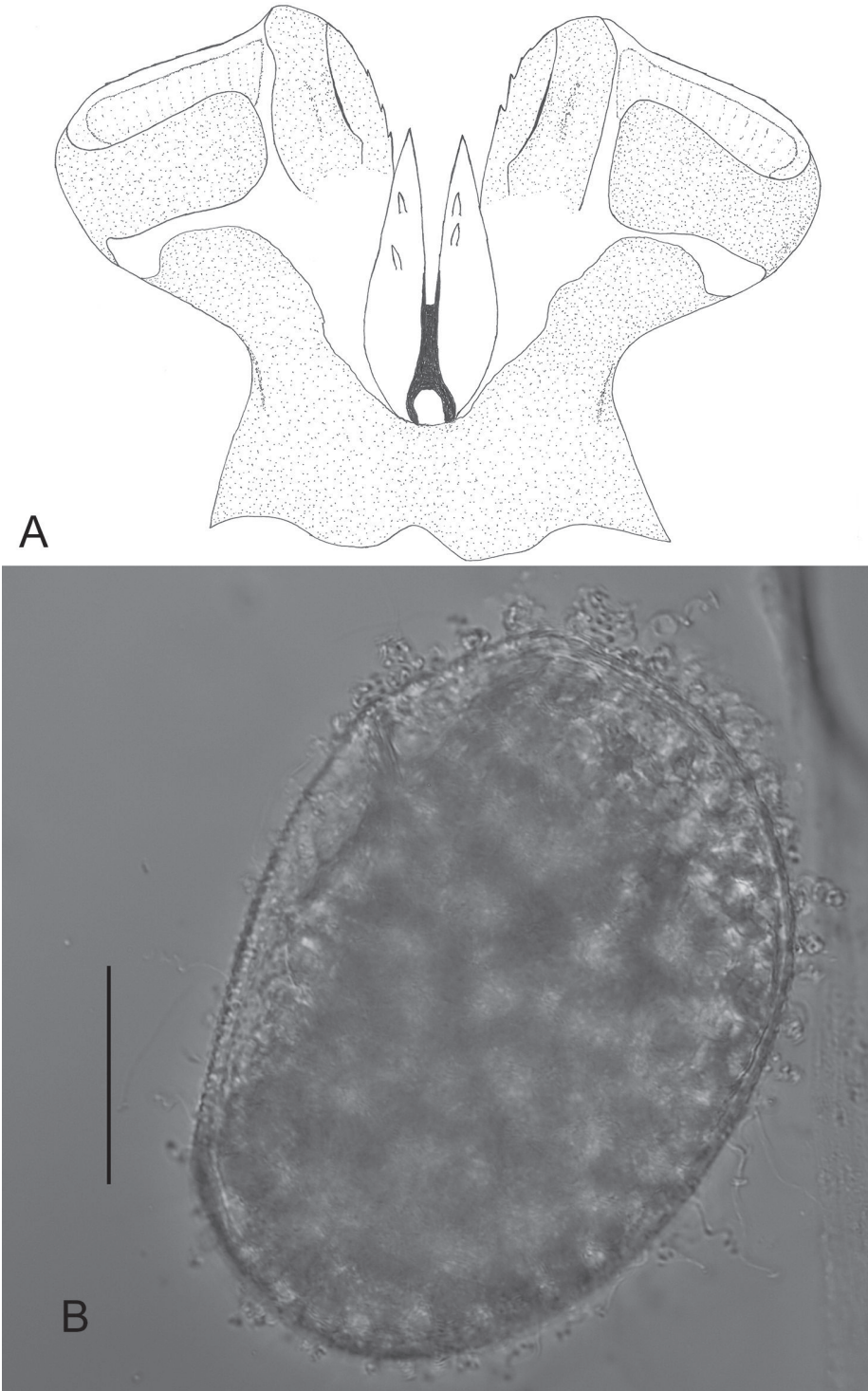


Figure 5. *Ecdyonurus aurasius* sp. nov. **A** penes in dorsal view **B** egg. Scale bar: 0.05 mm.

Female imago. Size: body length: 9.9–13.3 mm; forewings length: 10.5–12.9 mm; cerci length: 17.9–21.3 mm. General color of body similar to that in male imago, markedly paler. **Head.** yellowish-brown; eyes grayish. **Thorax.** Prothorax yellowish gray to brown. Mesothorax dorsally pale, yellow to yellowish-brown, basisternum and furcasterum medium brown. **Abdomen.** Terga yellowish laterally and tawny to rusty tawny dorsally. Terga I–VIII with central longitudinal rusty tawny parallel bands and lateral stripes (Fig. 3B). Abdominal sterna yellowish to light brown, especially VIII–IX, segments I–VII generally with two central light short strokes; nervous ganglia strongly tinted with purple on sterna II–VII. Subgenital plate large, whitish and angular, reaching two third of sternum VIII length; subanal plate acutely rounded (Fig. 4C). Cerci brown, with joints blackish.

Female subimago. Size: body length: 12.0–12.4 mm; forewings length: 12.3 mm; cerci length: 14.0–14.8 mm. Measurements and body color similar to female imago; thorax and abdomen slightly paler. Wings dull grey.

Male subimago. Size: body length: 9.8–10.5 mm; forewings length: 10.5–11.4 mm; cerci length: 13.3–26.9 mm. Head brown to reddish-brown. Eyes grayish blue. Ocelli as in male imago. Antennae yellowish, brown basally, same than in male imago. Fore legs darker than middle and hind ones. Fore femora intensively brown distally. Middle and hind legs uniformly yellowish gray to yellow. Wings dark gray. Abdominal terga similar to male imago. Sterna slightly lighter than terga. Protuberances of styliiger plate well marked, slightly yellowish, gonostyli intensively brown, yellow to whitish-yellow apically. Typical shape of penis already well apparent. Cerci brown.

Mature nymp. Size: body length: up to 7.12 mm for male and 9.6 mm for female; cerci slightly longer than body length. General body color yellowish-brown with pale yellowish markings.

Head. Mean width/length ratio 1.4–1.6, yellowish-brown to brown, with two central light spots near fore margin, and two whitish stripes along the dehiscence line (Fig. 6A). Eyes blackish grey; ocelli whitish grey, antennae with scape and pedicel medium brown; flagellum yellowish-brown.

Mouthparts. Labrum. Mean length /labrum insertion length ratio 1.58; tips slightly turned backwards (Fig. 7A); anterior margin with a median single row of stout setae (Fig. 7B). Right mandible with prostheca composed of 8–11 feathered bristles; kinetodontium (inner incisor) much shorter than (outer) incisor (Fig. 7D). Left mandible with prostheca composed of 9–11 feathered setae, kinetodontium subequal in length to incisor. Hypopharynx with lingua quadratic with dorsal margin slightly concave in the middle; superlingua well developed, with long hair-like setae on outer margin becoming shorter and less dense near apex (Fig. 7E). Labium typical of the genus; glossae markedly rhomboid, with inner margin straight or slightly concave (Fig. 7F). Crown of the galealacinia of maxilla with 16–22 comb-shaped setae; median setae with ca 15–17 teeth (Fig. 7G). Maxillary palps 3-segmented, second segment slightly longer than third one.

Thorax. Pronotum. Mean width/length ratio 4.2–5.0, yellowish-brown to brown; lateral projections ca as long as the length of the pronotum; with lateral margin regularly convex, and tip slightly pointed (Fig. 6A). Mesonotum medium brown with yellowish markings.

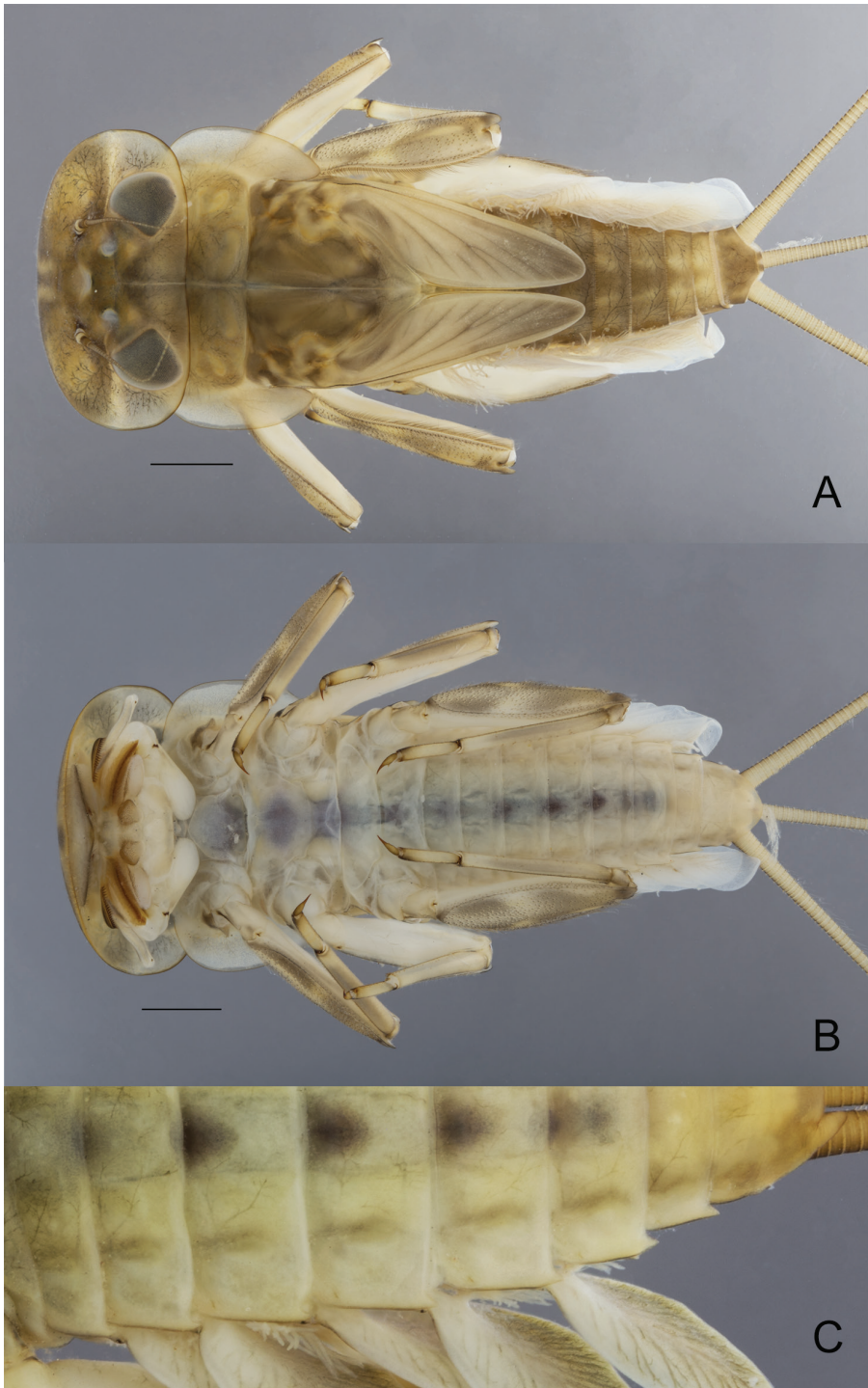


Figure 6. *Ecdyonurus aurasius* sp. nov., nymphal habitus **A** dorsal view **B** ventral view **C** posterolateral expansions of the abdomen. Scale bar: 1 mm.

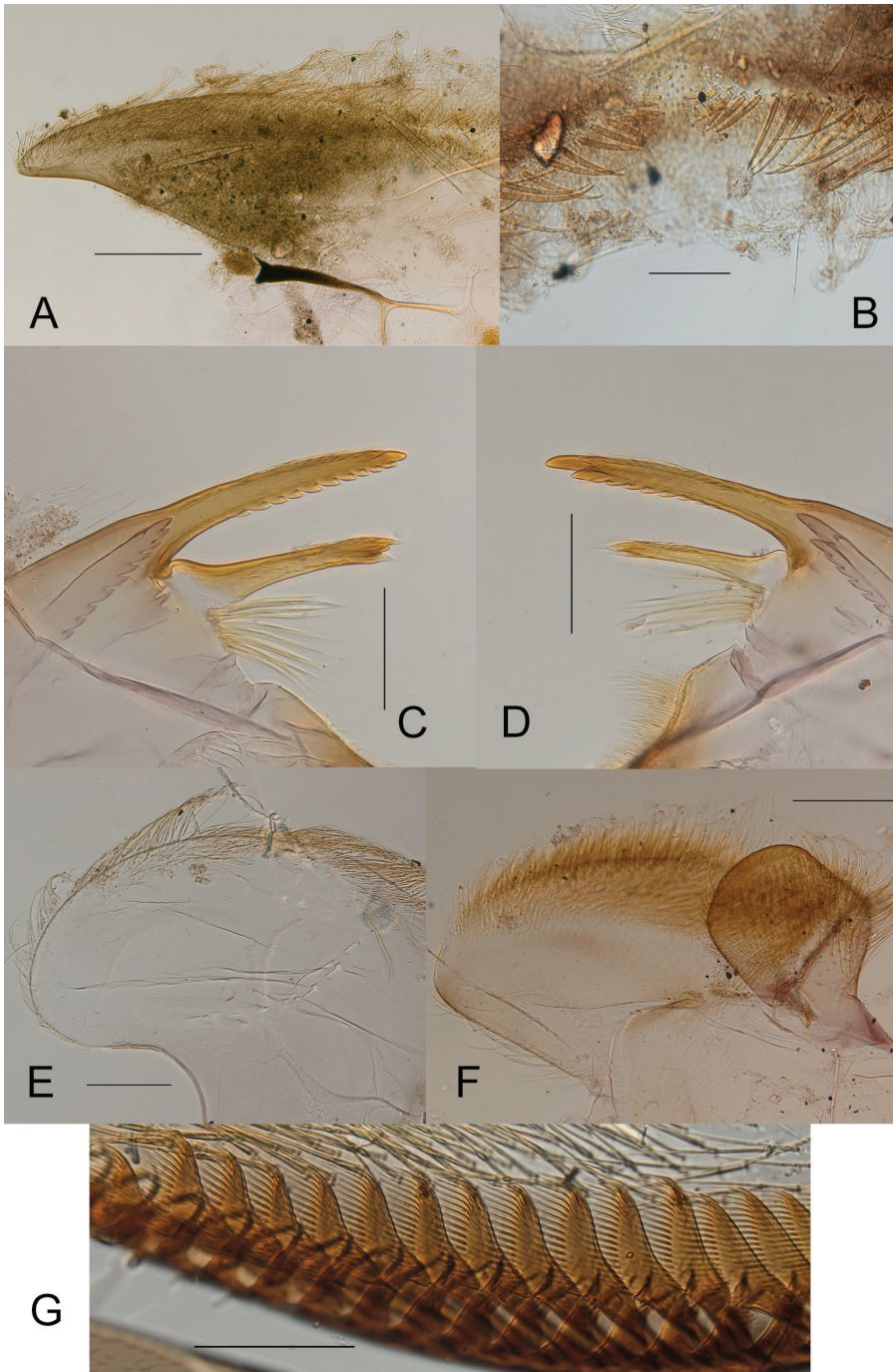


Figure 7. *Ecdyonurus aurasius* sp. nov., nymphal mouthparts: **A** hemi-labrum **B** detail of anteromedial part of labrum in ventral view **C** left mandible **D** right mandible **E** left half of hypopharynx **F** left half of labium **G** comb-shaped setae at the crown of the galea-lacinia. Scale bars: 0.2 mm (**A**, **F**); 0.1 mm (**B–E**, **G**).

Legs. Yellowish-brown to brown; dorsal surface of femora yellowish-brown washed with grayish brown; uniformly yellowish white ventrally. Tibiae yellowish-brown. Tarsi brownish. Middle and hind legs coloration similar to fore legs. Fore femora 2.0–2.2 times longer than wide; fore tibiae subequal in length to femora. Middle femora 2.2–2.3 times longer than wide; tibiae 0.8–0.9 times femora length. Hind femora 2.3–2.4 longer than wide; tibiae 0.80–0.85 times femora length. Mid- and hind femora length 1.1–1.3 times fore-femora length. Stout setae on dorsal surface of femora similar on all legs, elongated with subparallel margins, tip truncate or slightly rounded (Fig. 8A); claws elongated and hooked with 2–4 small denticles (Fig. 8B).

Abdomen. Terga brownish gray; on terga II–VIII two centrally elongated yellowish spots increasing in size posteriorly and fused on tergum IX; tergum X uniformly medium brown (Fig. 6A). Abdominal sterna yellowish white, nervous ganglia tinted with purple. Posterior margin of terga with large pointed marginal teeth alternating with medium and short ones, and several rows of microdenticles above the margin (Fig. 8C). Posterolateral projections short, weakly sclerotized, reaching from slightly above 1/7 to 1/5 of the length of the following segment (Fig. 6C). Gills grayish brown with distinct brown and developed tracheation; gill I tongue-shaped, gills II–VII leaf-shaped, asymmetrical, gills III–IV slightly longer than wide (Fig. 8D–J). Cerci and paracercus yellowish-brown; each segment with a row of pointed stout setae.

Egg. Length 165–175 μm ; width 120–130 μm ; numerous KCT's densely arranged at one pole (Fig. 5B); chorionic surface covered with micro granulations.

Discussion

Ecdyonurus aurasius sp. nov. belongs to the subgenus *Ecdyonurus* by the shape of the apical sclerite of male genitalia and the single row of stout setae on the ventral side of the labrum. However, this species presents some intermediate characters between the subgenera *Ecdyonurus* and *Helevetoraeticus*; the number of comb-shaped setae on the crown of the galea-lacinia is generally less than 20 in *Ecdyonurus* s.s., whereas our species exhibits a range from 16 to 22 setae; the setae on the lateral margin of superlingua are supposed to be long, including the tip, whereas in our species, those at the tip are shorter. We can also add the posterolateral projections on the abdomen which are very short, and the nervous ganglia tinted in purple, two characters not frequent in *Ecdyonurus* s.s. but more common in *Helvetoraeticus*. Nevertheless, we are confident that our new species belongs to the subgenus *Ecdyonurus*.

By the shape of the penis lobes and the posterolateral projections of the abdomen, *E. aurasius* sp. nov. is closely related to *E. aurantiacus*, *E. dispar*, *E. rothschildi*, and *E. ifranensis*. The first two are considered as Mediterranean faunal elements, expanding to Central Europe or even the British Islands for *E. dispar* (Bauernfeind and Soldán 2012). The nymph of *E. aurasius* sp. nov. can be separated from those of *E. aurantiacus* and *E. dispar* by the nervous ganglia tinted with purple, and the tongue-shaped gill I,

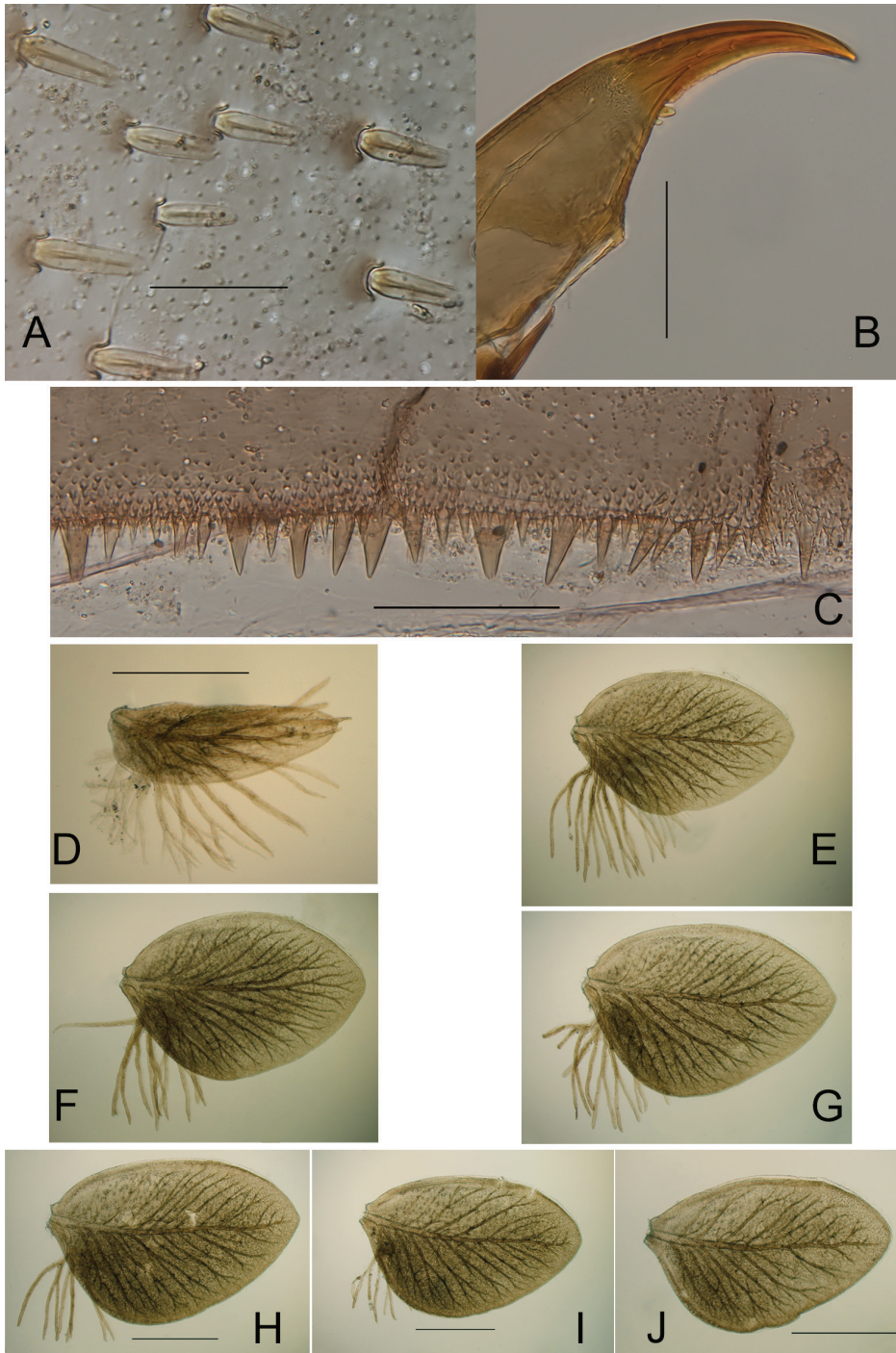


Figure 8. *Ecdyonurus aurasius* sp. nov., nymphal structures **A** stout setae on the dorsal surface of femora **B** claw **C** posterior margin of tergum IV **D–J** Gill I to VII. Scale bars: 0.05 mm (**A**); 0.1 mm (**B–J**); 0.5 mm (**E–G** same bar as **H**).



Figure 9. Sampling sites where *Ecdyonurus aurasius* sp. nov. was collected **A** Oued Chaâba **B** Inoughissen **C** Charchar **D** Berbaga (photos Besma Dambri).

from *E. dispar* also by the shape of the stout setae on the dorsal surface of femora (acute and pointed in the latter). The new species presents more affinities with the two other North African endemics but can be distinguished from *E. rothschildi* by the much longer pronotal projections, the shape of the stout setae on the dorsal surface of femora (pointed in the latter), the shape of the gills (more symmetrical in *E. rothschildi*) and the shape of the glossae ((inner margin rounded and convex in *E. rothschildi*). *Ecdyonurus aurasius* sp. nov. differs from *E. ifranensis* by the shape of the labrum (less broad in *E. ifranensis*), the shape of the stout setae on the dorsal surface of femora (pointed in *E. ifranensis*), and the shape of the glossae similar to *E. rothschildi*. In males, *E. aurasius* sp. nov. differs from *E. rothschildi*, *E. dispar* and *E. aurantiacus* by the compound eyes separated and not touching (character not stated in *E. ifranensis* description), from *E. aurantiacus* and *E. dispar* by the posterior margin of the basal sclerite smooth, and from *E. ifranensis* by the first transversal vein in the costal field surrounded by a dark brown maculation (the same in *E. rothschildi*), and by the shape of the posterior margin of the basal sclerite rounded (straight in *E. ifranensis*). It is also worth noting that *E. aurasius* sp. nov. differs from the two other North African species by the nervous ganglia tinted in purple in female imagos, whereas they are colorless in *E. rothschildi* and *E. ifranensis*.

Distribution and biology

Ecdyonurus aurasius sp. nov., as known so far, is restricted to the Aurès region. The species has been recorded from only six localities in the Western Aurès area; most habitats are located in the highest part of the streams, within altitudes ranging from 1010 to 1800 m a.s.l. These sites are represented by small mountain watercourses with gravel substrate (Fig. 9). The average annual water temperature ranges from 5 °C to 18 °C with high concentration of dissolved oxygen (6.5 to 9.35 mg/L). The nymphs were sampled under current velocity ranging from 0.24 to 0.48 m/sec, the average streams width from 60 cm to 1.50 m, with depth from 10 to 35 cm, and pH from 6.8 to 7.2. The highest population density was recorded at the Charchar site (60 individuals/m²) and the lowest one was observed at the Bouailef site (2–5 individuals/m²).

The mature nymphs and subimagos (together with early-instar nymphs) were observed in May/June and another generation observed in September/October, thus suggesting a bivoltine life cycle. The other Ephemeroptera species sporadically occurring in the same sites were *Caenis luctuosa* (Burmeister, 1839), *Baetis chelif* Soldan, Godunko & Thomas, 2005 and *Baetis sinespinosus* Soldán & Thomas, 1983.

Acknowledgements

We would like to thank the General Directorate of Forests of Batna province for their accompany on the difficult access sites. We want to express our appreciation to Professor Abdelkrim Si Bachir, Director of the Faculty of Natural and Life Sciences, for facilitating the work in the laboratory, and Dr Abdelkrim Arar for his help with the map

production. Our sincere thanks to Sonia Zrelli (Bizerte, Tunisia), Mokhtar Benlasri (Marrakech, Morocco) Lina Kechemir (Tizi-Ouzou, Algeria) and Boudjéma Samraoui (Guelma, Algeria) for providing material useful for this study. Céline Stoffel (MZL) is thanked for her dedicated work with the molecular lab. We also express our gratitude to Robert Czerniawski, Director of IB-US for encouraging this collaboration and Tomasz Krepeski for providing support and lab material for morphological observations in IB-US laboratory. Comments from and discussion with the two reviewers, Lubos Hrivniak and Ernst Bauernfeind, greatly helped to improve the manuscript.

This research was supported by the Algerian Ministère de l'Enseignement Supérieur et de la Recherche Scientifique.

References

- Bajkova OY (1975) Izvestiya Sibirskogo Otdelnriya Akademii Nauk SSSR 1: 54–57. [New genus of Ephemeroptera from the Primor'ye] [in Russian]
- Barber-James HM, Gattolliat J-L, Sartori M, Webb JM (2013) World checklist of freshwater Ephemeroptera species. <http://fada.biodiversity.be/group/show/35>
- Bauernfeind E, Soldán T (2012) The Mayflies of Europe. Apollo Books, Ollerup, 781 pp.
- Benhadji N, Sartori M, Hassaine KA, Gattolliat JL (2020) Reports of Baetidae (Ephemeroptera) species from Tafna Basin, Algeria and biogeographic affinities revealed by DNA barcoding. Biodiversity Data Journal 8: e55596. <https://doi.org/10.3897/BDJ.8.e55596>
- Bouhala Z, Marquez-Rodriguez J, Chakri K, Samraoui F, El-Serehy FA, Ferreras-Romero M, Samraoui B (2020) The life cycle of the Maghrebian endemic *Ecdyonurus rothschildi* Navas, 1929 (Ephemeroptera: Heptageniidae) and its potential importance for environmental monitoring. Limnology 22: 17–26. <https://doi.org/10.1007/s10201-020-00625-z>
- Boumaiza M, Thomas AGB (1995) Distribution and ecological limits of Baetidae vs the other mayfly families in Tunisia: A first evaluation (Insecta, Ephemeroptera). Bulletin de la Société d'Histoire Naturelle de Toulouse 131: 27–33.
- Burmeister H (1839) Ephemerina. Handbuch der Entomologie 2: 788–804.
- Crass RS (1947) The May-flies (Ephemeroptera) of Natal and the Eastern Cape. Annals of the Natal Museum 11: 37–110.
- Curtis J (1834) Descriptions of some nondescript British species of May-flies of Anglers. The London and Edinburgh Philosophical Magazine and Journal of Science 4(20): 120–125. <https://doi.org/10.1080/14786443408648276>
- Darriba D, Taboada G, Doallo R, Posada D (2012) jModelTest 2: More models, new heuristics and parallel computing. Nature Methods 9(8): 772–772. <https://doi.org/10.1038/nmeth.2109>
- Eaton AE (1868) An outline of re-arrangement of the genera of Ephemeridae. Entomologist's Monthly Magazine 5: 82–91.
- El Alami M, El Yaagoubi S, Gattolliat J-L, Sartori M, Dakki M (2022) Diversity and distribution of Mayflies from Morocco (Ephemeroptera, Insecta). Diversity 14(6): e498. [19 pp] <https://doi.org/10.3390/d14060498>
- Fabricius JC (1793) 2 Entomologia systematica emendata et aucta. <https://doi.org/10.5962/bhl.title.122153>

- Flowers RW (1980) Two new genera of Nearctic Heptageniidae (Ephemeroptera). *The Florida Entomologist* 3(3): 296–307. <https://doi.org/10.2307/3494626>
- Gauthier H (1928) Recherche sur la faune des eaux continentales de l'Algérie et de la Tunisie. Minerva, Alger, 149 pp.
- Hrivniak L, Sroka P, Godunko RJ, Palatov D, Polasek M, Manko P, Obona J (2018) Diversity of Armenian mayflies (Ephemeroptera) with the description of a new species of the genus *Ecdyonurus* (Heptageniidae). *Zootaxa* 4500(2): 195–221. <https://doi.org/10.11646/zootaxa.4500.2.3>
- Kimura M (1980) A simple method for estimating evolutionary rate of base substitutions through comparative studies of nucleotide sequences. *Journal of Molecular Evolution* 16(2): 111–120. <https://doi.org/10.1007/BF01731581>
- Kluge NJ (2004) The phylogenetic system of Ephemeroptera. Kluwer Academic Publishers, Dordrecht, 442 pp. <https://doi.org/10.1007/978-94-007-0872-3>
- Kumar S, Stecher G, Li M, Knyaz C, Tamura K (2018) MEGA X: Molecular Evolutionary Genetics Analysis across Computing Platforms. *Molecular Biology and Evolution* 35(6): 1547–1549. <https://doi.org/10.1093/molbev/msy096>
- Lestage J-A (1924) Les Ephémères de l'Afrique du Sud. Catalogue critique et systématique des espèces connues et description de trois genres nouveaux et de sept espèces nouvelles. *Revue de Zoologie Africaine* 12: 316–352.
- Lestage J-A (1925) Ephéméroptères, Plécoptères et Trichoptères recueillis en Algérie par M. H. Gauthier et liste des espèces connues actuellement de l'Afrique du Nord. *Bulletin de la Société d'Histoire Naturelle de l'Afrique du Nord* 16: 8–18.
- Leticia I, Bork P (2021) Interactive Tree Of Life (iTOL) v5: An online tool for phylogenetic tree display and annotation. *Nucleic Acids Research* 49(W1): W293–W296. <https://doi.org/10.1093/nar/gkab301>
- Martynov AV, Sivaruban T, Palatov DM, Srinivasan P, Barathy S, Isack R, Sartori M (2022) Contribution to Teloganodidae (Ephemeroptera, Ephemeroidea) of India. *ZooKeys* 1113: 167–197. <https://doi.org/10.3897/zookeys.1113.85448>
- Navás L (1929) Insectes Névroptères et voisins de Barbarie. *Bulletin de la Société d'Histoire Naturelle de l'Afrique du Nord* 20: 57–60.
- Puillandre N, Lambert A, Brouillet S, Achaz G (2012) ABGD, Automatic Barcode Gap Discovery for primary species delimitation. *Molecular Ecology* 21(8): 1864–1877. <https://doi.org/10.1111/j.1365-294X.2011.05239.x>
- Puillandre N, Brouillet S, Achaz G (2021) ASAP: Assemble species by automatic partitioning. *Molecular Ecology Resources* 21(2): 609–620. <https://doi.org/10.1111/1755-0998.13281>
- Rambaut A, Drummond A, Xie D, Baele G, Suchard M (2018) Posterior Summarization in Bayesian Phylogenetics Using Tracer 1.7. *Systematic Biology* 67(5): 901–904. <https://doi.org/10.1093/sysbio/syy032>
- Ronquist F, Teslenko M, van der Mark P, Ayres D, Darling A, Höhna S, Larget B, Liu L, Suchard M, Huelsenbeck J (2012) MrBayes 3.2: Efficient Bayesian Phylogenetic Inference and Model Choice Across a Large Model Space. *Systematic Biology* 61(3): 539–542. <https://doi.org/10.1093/sysbio/sys029>

- Sartori M (2014) Status of the enigmatic Oriental genus *Rhithrogeniella* Ulmer, 1939 (Ephemeroptera, Heptageniidae). *ZooKeys* 429: 47–61. <https://doi.org/10.3897/zookeys.429.8116>
- Soldán T, Gagneur J (1985) *Ecdyonurus rothschildi* Navás, 1929: Description de la larve (Ephemeroptera, Heptageniidae). *Annales de Limnologie* 21(2): 141–144. <https://doi.org/10.1051/limn/1985013>
- Stecher G, Tamura K, Kumar S (2020) Molecular Evolutionary Genetics Analysis (MEGA) for macOS. *Molecular Biology and Evolution* 37(4): 1237–1239. <https://doi.org/10.1093/molbev/msz312>
- Thomas AGB (1998) A provisional checklist of the mayflies of North Africa (Ephemeroptera). *Bulletin de la Société d'Histoire Naturelle de Toulouse* 134: 13–20.
- Thomas AGB, Dakki M (1979) Ephéméroptères d'Afrique du Nord: I. *Ecdyonurus rothschildi* Navás, 1929. Description des imagos. *Annales de Limnologie* 14(3): 197–201. <https://doi.org/10.1051/limn/1978008>
- Ulmer G (1920) Neue Ephemeropteren. *Archiv für Naturgeschichte, Abteilung A* 11: 1–80. [1919]
- Vitte B, Thomas AGB (1988) Compléments et corrections à la faune des Ephéméroptères d'Afrique du Nord. 3. *Ecdyonurus ifranensis* n. sp. du Moyen Atlas marocain (Ephemeroptera). *Annales de Limnologie* 24(3): 269–273. <https://doi.org/10.1051/limn/1988023>
- Vuataz L, Sartori M, Gattolliat JL, Monaghan MT (2013) Endemism and diversification in freshwater insects of Madagascar revealed by coalescent and phylogenetic analysis of museum and field collections. *Molecular Phylogenetics and Evolution* 66(3): 979–991. <https://doi.org/10.1016/j.ympev.2012.12.003>
- Wang TQ, McCafferty WP (2004) Heptageniidae (Ephemeroptera) of the world. Part I: Phylogenetic higher classification. *Transactions of the American Entomological Society* 130: 11–45.
- Webb JM, McCafferty WP (2008) Heptageniidae of the world. Part II: Key to the Genera. *Canadian Journal of Arthropod Identification* 7: 1–55.
- Yanai Z, Sartori M, Dor R, Dorchin N (2017) Molecular phylogeny and morphological analysis resolve a long-standing controversy over generic concepts in Ecdyonurinae mayflies (Ephemeroptera: Heptageniidae). *Systematic Entomology* 42(1): 182–193. <https://doi.org/10.1111/syen.12203>
- Zrelli S, Boumaiza M, Bejaoui M, Gattolliat J-L, Sartori M (2016) New data and revision of the Ephemeroptera of Tunisia. In: Yoshimura M, Takemon Y (Eds) *Biology of Inland Waters supplement N°3*, Wakayama, Japan, 99–106.
- Zurwerra A, Tomka I (1985) *Electrogena* gen. nov. eine Gattung der Heptageniidae (Ephemeroptera). *Entomologische Berichte (Luzern)* 13: 99–104.

Taxonomy of *Homoeusa* Kraatz, 1856 (Coleoptera, Staphylinidae) from the East Palearctic: I. *Homoeusa rufescens* (Sharp, 1874) and a new allied species

Tsubasa Nozaki^{1,2}, Munetoshi Maruyama²

1 Entomological Laboratory, Graduate School of Bioresource and Bioenvironmental Sciences, Kyushu University, Fukuoka 819-0395, Japan **2** The Kyushu University Museum, Fukuoka 812-8581, Japan

Corresponding author: Tsubasa Nozaki (dosanko.lathrobium@gmail.com)

Academic editor: Volker Assing | Received 19 April 2022 | Accepted 21 June 2022 | Published 12 September 2022

<https://zoobank.org/5548DAFD-60EA-4FF7-9418-9702D58FF602>

Citation: Nozaki T, Maruyama M (2022) Taxonomy of *Homoeusa* Kraatz, 1856 (Coleoptera, Staphylinidae) from the East Palearctic: I. *Homoeusa rufescens* (Sharp, 1874) and a new allied species. ZooKeys 1121: 39–58. <https://doi.org/10.3897/zookeys.1121.85489>

Abstract

There is insufficient information to identify most species of the myrmecophilous rove beetle genus *Homoeusa*. In this paper, after examining the type material, *Homoeusa rufescens* (Sharp, 1874) is redescribed in detail and its new allied species *Homoeusa ovata* **sp. nov.** is described. We also observed the behavior of these two species in the field; the behavior was similar to that reported for *H. acuminata* (Märkel, 1842). A checklist of *Homoeusa* from the Palearctic and Nearctic is also provided.

Keywords

Aleocharinae, description, Dinardina, *Homoeusa ovata* sp. nov., *Lasius*, myrmecophily, new species, rove beetle

Introduction

Nine species of the myrmecophilous genus *Homoeusa* Kraatz, 1856 (tribe Oxyopini) are known from the Palearctic region, of which eight are recorded from the East Palearctic, i.e., China, Taiwan, Far East Russia, and Japan (Smetana 2004; Pace 2010; Maruyama et al. 2013). Most species have not been redescribed since

their original descriptions 90–120 years ago, which are very short and almost useless for identification. This series of papers aims to revise the East Palearctic species of *Homoeusa*.

Homoeusa is distinguishable from the other myrmecophilous oxypodine genera of the Palearctic by its sub-limuloid body shape and unilobed ligula; the latter distinguishes it from the similar genus *Thiasophila* Kraatz, 1856, which has a bifid ligula. Maruyama and Zerche (2014) suggested that *Thiasophila rufescens* Sharp, 1874 described from Japan could be a member of *Homoeusa*. Probably based on this statement, Schülke and Smetana (2015) listed *T. rufescens* as a *Homoeusa* species. Here, we confirmed that *T. rufescens* should be transferred to *Homoeusa*. We found that another species allied to *T. rufescens* is included in the syntypes of *T. rufescens* and is very common in the nests of *Lasius* species in the *fuliginosus* group (formerly members of the subgenus *Dendrolasius*). It was found to be a new species and is also described here. The taxonomy of *Homoeusa* is very difficult and some species complexes still require time to work. Therefore, this paper treats these two species, which are very common and need to be identified, prior to the revision of the whole genus. We discuss the feeding behavior of these species and provide a checklist of the world species of *Homoeusa*.

Materials and methods

The material examined in this study is deposited mostly in the Kyushu University Museum (**KUM**), and some in The Hokkaido University Museum, Sapporo (**HUM**), National Museum of Nature and Science, Tsukuba (**NSMT**), Sagami-hara City Museum, Kanagawa, Japan (**SCM**), and private collections of Hiromu Kamezawa (Saitamaken) (cKam). Type material of *Homoeusa rufescens* is deposited in the Natural History Museum, London (**NHM**). Part of the paratypes from the Russian Far East are in the Institute of Biology and Soil Science, Vladivostok, Russia (**IBSS**).

The morphological observations and measurements were conducted using an Olympus SZX10. On the methods of dissection and preparation of permanent slides, we followed Maruyama (2004). Habitus photos were taken using a Canon 7D camera with a Canon MP-E 65 mm f/2.8 1–5X macro lens, and Nee-er TT560/1Y strobe, and image stacking was conducted using Zerene Stacker ver. 1.04 (Zerene Systems LLC). Drawings were made using a microscope Olympus BX50 with an Olympus drawing tube attached.

Measurement definitions and abbreviations are shown as follows: BL, approximate body length; AL, antennal length; HW, head width; PL, pronotal length; PW, pronotal width; EL, elytral length (sutural length from apex of scutellum to posterior margin of elytra); EW, elytral width; HTL, hind tibial length. Measurements of dorsal morphology were made on 20 specimens of each species, and then the sexes were identified. Measurements of each segment of the antenna (six specimens of each species) were made on dissected specimens mounted in Euparal.

Symbiotic hosts were mostly identified by MM, F. Ito, and some by TN and K. Kinomura.

Host ants

The scientific names of *Lasius* ants follow Bolton (1995), Radchenko (2005), and Boudinot et al. (2022). *Lasius fuji* was formerly recognized as the eastern Palearctic population of *L. fuliginosus*. Recently, the Japanese population of “*Lasius fuji*” has been suggested to be a species complex (Maruyama et al. 2013). Therefore, ‘*Lasius* cf. *fuliginosus*’ is adopted as the name of the Japanese population here. *Lasius fuliginosus* and allied species have long been classified in the subgenus *Dendrolasius*. However, Boudinot et al. (2022) synonymized all the subgenera of *Lasius* with the genus *Lasius* and recognized five species groups, which is adopted here.

The species names of symbiotic hosts are abbreviated in “Type material” and “Additional material” as follows: *Lasius fuliginosus* Group: *LFFJ*, *L. fuji* Radchenko, 2005; *LFFL*, *L. fuliginosus* (Latreille, 1798); *LFcF*, *Lasius* cf. *fuliginosus*; *LFM*, *Lasius morisitai* Yamauchi, 1979; *LFN*, *L. nipponensis* Forel, 1912; *LFO*, *L. orientalis* Karawajew, 1912; *LFS*, *L. spathepus* Wheeler, 1910; *LJ*, *Lasius japonicus* Santschi, 1941 (the *niger* group).

The distribution and host ant species of each species in the checklist is a synthesis of information from mostly Schülke and Smetana (2015), Maruyama et al. (2013), and this paper.

Results

Tribe Oxypodini Thomson, 1859

Subtribe Dinardina Mulsant & Rey, 1873

Genus *Homoeusa* Kraatz, 1856

Homoeusa Kraatz, 1856: 76 (original description, type species: *Euryusa acuminata* Märkel, 1842, by monotypy); Kraatz 1857: 16 (diagnosis); Jacquelin du Val 1857: 11 (catalogue); Fenyes 1919: 389 (redescription); Bernhauer and Scheerpeltz 1926: 736 (synonymy, catalogue); Smetana 2004: 467 (catalogue); Schülke and Smetana 2015: 682 (catalogue).

Myrmobiota Casey, 1893: 594 (original description, type species: *M. crassicornis* Casey, 1893, by monotypy); Fenyes 1919: 392 (redescription); Bernhauer and Scheerpeltz 1926: 736 (catalogue; synonym of *Homoeusa*); Seevers 1978: 75 (redescribed).

Soliusa Casey, 1900: 53 (original description, type species: *S. crinitula* Casey, 1900, by monotypy); Fenyes 1919: 389 (synonym of *Homoeusa*); Bernhauer and Scheerpeltz 1926: 736 (catalogue; synonym of *Homoeusa*).

Diagnosis. This genus is distinguished by the following combination of characteristics: body somewhat sub-limuloid; apex of ligula unilobed and round; antennae not or weakly clubbed; posterior margin of antennal insertion forming distinct latitudinal carina extending medially; spermatheca somewhat S-shaped.

Remarks. As mentioned in Maruyama (2009), this genus is similar to *Losiusa* and *Aspidobactrus*, which are called the “*Homoeusa* genus complex”. Together with some other genera, these genera are classified in the subtribe Dinardina of the tribe Oxy-podini (Schülke and Smetana 2015). The subtribe Dinardina is defined based on its limuloid body and shield-like pronotum (Seevers 1978). However, the monophyly of Dinardina (sensu Seevers 1978) has been rejected; the *Dinarda*+*Thiasophila* clade was distant from *Myrmobiota* (Osswald et al. 2013), which is a close relative of *Homoeusa* and often regarded as a junior synonym of *Homoeusa*. The *Homoeusa* genus complex is assumed to form a clade with *Myrmobiota* distant from *Dinarda*+*Thiasophila* given their symbiotic hosts and morphological characteristics of the head, ligula, and facial structure of the body. The relatedness of the *Homoeusa* genus complex and Nearctic genus *Decusa* Casey, 1900 was also suggested (see also Wasmann 1901). To reveal the relationships among these genera in detail, future phylogenetic research is necessary.

***Homoeusa rufescens* (Sharp, 1874), combination confirmed**

Japanese name: Hoso-hirata-ariyadori

Figs 1–4, 6–16, 28, 29

Thiasophila rufescens Sharp, 1874: 5; Fenyés 1919: 393 (catalogue); Bernhauer and Scheerpeltz 1926: 771 (catalogue); Smetana 2004: 488 (catalogue).

Homoeusa rufescens: Maruyama and Zerche 2014: 17 (mentioning actual generic affiliation); Schülke and Smetana 2015: 682 (catalogue).

Type material. Lectotype (Figs 1–3), here designated, ♂, “Japan. Lewis.” / “Sharp Coll 1905-313” / “Syn-type” (blue round curator label) / “Lectotype *Thiasophila rufescens* det. Maruyama, 2003” (dissected by MM) (NHM). **Paralectotypes**, 1 ♀, same data as lectotype but labelled “Type” (red round curator label) / “*Thiasophila rufescens* type D.S.” (NHM); 5 unsexed, same data as lectotype, but one is labelled “Nagasaki” (NHM).

Additional material. JAPAN: Honshû: Fukushima-ken: 1 unsexed, Yukiwari-bashi, Nishigô-mura, 29. VII. 2000, T. Kobayashi. **Ibaraki-ken:** 2 unsexed, Inohana Pass, 29. V. 1994, Y. Hagino. **Tochigi-ken:** 1 unsexed, Tobiyama Castle, Utsunomiya-shi, 17–18. VI. 1998, M. Maruyama (*LFS*); 2 unsexed, 1 ♀, same locality, 17. VI. 1998, M. Maruyama (*LFcfF*); 2 unsexed, Shimokomoriya, Utsunomiya-shi, 6. VII. 1999, M. Maruyama; 3 unsexed, Sayado, Môka-shi, 15. VI. 2000, T. Kobayashi & H. Obata; 81 unsexed, Ichikai-machi, Haga-gun, 29. IV.–2. V. 2002, Seidai Nagashima. **Gunma-ken:** 27 unsexed, Mt. Sakurayama, Onishi-chô, 22. V. 1999, Shiho Arai (*LFS*); 2 unsexed, Sakurayama Park, Onishi-chô, 18. V. 1998, Shiho Arai (*LFS*); 26 unsexed, 7 ♂, 3 ♀, same locality, 9. V. 1998, Shiho Arai (*LJ*); 10 unsexed, Sakurayama, Onishi-chô, 9. V. 1998, Koji Toyoda (*LFS*); 5 unsexed, Nakanojo Forest Park, Nakanojô-machi, 8. VI. 2001, T. Watanabe. **Saitama-ken:** 15 unsexed, Shioyama, Ranzan-machi, 21. VI. 1996, Koji Toyoda; 10 unsexed, same locality, 8. VI. 1997, Koji



Figures 1–5. 1–3 Lectotype of *Homoeusa rufescens* (Sharp, 1874): **1** habitus of the lectotype, male **2** labels of the lectotype **3** dissected parts of the lectotype **4** habitus of *Homoeusa rufescens* from non-type specimens, female **5** habitus of the holotype of *Homoeusa ovata* sp. nov., male.

Toyoda (LFcfF); 16 unsexed, same locality, 10. V. 1998, K. Toyoda (LFcfF); 3 unsexed, Shôgunsama, Ranzan-machi, 21. IV. 1999, K. Toyoda; 1 unsexed, Sugiyama, Ranzan-machi, 13. VII. 1998, K. Toyoda; 13 unsexed, Toki-gawa, Kamagata-mura, Ranzan-machi, 25. IV. 1999, K. Toyoda; 2 unsexed, Shiro-yama, Kamagata-mura, Ranzan-machi, 17. VI. 2000, K. Toyoda (LFcfF); 4 unsexed, Ranzan-keikoku, Kamagata-mura, Ranzan-machi, 14. V. 2000, K. Toyoda; 2 unsexed, Hashidake, Chichibu-shi, 26.

IV. 1998, S. Arai; 2 unsexed, Nakano, Showa-machi, 4. V. 2002, Hiromu Kamezawa (*LFS*) (cKam); 1 unsexed, same locality, 26. VI. 2001, H. Kamezawa (*LFcfF*) (cKam); 2 unsexed, same locality, 4. V. 2002, H. Kamezawa (*LFcfF*) (cKam); 5 unsexed, same locality, 4. V. 2003, H. Kamezawa (*LFcfF*) (cKam); 1 unsexed, Yokoze-machi, Chichibu-shi, 10–11. V. 1995, Yoshinori Kaneko, Akio Ito, Satoshi Tsuboyama. **Chiba-ken:** 1 unsexed, Mt. Kiyosumi, Amatsukominato, 9. VI. 1991, T. Takeda; 1 unsexed, Azeta, Sakura-shi, 20. VI. 1998, M. Maruyama (*LFS*); 1 unsexed, 1♀, same locality, 23–24. VI. 1998, M. Maruyama (*LFS*); 2 unsexed, same locality, 26. VI. 1998, M. Maruyama (*LFS*). **Tōkyō-to:** 1 unsexed, Mt. Takao, 1. V. 1985, S. Nomura; 2 unsexed, same locality, 13. V. 1985, S. Nomura; 2 unsexed, Takao-san (450 m in alt.), Hachioji-shi, 4. VI. 2001, M. Maruyama (*LFS*); 1 unsexed, Otomeyama Park, Shinjuku-ku, 13. V. 1985, S. Kubota; 3 unsexed, Dokan-bori, Imperial Palace, 17. V. 2000, T. Shimada (NSMT); 34 unsexed, Kami-dokan-bori, Imperial Palace, 17. V. 2000, Shiho Arai (*LFcfF*) (MSMT). **Kanagawa-ken:** 2 unsexed, Kawasaki-shi, 1. V. 1985, S. Kubota; 3 unsexed, Ikuta-Ryokuchi, Kawasaki-shi, 13. IV. 2002, K. Matsumoto; 1 unsexed, Mt. Masukata, Kawasaki-shi, 15. VI. 1996, K. Kawada; 1 unsexed, Jinmu-ji, Zushi-shi, 20. VI. 2003, M. Maruyama; 1 unsexed, Mt. Tanzawa, 26. VI. 1983, Y. Hirano; 1 unsexed, Kawana, Fujisawa, 19. VI. 2000, T. Watanabe (*LFS*); 1 unsexed, same locality, 7. V. 2001, T. Watanabe (*LFcfF*); 3 unsexed, 1♂, same locality, 14. V. 2001, T. Watanabe; 6 unsexed, Toya, Tsukui, 11. V. 1976, Ryo Kiryu (SCM); 6 unsexed, same locality, 29. IV. 1977, Ryo Kiryu (SCM); 2 unsexed, Mikage, Tsukui, 18. V. 1976, Ryo Kiryu (SCM); 1 unsexed, same locality, 23. IV. 1977, Ryo Kiryu (SCM); 1 unsexed, same locality, 9. VI. 1979, Ryo Kiryu (SCM). **Yamanashi-ken:** 2 unsexed, Karumizu-rindō, (1400 m in alt.), Narusawa, 29. VI. 2011, T. Watanabe. **Shimane-ken:** 1 unsexed, Urahikimi, 6. VI. 1988, S. Nomura. **Okayama-ken:** 1 unsexed, Ono Shine, Kawakami, Ohara-chō, Mimasaka-shi, 7. VI. 2009, Yoshifumi Fuzitani; 5 unsexed, same locality, 5. V. 2009, Yoshifumi Fuzitani (*LFS*). **Yamaguchi-ken:** 3 unsexed, Nishimagura, (100 m in alt.), Kusunoki, 30. V.–1. VI. 2000, Toshio Kishimoto. **Shikoku: Kagawa-ken:** 7 unsexed, 1♂, Usa-Jinja, Nagaona, Sanuki-shi, 31. V. 2001, M. Maruyama (*LFS*); 11 unsexed, 1♂, 1♀, Ôtaki-san, Shionoe-chō, 2. VI. 2001, M. Maruyama (*LFN*); 1 unsexed, Fujio-Jinja, Nishiuta-chō, Takamatsu-shi, 31. V. 2001, M. Maruyama (*LFS*); 4 unsexed, same locality, 1. VI. 2001, M. Maruyama (*LFN*); 5 unsexed, Furodani, Miki-chō, 30. VII. 2000, K. Izawa; 1 unsexed, Kamiyama, Miki-chō, 1. VI. 2001, M. Maruyama (*LFS*); 4 unsexed, Ôtawara, Nagano-chō, 22. V. 2000, F. Ito; 11 unsexed, Atago-yama, Kotohira-chō, 1. VI. 2001, M. Maruyama (*LFS*). **Ehime-ken:** 1♂, Sugitate, 17. VI. 2017, Yu Hisasue. **Kyūshū: Fukuoka-ken:** 1 unsexed, Hikosan, Biol. Lab. KU, Soeda-machi, 8–10. V. 1957, K. Morimoto; 1 unsexed, same locality, 7. VI. 1993, S. Nomura; 3 unsexed, Hikosan, Biol. Lab. KU (750 m in alt.), Soeda-machi, 22. V. 2011, M. Maruyama (*LFcfF*); 1 unsexed, Kusaba, Nishi-ku, Fukuoka-shi, 28. IV. 2018, Tsubasa Nozaki; 1 unsexed, Motooka, Nishi-ku, Fukuoka-shi, 29. IV. 2020, Tsubasa Nozaki; 1 unsexed, Mt. Shioji, Otogana, Onojo-shi [33.5416°N, 130.5023°E], 28. V. 2017, Yu Hisasue (*LFS*). **Saga-ken:** 1 unsexed, Tōsen-zan, Ureshino-shi, 29. IV. 2018, Mitsuyasu Nishida (fit). **Nagasaki-ken:** 4 unsexed, Tanukinoo,

Masuragahara-machi, Ômura-shi, 5. V. 2018, Mitsuyasu Nishida. **Kumamoto-ken:** 1 unsexed, Shiraga-dake, 4. XI. 1984, M. Ohara (HUM).

Diagnosis. It is distinguished from the other species of the genus by the following combination of characteristics: body small, slender and subparallel-sided; pronotum less transverse (PW/PL, 1.38–1.47), widest near middle, posterolateral angle obtuse, posterior margin hardly sinuate; apical lobe of male aedeagus thick with round sheet-like projection; apical lobe of paramere straight; velum broad and round.

Redescription. *Body* (Figs 1, 4) small, very slender, subparallel-sided; dorsal surface mostly slightly polished.

Head (Fig. 6) relatively large, reddish brown; frontal margin with few long setae; carina of antennal insertion gently sinuate; eye large. Antennae (Fig. 7) stout, as long as head and pronotum combined, reddish brown, but segments I–IV and XI paler; segment I dilated, widest near apex; segment II slightly longer than III, widened apically; segment III widened apically; segment IV–X widened apically, each apical margin fringed with small teeth and longer than wide; segments IV as long as wide; segments V–X slightly wider than long; segment XI oblong oval. Labrum (Fig. 8), apical margin concave, surface with 20 setae; epipharynx with 2 pairs of sensillae on anterior margin, and 3 pairs of micro setae on lateral margin. Mentum (Fig. 9) with 3 pairs of setae and 1 pair of microsetae; anterior margin deeply concave. Prementum (Fig. 10) with many pseudopores, and with 2–3 real pores and 1 setal pore on each side near middle lateral margin. Ligula elongate, apical margin with 1 pair of spinule and several sensilla. Labial palpus, segment II and III each with 5 setae.

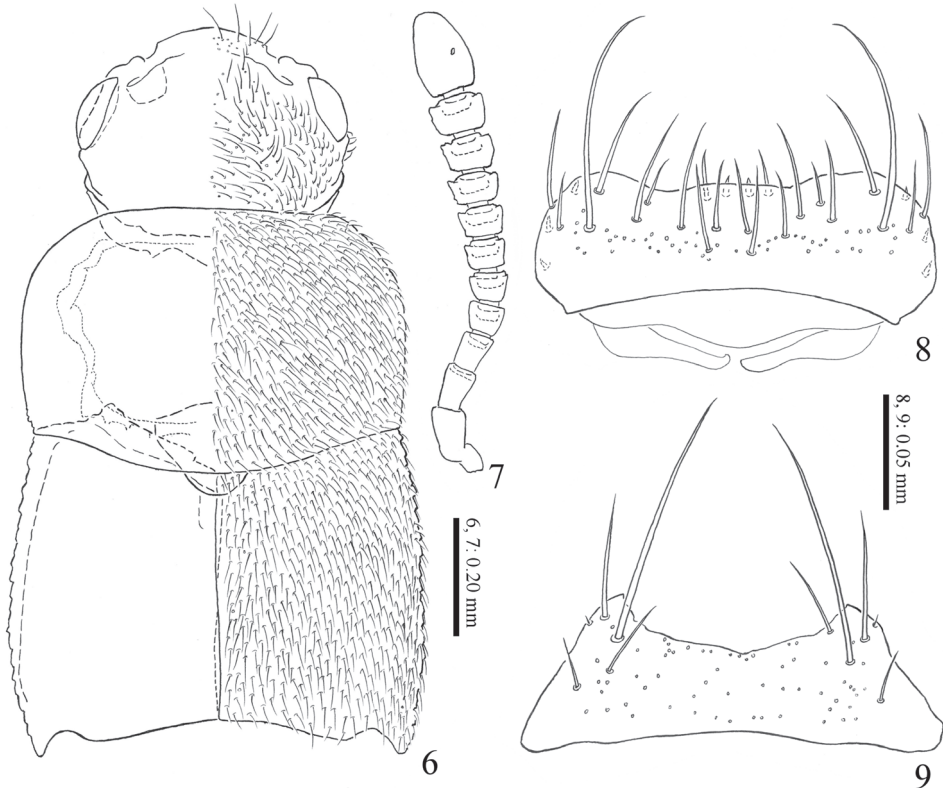
Pronotum (Fig. 6) convex, subrectangular, less transverse, widest near middle; posterolateral angle obtuse, posterior margin hardly sinuate, brownish red to brownish black; surface finely covered with setae and punctures. Elytra (Fig. 6) slightly widened posteriorly, posterior margins shallowly notched near lateral corners, brownish red; surface finely covered with setae and punctures, moderately reticulated. Mesoventral processes (Fig. 11) narrow, with medial carina forming Y-shaped, apex rounded; meso-coxal cavities separated; metaventral process weakly produced.

Abdomen elongate, slightly narrowed posteriad; surface sparsely covered with short setae and each posterior margin with long stout setae; polished and weakly reticulated.

Male: 8th sternite longer than wide, weakly rounded apically. Median lobe of aedeagus (Fig. 12), apical lobe of aedeagus thick with round flattened projection on ventral side; apical lobe of paramere (Fig. 13) short and straight; velum broad and round; ventral margin of paramerite almost straight.

Female: 8th sternite longer than wide, weakly rounded apically. Spermatheca (Figs 14–16), apical part moderately swollen; apical 3/5 with inner wall densely reticulated.

Measurements. Body shape ($N = 20$): BL \approx 1.6–2.7; AL, 0.64–0.75; HW, 0.41–0.47; PL, 0.44–0.50; PW, 0.61–0.70; EL, 0.38–0.44; EW, 0.65–0.73; HTL, 0.42–0.48; PW/PL, 1.38–1.49; PW/HW, 1.38–1.57; AL/HW, 1.45–1.77. Aspect ratio (length/width) of each antennal segment from I to XI ($N = 6$): 1.36–1.58, 1.43–1.71, 1.15–1.22, 0.63–0.77, 0.52–0.63, 0.43–0.53, 0.44–0.50, 0.39–0.49, 0.43–0.51, 0.49–0.56, 1.26–1.54.



Figures 6–9. *Homoeusa rufescens* Sharp, 1874 **6** fore body **7** right antenna **8** labrum **9** mentum.

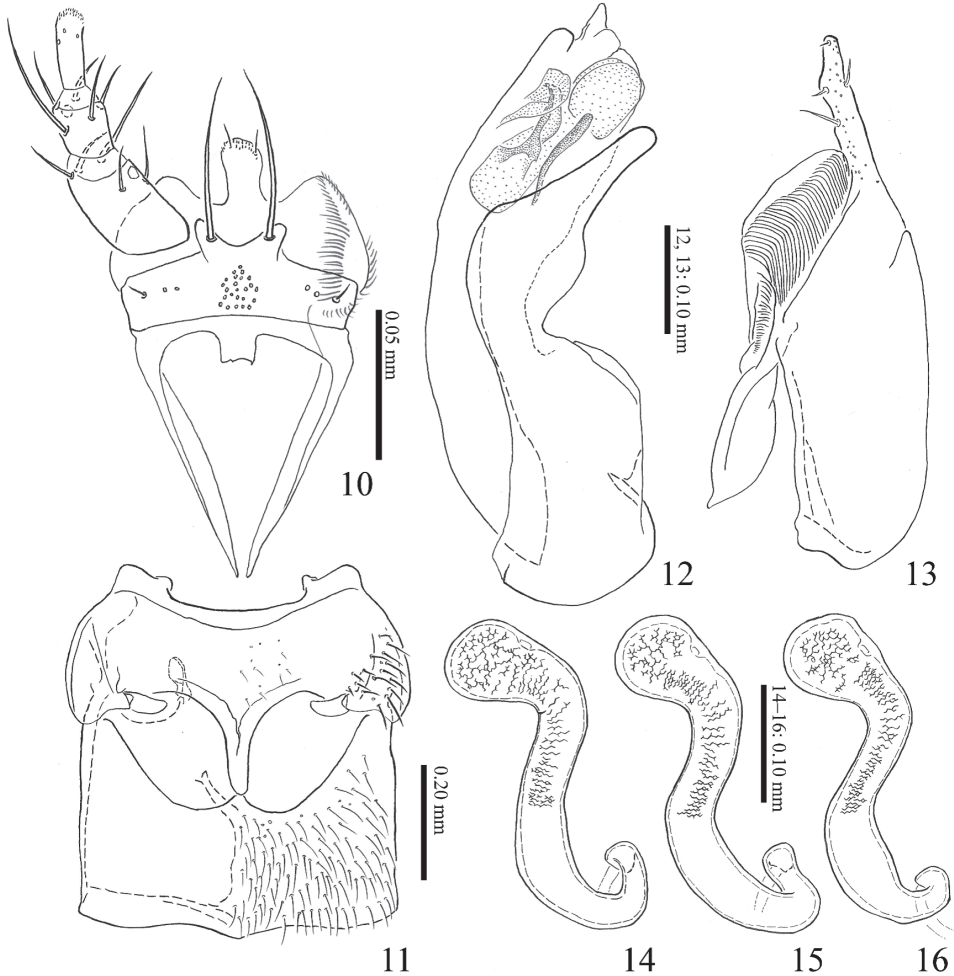
Variation. In most individuals, the pronotum tends to be brownish red, but the color varies from brownish red to brownish black.

Distribution. Japan (Honshû, Shikoku, Kyûshû).

Bionomics. From April to July, this species can be found in the trails of the *Lasius fuliginosus* species group (Fig. 28). When they encounter host ants, they pause briefly until the ants ignore them and then start walking. TN observed that they ate prey that the ants were trying to carry but dropped. This species is sometimes observed to climb on food that the host ant is carrying and eat it (Fig. 29).

Symbiotic hosts. *Lasius* cf. *fuliginosus*, *L. morisitai*, *L. nipponensis*, *L. spathepus*.

Remarks. The original description suggested that the syntypes included another species (Sharp 1874). Based on our examination of the syntype, it includes two species, as mentioned in the original description. Here, the specimens of the more slender species that more closely match the original description are designated as the lectotype and paralectotype. The specimens that were judged a different species were excluded from the syntypes of *H. rufescens* and included in the paratypes of the following species. As is often the case with old specimens, the proteins in the lectotype



Figures 10–16. *Homoeusa rufescens* Sharp, 1874 **10** labium **11** meso-, metaventrite **12** median lobe of aedeagus from lateral view **13** paramere of aedeagus from lateral view **14–16** spermatheca.

were denatured and potassium hydroxide did not sufficiently dissolve the muscle of the genital organs (Fig. 3), but the morphological characteristics of this species were fully observed.

In the original description, “*Thiasophila rufescens*” is “found with *Formica japonica*” (Sharp 1874). Ruzsky (1912) established the subgenus ‘*Dendrolasius*’ (= *Lasius fuliginosus* species group), with “*Formica fuliginosa*” as the type species. There were no *Homoeusa rufescens* specimens collected from *Formica* ants in the present study, so the syntypes were also likely collected from the *Lasius fuliginosus* species group. A single specimen was pinned with a *Lasius japonicus* (*niger* group), but this is considered to be a coincidence.

***Homoeusa ovata* Nozaki & Maruyama, sp. nov.**

<https://zoobank.org/6638F337-2AAC-419F-9334-01EA46D98C90>

Japanese name: Hime-hirata-ariyadori

Figs 5, 17–27, 30, 31

Type material. Holotype. “Mt. Maruyama / Sapporo-shi / <Hokkaido, JAPAN> / 6. VI. 1988 / M. Maruyama leg. / trail of ants” (*LFcfF*). **Paratypes.** 1♂, (ex type series of “*Thiasophila rufescens*”), “Japan. Lewis.” / “Sharp Coll 1905-313” (no other data) (NHM). Paratypes. 1 unsexed (ex type series of “*Thiasophila rufescens*”), same data but labelled “*rufescens* var.?” (NHM). **RUSSIA: Primorskyi kraii:** 1 unsexed, Kamenushka, Ussuryisk (MMLASRUS07), 28. V. 2005, M. Maruyama (*LFO*); 1 unsexed, same locality (MMLASRUS09), 28. V. 2005, M. Maruyama (*LFO*) (IBSS); 1 unsexed, 1♂, same locality (MMLASRUS11), 28. V. 2005, M. Maruyama (*LFN*); 1 unsexed, Bukhta Vityaz, Poluostrov Gamov, Khasanskyi (MMLASRUS14), 29. V. 2005, M. Maruyama (*LFO*); 2 unsexed, same locality (MMLASRUS17), 31. V. 2005, M. Maruyama (*LFO*) (IBSS); 2 unsexed, same locality (MMLASRUS19), 31. V. 2005, M. Maruyama (*LFF*); 6 unsexed, 2♀, Okeanskaya, Vladivostok (MMLASRUS23), 1. VI. 2005, M. Maruyama (*LFO*); 6 unsexed, 1♂, 1♀, Nadezhdinskyi, Khasanskyi, 1. VI. 2005, M. Maruyama (*LFF*) (IBSS); 2 unsexed, 3♂, Arisimovka, 70 km E Vladivostok, [43.11°N, 132.41°E], 5. VI. 1993, L. Zerche (*LFO*); 2 unsexed, Sibir or. Ussuri Vladivostok, 1919, Dr. Jureček. **KOREA:** 8 unsexed, 1♂, Janggoksa, Chilgab-san, Cheongyang-gun, Chungnam, 23. VI. 2000, Shuhei Nomura (*LFS*); 70 unsexed, 1♂, Jeonglyeong Chi Samnae Myeon Cheonla-buk Do, 12. VII. 1991, S. Nomura (*LFO*); 18 unsexed, 3♂, 1♀, same locality, 12. VII. 1991, S. Nomura. **JAPAN: Hokkaido:** 23 unsexed, Hyakumatsu-zawa, Sapporo-shi, 8. VI. 1998, M. Maruyama (*LFcfF*); 50 unsexed, Hakkenzan, Sapporo-shi, 31. V. 2002, M. Maruyama (*LFcfF*); 54 unsexed, same locality, 31. VI. 2002, M. Maruyama (*LFcfF*); 17 unsexed, 1♀, same locality, 1. VI. 2002, M. Maruyama (*LFO*); 92 unsexed, 1♂, 1♀, same locality, 1. VI. 2002, M. Maruyama (*LFN*); 267 unsexed, 2♂, 2♀, same locality, 1. VI. 2002, M. Maruyama (*LFcfF*); 2 unsexed, Kannon-zawa, Sapporo-shi, 1. V. 2002, M. Maruyama; 6 unsexed, same locality, 20. V. 2002, M. Maruyama; 27 unsexed, same locality, 31. V. 2002, M. Maruyama (*LFcfF*); 4 unsexed, 1♂, 5♀, same locality, 1 VI 2002, M. Maruyama (*LFcfF*); 23 unsexed, Maruyama, Sapporo-shi, 6. VI. 1998, M. Maruyama (*LFcfF*) (same data as holotype); 3 unsexed, Hitsujigaoka, Sapporo-shi, 18. V. 2000, M. Maruyama (*LFS*); 2 unsexed, Nopporo, 17. VII. 1990, M. Ohara (HUM); 12 unsexed, Nopporo, Ebetsu-shi, 13. VI. 1999, M. Maruyama (*LFcfF*); 20 unsexed, 2♀, Ôsawaguchi, Nopporo-shinrin-kôen, Ebetsu-shi, 16–19. VI. 2001, S. Hori; 46 unsexed, same locality, 16–19. VI. 2001, S. Hori (*LFO*); 25 unsexed, same locality, 2. VI. 1999, M. Maruyama; 2 unsexed, Tomambetsu, Nopporo, Ebetsu-shi, 29. V. 2002, M. Maruyama (*LFcfF*); 1 unsexed, Nozaki, Bihoro-chô, 23. VI. 2001, Y. Kida; 1 unsexed, Taihei, Maruseppuchô, 29–31. V. 2000, Y. Kida; 104 unsexed, 1♀, same locality, 16–17. VI. 2000, Y. Kida; 4 unsexed, same locality, 11–12. VIII. 2000, Y. Kida (*LFcfF*); 36 unsexed, same locality, 19–21. VIII. 2000, Y. Kida (*LFcfF*); 1 unsexed, 2♂, 1♀, same locality, 25. VIII. 2000, M. Maruyama (*LFcfF*); 1 unsexed, Makoi, Shari-chô, 27. V. 2000, Y.

Kida; 2 unsexed, same locality, 28. V. 2000, Y. Kida; 53 unsexed, 1♂, same locality, 24. VI. 2002, Y. Kida; 4 unsexed, same locality, 13. VI. 2002, Y. Kida; 44 unsexed, Kanayama, same locality, 18–24. VI. 2002, Yasunari Kida; 7 unsexed, Midorioka-kôen, Kitami-shi, 17. VI. 2001, M. Maruyama; 3 unsexed, Hebinuma, Teshio-gawa, Teshio-chô, 9. VII. 1992, S. Hori; 2 unsexed, Kamishunbetu, 20. VII. 1977, Naomi; 2 unsexed, Yûtoku, Ôtaki-mura, 24. VIII. 2001, M. Maruyama; 4 unsexed, Mukôengaru Engaru-chô, 25. V. 2000, Y. Kida (*LFcfF*); 2 unsexed, Miwa, Koshimizu-chô, 28. VII. 2001, S. Kuwahara; 1 unsexed, Mt. Kariba, Shiribeshi, 13. VI. 1986, S. Nomura; 1 unsexed, Himenuma, Rishiri Is, 4. IX. 1990, T. Kishimoto. **Honshû: Aomori-ken:** 1 unsexed, Hirosaki, 3. VII. 1960, Y. Murakami; 2 unsexed, same locality, 5. VII. 1960, Y. Murakami. **Miyagi-ken:** 1 unsexed, Aoba-yama, Sendai-shi, 17. VII. 2004, K. Mizota; 6 unsexed, Naruko-onsen, Naruko-chô, 14–17. VI. 1999, M. Sano (*LFO*). **Akita-ken:** 7 unsexed, 1♀, Tamagawa, Tazawako-machi, 12–13. VI. 1999, M. Sano (*LFcfF*). **Fukushima-ken:** 6 unsexed, Mizuhiki, Toteiwa-mura, 12. VI. 2004, H. Kamezawa (cKam); 33 unsexed, 2♂, Kashi Spa., Nishigo-mura, 16. VI. 1998, M. Maruyama (*LFcfF*); 12 unsexed, same locality, 17. VI. 1998, M. Maruyama (*LFcfF*); 1 unsexed, Nanairi, Hinoemata, 25. VII. 1996, S. Naomi. **Ibaraki-ken:** 2 unsexed, Inohana Pass, 29. V. 1994, Y. Hagino. **Tochigi-ken:** 1 unsexed, Yumoto, Nikkô, 29. IV. 1982, S. Naomi; 1 unsexed, Ichikai-machi, Haga-gun, 29. IV.–2. V. 2002, Seidai Nagashima. **Gunma-ken:** 5 unsexed, Sakurayama, Onishi-chô, 9. V. 1998, Koji Toyoda (*LFS*); 5 unsexed, same locality, 9. V. 1998, Shiho Arai (*LFS*); 2 unsexed, same locality, 9. V. 1998, Shiho Arai (*L*); 1 unsexed, same locality, 22. V. 1999, Shiho Arai (*LFS*); 10 unsexed, Nageishi-tôge, Fujioka-shi, 5. VI. 2001, T. Watanabe; 8 unsexed, Nakanojô-forest-park, Nakanojô-machi, Agatsuma-gun, 8. VI. 2001, T. Watanabe. **Saitama-ken:** 3 unsexed, Shiro-yama, Kamagata, Ranzan-machi, 17. VI. 2000, K. Toyoda; 1 unsexed, 1♂, Ranzan-keikoku, Kamagata-mura, Ranzan-machi, 14. IV. 2000, K. Toyoda; 1 unsexed, same locality, 25. IV. 2000, K. Toyoda; 1 unsexed, same locality, 21. IV. 1999, K. Toyoda; 4 unsexed, Shioyama, Ranzan-machi, 8. V. 1998, K. Toyoda; 7 unsexed, same locality, 10. V. 1998, K. Toyoda; 11 unsexed, same locality, 10. V. 1998, K. Toyoda (*LFcfF*); 3 unsexed, 1♂, Toki-gawa, Kamagata-mura, Ranzan-machi, 25. IV. 1999, K. Toyoda; 5 unsexed, Shiroishi-toge, Higashichichibu-mura, 20. VI. 1999, Shiho Arai; 1 unsexed, same locality, 17. VI. 2000, K. Toyoda (*LFS*); 4 unsexed, Nr. Shiroishi Pass Higashichichibu-mura, 27. VI. 1998, K. Toyoda; 1 unsexed, Chichibu-kôgen, Higashichichibu-mura, 3. VII. 1999, K. Toyoda; 1 unsexed, same locality, 3. VII. 1999, K. Toyoda; 3 unsexed, Hashidake, Chichibu-shi, 17. VII. 1999, Shiho Arai (*L*); 1 unsexed, same locality, 26. IV. 1998, K. Toyoda (*LFS*); 1 unsexed, Koakazawa, (1,000 m in alt), Iri Kawa, Mt. Hakutai san, Ootaki-chiku, Chichibu-shi, 7. VI. 2002, Koji Toyoda; 1 unsexed, Hashidate Riv., Chichibu-shi, 7. VI. 2002, Koji Toyoda; 3 unsexed, Mt. Jyouminesan Minao-chô, 29. V. 1999, Shiho Arai (*LFcfF*); 1 unsexed, Nr. Ohno Pass Takigawa-mura, 5. VIII. 1998, K. Toyoda (*LFS*). **Chiba-ken:** 2 unsexed, Matuzaki, Inzai-shi, 3. V. 1991, T. Takeda. **Tôkyô-to:** 1 unsexed, Mt. Takao, 1. V. 1985, S. Kubota; 35 unsexed, 3♂, 2♀, Takao-san (450 m in alt.), Hachiôji-shi, 4. VI. 2001, M. Maruyama (*LFS*); 4 unsexed, Takao-san, Hachiôji-shi, 1. VII. 1998, M. Maruyama; 2 unsexed, same locality, 4. VII. 1998, M. Maruyama; 1

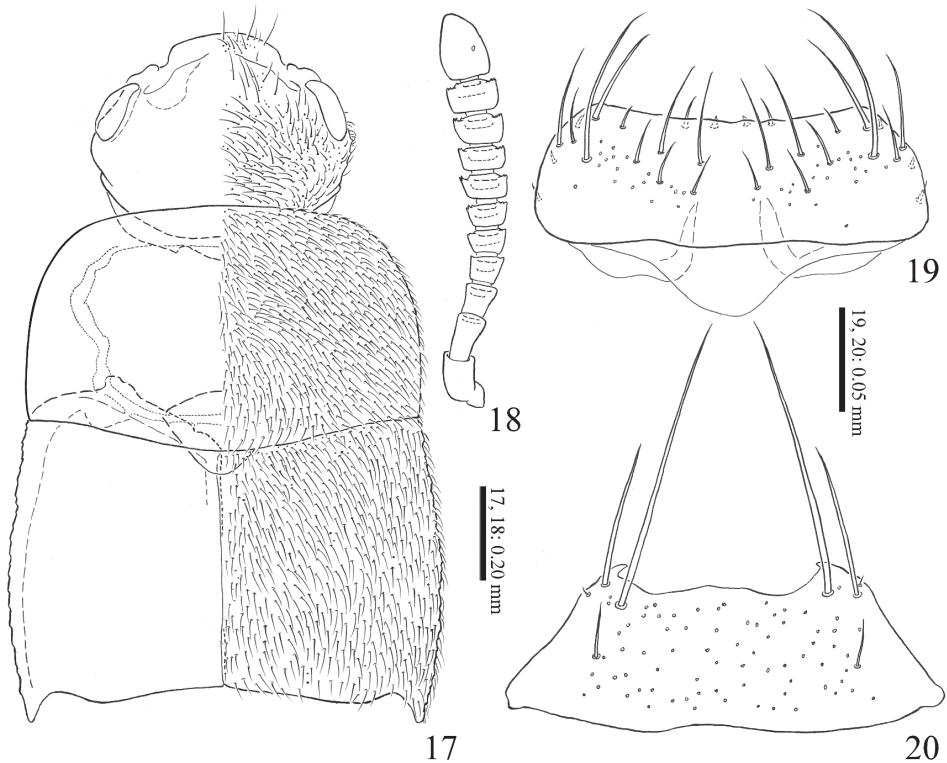
unsexed, same locality, 4. VII. 1998, M. Maruyama (*LFS*); 1 unsexed, Oyama, Machida-shi, 19. V. 1991, T. Kishimoto. **Kanagawa-ken:** 6 unsexed, Kawana, Fujisawa-shi, 14. V. 2001, T. Watanabe (*LFS*); 4 unsexed, Jimmu-ji, Zushi-shi, 20. VI. 2003, M. Maruyama; 1 unsexed, Toya, Tsukui, 29. IV. 1977, Ryo Kiryu (*SCM*); 1 unsexed, same locality, 14. V. 1976, Ryo Kiryu (*SCM*); 1 unsexed, Nanzawa, Tsukui, 14. V. 1977, Ryo Kiryu (*SCM*); 1 unsexed, Hasuge-san, Aikô, 3. V. 1963, Ryo Kiryu (*SCM*); 1 unsexed, Minami-Ashigara, 11. II. 1975, Y. Hirano; 2 unsexed, Fudakake, Higashi-Tanzawa, 16. VI. 1984, Y. Hirano; 1 unsexed, Mt. Tanzawa, 26. II. 1973, Y. Hirano; 1 unsexed, Kawasaki, 1. V. 1985, 1. V. 1985; 1 unsexed, Kozuka-yama, Hakozaki-chô, 25–26. V. 1995, Yoshinori Kaneko, Akio Ito, Satoshi Tsuboyama; 6 unsexed, 1♂, Niiharu-shiminno-mori, Yokohama-shi, 21. V. 2001, T. Watanabe (*LFO*). **Niigata-ken:** 2 unsexed, Yuzawa-machi, Minami-uonuma-gun, 20–22. VI. 2002, S. Nagashima (*LFS*); 2 unsexed, Tairai, 3. VII. 1985, S. Nomura. **Ishikawa-ken:** 2 unsexed, Ichinose pass Shiramine-Village, 25. V–7. VI. 2003, Katsuyuki Nakata (fit). **Yamanashi-ken:** 8 unsexed, Hikawarindô, Daibosatsu-rei, Koushû-shi, 24. VI. 2001, T. Watanabe; 4 unsexed, Ashiyu-onsen, Ashiyu-mura, 23. V. 2001, T. Watanabe (*LFcfF*); 1 unsexed, same locality, 24. V. 2001, T. Watanabe; 3 unsexed, Shiroidaira Dôshi-mura, 17. VII. 2001, T. Watanabe; 4 unsexed, Gozaishi-kôsen (900 m in alt.), Nirasaki-shi, 25. VII. 2002, S. Nomura (*LFN*); 2 unsexed, Karumizu-rindô, (1400 m in alt.), Narusawa, 29. VI. 2011, T. Watanabe. **Nagano-ken:** 1 unsexed, Kakuma Valley, Sanadamachi, 17. VI. 2001, T. Watanabe; 1 unsexed, Midarebashi, Honjô-mura, 21. VII. 1999, T. Watanabe; 52 unsexed, Pensionsmura, Hara-mura, 11. VII. 1999, Shiho Arai (*LFO*); 2 unsexed, Otari-onsen (1100 m in alt.), Otari-mura, Kita-azumi-gun, 16. V. 2004, H. Kamezawa (*cKam*); 2 unsexed, Fujii, Satoyamabe, Matsumoto-shi, 9. VI. 2004, T. Komatsu; 1 unsexed, same locality, 11. VI. 2004, T. Komatsu; 1 unsexed, same locality, 21. VI. 2004, T. Komatsu. **Gifu-ken:** 6 unsexed, Ogamigo (800 m in alt.) Shôkawa-mura, 5–6. VIII. 1998, M. Maruyama (*LFS*); 4 unsexed, Mt. Kinkazan, Gifu-shi, 11. VI. 2003, K. Kinomura (*LFS*); 1 unsexed, Isshiki, Shôkawa-chô, Takayama-shi, 1. VIII. 2004, K. Kinomura (*LFN*); 51 unsexed, Isshiki, Shôkawa-chô, Takayama-shi, 8. VI. 2013, K. Kinomura (*LFM*); 29 unsexed, Nabedaira-kôgen, Kansaka, Okuhida-onsenkyô, Takayama-shi, 30. VI. 2013, K. Kinomura (*LFN*); 20 unsexed, Nabedaira-kôgen, (1305 m in alt.) Kansaka, Okuhida-onsenkyô, Takayama-shi, (1305 m in alt.), 30. VI. 2013, K. Kinomura (*LFN*). **Wakayama-ken:** 1 unsexed, Mt. Gomandan, 22–23. VI. 1981, S. Naomi. **Tottori-ken:** 1♂, Mt. Daisen, 3–5. VI. 1980, S. Naomi; 3 unsexed, same locality, 10. VI. 1986, S. Nomura (*LFS*); 10 unsexed, 1♂, Urahikimi, Shimane-ken, 6. VI. 1988, S. Nomura (*LFS*). **Okayama-ken:** 2 unsexed, Ono Shine, Kawakami, Ohara-chô, Mimasaka-shi, 5. V. 2009, Yoshifumi Fujitani; 1 unsexed, same locality, 24. V. 2009, Yoshifumi Fujitani; 1 unsexed, same locality, 7. VI. 2009, Yoshifumi Fujitani. **Hiroshima-ken:** 11 unsexed, Nakatsuya, Hatsu-kaichi-shi, 7. VI. 1987, S. Nomura; 1 unsexed, Mt. Garyu, 27. VI. 1987, S. Nomura (*LFcfF*). **Yamaguchi-ken:** 10 unsexed, Nishimagura, (100 m in alt.), Kusunoki, 30. V. – 1. VI. 2000, Toshio Kishimoto; 3 unsexed, Momijidani park, Yokoyama, Iwakuni-shi, 28. V. 2011, M. Shimono (*LFS*). **Shikoku: Kagawa-ken:** 5 unsexed, Furodani, Miki-chô, 30. VII. 2000, K. Izawa (*LFcfF*); 108 unsexed, 3♂, 1♀, Ôtaki-san, Shionoe-chô,

2. VI. 2001, M. Maruyama et al. (*LFN*); 21 unsexed, Atago-yama, Kotohira-chô, 1. VI. 2001, M. Maruyama et al. (*LFS*); 22 unsexed, Fujio-jinja, Nishi-ueta-chô, Takamatsu-shi, 31. V. 2001, M. Maruyama et al. (*LFN*); 2 unsexed, same locality, 1. VI. 2001, M. Maruyama et al. (*LFN*); 22 unsexed, Daisen-zan, Kotonami-chô, 1. VI. 2001, M. Maruyama et al. (*LFM*); 13 unsexed, Usa-jinja, Nagaona, Sanuki-shi, 31. V. 2001, M. Maruyama et al. (*LFS*); 3 unsexed, Shirahige-jinja, Ayakami-chô, 25. IV. 2004, H. Fujimoto (*LFM*). **Ehime-ken:** 1♂, Sugitate, 17. VI. 2017, Yu Hisasue; 2 unsexed, Waki-ga-fuchi Park (120–220 m in alt.), Sue-machi, Matsuyama-shi [33.87°N, 132.83°E], 4. V. 2017, Yu Hisasue (Tullgren); 1 unsexed, Mt. Ishizuchi (1400 m in alt.), Saijô-shi, 29. VI. 2014, Yu Hisasue; 1 unsexed, Minamikume-machi, Matsuyama-shi [33.8333°N, 132.8184°E], 25. IV. 2015, Yu Hisasue (Tullgren). **Kyûshû: Fukuoka-ken:** 1 unsexed, Hakozaki, Fukuoka-shi, 12. V. 1979, K. Yamagishi; 2 unsexed, 1♂, Hikosan, Biol. Lab. KU (750 m in alt.), Soeda-machi, 22. V. 2011, M. Maruyama (*LFcfF*). **Saga-ken:** 2 unsexed, Mt. Mifume, 15. V. 2019, S. Nomura; 2 unsexed, Mt. Kurokami-yama (400 m in alt.), Takeo-shi [33.2130°N, 129.9044°E], 9. V. 2021, Yu Hisasue (*LFcfF*); 4 unsexed, 1♂, Kurokami-yama, Arita-chô, 15. V. 2019, Mitsuyasu Nishida. **Nagasaki-ken:** 3 unsexed, 1♂, Tanukinoo, Masuragaharomachi, Ômura-shi, 5. V. 2018, Mitsuyasu Nishida; 1 unsexed, Todoroki Valley, 1. VI. 1987, S. Naomi; 1♂, Suwa Shine, Nagasaki-shi, 2. V. 1985, S. Nomura; 1 unsexed, Tomikawa-keikoku, Isahaya-shi, 28. IV.–1. V. 2008, T. Iwai.

Diagnosis. It is distinguished from the other species of the genus by the following combination of characteristics: body subparallel-sided; pronotum convex and strongly transverse (PW/PL, 1.54–1.68), widest near middle, sides barely protrude, posterolateral angle obtuse and posterior margin hardly sinuate; apical lobe of male aedeagus S-shaped with small lanceolate sheet-like projection; apical lobe of paramere (Fig. 24) curved ventrally and thickened apicad with four setae gathering to apex; velum emarginate at middle. This species is especially similar to *H. rufescens* and slightly resembles *H. japonica* and *H. prolongata* in habitus. However, this species is easily separated from the three species by the shape of aedeagus and dorsal characteristics: *H. rufescens* by pronotum aspect ratio (less transverse in *H. rufescens*); *H. japonica* by body size and pronotum shape (posterior margin is moderately sinuate in *H. japonica*); and *H. prolongata* by pronotum shape (more flattened and hemicircular, posterolateral angle gently acute in *H. prolongata*).

Description. Body (Fig. 5) small, slender, subparallel-sided; dorsal surface mostly moderately polished.

Head (Fig. 17) relatively large, reddish brown; frontal margin with few long setae; carina of antennal insertion simply bent; eye large. Antennae (Fig. 18) stout, as long as head and pronotum combined, reddish brown, but segments I–III and XI paler; segment I dilated, widest near apex; segment II longer than III, widened apically; segment III widened apically; segment IV–X widened apically, each apical margin fringed with small teeth and longer than wide; segments IV as long as wide; segments V–X slightly wider than long; segment XI oblong oval. Labrum (Fig. 19), apical margin weakly concave surface with 20 setae; epipharynx with 2 pairs of sensillae on anterior margin, and 3 pairs of micro setae on lateral margin. Mentum (Fig. 20) with 3 pairs of setae and 1 pair of microsetae; anterior margin shallowly concave. Prementum (Fig. 21) with many



Figures 17–20. *Homocusa ovata* sp. nov. **17** fore body **18** right antenna **19** labrum **20** mentum.

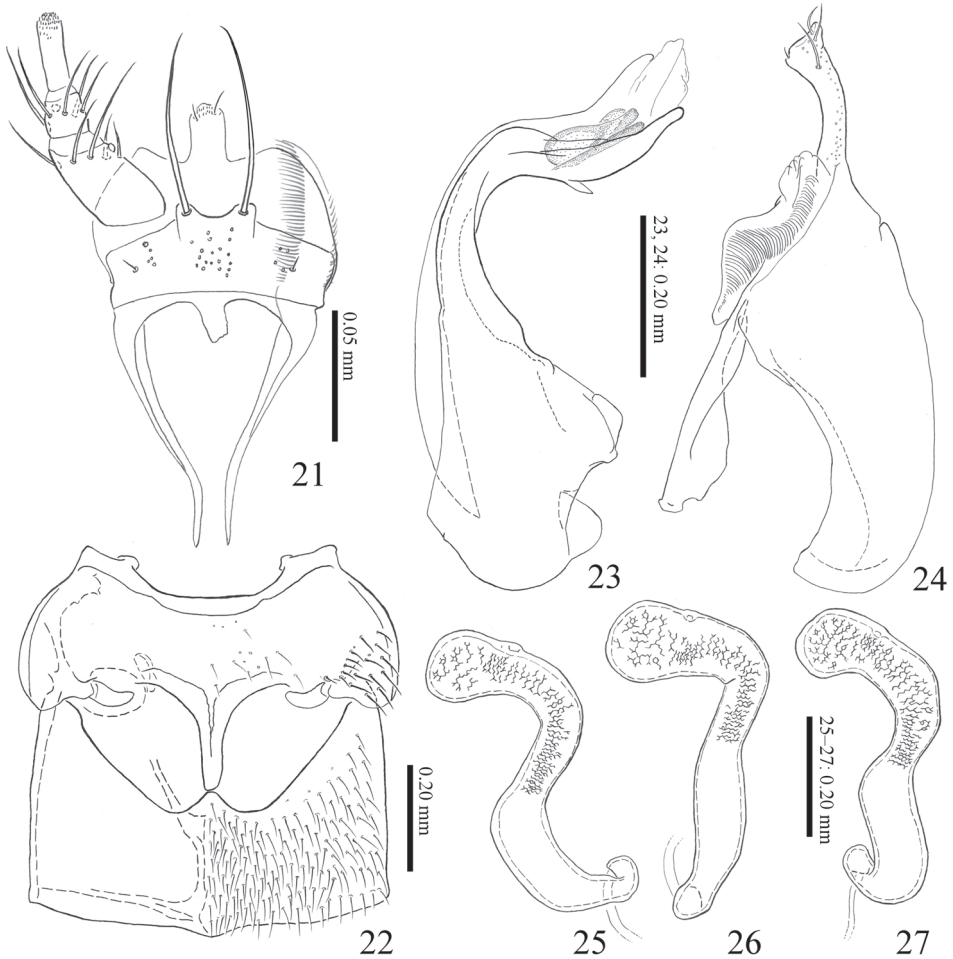
pseudopores, and with 4–5 real pores and 1 setal pore on each side near middle lateral margin. Ligula elongate, apical margin with 1 pair of spinula and several sensilla. Labial palpus (Fig. 21), segment II and III each with 5 setae.

Pronotum (Fig. 17) convex, subrectangular, strongly transverse, widest near middle, posterolateral angle obtuse, posterior margin hardly sinuate; brownish red to brownish black; surface finely covered with setae and punctures, gently polished. Elytra (Fig. 17) slightly widened posteriorly, posterior margins shallowly notched near lateral corners, brownish red; surface finely covered with setae and punctures, gently polished. Mesoventral (Fig. 22) processes narrow, with medial carina, forming Y-shaped, apex rounded; mesocoxal cavities almost separated; metaventral process gently produced.

Abdomen elongate, gently narrowed posteriad; surface sparsely covered with short setae and each posterior margin with long stout setae; gently polished and weakly reticulated.

Male: 8th sternite longer than wide, rounded apically. Median lobe of aedeagus (Fig. 23), apical lobe of male aedeagus s-shaped with small lanceolate flattened projection; apical lobe of paramere (Fig. 24) curved ventrally and thickened apicad with 4 setae gathering to apex; velum emarginated at middle; ventral margin of paramerite strongly concaved.

Female: 8th sternite longer than wide, rounded apically. Spermatheca (Figs 25–27), apical part weakly swollen; apical half with inner wall densely reticulated.



Figures 21–27. *Homoeusa ovata* sp. nov. **21** labium **22** meso-, meta-ventrite **23** median lobe of aedeagus from lateral view **24** paramere of aedeagus from lateral view **25–27** spermatheca.

Measurements. Body shape ($N = 20$): BL \approx 1.91–2.97; AL, 0.61–0.76; HW, 0.45–0.51; PL, 0.45–0.53; PW, 0.72–0.84; EL, 0.38–0.48; EW, 0.73–0.87; HTL, 0.47–0.53; PW/PL, 1.55–1.68; AL/PL, 1.26–1.68; HTL/PL, 0.93–1.12. Aspect ratio (length/width) of each antennal segment from I to XI ($N = 6$): 1.29–1.67, 1.29–1.75, 0.87–1.2, 0.72–0.82, 0.50–0.55, 0.43–0.50, 0.41–0.55, 0.33–0.61, 0.38–0.48, 0.41–0.54, 1.25–1.48.

Variation. In most individuals, the pronotum tends to be darker, but the color varies from brownish red to brownish black.

Distribution. Russia (Primorskyi krai), Korea, Japan (Hokkaido, Honshû, Shikoku, Kyûshû).

Bionomics. This species behaves almost the same as *H. rufescens*. It is also observed to feed on prey among ants and sometimes climbs on, and eats food carried by ants (Fig. 31).



Figures 28–31. Photos of alive individuals of *Homoeusa* spp. in trails of *Lasius fuliginosus* species group in field environments **28, 29** *H. rufescens*: **28** waking on a trail of *Lasius morisitai* **29** feeding on food being carried by ant workers (photographed by Taku Shimada) **30, 31** *H. ovata* sp. nov.: **30** waking on a trail of *Lasius* cf. *fuliginosus* **31** feeding on food being carried by ant workers (photographed by Kyoichi Kinomura).

Symbiotic hosts. *Lasius fuji*, *L. cf. fuliginosus*, *Lasius morisitai*, *L. nipponensis*, *L. orientalis*, *L. spathepus*.

Discussion

As Quinet and Pasteels (1996) reported, *Homoeusa acuminata* has been observed to climb on prey being carried by ants and feed on it, simultaneously hitchhiking and stealing food. This beetle has also been reported to rarely feed directly on food not yet carried by ants (Quinet and Pasteels 1995). Similar behaviors have been observed in *H. rufescens* and *H. ovata* sp. nov., such as stealing food while boarding and being ignored by the ants during the process. However, *H. rufescens* and *H. ovata* sp. nov. have also been observed feeding on food that ants are trying to carry and on prey dropped by ants. These two species may have a wider range of foraging strategies than *H. acuminata* and may also scavenge and not merely be kleptoparasitic. The optimal foraging strategy for these beetles near an ant trail may depend on the level of ant activity.

Checklist of the genus *Homoeusa* Kraatz, 1856

Palearctic

1. *Homoeusa acuminata* (Märkel, 1842): 143.*Euryusa acuminata* Märkel, 1842*Homoeusa tomentosa* Reitter, 1909: 38

Distribution. Azerbaijan, Austria, Belgium, Belarus, Croatia, Russia (Central European Territory), Czech Republic, France, Great Britain, Germany, Georgia, Greece, Hungary, Italy, The Netherlands, Poland, Romania, Slovakia, Spain, Russia (South European Territory), Switzerland, Russia (Far East).

Host. *Lasius fuliginosus*.

2. *Homoeusa chinensis* Pace, 1999: 150.

Distribution. China (Beijing).

Host. Unknown.

3. *Homoeusa japonica* Sharp, 1874: 5.

Distribution. Japan (Honshu, Shikoku, Kyushu).

Host. *L. cf. fuliginosus*, *L. morisitai*, *L. spathepus*.

4. *Homoeusa laevigata* Sharp, 1888: 283.

Distribution. Japan (Honshu).

Host. *L. nipponensis*.

5. *Homoeusa longicornis* Sharp, 1888: 283.

Distribution. Japan (Hokkaido, Honshu).

Host. *L. cf. fuliginosus*, *L. morisitai*, *L. spathepus*.

6. *Homoeusa ovata* sp. nov.

Distribution. Russia (Primorskyi krai), Korea, Japan (Hokkaido, Honshu, Shikoku, Kyushu).

Host. *L. fuji*, *L. cf. fuliginosus*, *L. morisitai*, *L. nipponensis*, *L. orientalis*, *L. spathepus*.

7. *Homoeusa prolongata* Sawada, 1970: 57.

Distribution. Japan (Hokkaido, Honshu, Shikoku, Kyushu).

Host. *L. japonicus*.

8. *Homoeusa rufescens* (Sharp, 1874): 5.

Thiasophila rufescens Sharp, 1874

Distribution. Japan (Honshu, Shikoku, Kyushu).

Host. *L. cf. fuliginosus*, *L. morisitai*, *L. nipponensis*, *L. spathepus*.

9. *Homoeusa sibirica* Rambousek, 1921: 86.

Distribution. Russia (Far East), Korea (South).

Host. Unknown.

10. *Homoeusa taiwanensis* Pace, 2010: 29.

Distribution. Taiwan (Kaohsiung).

Host. Unknown.

Nearctic

11. *Homoeusa crinitula* (Casey, 1900): 53.

Soliusa crinitula Casey, 1900

Homoeusa frosti (Casey, 1911): 53

Soliusa frosti Casey, 1911

Distribution. America (New York, Massachusetts).

Host. Unknown.

12. *Homoeusa crassicornis* (Casey, 1893): 595.

Myrmobiota crassicornis Casey, 1893

Distribution. America (Iowa).

Host. Unknown.

Acknowledgements

We would like to express our gratitude to Dr Takato Kobayashi (Yamanashi Institute of Environmental Science, Yamanashi pref., Japan), Mr Hiromichi Obata (Kanagawa pref., Japan), Dr Shuhei Nomura (NSMT), Mr Shigehisa Hori (Hokkaido Museum, Hokkaidô, Japan), Dr Fuminori Ito (Kagawa University), Mr Yasunari Kida (Marusep-

pu Insectarium, Hokkaidô, Japan), Mr Takashi Watanabe (Kanagawa pref., Japan), Mr Koji Arai [Koji Toyoda], Ms Shiho Arai (Ranzan-machi, Saitama pref.), Mr K. Izawa, Mr Hiromu Kamezawa (Saitama pref.), Mr Kyoichi Kinomura (Gifu pref.), Mr Yu Hisasue (Kyushu University, Fukuoka, Japan), and all other collectors for kindly offering the specimens. We would like to show our great appreciation Mr Taku Shimada (Tokyo pref.), K. Kinomura and Ms Mari Muto (Gifu pref.) for kindly allowing the use of photos of alive individuals in fields. MM thanks Dr Roger Booth (NHM) for making loan of the type material, Dr Victor Kuznetsov and Dr Yuri Tshistjakov (IBSS) for arranging his research permit and collecting trip around Vladivostok in 2005 and Mr Yoshiyuki Nagahata for helping him during the trip. We also greatly appreciate Dr Kazuo Ichikawa for his financial support for our research. This study was supported in part by a JSPS KAKENHI Grant Number 19H03285. Finally, we would like to express our gratitude to anonymous reviewers for their helpful comments on the manuscript.

References

- Bernhauer M, Scheerpeltz O (1926) Staphylinidae VI. (Pars 82). In: Junk W, Schenkling S (Eds) Coleopterorum Catalogus Vol.5. W. Junk, Berlin, 499–988.
- Bolton B (1995) The new general catalogue of the ants of the world. Harvard University Press, London, 504 pp.
- Boudinot BE, Borowiec ML, Prebus MM (2022) Phylogeny, evolution, and classification of the ant genus *Lasius*, the tribe Lasiini and the subfamily Formicinae (Hymenoptera: Formicidae). Systematic Entomology 47(1): 113–151. <https://doi.org/10.1111/syen.12522>
- Casey TL (1893) Coleopterological notices V. Annals of the New York Academy of Sciences 7(1): 129–606. <https://doi.org/10.1111/j.1749-6632.1893.tb55411.x>
- Casey TL (1900) Review of the American Corylophidae, Cryptophagidae, Tritomidae and Dermestidae, with Other Studies. Journal of the New York Entomological Society 8: 51–172.
- Casey TL (1911) New American species of Aleocharinae and Myllaeninae. In: Casey TL (Ed.) Memoirs on the Coleoptera II. The New Era Printing Company, Lancaster (Pennsylvania), 1–125.
- Fenyés A (1919) Coleoptera. Fam. Staphylinidae. Subfam. Aleocharinae. In: Wytzman P (Ed.) Genera Insectorum. Louis Desmet-Verteneuil, Brussels, 1–453.
- Jacquelin du Val PNC (1857) Famille Des Staphylinides. In: Manuel Entomologique. Genera des coléoptères d'Europe comprenant leur classification en familles naturelles, la description de tous les genres, des tableaux synoptiques destinés à faciliter l'étude, le catalogue de toutes les espèces, de nombreux dessins. Chez A. Deyrolle, Paris, 1–95. <https://doi.org/10.5962/t.173866>
- Kraatz G (1856) Naturgeschichte der Insekten Deutschlands. Abteilung 1. Coleoptera. Vol. 2. Staphylinii. Lief. 1–2. Nicolaische Buchhandlung, Berlin, [vii +] 376 pp.
- Kraatz G (1857) Genera Aleocharinorum illustrata. Linnaea Entomologica 11: 1–43.
- Märkel F (1842) Anfrage und Bitte. Entomologische Zeitung 3: 142–144.
- Maruyama M (2004) A permanent Slide Pinned under a Specimen. Elytra 32(2): 276.
- Maruyama M (2009) On the Myrmecophilous Genus *Losiusa* Seever, 1978 (Coleoptera, Staphylinidae, Aleocharinae). Esakia 49: 111–116. <https://doi.org/10.5109/16153>

- Maruyama M, Zerche L (2014) Japanese species of Myrmecophilous genus *Thiasophila*. *Esakia* 54: 17–25. <https://doi.org/10.5109/1516263>
- Maruyama M, Komatsu T, Kudo S, Shimada T, Kinomura K (2013) *The Guests of Japanese Ants*. Tokai University Press, Kanagawa, [xii+] 208 pp.
- Osswald J, Bachmann L, Gusarov VI (2013) Molecular phylogeny of the beetle tribe Oxypodini (Coleoptera: Staphylinidae: Aleocharinae). *Systematic Entomology* 38(3): 507–522. <https://doi.org/10.1111/syen.12011>
- Pace R (1999) Aleocharinae della Cina: Parte V (conclusione) (Coleoptera, Staphylinidae). *Revue Suisse de Zoologie* 106: 107–164. <https://doi.org/10.5962/bhl.part.80073>
- Pace R (2010) Thamaraeini, Lomechusini, Oxypodini, Hoplandriini e Aleocharini di Taiwan (Coleoptera, Staphylinidae). *Bollettino del Museo Civico di Storia Naturale di Verona* 34: 19–54.
- Quinet Y, Pasteels JM (1995) Trail following and stowaway behaviour of the myrmecophilous staphylinid beetle, *Homoeusia acuminata*, during foraging trips of its host *Lasius fuliginosus* (Hymenoptera: Formicidae). *Insectes Sociaux* 42(1): 31–44. <https://doi.org/10.1007/BF01245697>
- Quinet Y, Pasteels JM (1996) Food and reproductive strategies of the myrmecophilous staphylinid beetle *Homoeusia acuminata* (Aleocharinae) on the foraging trails of its host ant *Lasius fuliginosus* (Hymenoptera: Formicidae). *Insectes Sociaux* 43(1): 105–108. <https://doi.org/10.1007/BF01253961>
- Radchenko (2005) A review of the ants of the genus *Lasius* Fabricius, 1804, subgenus *Dendrolasius* Ruzsky, 1912 (Hymenoptera: Formicidae) from East Palaearctic. *Annales Zoologici* 55: 83–94.
- Rambousek F (1921) Vědecké výsledky Českoslov. armády v Rusku a na Sibiři. III. Novi Staphylinidi z vých. Sibiře. *Časopis Československé Společnosti Entomologické* 18: 82–87.
- Reitter E (1909) *Fauna Germanica. Die Käfer des Deutschen Reiches*, Vol. 2. K.G. Lutz, Stuttgart, 392 pp.
- Ruzsky M (1912) Mirmekologische заметки. *Uchenye Zapiski Kazanskago Vetrinarago Instituta* 29: 629–636.
- Sawada K (1970) Aleocharinae (Staphylinidae, Coleoptera) of the IBP-Station in the Shiga Heights, Central Japan, II. *Contributions from the Biological Laboratory Kyoto University* 23: 33–60.
- Schülke M, Smetana A (2015) Staphylinidae Latreille, 1802. In: Löbl I, Löbl D (Eds) *Catalogue of Palaearctic Coleoptera. Volume 2/1–2. Revised and updated edition. Hydrophiloidea Staphyloidea*. Brill, Leiden, 304–1134.
- Seevers CH (1978) A generic and tribal revision of the North American Aleocharinae (Coleoptera: Staphylinidae). *Fieldiana. Zoology* 71: 1–289.
- Sharp D (1874) I. The Staphylinidae of Japan. *Transactions of the Royal Entomological Society of London* 22(1): 1–103. <https://doi.org/10.1111/j.1365-2311.1874.tb00159.x>
- Sharp D (1888) The Staphylinidae of Japan. *Annals & Magazine of Natural History* 2(6): 277–295. <https://doi.org/10.1080/00222938809460928>
- Smetana A (2004) Subfamily Aleocharinae Fleming, 1821. In: Löbl I, Smetana A (Eds) *Catalogue of Palaearctic Coleoptera. Vol. 2. Hydrophiloidea-Histeroidea, Staphyloidea*. Apollo Books, Stenstrup, 353–494. <https://doi.org/10.1603/008.104.0301>
- Wasmann E (1901) On Some Genera of Staphylinidae, Described by Thos. L. Casey. *Canadian Entomologist* 33(9): 249–252. <https://doi.org/10.4039/Ent33249-9>

Morphology of immature stages, biology, and systematic position of the Violet seed weevil, *Orobitis cyanea* (Linnaeus, 1758) (Curculionidae, Conoderinae, Orobitiditae, Orobitidini)

Rafał Gosik¹, Peter Sprick²

1 Department of Zoology and Nature Protection, Faculty of Biology and Biotechnology, Maria Curie–Skłodowska University, Akademicka 19, 20–033 Lublin, Poland **2** Curculio–Institute e.V. (CURCI), Weckenstraße 15, 30451 Hannover, Germany

Corresponding author: Rafał Gosik (r.gosik@poczta.umcs.lublin.pl)

Academic editor: Miguel Alonso-Zarazaga | Received 23 May 2022 | Accepted 18 August 2022 | Published 12 September 2022

<https://zoobank.org/C3FEAEC9-DA17-4B29-A359-54EEB1A5FECF>

Citation: Gosik R, Sprick P (2022) Morphology of immature stages, biology, and systematic position of the Violet seed weevil, *Orobitis cyanea* (Linnaeus, 1758) (Curculionidae, Conoderinae, Orobitiditae, Orobitidini). ZooKeys 1121: 59–82. <https://doi.org/10.3897/zookeys.1121.86888>

Abstract

The mature larva of the weevil species *Orobitis cyanea* (Linnaeus, 1758), one of only two Palaearctic members of the supertribe Orobitiditae, is re-described, while the pupa is described for the first time. The biology of this species was studied at two sites in Germany. It was reared from seed capsules of *Viola canina* L. (Violaceae), and feeding holes were observed on *V. riviniana* Rchb. Adults of *Orobitis cyanea* and *O. nigrina* Reitter, 1885, specialists of *Viola*, show a well-developed escape mechanism, to which contribute a smooth surface, a rounded, nearly spherical body shape, and a seed-imitating thanatosis behaviour. The molytine weevil *Leiosoma cribrum* (Gyllenhal, 1834), the only other known weevil specialist of *Viola* in Europe, has a smooth surface, also, and is the most spherical species of the genus. The unique characters of the larva and pupa of *Orobitis cyanea* are discussed in regard to the systematic position of this taxon.

Keywords

Blacus, escape mechanism, life cycle, mimicry, parasitoid, thanatosis

Introduction

The subfamily Conoderinae Schoenherr, 1833, in the broad sense of some current classifications (Prena et al. 2014; Alonso-Zarazaga et al. 2017), is distributed worldwide and contains four supertribes: Bariditae Schoenherr, 1836; Ceutorhynchitae Gistel, 1848; Conoderitae Schoenherr, 1833 (also known as Zygopinae Lacordaire, 1865), and Orobittidae C. G. Thomson, 1859. From the total number of 7571 described Conoderinae species in 940 genera, approximately 4032 belong to Bariditae, 2164 to Conoderitae, ~ 1371 to Ceutorhynchitae, and just four to Orobittidae (Prena et al. 2014). The Violet Weevils (Orobittidae) include two genera: 1) *Parorobitis* Korotyaev, Konstantinov & O'Brien, 2000 with two Neotropical species: *P. gibbus* Korotyaev, Konstantinov & O'Brien, 2000 and *P. minuta* Korotyaev, Konstantinov & O'Brien, 2000; 2) *Orobittis* Germar, 1817 with two Palaearctic species: *O. nigrina* Reitter, 1885 and *O. cyanea* (Linnaeus, 1758) (Korotyaev et al. 2000). Orobittidae are a very uniform group, owing to the extraordinarily convex body, 1.8–3.5 mm in size, the rostrum bent at the antennal insertion, the fused meso- and metasternum, the first ventrite no longer than the second, the claws with appendages fused in an entire median process, and the unique structure of the stridulatory device (Lyal and King 1996; Korotyaev et al. 2000). The distribution of *Orobittis cyanea* includes Europe from the Arctic Circle to the Mediterranean, Siberia, central and east Asia with Asia Minor (Morris 2012; Alonso-Zarazaga et al. 2017). As *Orobittis cyanea* has limited dispersal abilities owing to its reduced or non-existent wings (Dieckmann 1972), it inhabits a wide range of natural or near-natural habitats: well-insolated deciduous woodlands and forest edges, nutrient-poor grasslands, limestone grasslands, marshes, sand dunes, and cliffs (Smreczyński 1974; Morris 2012). Interestingly, it has also been reported as a pest species in nurseries (Dieckmann 1972), but this latter observation, dating 50 or more years ago, could indicate that nurseries were then situated close to natural habitats or that plant material was exchanged between them.

To date, the systematic placement of Orobittidae has been changed many times. Van Emden (1938) accepted the status of Orobittidae (sic) in the rank of a subfamily. At the same time, taking into account the morphology of the larval stage, he drew attention to their fundamental distinctiveness from Ceutorhynchinae (originally Ceutorrhynchinae), and he noticed some similarities between Orobittidae, Apioninae, and Gonatoceri. Dieckmann (1967, 1972), Lohse (1983), and Smreczyński (1974) included Orobittidae in Ceutorhynchinae, whereas Zherikhin and Gratshev (1995) placed *Orobittis* in an enlarged concept of Barididae.

However, Alonso-Zarazaga and Lyal (1999) extracted them as a separate subfamily. Also, Korotyaev et al. (2000), based on a very detailed morphological analysis of the adult stage of Ceutorhynchinae, Zygopinae (i.e., Conoderinae sensu stricto), Baridinae, and Orobittidae, left all these groups in the rank of subfamilies, emphasising especially the distinctiveness of Orobittidae from the others. At the same time,

they noted that the final decision about their placement required further research. The treatment of Orobittidae as a separate subfamily was also upheld by Lyal (2013). In contrast, Prena et al. (2014) reduced this subfamily to supertribe rank within the subfamily Conoderinae, while still highlighting the significant differences (both in adults and in larvae) between Orobittidae and the other taxa grouped in Conoderinae sensu lato. The position of Orobittidae in the supertribe rank within Conoderinae was subsequently retained by Alonso-Zarazaga et al. (2017).

In view of the difficulty in clarifying of the taxonomic position of this widespread Palearctic species, the critical morphological differences to other Conoderinae, some important discrepancies between previously published information on the larval stage (Urban 1925; van Emden 1938), our observations concerning the biology of the Violet seed weevil, and the lack of a description of its pupa, the purpose of this contribution is to provide new morphological information on the larval stage and to describe the pupa of the taxonomically isolated genus *Orobittis*, that may be valuable to clarify its systematic position. In his excellent paper, van Emden (1938) listed only some of the features of *Orobittis* that are different from other Conoderinae.

Materials and methods

Study sites

On 3 July 2020, *Orobittis cyanea* was detected in stands of *Viola canina* L. in nutrient-poor grassland on a military training area near the village of Scheuen in the Celle district of Lower Saxony (Niedersachsen) (Fig. 1A, B). Two other *Viola* species, present at the same site and in the same habitat, were *Viola arvensis* Murr. and *Viola tricolor* L. subsp. *tricolor*. Whereas *V. arvensis* occurred mainly in small numbers, *V. tricolor* was very common at several spots there. In 2021, this site was visited once again, and the search for larvae and pupae was repeated on 19 June 2021. On 17 July 2021, the species was found in the 'Kleines Sandtal' ('Small Sand Valley') locality in the Harz National Park in the federal state of Sachsen-Anhalt, 3.6 km south-west of Ilsenburg. The specific microhabitat lays at the foot of a well-insolated south-facing slope, mainly along the border of a ditch with *Viola riviniana* Rchb. (Fig. 1C). The altitude is ~ 470 m a.s.l.

Material studied

Larvae: 10 exx. 03.07.2020, Scheuen (Celle), military training area, dry, nutrient-poor grassland on sandy soil, in *Viola canina* seed capsules (Fig. 2A).

Pupae ♀: 1 ex. 03.07.2020, 2 exx. 19.06.2021, Scheuen (Celle), military training area, dry, nutrient-poor grassland on sandy soil, in *Viola canina* seed capsules (Fig. 2B).



Figure 1. Biotopes of *Orobitis cyanea* **A, B** dry, nutrient-poor grassland on sandy soil near Scheuen **C** clearing on a well-insolated south-facing slope in the Harz National Park, 470 m a.s.l.

Methods

Before description, all the specimens were fixed in 75% ethanol and examined under an optical stereomicroscope (Olympus SZ 60 and SZ11) with calibrated oculars. The following measurements of the larva were made: body length (**BL**), body width (**BW**) (at the third thoracic segment), head capsule width (**HW**) and head capsule height (**HH**, measured from the apex to the epistoma). The pupal measurements included body length (BL), body width (BW) (at the level of the mid-legs), head width (HW) (at the level of the eyes), length of rostrum (**RL**) and width of pronotum (**PW**). Drawings and outlines were made using a drawing tube (MNR-1), installed on a stereomicroscope (Amplival), and were processed with computer software (Corel Photo-Paint X7, Corel Draw X7).

Slide preparation basically followed May (1994). The larva selected for study under the microscope was cut off and clear, next the mouth parts were separated. The

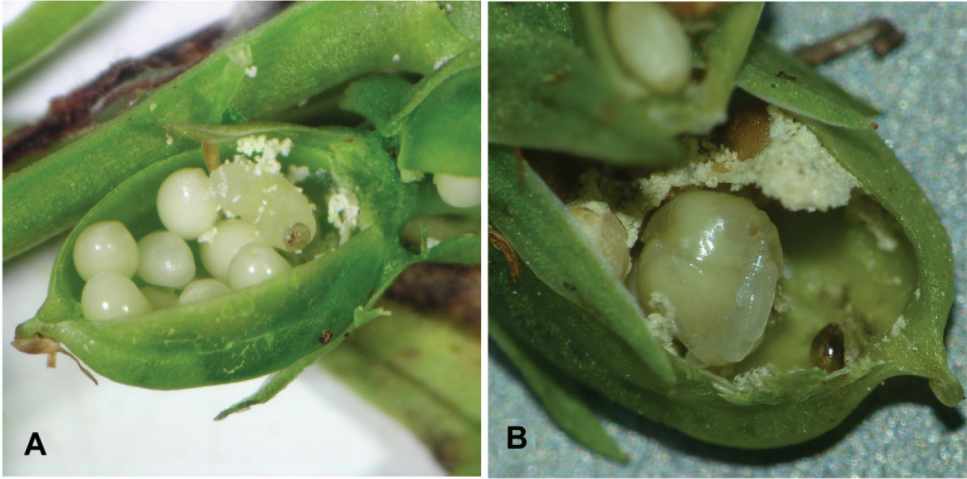


Figure 2. *Orobitis cyanea* **A** larva and seeds in a fruit of *Viola canina* **B** pupa in seed capsules of *V. canina*.

remaining part of the body was cleared in 10% potassium hydroxide (KOH), then rinsed in distilled water and dissected. Consequently, the head, mouthparts and body (thoracic and abdominal segments) were separated and mounted on permanent microscope slides in Faure–Berlese fluid (50 g gum arabic and 45 g chloral hydrate dissolved in 80 g distilled water and 60 cm³ glycerol) (Hille Ris Lambers 1950).

The photographs were taken using an Olympus BX63 microscope and processed with Olympus cellSens Dimension software. The larvae selected for SEM imaging (scanning electron microscope) were first dried in absolute ethanol (99.8%), then rinsed in acetone, treated by CPD (Critical Point Drying) and finally gold-plated. TESCAN Vega 3 SEM was used to examine selected structures.

The general terminology and chaetotaxy follow Anderson (1947), May (1994), Marvaldi (1999, 2003), and Skuhrovec et al. (2015); the terminology for the antennae follows Chaika and Tomkovich (1997). Larval instar determination and calculation of the Growth Factor (GF) are based on Willis (1964) and Gosik et al. (2019).

Results

Description of the larva of *Orobitis cyanea*

BL: 1.00–4.00; **BH:** 0.57–1.43; **HW:** 0.37–0.58 (all measurements are given in mm). The detailed results of measurements and the Growth Factor calculation are listed in Table 1.

General habitus and chaetotaxy. Live larva pure white, with yellow head capsule (Fig. 2A). All spiracles unicameral; thoracic (Fig. 3A) placed laterally between pro- and mesothorax; abdominal spiracles (Fig. 3B) placed medio-laterally on segments I–VIII. Body rather elongate, curved, rounded in cross section.

Table 1. Measurements and Growth Factor calculation in *Orobitis cyanea* larvae (measurements are given in mm, ⁿ–number of specimens; HW is relevant to GF calculation; abbreviations: BL–body length, BW–body width, HW–head width; HH–head height).

Instar	HW	HH	BL	BH	GF
1 st instar	0.37 ¹ ; 0.38 ¹	0.35 ¹ ; 0.55 ¹	1.00 ¹ ; 1.05 ¹	0.57 ¹ ; 0.60 ¹	
2 nd instar	0.46 ² ; 0.47 ¹	0.40 ² ; 0.42 ¹	3.00 ² ; 3.16 ¹	0.83 ² ; 1.00 ¹	1.23
3 rd instar (mature)	0.57 ² ; 0.58 ³	0.46 ² ; 0.50 ² ; 0.53 ¹	3.00 ¹ ; 3.66 ² ; 4.00 ²	1.00 ¹ ; 1.16 ¹ ; 1.33 ² ; 1.43 ¹	1.24

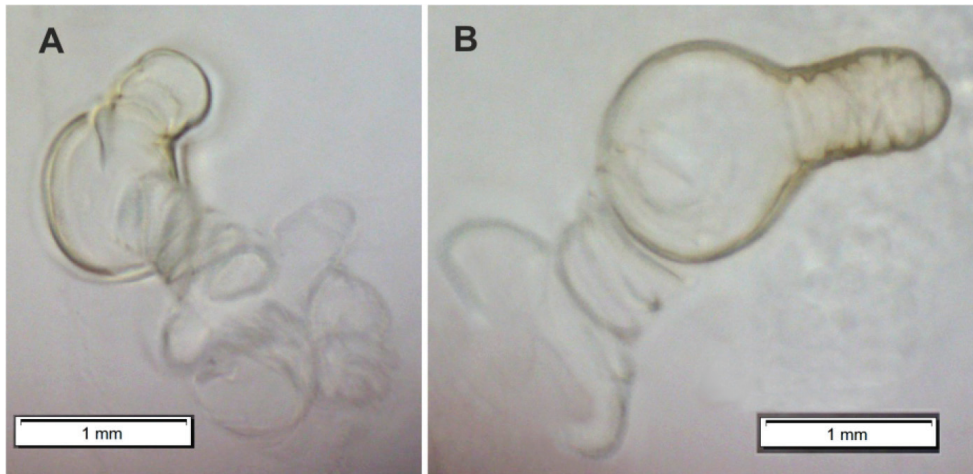


Figure 3. *Orobites cyanea* mature larva, spiracles **A** spiracle of prothorax **B** spiracle of abdominal segment I.

Head and antenna. Head capsule (Fig. 4A–C) almost rounded; endocarina reaches 4/5 of the frons; frontal sutures distinct along entire length up to antennae; stemmata (st) invisible. Hypopharyngeal bracon without median sclerome. Setae of head minute, only *des*₅ and setae on frons short, hair-like. Cranial setae: *des*₁ placed medially, *des*₂ placed posterolaterally, *des*₃ and *des*₄ placed suture on epicranium away from frontal suture, *des*₅ placed anterolaterally, *fs*₂ placed medially, *fs*₃ placed anteromedially, *fs*₅ placed anterolaterally, close to epistome, *les*₁ and *les*₂ placed close to *des*₅, postepicranial area with one *pes*. Antennae (Fig. 4D) placed on each side at anterior margin of head; membranous basal segment convex, semi-spherical, bearing conical, distinctly elongated sensorium and nine sensilla: five basiconica (sb) and three styloconica (ss).

Mouthparts. Clypeus (Fig. 5A) ~ 4.5× wider than long, with single *cls* medium in size, placed posteromedially, sensillum (*clss*) posterolaterally. Anterior margin of clypeus distinctly concave. Labrum (Fig. 5A, B) ~ 2× wider than long, anterior margin sinuated; *lrs*₁ medium, placed anteromedially, *lrs*₂ absent and *lrs*₃ medium, placed posterolaterally. Epipharynx (Fig. 5C) with two *als* and one *ams*, all semi-circular, *mes* absent. Labral rods (lr) absent as such but five sclerotisations like ribs distinct between the *ams* and *als* (Fig. 5D). Clypeus and labrum distinct, with transverse, median furrow.

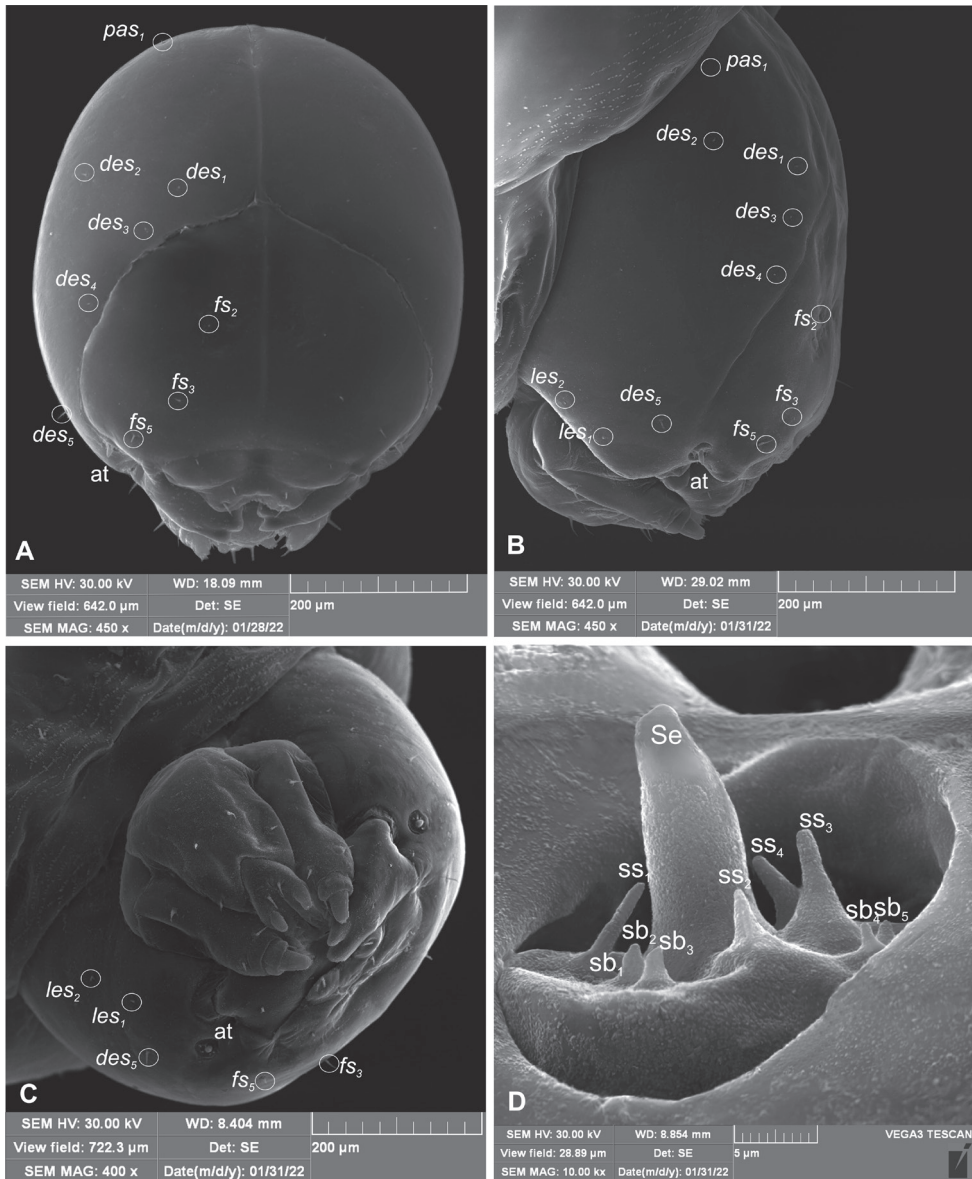


Figure 4. *Orobitis cyanea* mature larva, head and antenna (SEM micrograph) **A** frontal view **B** lateral view **C** ventral view **D** antenna. Abbreviations: at – antenna, sb – sensillum basiconicum, Se – sensorium, ss – sensillum styloconicum, setae: *des* – dorsal epicranial, *fs* – frontal, *les* – lateral epicranial, *pes* – postepicranial.

Mandible (Fig. 6) with two apical teeth of almost equal height, the inner one subapical and slightly smaller; cutting edge smooth, without additional protuberance; setae: *mds*₁ and *mds*₂ minute, both placed medially in shallow pits. Maxillolabial complex: (Figs 7A, B, 8A) stipes with a medium *stps*, two short *pf*s, and one minute *mbs* plus

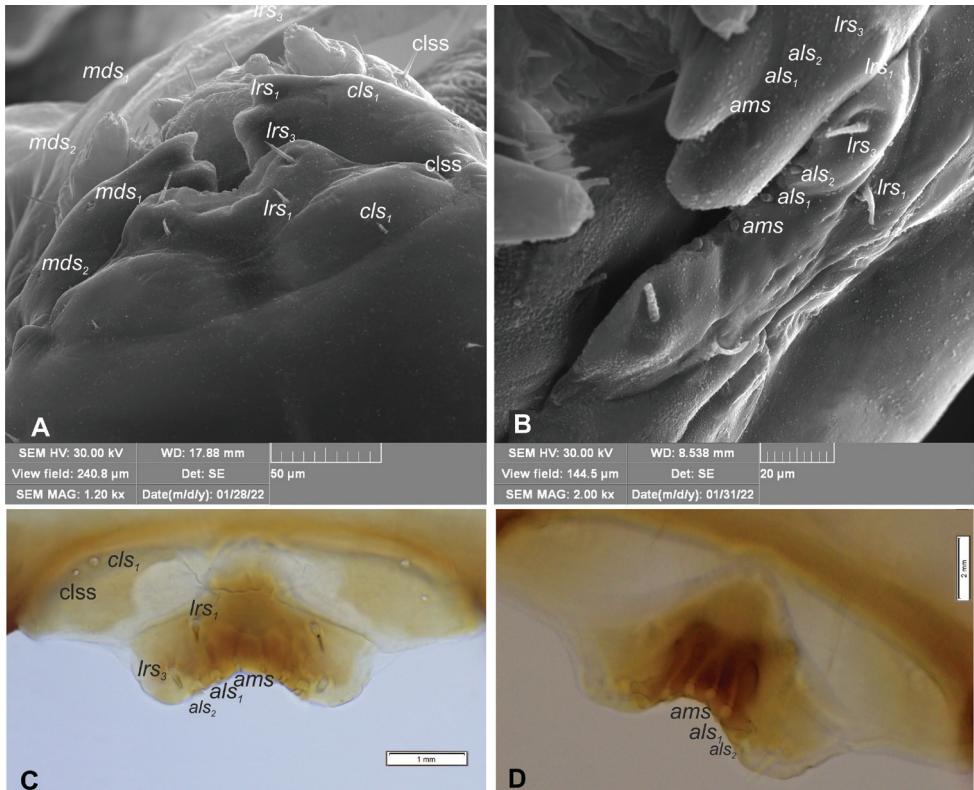


Figure 5. *Orobitis cyanea* mature larva, clypeus, labrum, epipharynx and mandible **A, B** clypeus and labrum (SEM micrographs) **C** clypeus, labrum and epipharynx **D** epipharynx with ribs. Abbreviations: cls – clypeal sensorium, setae: *ams* – anteromedial, *als* – anterolateral, *cls* – clypeal, *lrs* – labral.

sensillum; mala with row of four *dms* various in shape and size (first semi-circular, second and third elongated, pointed, fourth short, blunt) and a group of four digitate, medium *vms*; maxillary palpi bi-segmented; basal palpomere distinctly wider and shorter than distal one; length ratio of basal and distal palpomeres 2:1; basal palpomere with medium short *mps* and one pore, distal palpomere (Fig. 8B) with one digitiform sensillum (*ds*) and a group of 13 apical sensilla (ampullacea) on terminal receptive area (*tra*) (Fig. 8C); dorsal parts of mala partially covered with fine asperities; labium with cup-shaped prementum, with one medium *prms* placed medially (Fig. 7A); ligula divided, with two minute *ligs*, at margin covered with prominent asperities (Fig. 8B, E, F); premental sclerite C-shaped; postmentum rather elongate, and narrow, membranous, triangular, with two medium *pms*: *pms*₁ situated posterolaterally and *pms*₂ mediolaterally; labial palpi one-segmented; each palpus with single pore, distal palpomere with a group of 12 apical sensilla (ampullacea) on terminal receptive area (Fig. 8D); surface of labium smooth.

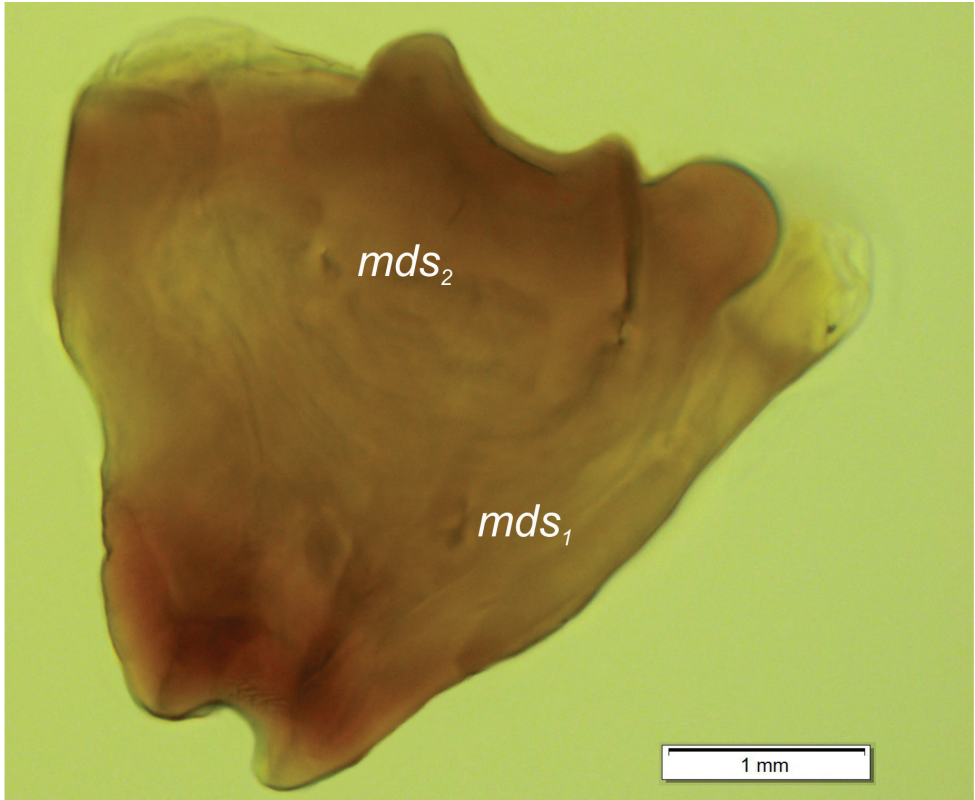


Figure 6. *Orobitis cyanea* mature larva, left mandible. Abbreviation: *mds* – mandibular setae.

Body. Prothorax small, pronotal shield not pigmented; mesothorax slightly smaller than metathorax. Meso- and metathorax each divided dorsally into two lobes (pro-dorsal and postdorsal lobes almost equal in size). Pedal lobes of thoracic segments isolated, conical, prominent. Abdominal segments I–III of similar size, slightly smaller than metathorax (Figs 9, 10A). Segments IV–IX tapering towards posterior body end. Abdominal segments I–VII each with weakly developed prodorsal fold and prominent, undivided postdorsal lobe (Figs 9, 10B). Segments VIII–IX dorsally undivided. Epipleural lobes of segments I–VII slightly conical, on segments VIII and IX almost invisible. Laterosternal and eusternal lobes of segments I–VIII conical, weakly isolated (Figs 9, 10C). Abdominal segment X divided into three lobes, dorsal small, lateral lobes prominent, of almost equal size. Anus situated terminally. Body cuticle with asperities forming rows and circles (Fig. 9D). Lateral part of prothorax densely covered with thorn-like asperities, arranged in vertical rows (Fig. 9E, F).

Chaetotaxy: distinctly reduced, most setae minute, thorn-like, only on dorsal part of abdominal segment IX very short, hair-like. Thorax (Fig. 9A): prothorax with seven equal in size *prns*, two *ps*, and one *eus*. Meso- and metathorax each with one *prns* and one

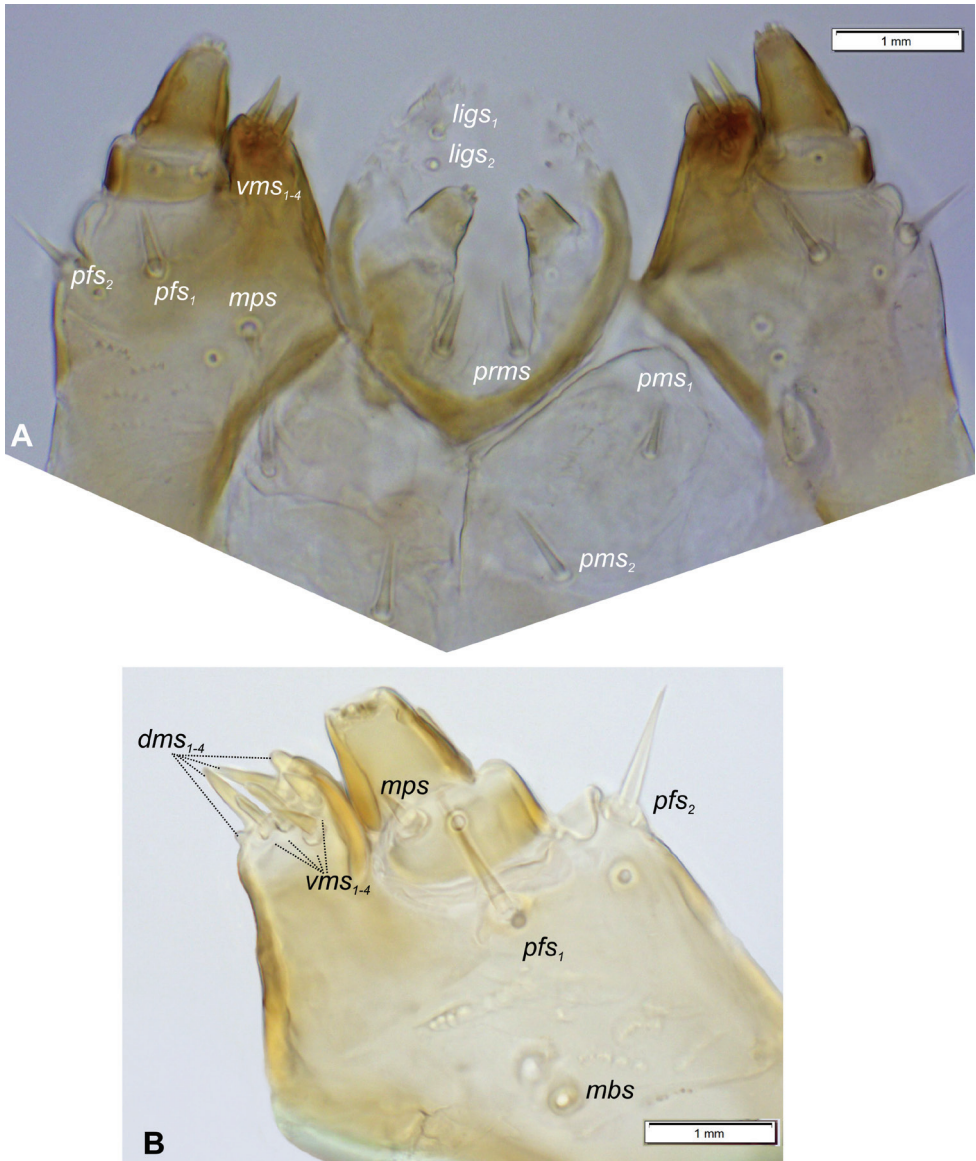


Figure 7. *Orobitis cyanea* mature larva, maxillolabial complex and apical part of maxilla **A** maxillolabial complex, ventral aspect **B** apical part of left maxilla, photo. Abbreviations: setae: *dms* – dorsal malar, *lig*s – ligular, *mbs* – malar basiventral, *mps* – maxillary palp, *pfs* – palpiferal, *prms* – prelabial, *pms* – postlabial, *stps* – stipal, *vms* – ventral malar.

pds, two *ss*, one *eps*, one *ps* and one *eus*. Pedal areas of thoracic segments each with three *pda*. Abdomen (Fig. 9B, C): segments I–VI with one *prs*, one *pds*, one *ss*, one *eps*, one *lts*, and one *eus*. Abdominal segments VII and VIII with one *pds*, one *ss*, one *eps*, one *lts*, and two *eus*. Abdominal segment IX with two *ds*, two *ps*, and two *sts*. Abdominal segment X without setae.

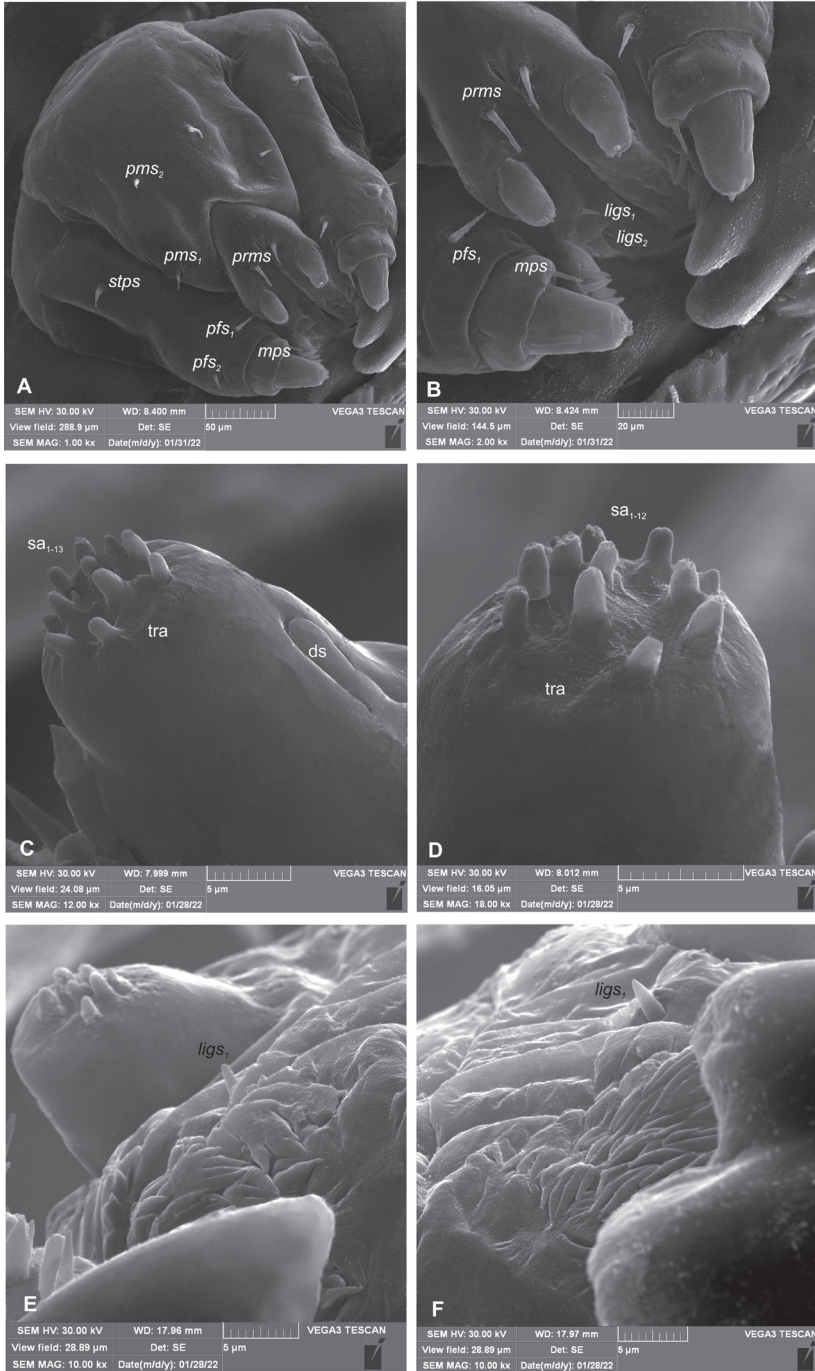


Figure 8. *Orobitis cyanea* mature larva, maxillolabial complex (SEM micrographs) **A** maxillolabial complex, ventral aspect **B** prementum, ventral aspect **C** apical part of distal maxillary palp **D** apical part of labial palpomere **E, F** surface of ligulae. Abbreviations: ds—digitiform sensillum, sa – sensillum ampullaceum, tra – terminal receptive area, setae: *dms* – dorsal malar, *ligs* – ligular, *mbs* – malar basiventral, *mps* – maxillary palp, *pfs* – palpiferal, *prms* – prelabial, *pms* – postlabial, *stps* – stipal, *vms* – ventral malar.

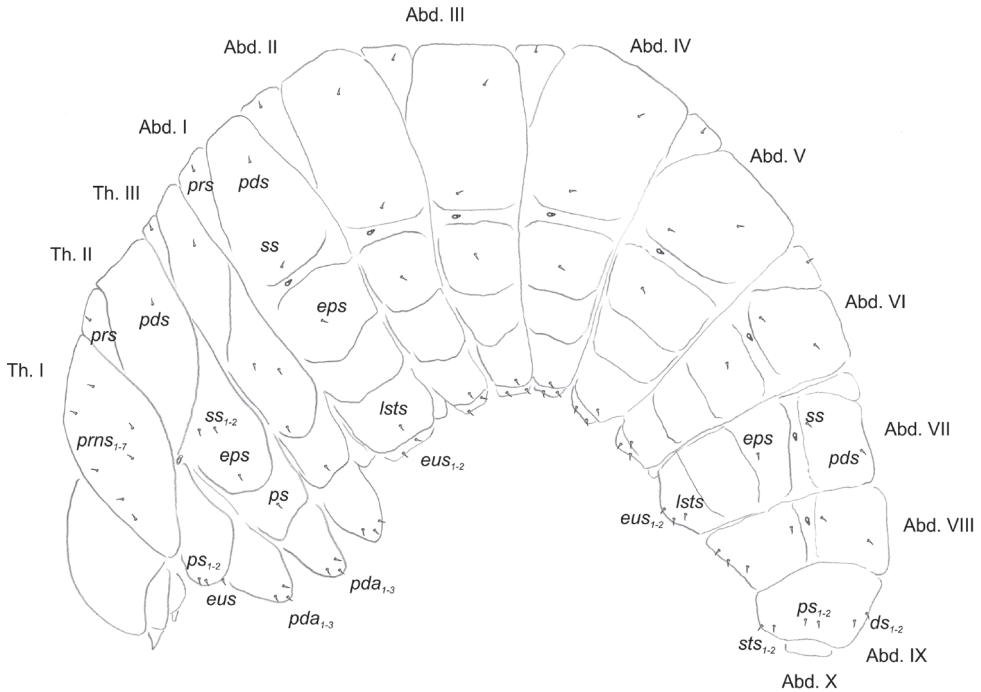


Figure 9. *Orobitis cyanea* mature larva, lateral view, habitus and chaetotaxy. Abbreviations: Th. I–III—thoracic segments 1–3, Abd. I–X—abdominal segments 1–10, setae: *ds*—dorsal *eps*—epipleural, *eus*—euster nal, *ps*—pleural, *pda*—pedal, *pds*—postdorsal, *prns*—pronotal, *prs*—prodorsal, *ss*—spiracular, *sts*—sternal.

Description of the pupa of *Orobitis cyanea*

Female: BL: 2.00¹; 2.16¹; 2.20¹; BW: 2.16¹; 2.33¹; HW: 0.55¹; 0.57²; RL: 1.00¹; 1.05¹; 1.10¹; PW: 1.23¹; 1.30¹ (one pupa partially deformed). ⁿ—number of specimens.

General habitus and chaetotaxy. Body white, compact, almost round in outline (Figs 2B, 11A, B), partially (femora and tarsi) covered with fine asperities, rest of body smooth (Fig. 11C–E). Rostrum elongate, almost 4× as long as wide, reaching metacoxae. Pronotum trapezoidal, 2× wider than long. Mesonotum wider than metanotum, with prominent triangular scutellar shield. Abdominal segments I–V of equal length, segments VI–VIII tapering gradually towards end of body, segment IX terminal. Gonotheca in female divided. Urogomphi (posterior processes) absent. Spiracles placed laterally on abdominal segments I–VI, functional on segments I–V, vestigial on segment VI. Chaetotaxy completely reduced, invisible even under the highest magnification.

Biological observations on host plants, life cycle, and antagonists of *Orobitis cyanea*

A search for immature stages at the site near Scheuen yielded several larvae and a few pupae on 19 June 2020 and 3 July 2021. They were found only in seed capsules of *Viola canina* (Fig. 12A). The examination of more than 20 capsules of *V. tricolor* did

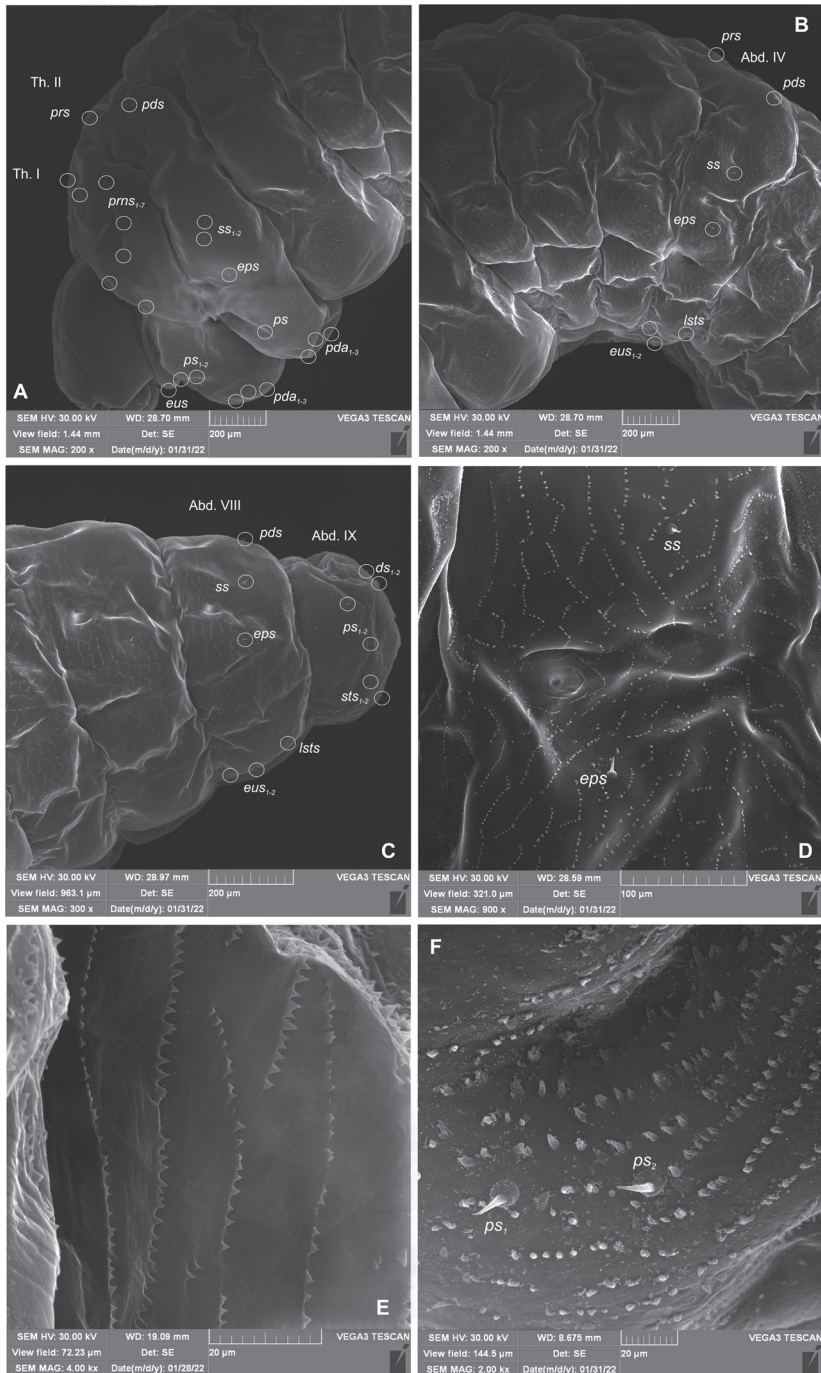


Figure 10. *Orobitis cyanea* mature larva, habitus and cuticle (SEM micrographs) **A** lateral view of head and thorax **B** lateral view of abdominal segments I–V **C** lateral view of abdominal segments VII–IX **D** lateral view of abdominal segment V (magnification) **E** structure of cuticle of dorsolateral part of prodorsum **F** structure of cuticle of ventrolateral part of prodorsum. Abbreviations: setae: *ds*–dorsal *eps*–epipleural, *eus*–eusternal, *ps*–pleural, *pda*–pedal, *pds*–postdorsal, *prms*–pronotal, *prs*–prodorsal, *ss*–spiracular, *sts*–sternal.

not reveal a single immature specimen or any feeding traces similar to those seen on *V. canina* leaves (Fig. 12B). Likewise, we did not obtain any larva or pupa at the Harz Mountains site on 17 July, but from the numerous feeding traces on the leaves and seed capsules and from the emergence holes in the capsules, the conclusion was drawn that development must have taken place in *V. riviniana* seed capsules, too (Fig. 13A, B).

In April and May, overwintering adults make small feeding holes in the leaves of their host plants, eating for maturation. At dry sites with early-flowering *Viola* species, such as *V. canina* L. or *V. hirta* L., eggs are laid mainly in April and May in the immature ovaries of the flowers. Larvae feed from young seeds, generating sufficient room to develop into the pupal stage at their feeding sites. Pupation occurred at both study sites inside the seed capsules in June and the first half of July. Adults left the seed capsules actively through feeding holes, or at the latest in July, by which time the seeds had ripened and the seed capsules burst open. Even in the Harz Mountains, the new generation had totally abandoned its place of development at the well-insolated site by mid-July, and some individuals were now occurring on their host plants; at that time, many adult weevils were present only in less exposed places. There were many feeding traces and adult weevils on the plants, but there were no more larvae or pupae inside the seed capsules. These were either still closed along the shady trench or had burst open on the sun-exposed slope.

Discussion

Comments and inferences regarding the host plants, biology and parasitoids of *Orobitis cyanea*

Our observations regarding the feeding and development of *Orobitis cyanea* on *Viola riviniana* seed capsules are in accordance with those of Scherf (1964), who listed the following *Viola* species as host plants of this weevil: *V. canina*, *V. epipsila* Ledeb., *V. odorata* L., *V. palustris* L., *V. reichenbachiana* Jord. ex Bor. (as *V. silvatica* Fr. ex Hartm.) and *V. riviniana*. In addition, Urban (1925) listed *Viola canina* (once under this name and once as *V. stricta* Hornem.), *V. odorata*, *V. palustris*, *V. pumila* Chaix (as *V. pratensis* Mert. & Koch), and *V. reichenbachiana* Jord. ex Bor. (as *V. silvestris* auct.). The only species to add from our own observations is *V. hirta* L., from which *O. cyanea* was swept on one occasion in Luxembourg. But as this was only a singular finding without observation of feeding traces, the host plant status of *V. hirta* for *O. cyanea* has still to be confirmed. All these *Viola* species are violet in colour, and none are pansy species like *V. arvensis*, *V. tricolor* or *V. × wittrockiana* Gams ex Neuenb. & Buttl., which are also members of the genus *Viola*. Dieckmann (1972) described the development of *O. cyanea* in seed capsules, but he did not list any particular *Viola* species. His statement that *O. cyanea* was found to be a pest on pansy species has therefore to be regarded as doubtful. According to our observations, *O. cyanea* is related to natural habitats, but Morris (2012) reported it also from cultivated areas like pastures and gardens.

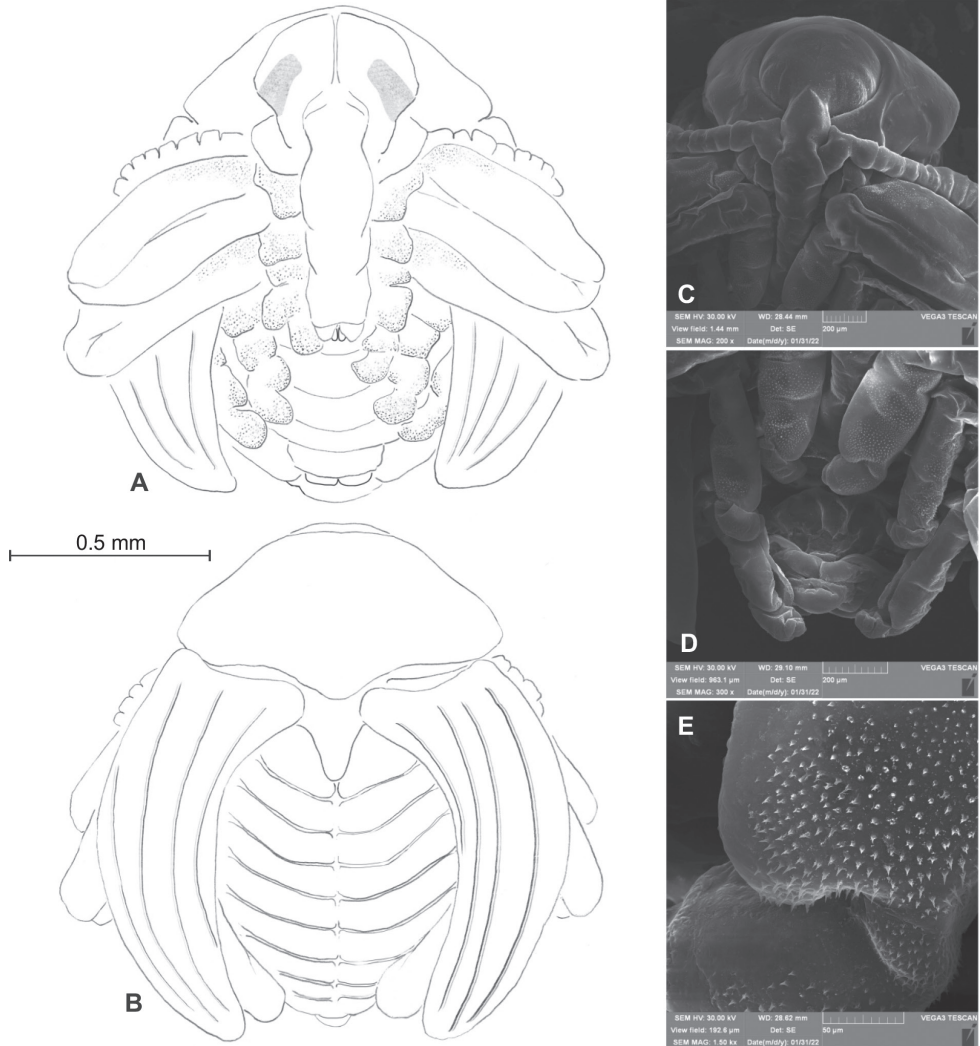


Figure 11. *Orobitis cyanea* pupa, habitus and structure of cuticle **A** ventral view **B** dorsal view, scheme **C** head and rostrum, frontal view **D** abdomen, ventral view **E** tarsi of first pairs of fore legs, magnification (SEM micrographs).

On the other hand, we confirm the information given by Dieckmann (1972) regarding the phenology and pupation of *Orobitis cyanea* in a cocoon, in the immediate vicinity of the feeding place or directly there. Our observations are contrary to those of Urban (1925), who reported a late start of development in the season, and violet seed capsules with larvae, pupae, fresh and fully coloured adults of *O. cyanea* that were studied in September. As Urban (1925) did not supply any data on either site or host plants, it can only be assumed that he studied the development of this weevil in moist, shady or cool sites with late-flowering host plant species, such as *Viola epipsila*



Figure 12. *Viola canina* **A** flowering host plant **B** host plant with some feeding holes after flowering.

or *V. palustris*. There, the first adults of the new generation should occur considerably later, in July and August, and the latest adults may hibernate at the pupation sites inside the capsules. Obviously, the activity of this oligophagous weevil is closely linked to plant development and may even differ from one locality to another as a result of microclimatic differences, as observed at the study site in the Harz Mts.

Some specimens of a parasitoid wasp, *Blacus* sp. (Fig. 14), were found in the samples of seed capsules containing *Orobitis cyanea* larvae from Scheuen, taken to the laboratory for rearing. Wasps of the genus *Blacus* Nees, 1818 (Blacini, Braconidae) are common parasitoids of weevil larvae and are frequently reported from weevil genera like *Scolytus*, *Stereonychus*, *Gymnetron* and *Barynotus* (Belokobylskii 1995; Farahani and Talebi 2013).

Larval instar determination and Growth Factor calculation

The method of larval instar determination worked out by Dyar (1890) has been widely accepted (Leibee et al. 1980; Rowe and Kok 1985). It was ultimately popularised under the name of Growth Factor (GF) (Sprick and Gosik 2014; Gosik et al. 2019), which is in fact Dyar's ratio⁻¹, which bears a closer relationship with natural development. The results of measurements and the Growth Factor calculation indicates three larval instars in *Orobitis cyanea* (Table 1) and GF values of 1.23 and 1.24 from the first to the second, and from the second to the third instar, respectively.

The number of larval instars in weevils is correlated primarily with the body size of a species. Thus, small species (head width of the mature larva below ~ 0.65 mm) usually have only three larval instars (Dosdall et al. 2007; Gosik et al. 2020; Skuhrovec et al. 2022), whereas larger species can have up to seven instars (Skuhrovec et al. 2022).

In some previously studied Entiminae species, GF usually varied between 1.38 and 1.44 (Leibee et al. 1980; Sprick et al. 2022). There is only one GF value each for a Ceutorhynchinae and Lixinae species: in *Ceutorhynchus subpubescens* LeConte, 1876 it

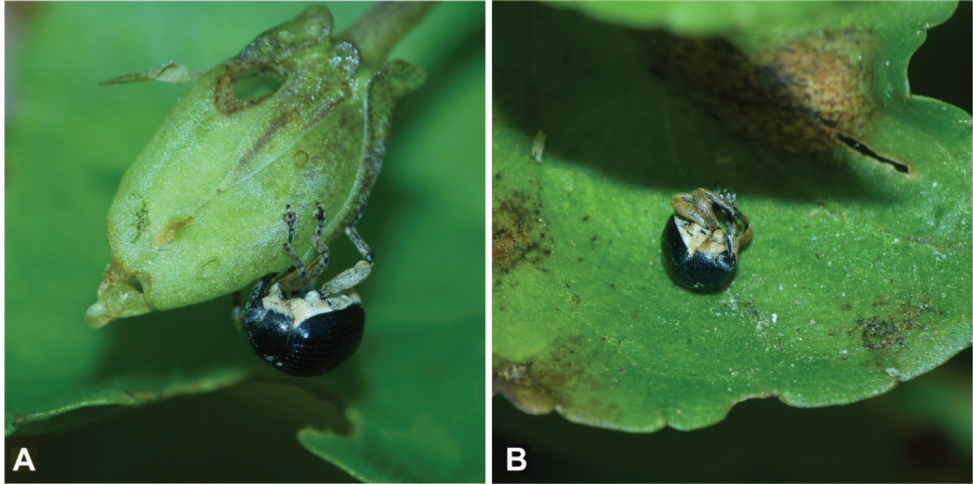


Figure 13. *Orobitis cyanea* on *Viola riviniana* **A** adult on seed capsule with feeding traces and emergence hole **B** adult exhibiting thanatosis.

was calculated at 1.43 (Dosdall et al. 2007) and in *Rhinocyllus conicus* (Frölich, 1792) at 1.538 (Rowe and Kok 1985). In the case of *Orobitis cyanea*, the significantly low GF value is probably correlated with the relatively big size of the first larval instar. There is usually only one larva per seed capsule (Urban 1925). Taking into consideration the limited dispersion capability and the close host plant affinities of *O. cyanea*, females invest more in the size than in the number of eggs.

Morphological adaptations and behaviour

When disturbed, *Orobitis cyanea* shows death-feigning or thanatosis behaviour and appears to imitate a *Viola* seed, which may be a form of mimicry: the dark part of the weevil may imitate the main part of the seed, the light part the elaiosome (Morris 2012; Kutzelnigg 2013). Thanatosis, the spherical shape and the colouring prove to be effective components of a shelter mechanism when escaping from danger, as they allow rapid down-rolling and concealment in vegetation or leaf litter below the plants, possibly among seeds or dark soil particles at the same time (Fig. 13B), especially as the smooth leaves of most *Viola* species support this escape mechanism. In addition, the behavioural data relating to *Orobitis cyanea* are presumably applicable to the closely related *O. nigrina* Reitter, 1885, which lives on *Viola biflora* L. in the Alps (Penecke 1922). Escape mechanisms similar to those described here for *Orobitis* species from *Viola* are widespread in weevils or even other beetles. Apparently, they have developed independently many times.

It seems worth mentioning that the only other European *Viola*-inhabiting weevil specialist, *Leiosoma cribrum* (Molytinae), occupies the top position in spherical body shape among all available *Leiosoma* species, where this could be tested (Table 2). In 21

of ~ 44 *Leiosoma* species, available as adult specimen or as habitus photo from different sources, e.g., Pedroni (2010, 2012) or Bahr (2021), we determined the length-width ratio of the body to demonstrate the degree of spherical body shape (Table 2).

Leiosoma cribrum is the most rounded, shortest, and smallest species of this genus, approximating mostly the nearly perfect spherical shape of both *Orobitis* species. All other *Leiosoma* species are more elongate, closest are *L. reitteri* Bedel, 1884, *L. apionides* (Wollaston, 1864) (both ~ 1.88:1), and *L. deflexum* (Panzer, 1795) (1.91:1). The bulk of the species ranges between ~ 2.00:1 in *L. diottii* Pedroni, 2018, *L. osellai* Diotti & Caldara, 2020, and *L. senex* Pedroni, 2018, and 2.42 – 2.43:1 in *L. hemicum* Pedroni, 2012 and *L. komovicum* Pedroni, 2018.

Even if only for a small part of *Leiosoma* species the host plant species are known (Sprick and Krämer-Klement, in press), it is noticeable that there should be some selection pressure to weevil specialists that live on *Viola* species, which are unable to fly, to improve the escape mechanisms by falling down, rolling away or imitate biotic or abiotic structures of the environment in which they live, e.g., seed in *Orobitis*, or soil or underground in *Leiosoma*. Night activity of *Leiosoma* species may be another behavioural adaptation to reduce the possible loss of adult weevils by unspecific predators.

The taxonomic placement of Orobitidae - based on morphological studies of immature stages

In his comprehensive work, van Emden (1938) omitted several notable features that are probably almost impossible to notice in first-instar larvae, especially if only a light microscope is available. Above all, these are the deeply divided ligula, the T-shaped anus, the extreme reduction in head bristle size, the lack of stemmata, and the clypeus divided by a transverse furrow.

The larva of *Orobitis cyanea* is easily recognised by the following features: 1) post-dorsal folds of abdominal segments I–VII undivided; 2) abdominal segments VIII and IX without prodorsal folds; 3) anus T-shaped, with dorsal and lateral lobes; 4) body cuticle with asperities forming rows and circles; 5) all spiracles unicameral; 6) epicranial

Table 2. Comparison of length-width ratio of the body of *Viola*-inhabiting species (A) and from species with other or unknown host plants (B). Measured from the front margin of the eyes to the apex of elytra and at the widest part of the elytra. *Groups defined by Pedroni (2010, 2012, 2018).

Host	Species/Species group*	Ratio	Data source
A	<i>Orobitis cyanea</i>	1.51:1	own data
	<i>O. nigrina</i>	1.58:1	own data
	<i>Leiosoma cribrum</i>	1.72:1	own data
B	<i>Leiosoma cribrum</i> group (five further species)	1.99:1 – 2.24:1	Pedroni (2018) Bahr (2021)
	<i>Leiosoma oblongulum</i> group (four species)	2.00:1 – 2.16:1	Pedroni (2010), Diotti and Caldara (2017, 2020); own data
	<i>Leiosoma scrobiferum</i> group (six species)	2.22:1 – 2.43:1	Pedroni (2012)
	Species from undefined species groups: <i>L. apionides</i> , <i>L. bosnicum</i> , <i>L. deflexum</i> , <i>L. kirschii</i> , <i>L. reitteri</i>	1.88:1 – 2.28:1	Stüben (2011), Sabaljev (2013), Pedroni (2016), own data (coll. J. Messutat, coll. M. Stern)

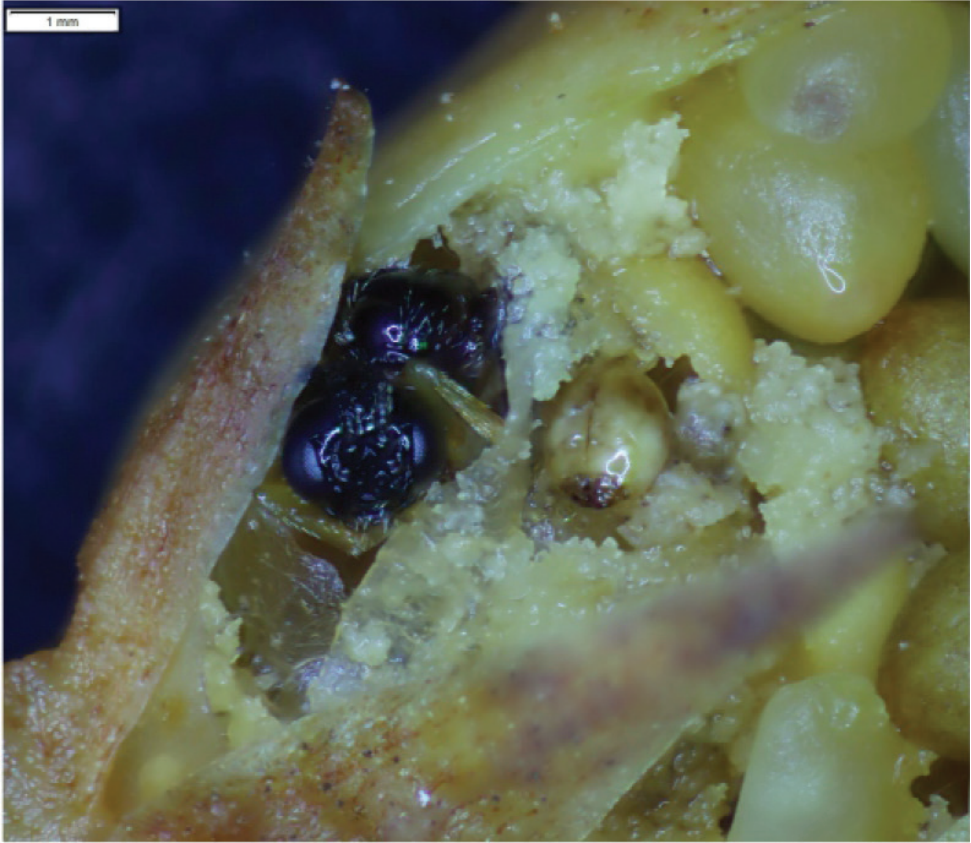


Figure 14. *Orobitis cyanea* larva and the parasitoid wasp.

setae minute; 7) stemmata absent; 8) extremely elongate endocarina, almost reaching the epistome; 9) antennal sensorium elongate; 10) clypeus with prominent median depression and curved to inside anterior margin; 11) labrum extremely narrow with anterior margin deeply rounded inwards (concave); 12) clypeus with only one pair of *cls*; 13) labrum with two pairs of *lrm*; 14) labrum with one pair of *ams*, two pairs of *als* but no *mes*; 15) labral rods absent but presence of multiple rib like sclerotisations; 16) post-labium with two pairs of *pms*; 17) labial palpi uni-segmented; and 18) ligula divided.

Knowledge of the immatures of the various Conoderinae supertribes is uneven. This is mainly because the supertribes of this subfamily differ in species numbers, distribution, individual abundance and economic importance. Bariditae and Ceutorhynchitae have been relatively well studied (Scherf 1964; Pakaluk 1993, 1994; Prena et al. 2014). Conoderitae, on the other hand, have a rather small number of species with the preimaginal stages described (Gosik et al. 2021). Nevertheless, the available material is sufficient to discover the characteristics of each group. Since the larva of *Orobitis cyanea* is the only one in the genus *Orobitis* described so far and there are only two genera in the entire supertribe Oorbitiditae, the above-mentioned features can be considered diagnostic of this suprageneric taxon, although it may change with further studies.

Finding features common to all known larvae that would be diagnostic of Conoderinae sensu lato is not possible. Some larval characteristics present in all the supertribes belonging to this subfamily are in fact common to the family Curculionidae (May 1994), and then cannot be diagnostic of such a subfamily, such as 1) the numbers of *des* and *les*; 2) the numbers of some thoracic setae, i.e., two *ps*, one *eus*, one *prs*, one *eps*, one *ps*; 3) the numbers of some abdominal setae: one *lsts*, two *eus*, two *ds*, two *sts*, two *ps*; and 4) the numbers of mandibular and maxillary setae. Even though larvae from the subfamily Conoderinae Schoenherr, 1833 constitute a group that is morphologically very diverse, it is still possible to find larval features common to all of them, so long as Orobittidae are excluded. But again, these common features are typical of the family Curculionidae: 1) abdominal segments I–VII with well-separated prodorsal folds and always divided postdorsal folds; 2) anal lobes divided into four X-shaped lobes; 3) thoracic and abdominal spiracles bicameral; 4) epicranial setae elongate; 5) endocarina absent or extending to mid-length of frons; 6) ocelli present; 7) antennal sensorium short, conical; 8) clypeus trapezium-shaped with two pairs of *cls*; 9) labrum semi-circular with rounded or slightly sinuate anterior margin, always with three pairs of *lrs*; 10) labral rods elongate, well visible; 11) labrum with three pairs of *ams*, three pairs of *als* and two *mes*; 12) labial palpi bi-segmented; 13) postlabium with three pairs of *lrm*; and 14) premental sclerite tridentate, with elongate posterior extension.

In addition, the GF measurements indicate that there are three larval stages in *Orobittis cyanea*, as in Ceutorhynchitae (Scherf 1964; Dossdal et al. 2007), but not in Conoderitae (5 instars) (Gosik et al. 2021).

The features given by Prena et al. (2014) as characteristic of Conoderinae pupae are very general and are widespread in other weevil subfamilies, also. Among those mentioned by these authors, there is not a single feature unique to Conoderinae. Moreover, many of the cited features are additionally annotated “present or absent”.

In the pupae, the differences between Orobittidae and other Conoderinae are more clearly visible: setae on head, rostrum, pronotum and abdomen always clearly visible vs no setae entirely; pupal urogomphi, which are more or less developed or reduced in Conoderinae, are completely absent in Orobittidae.

In general, endophagous larvae have significantly shorter segmental setae than exophagous larvae (Gosik et al. 2016). However, in the case of the head bristles, the difference between the two groups is not so obvious. On the other hand, one of the characteristics of *Orobittis cyanea* larvae is the complete absence of long and medium-length setae on both body and head. The longest bristles are considered at best to be microsetae. The others are almost indistinguishable from cuticular asperities.

It is worth noting that a structure similar to “ligula with depression in middle” has been described as characteristic of the larva of only one species of Baridini, namely *Aulacobaris johanni* (Korotyaev, 1988) (Nikulina 2013). However, it is difficult to draw any further conclusions about the relationship between these species from this feature.

Both larva and pupa of *Orobittis cyanea* display many diagnostic features and at the same time differences from other Conoderinae species that it is difficult to find arguments supporting the current systematic position of this species. We consider,

therefore, that there is ample justification for retaining *Orobitiditae* as a separate subfamily (as suggested by Korotyaev et al. 2000).

The study of immatures of the two Neotropical *Orobitiditae* species could well provide new data, but at this stage, the placement of *Orobitiditae* within an enlarged concept of *Conoderinae* is not supported. Finding features unique to immatures of *Orobitis* is rather easy, but associating them with any other *Curculionidae* group is problematic. Therefore, leaving *Orobitiditae* as the subfamily *Orobitidinae*, as suggested by Alonso-Zarazaga and Lyal (1999) and Korotyaev et al. (2000), is best supported by our results.

Acknowledgements

We thank Andreas Marten for his assistance with the fieldwork, Marek Wanat and Michael Morris for their help with the literature queries. We would like to express our cordial thanks to Werner Ulrich for his help in identifying the parasitoid. We are indebted to Peter Senn for the linguistic editing of the text.

References

- Alonso-Zarazaga MA, Lyal CHC (1999) A world catalogue of families and genera of Curculionoidea (Insecta: Coleoptera) (excepting Scolytidae and Platypodidae). *Entomopraxis*, SCP, Barcelona, 315 pp.
- Alonso-Zarazaga MA, Barrios H, Borovec R, Bouchard P, Caldara R, Colonnelli E, Gültekin L, Hlaváč P, Korotyaev B, Lyal CHC, Machado A, Meregalli M, Pierotti H, Ren L, Sánchez-Ruiz M, Sforzi A, Silfverberg H, Skuhrovec J, Trýzna M, Velázquez de Castro AJ, Yunakov NN (2017) Cooperative Catalogue of Palaearctic Coleoptera. Curculionoidea. Sociedad Entomológica Aragonesa, Monografías electrónicas SEA, 8, November 10: 2017, 729 pp. www.sea-entomologia.org
- Anderson WH (1947) A terminology for the anatomical characters useful in the taxonomy of weevil larvae. *Proceedings of the Entomological Society of Washington* 49: 123–132.
- Bahr F (2021) Fotokatalog ausgewählter Rüsselkäfer der paläarktischen Region. / Le Charançon No. 5. www.curci.de [accessed on 26 April 2022]
- Belokobylskii SA (1995) New and rare species of the genus *Blacus* (Hymenoptera: Braconidae) from the Russian Far East. *European Journal of Entomology* 92: 449–467.
- Chaika SYu, Tomkovich KP (1997) Sensory organs of weevils (Coleoptera, Curculionidae). *Entomological Review* 4: 486–496.
- Dieckmann L (1967) Zur Gattung *Orobitis* Germar. *Entomologische Blätter* 63: 50–54.
- Dieckmann L (1972) Beiträge zur Insektenfauna der DDR: Coleoptera – Curculionidae: Ceutorhynchinae. *Beiträge zur Entomologie* 22: 3–128.
- Diotti L, Caldara R (2017) *Leiosoma matesiense* n. sp. dei Monti del Matese (Coleoptera, Curculionidae, Molytinae). *Giornale Italiano di Entomologia* 14(62): 647–650.

- Diotti L, Caldara R (2020) *Leiosoma osellai* n. sp. dei Monti del Cilento (Coleoptera, Curculionidae, Molytinae). *Giornale Italiano di Entomologia* 15(64): 711–714.
- Dosdall LM, Ulmer BJ, Bouchard P (2007) Life History, Larval Morphology, and Nearctic Distribution of *Ceutorhynchus subpubescens* (Coleoptera: Curculionidae). *Annals of the Entomological Society of America* 2(2): 178–186. [https://doi.org/10.1603/0013-8746\(2007\)100\[178:LHLMAN\]2.0.CO;2](https://doi.org/10.1603/0013-8746(2007)100[178:LHLMAN]2.0.CO;2)
- Dyar HG (1890) The number of molts of lepidopterous larvae. *Psyche* (Cambridge, Massachusetts) 5(175–176): 420–422. <https://doi.org/10.1155/1890/23871>
- Farahani S, Talebi AA (2013) A study of the genus *Blacus* Nees (Hymenoptera: Braconidae: Blacinae) in Iran with three new records. *Ukrainska Entomofaunistyka* 4: 3–11.
- Gosik R, Sprick P, Skuhrovec J, Derús M, Hommes M (2016) Morphology and identification of the mature larvae of several species of the genus *Otiiorhynchus* (Coleoptera, Curculionidae, Entiminae) from Central Europe with an update of the life history traits. *Zootaxa* 4108(1): 1–67. <https://doi.org/10.11646/zootaxa.4108.1.1>
- Gosik R, Sprick P, Morris MG (2019) Descriptions of immature stages of four species of the genera *Graptus*, *Peritelus*, *Philopedon*, and *Tanymecus* and larval instar determination in *Tanymecus* (Coleoptera, Curculionidae, Entiminae). *ZooKeys* 813: 111–150. <https://doi.org/10.3897/zookeys.813.30336>
- Gosik R, Skuhrovec J, Caldara R, Toševski I (2020) Immature stages of Palearctic *Mecinus* species (Coleoptera, Curculionidae, Curculioninae): Morphological characters diagnostic at genus and species levels. *ZooKeys* 939: 87–165. <https://doi.org/10.3897/zookeys.939.50612>
- Gosik R, Wanat M, Bidas M (2021) Adult Postabdomen, Immature Stages and Biology of *Euryommatus mariae* Roger, 1856 (Coleoptera: Curculionidae: Conoderinae), a Legendary Weevil in Europe. *Insects* 2(2): e151. <https://doi.org/10.3390/insects12020151>
- Hille Ris Lambers D (1950) On mounting aphids and other soft-skinned insects. *Entomologische Berichten* 13: 55–58.
- Korotyaev BA, Konstantinov AS, O'Brien CW (2000) A new genus of Orobittidae and discussion of its relationships (Coleoptera: Curculionidae). *Proceedings of the Entomological Society of Washington* 102: 929–956.
- Kutzelnigg H (2013) Rekordverdächtige Konvergenzen. Beziehungen zwischen Pflanzen und Ameisen. *Studium Integrale Journal* 20(2): 76–83. <http://www.si-journal.de/index2.php?artikel=jg20/heft2/sij202-2.html>
- Leibee GL, Pass BC, Yeagan KV (1980) Instar determination of Clover Root Curculio, *Sitona hispidulus* (Coleoptera: Curculionidae). *Journal of the Kansas Entomological Society* 53: 473–475. <https://www.jstor.org/stable/pdf/25084061.pdf>
- Lohse GA (1983) 28. U.Fam. Ceutorhynchinae. In: Freude H, Harde KW, Lohse GA (Eds) *Die Käfer Mitteleuropas*. Band 11. Goecke & Evers, Krefeld, Germany, 180–253. [340 pp]
- Lyal CHC (2013) Conoderinae. In: Smetana A (Ed.) *Catalogus Coleopterorum Palearcticae, Curculionoidea II*; Löbl I; vol. 8. Brill, Leiden/Boston, 214–217.
- Lyal CHC, King T (1996) Elytro-tergal stridulation in weevils (Insecta: Coleoptera: Curculionoidea). *Journal of Natural History* 30(5): 703–773. <https://doi.org/10.1080/00222939600770391>

- Marvaldi AE (1999) Morfología larval en Curculionidae. *Acta Zoológica Lilloana* 45: 7–24.
- Marvaldi AE (2003) Key to larvae of the South American subfamilies of weevils (Coleoptera, Curculionoidea). *Revista Chilena de Historia Natural* 76(4): 603–612. <https://doi.org/10.4067/S0716-078X2003000400005>
- May BM (1994) An introduction to the immature stages of Australian Curculionoidea. In: Zimmerman EC (Ed.) *Australian weevils. Volume II: Brentidae, Eurhynchidae, Apionidae and a chapter on the immature stages* by Brenda May. CSIRO Publications, Melbourne, Victoria, 365–728.
- Morris MG (2012) True Weevils. (Coleoptera: Curculioninae, Baridinae, Orobittidinae). Part III. Royal Entomological Society of London. *Handbook* 5(17d): 1–246.
- Nikulina ON (2013) New data on the larvae of the weevil tribe Baridini (Coleoptera, Curculionidae) from Mongolia and Middle Asia. *Entomological Review* 93(2): 199–207. <https://doi.org/10.1134/S0013873813020085>
- Pakaluk J (1993) Review of the immature stages of Baridinae I: Nertinini (Coleoptera: Curculionidae). *Elytron* 7: 165–170.
- Pakaluk J (1994) Review of the immature stages of Baridinae II: Madarini (Coleoptera: Curculionidae). *Annales Zoologici* 45: 1–14.
- Pedroni G (2010) *Leiosoma talamellii* n. sp. della Majella (Appennino centrale) con alcune note di ecologia (Insecta Coleoptera Curculionidae). *Quaderno di Studi e Notizie di Storia Naturale della Romagna* 30: 203–210.
- Pedroni G (2012) Le specie italiane del gruppo di *Leiosoma scrobiferum* con descrizione di sei specie nuove (Coleoptera, Curculionidae, Molytini). *Bollettino del Museo Civico di Storia Naturale di Verona. Botanica, Zoologia* 36: 73–90.
- Pedroni G (2016) Designazione del lectotypus di *Leiosoma kirschii* Gredler, 1866 (Coleoptera: Curculionidae: Molytinae). *Gredleriana* 16: 133–140.
- Pedroni G (2018) Revisione tassonomica delle specie del gruppo di *Leiosoma cribrum* (Coleoptera: Curculionidae: Molytinae). - *Atti della Società italiana di scienze naturali e del Museo civico di storia naturale di Milano* 5(1): 19–32.
- Penecke KA (1922) Beiträge zur Kenntnis der geographischen Verbreitung und der Nährpflanzen von Curculioniden. *Wiener Entomologische Zeitung* 39(5–10): 183–188. <https://doi.org/10.5962/bhl.part.2574>
- Prena J, Colonnelli E, Hespeneheide HA (2014) Conoderinae Schoenherr, 1833. In: Leschen RAB, Beutel RG (Eds) *Handbook of Zoology, Coleoptera, vol. 3*. DeGruyter Berlin, 577–589.
- Rowe DJ, Kok LT (1985) Determination of larval instars, and comparison of field and artificial diet-reared larval stages of *Rhinocyllus conicus* (Col: Curculionidae). *Virginia Journal of Science* 36: 277–280.
- Sabaljuev IA (2013) Dolgonosik [Δολγονοσικ] *Leiosoma reitteri* Bedel, 1884. <https://www.zin.ru/animalia/coleoptera/rus/leireiza.htm> [accessed on 26 April 2022]
- Scherf H (1964) Die Entwicklungsstadien der mitteleuropäischen Curculioniden (Morphologie, Bionomie, Ökologie). *Abhandlungen der Senckenbergischen Naturforschenden Gesellschaft* 506: 1–335.
- Skuhrovec J, Gosik R, Caldara R, Košťál M (2015) Immatures of Palaearctic species of the weevil genus *Sibinia* (Coleoptera, Curculionidae): New descriptions and new bionomic

- data with suggestions on their potential value in a phylogenetic reconstruction of the genus. *Zootaxa* 3955: 151–187. <https://doi.org/10.11646/zootaxa.3955.2.1>
- Skuhrovec J, Gosik R, Caldara R, Toševski I, Batyra A (2022) Description of immature stages of *Gymnetron* species (Coleoptera, Curculionidae, Curculioninae), with particular emphasis on the diagnostic morphological characters at the generic and specific levels. *ZooKeys* 1090: 45–84. <https://doi.org/10.3897/zookeys.1090.78741>
- Smreczyński S (1974) Chrząszcze – Coleoptera. Ryjkwce – Curculionidae. Podrodzina Curculioninae. *Plemiona Barini, Coryssomerini, Ceutorhynchini*, vol. 83 (XIX, 98e). *Klucze do Oznaczenia Owadów Polski*, Warszawa, 180 pp.
- Sprick P, Gosik R (2014) Biology and morphology of the mature larva of *Mitoplinthus caliginosus caliginosus* (Curculionidae, Molytinae). *SNUDEBILLER: Studies on taxonomy, biology and ecology of Curculionoidea* 15, 229, 10 pp.
- Sprick P, Krämer-Klement K (2022[in press]) Oxalidaceae, eine neue Wirtspflanzenfamilie für die Gattung *Leiosoma* Stephens, 1829 - mit Bemerkungen zu den Wirtspflanzen von *Leiosoma*-Arten (Curculionidae: Molytinae). *Weevil News*.
- Sprick P, Gosik R, Graba S (2022) Morphology, instar determination and larval biology of *Otiorrhynchus (Otiorrhynchus) coecus coecus* Germar, 1823 and pupal morphology of *O. (Nibus) carinatopunctatus* (Retzius, 1783) and *O. (Postaremus) nodosus* (O. F. Müller, 1764) from Central and Northern Europe (Coleoptera, Curculionidae, Entiminae). *Weevil News* 99: 1–24.
- Stüben PE (2011) Die Curculionoidea (Coleoptera) La Gomeras. *Snudebiller : Studies on Taxonomy, Biology, and Ecology of Curculionoidea* 12(177): 85–129.
- Urban C (1925) Der Veilchenkäfer. *Entomologische Blätter* 21: 139–141.
- Van Emden FI (1938) On the taxonomy of Rhynchophora larvae (Coleoptera). *The Transactions of the Entomological Society of London* 8(1): 1–37. <https://doi.org/10.1111/j.1365-2311.1938.tb01800.x>
- Willis RJ (1964) The bionomics and larval morphology of the otiorrhynchid pests of soft fruit crops. – Thesis, The Queen's University of Belfast, Northern Ireland, 250 pp. [and appendix of 60 pp.]
- Zherikhin VV, Gratshev VG (1995) A comparative study of the hind wing venation of the superfamily Curculionoidea, with phylogenetic implications. In: Pakaluk J, Ślipiński SA (Eds) *Biology, phylogeny and classification of Coleoptera: Papers celebrating the 80th birthday of Roy A. Crowson*. Vol. 2. Muzeum i Instytut Zoologii PAN, Warsaw, 633–777. [i–vi + 559–1092 pp]

Evaluation of genetic diversity and population structure in *Leptobotia microphthalmal* Fu & Ye, 1983 (Cypriniformes, Cobitidae)

Dongqi Liu^{1*}, Shiming Zhang^{2*}, Xinyu Zuo², Yi Zheng¹, Jing Li¹

1 Sichuan Province Key Laboratory of Characteristic Biological Resources of Dry and Hot River Valley, School of Biological and Chemical Engineering, Panzhihua University, Panzhihua, 617000, China **2** Upper Changjiang River Bureau of Hydrological and Water Resources Survey, Chongqing, 400000, China

Corresponding author: Shiming Zhang (shimingzhang1970@163.com)

Academic editor: Maria Elina Bichuette | Received 4 May 2022 | Accepted 29 August 2022 | Published 12 September 2022

<https://zoobank.org/FA219A45-622D-46FF-B9CE-2483FA864711>

Citation: Liu D, Zhang S, Zuo X, Zheng Y, Li J (2022) Evaluation of genetic diversity and population structure in *Leptobotia microphthalmal* Fu & Ye, 1983 (Cypriniformes, Cobitidae). ZooKeys 1121: 83–95. <https://doi.org/10.3897/zookeys.1121.85953>

Abstract

This paper reports the first account about dynamic changes on genetic diversity and population structure of *Leptobotia microphthalmal* in the Yangtze River drainage due to dam constructions. The genetic diversity and population structure of twelve populations of *L. microphthalmal* collected in 2010 and 2020 were estimated using 12 nuclear microsatellite markers. Reduction of genetic diversity between 2010 and 2020 was not significant in a paired *t*-test ($p > 0.05$), but population structure of *L. microphthalmal* had a tendency to change: the genetic differentiation (F_{st}) among the five populations collected in 2010 were all insignificant ($p > 0.05$). However, differentiation (F_{st}) among some populations collected in 2020 were significant ($p < 0.05$), which indicated the population structure of *L. microphthalmal* was changing. Correlation analysis indicated that negative correlations between the genetic diversities and geographical elevations among populations were significant for seven populations collected in 2020 ($r = -0.819$, $p = 0.039$), which means that populations of *L. microphthalmal* in high elevation regions were more vulnerable than those in low elevation regions. Finally, some suggestions for conservation and restoration are proposed, such as artificial propagation, to prevent the further reduction of genetic diversity and population resources.

Keywords

Conservation biology, fish ecology, microsatellites, restoration

* These authors contributed equally to this work.

Introduction

Leptobotia microphthalmalma Fu & Ye, 1983 (Cypriniformes: Cobitidae) is an important benthic commercial fish with high ornamental and edible value. It is a unique Chinese species (Ding 1994) and endemic to the middle and upper reaches of the Yangtze River and its tributaries. It is known in China and international markets for its vivid color (Cao et al. 2007). In recent years, *L. microphthalmalma* populations have declined greatly due to dam construction, over-fishing, and environmental deterioration, including the destruction of prey and breeding grounds (Yue and Chen 1998). The annual catch was 2000 kg prior to the 2000s, but has decreased to no more than 500 kg per year in recent years (Shen et al. 2017).

The species is often found near gravel and rock crevice habitats on the bottom of rivers and streams with swift currents (Ding 1994). This species often goes up-stream to spawn, and spawning occurs from April to June, with eggs and developing larvae drifting with the currents (Liang et al. 2009). Thus, the development of embryos and the growth of larvae requires relatively long and continuous rivers. However, this natural requirement conflicts with the construction of hydropower stations on the Yangtze River (Yue and Chen 1998). With the construction of Three Gorges Dam and other cascade hydropower stations within its distribution, *L. microphthalmalma* is suffering from severe threats to its survival (Liu et al. 2014a). Thus, the genetic connection and communication between populations may be interrupted, resulting in bottlenecks and inbreeding. As a result, the genetic diversities may decrease. If wild species are to survive environmental changes beyond the limits of developmental plasticity, they must have an available and viable genetic diversity pool. If not, extinction would appear to be inevitable (Frankel 1983). Today, artificial propagation and breeding techniques are successful (Ku et al. 1999), and the release of cultured juveniles into rivers has been proposed as one conservation strategy, and has been carried out for several years on a small scale in the upper reaches of the Yangtze River (Zhou et al. 2007). These releasing programs can increase the quantity, but they may have influences on genetic diversities and structures of wild populations of *L. microphthalmalma*.

Considering the present and potential environmental threats from artificial negative factors to *L. microphthalmalma* populations and the influence of releasing program, it is necessary to monitor the dynamic population genetic status of *L. microphthalmalma*. Shen et al. (2017) studied the diversity of two populations (only 108 samples) using mtDNA control region. However, the comparative study of *L. microphthalmalma* during different times using different genetic markers in a larger quantity of samples has not been made to date. In the present study, twelve microsatellites were used to assess genetic diversity and population structure of twelve *L. microphthalmalma* populations including 280 individuals collected in upper and middle drainages of the Yangtze River from 2010 to 2020. The genetic diversity and population structure of *L. microphthalmalma* in 2010 was then compared with that in 2020.

In this study, the population genetic diversity of *L. microphthalmalma* in the upper reaches of the Yangtze River was studied to understand the genetic background of

L. microphthalmal, and to provide basic knowledge for germplasm protection of *L. microphthalmal*. At the same time, it provides a scientific basis for evaluating and predicting the impact of cascade power station development on aquatic animals and ecological environments of the Yangtze River.

Materials and methods

Sample collection and microsatellites amplification

Fins from 280 individuals of *L. microphthalmal* were collected from the middle and upper Yangtze River drainage (Table 1). In fact, our sampling covered most of the distribution area of the species. Five populations of *L. microphthalmal* were collected from the Ertan part of the Yalong River (ET), the Anbian part of the Jinsha River (AB), the Shiyuanzi part of the Yangtze River (SYZ), the Hejiang part of the Yangtze River (HJ), and the Hechuan part of the Jialing River (HC) in 2010. Seven populations of *L. microphthalmal* were collected from the Zhuangshang part of the Jinsha River (ZS), the Laomatian part of the Jinsha River (LMT), the Juexi part of the Min River (JX), the Pingshan part of the Yangtze River (PS), the Wayao part of the Yangtze River (WY), the Xuyong part of the Yangtze River (XY), and the Qiping part of the Jialing River (QP) in 2020 (Fig. 1). In order to reduce experimental errors caused by different fish ages, 247 individuals, aged between 3 and 4 years old, were selected from 280 samples, according to the relationship between age and body length (Cao et al. 2007).

Twelve microsatellite loci (XY12, XY13, XY14, XY21, XY27, XY32, XY35, XY37, XY38, XY41, XY43, and XY45) specifically developed for *L. microphthalmal* (Liu et al. 2014a, b) were used as described in Liu et al. (2018). Procedures of polymerase chain reaction (PCR) amplification, electrophoresis, and fluorescent microsatellites were specifically developed in Liu et al. (2020) and the methodology was followed herein.

Table 1. Sample information of *L. microphthalmal*.

Population code	Population name	River	Sample size		Elevation (m)	Sampling time
			N ₁	N ₂		
HJ	Hejiang	Yangtze River	15	13	235	Apr 2010
HC	Hechuan	Jialing River	21	19	200	Jul 2010
ET	Ertan	Yalong River	22	17	991	Aug 2010
AB	Anbian	Jinsha River	24	23	421	May 2010
SYZ	Shiyuanzi	Yangtze River	22	21	281	Jun 2010
WY	Wayao	Yangtze River	24	22	272	Aug 2020
XY	Xuyong	Yangtze River	21	18	235	Sep 2020
JS	Juexi	Minjiang River	25	22	311	Nov 2020
QP	Qingping	Jialing River	28	23	284	Oct 2020
PS	Pingshan	Minjiang River	24	23	273	May 2020
ZS	Zhuangshang	Jinsha River	26	22	1103	May 2020
LMT	Laomatian	Jinsha River	28	24	890	Nov 2020
Total			280	247		

N₁, Number of samples collected; N₂, Number of samples used for analyses.

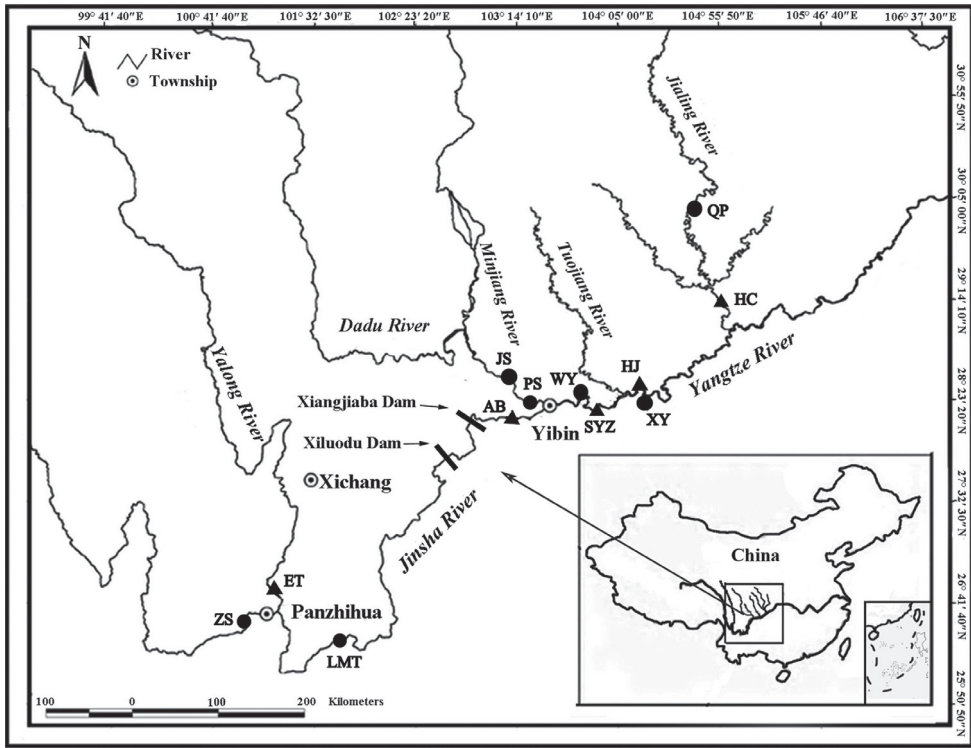


Figure 1. Sampling localities of China (black triangles indicate collection in 2010; black circles indicate collection in 2020) of *L. microphthalma*. For full names of population codes, see Table 1.

Genetic diversity and landscape analysis

The software GenAEx 6.501 was used to statistically analyze observed heterozygosity (*H_o*), expected heterozygosity (*H_e*), and polymorphism information content (*PI*C) (Peakall and Smouse 2006). Average allelic richness by population (*Ar*) and private allelic richness (*PAr*) across 12 nuclear loci were calculated using HP-RARE 2.2 (Kalinowski 2005), which uses the rarefaction procedure to account for variable sample sizes. Paired *t*-test was used to compare *Ar* and *PAr*. The correlation between genetic diversity and elevation was calculated.

The software POPGENE 2.4 was used to calculate Hardy–Weinberg equilibrium (HWE) and pairwise genetic differentiation (*F_{st}*) (Francis et al. 1999). A Bayesian approach was applied to explore the population genetic structure using STRUCTURE 2.2.1 (Pritchard et al. 2000). The number of groups *K* was set to 1–9, and each *K* was repeated five times. The calculation results were packaged, and the optimal *K* value was analyzed by STRUCTURE Harvester. As a best choice to maximize Δ*K* corresponding to the *K* value (including Δ*K* = mean|*L*'(*K*)| / sd(*K*)(*L*), *L*'(*K*) as the likelihood distribution rate averages, |*L*'(*K*)| for the second round of likelihood distribution rate the absolute value of the mean), Repeated sampling analysis is conducted on the results of structure operation to obtain the *Q* value corresponding to the optimal *K* value,

and the structure graph is drawn according to the Q value gene flow and landscape analyses (Evanno et al. 2005). Population structure was evaluated using the analysis of molecular variance model (AMOVA) in the ARLEQUIN 2.0 (Excoffier et al. 1992).

The BOTTLENECK tests for the departure from mutation drift equilibrium based on heterozygosity, excess or deficiency. The bottleneck compares heterozygosity expected (H_e) at Hardy-Weinberg equilibrium to the heterozygosity expected (H_{eq}) at mutation drift equilibrium in the same sample. All the three models of mutation were used to calculate H_{eq} : the strict one stepwise mutation model (SMM; Kimura and Ohta 1978), the infinite allele model (IAM; Kimura and Crow 1964) and two-phase model (TPM; Di Rienzo et al. 1994). FSTAT 1.8.2 was used to estimate inbreeding coefficient (F_{is}).

Results

Genetic data of diversities

The allelic richness (A_r) of populations ranged from 11.17 in XY to 15.36 in QP (Table 2). Average observed heterozygosity (H_o) varied from 0.753 in JX to 0.899 in XY. Average expected heterozygosity (H_e) varied from 0.839 in XY to 0.869 in PS. Most average values of H_o were lower than those of expected heterozygosity (H_e) in all populations except for ET, LMT, XY, and QP (Table 2). Average polymorphic information content (PIC) varied from 0.785 in ZS to 0.852 in HC (Table 2). The private allelic richness (PA_r) varied from 1.63 in ET to 21.36 in LMT, and LMT also showed the highest number of private alleles, while the lowest number of private alleles was found in ET (Table 2). All differences of genetic diversity (PIC and A_r) between the 12 populations were insignificant in paired t -tests ($p > 0.05$). Significant negative correlations between the genetic variability and elevations among populations were found for the seven populations in 2020 ($r = -0.819$, $p = 0.039$), but there were no significant correlations for the five populations in 2010.

Table 2. Genetic variability of *L. microphthalmia* populations. For full names of population codes, see Table 1.

Population	H_o	H_e	PIC	A_r	PA_r	F_{is}
HJ	0.838	0.849	0.844	13.25	6.45	0.134
HC	0.798	0.853	0.852	12.14	3.52	0.244
ET	0.878	0.846	0.808	13.72	1.63	0.102
AB	0.808	0.866	0.828	14.51	15.96	0.100
SYZ	0.793	0.862	0.838	14.62	7.01	0.217
WY	0.755	0.841	0.836	14.32	6.57	0.318
XY	0.899	0.839	0.842	11.17	8.13	0.198
JS	0.753	0.848	0.802	14.44	9.05	0.218
QP	0.863	0.846	0.814	15.36	8.9	0.651
PS	0.862	0.869	0.825	14.14	5.48	0.365
ZS	0.828	0.840	0.785	13.45	13.9	0.307
LMT	0.873	0.856	0.798	14.17	21.36	0.747

H_o , observed heterozygosity; H_e , expected heterozygosity; PIC , polymorphism information content; A_r , allelic richness; PA_r , private allelic richness; F_{is} , inbreeding coefficients.

Population genetic demography and structure analyses

The 12 populations were divided into three groups based on sampling locations: upper group (ET, ZS, and LMT), middle group (HJ, SYZ, AB, XY, JX, PS, and WY), and lower group (HC and QP). An AMOVA performed in five populations (SYZ, ET, HC, AB, and HJ) sampled in 2010 indicated molecular variance between groups, between populations, and within populations were all insignificant ($p > 0.05$). Although AMOVA in seven populations (XY, WY, QP, PS, LMT, ZS, and JX) sampled in 2020 indicated that molecular diversity between groups and between populations within sites were insignificant, variance within populations (98.16%) was significant ($p < 0.05$).

Pairwise F_{st} between populations varied from 0.022 to 0.330 (Table 3). F_{st} between five populations sampled in 2010 (HJ, HC, ET, AB, and SYZ) were all insignificant ($p > 0.05$; Table 3). However, some F_{st} between seven populations sampled in 2020 (JX, WY, XY, LMT, QP, PS, and ZS) were significant ($p < 0.05$), including F_{st} between QP and ZS, and LMT and JX (Table 3). Some F_{st} between five populations (2010) and seven populations (2020) were significant ($p < 0.05$) including F_{st} between ZS and SYZ, and between LMT and HC (Table 3). Two neighbor-joining trees were built based on F_{st} values among five populations (2010) and among seven populations (2020), respectively. HC and HJ populations were clustered together and the AB, SYZ, and ET populations were clustered together in the neighbor-joining tree (Fig. 2a). JX and XY, and QP and PS were clustered together in the neighbor-joining tree, respectively (Fig. 2b). LMT, WY, and ZS populations were also clustered together in the neighbor-joining tree (Fig. 2b).

STRUCTURE analysis was applied in five populations (2010), seven populations (2020), and all twelve populations. The optimal K value in five populations (2010) was 3. However, the five populations did not form independent clusters for $K = 3$, with each sample in effect having equal probability of belonging to any of those clus-

Table 3. Pairwise genetic differentiation of *L. microphthalmus* populations. For full names of population codes, see Table 1.

	HJ	HC	ET	AB	SYZ	WY	XY	JS	QP	PS	ZS
HC	0.037										
ET	0.079	0.063									
AB	0.046	0.037	0.068								
SYZ	0.075	0.022	0.048	0.073							
WY	0.048	0.023	0.062	0.065	0.066						
XY	0.078	0.048	0.077	0.078	0.047	0.078					
JS	0.074	0.056	0.079	0.057	0.050	0.089	0.056				
QP	0.032	0.053	0.083	0.056	0.080	0.058	0.078	0.047			
PS	0.047	0.067	0.050	0.040	0.058	0.057	0.054	0.064	0.064		
ZS	0.074	0.073	0.053	0.083	0.270*	0.060	0.064	0.058	0.330*	0.052	
LMT	0.069	0.160*	0.084	0.079	0.087	0.073	0.078	0.214*	0.080	0.073	0.062

* $P < 0.05$.

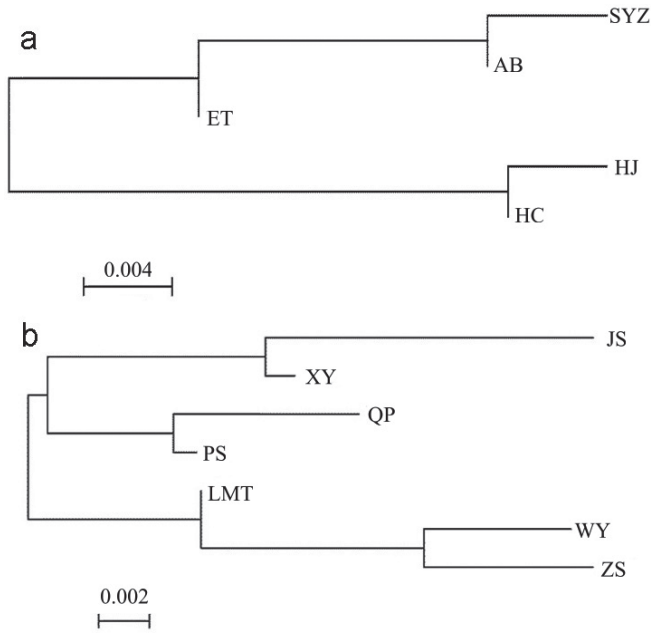


Figure 2. Neighbor-joining tree based on F_{st} . For full names of population codes, see Table 1.

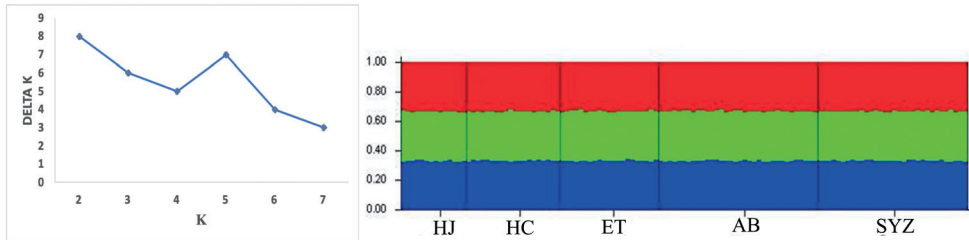


Figure 3. Structure results and maximum DK values of the *L. microphthalmal* populations collected in 2010. For full names of population codes, see Table 1.

ters in either analysis (Fig. 3). The ΔK statistic estimated the best supported number of a posterior genetic clusters at $K = 4$ in either seven populations (Fig. 4; 2020) or all twelve populations (Fig. 5). There was no apparent clustering of individuals into groups for $K = 4$ in seven populations (Fig. 4; 2020) or all twelve populations (Fig. 5), but there was a more-or-less unequal probability of every individual belonging to each cluster. Individuals in each population are becoming divergent to each other, which is consistent with the AMOVA analysis. As such, there was a trend of overall genetic clustering. Analysis using the coalescent-based method based on the IM model showed that the level of gene flow among populations was very limited: there was no significant gene flow in both five populations (2010) and seven populations (2020).

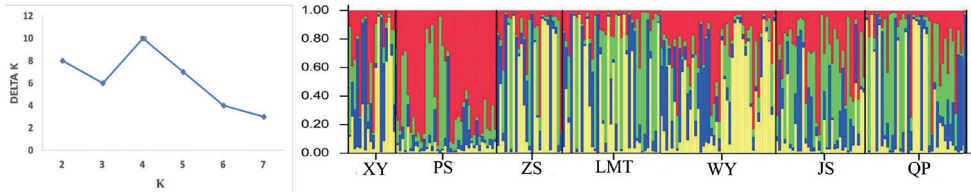


Figure 4. Structure results and maximum DK values of the *L. microphthalmal* populations collected in 2020. For full names of population codes, see Table 1.

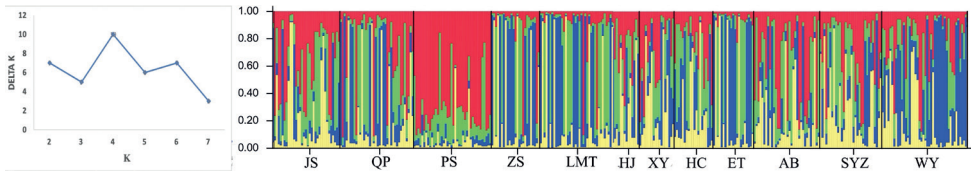


Figure 5. Combined structure results and maximum DK values of the *L. microphthalmal* populations collected in 2010 and 2020. For full names of population codes, see Table 1.

Table 4. Probabilities of Wilcoxon test of *L. microphthalmal* populations for mutation drift equilibrium (bottleneck) under three mutation models. For full names of population codes, see Table 1.

Population	I.A.M	S.M.M	T.P.M
HJ	0.1354	0.5542	0.3441
HC	0.0676	0.6883	0.7981
ET	0.0436*	0.7449	0.7448
AB	0.2358	0.2778	0.3509
SYZ	0.1557	0.9807	0.3127
XY	0.1829	0.1129	0.2030
WY	0.0659	0.3367	0.1873
JS	0.0359*	0.0514	0.0859
QP	0.0358*	0.0523	0.0750
PS	0.1235	0.2147	0.1209
ZS	0.0553	0.2445	0.0647
LMT	0.0485*	0.0559	0.0736

* $P < 0.05$ (rejection of mutation drift equilibrium).

The results of the bottlenecks are summarized in Table 4 and show every population tested under three possible mutation models. The probability values of one-tailed Wilcoxon test for heterozygosity excess (H_e) were < 0.05 in ET, JX, QP, and LMT in the infinite allele model (IAM). Nevertheless, under the stepwise mutation model (SMM) and the two-phase model (TPM), the excess heterozygosity of each population is not significant, and there has been no bottleneck effect or foundation effect in the past (Table 4). The inbreeding coefficient (F_{is}) of the 12 populations ranged from 0.100 in AB to 0.747 in ZS (Table 2). The inbreeding coefficient (F_{is}) of LMT and QP were significant ($P < 0.05$), while that of the other populations were not significant.

Discussion

Tendency of population genetic variabilities

The important indexes of population genetic diversity are heterozygosity and PIC. The higher the heterozygosity and PIC are, the greater the genetic variation; the higher the genetic diversity leads to greater stability of the population. Negative correlations among the genetic variabilities and geographical elevations between populations were significant for seven populations (2020), which indicates that rising elevation is always accompanied by reducing genetic variabilities. Therefore, populations of *L. microphthalmalma* in upper streams of the Yangtze (higher elevation area) are more fragile than those present downstream (lower elevation) flows. Hence, populations of *L. microphthalmalma* in upstream Yangtze River and its tributaries are extremely important in conservation and can serve as models for monitoring biodiversity in regions impacted by anthropogenic disturbances.

All populations indicated heterozygosity deficiencies except ET, LMT, XY, and QP. Two previous studies had examined how levels of heterozygosity varied during the course of well-documented demographic challenges. Ruzich et al. (2019) found that heterozygote go up during population reduces in six fish species, and Valsecchi et al. (2004) found that Mediterranean striped dolphins dying early in an epizootic environment were significantly less heterozygous than those dying later. These studies imply that natural selection may sometimes remove relatively homozygous individuals from populations during demographic declines, raising the counter-intuitive possibility that declining populations may in fact be more heterozygous than stable ones. Therefore, four populations (ET, LMT, XY and QP) may have experienced recession recently. Furthermore, the purging of genetic load during population bottlenecks could generate a scenario where relatively homozygous populations do better when faced with a challenge (Haxton et al. 2015).

Dynamics of population structure and landscape analysis

The AMOVA analysis indicated that five populations (2010) of *L. microphthalmalma* exhibited limited genetic differentiation between groups and between populations. *Fst* analysis indicated no significant population structure among the sampling locations. Also, the five populations did not form independent clusters in the population structure, with each sample in effect having the same possibility of belonging to any of those clusters in either analysis. There was significant correlation between the observed genetic differentiations and geographical distances in the five populations. This species spawn eggs which usually drift with flood currents downstream, and the adult fish usually swim upstream when the river are flooded (Li et al. 2015). Those life histories traits could accelerate genetic exchanges among groups across their distribution. In the Yangtze River region, the genetic differentiations between the populations of *Coreius guichenoti* (Sauvage & Dabry, 1874) is also not obvious, which is also due to the move-

ment of floating larvae and eggs (Liu et al. 2021). This is not different to the loss of population genetic structure of *L. microphthalmalma* due to similarity in breeding and life cycle characteristics, which may also be connected with the indeterminacy of counter-current swimming distance.

However, there were obvious differences in genetic structure between the seven populations in 2020: F_{st} indicated significant differences among some populations. There are no independent components in the structure of the seven populations, but the components of each population were not the same as the others. Although AMOVA indicated that genetic divergences among groups were finite, the genetic divergences that occurred between individuals in a population were significant ($p < 0.05$). Significant differentiation in all populations is not yet formed, but individuals are becoming different to each other within each population. The dams limit genetic connections between upstream and downstream populations of *L. microphthalmalma* and divide it into smaller independent populations. A robust barrier to dispersal likely exists to restrict genetic exchange among sample locations. The habitats of *L. microphthalmalma* will become isolated, which influences not only the breeding and development environments of *L. microphthalmalma*, but also prevents upstream and downstream gene flow. Therefore, there was no inapparent correlation between genetic differences and geographical distance in these seven populations (2020, $p > 0.05$). The individuals of populations are becoming different from each other because of a changing aquatic environment. Therefore, strong structures of populations might be formed in the future. This was evidenced by bottleneck analysis: microsatellite data indicated that some populations collected in 2020 suffered from bottleneck or founder effects under two models (IAM, SMM), which was consistent with F_{is} analysis. Also, the construction of the reservoir upstream of the Yangtze River vastly altered the aquatic environments, and might destroy the habitats and breeding areas of *L. microphthalmalma*. As a consequence of the lack of flowing water, juvenile fish may grow unsuccessfully; thus, many wild populations and their genetic variability will necessarily reduce.

Conservation and restoration guidance

In order to protect and restore the germplasm resources of *L. microphthalmalma*, the fishing of wild parents and back-up parents should be strictly controlled while protecting the spawning grounds and improving the water environmental conditions, so as to maintain the self-healing potential of natural water resources of *L. microphthalmalma*. Although relevant departments have long established breeding farms of *L. microphthalmalma*, the numbers of wild parents in the Yangtze River have decreased sharply in recent years, having died in fishing and transportation, which inevitably leads to the shortage of original parents. Seed farms usually breed F1 generations as back-up parents (Liu et al. 2014b). Due to the high cost, the long cycle (2–3 years), and limited seedling cultivation scale of F1 generation back-up parents in the seed farm, the supply of back-up parents in the seed farm is limited and the price is high. Some farms, in order to save costs, often introduce a small amount

of seed stock station back-up parents or fry from numerous progenies reserved for parents, and breed on a smaller scale (Liu et al. 2015); hence, the population is not big enough and it is easy to observe the bottleneck effect and inbreeding depression phenomena, which may also cause farms to produce parent group alleles lacking one of the important reasons.

At present, the proliferation and release of seedlings generally takes the form of bidding for government grants. Therefore, in order to better protect and utilize the germplasm resources of *L. microphthalmia*, it is suggested that the relevant functional departments should strictly examine the qualification, breeding scale, and parental source of the nursery before release, and strive to make the source of the nursery traceable and of high quality. The genetic background of the released population must be evaluated before release to ensure the stability of the genetic structure of the natural population. Sampling investigations and supervision of the specification, health status, and germplasm status of the released seedlings should be strengthened at the site of release. The growth, biology, genetic diversity, and genetic structure of natural populations in natural water bodies should be monitored regularly after discharge, and the discharge plan should be adjusted according to the monitoring results.

Acknowledgements

This work was supported by Upper Changjiang River Bureau of Hydrological and Water Resources Survey (no. SWJ20210501 and no. HX2022070), Science and Technology Bureau of Panzhihua (no. 2021ZD-R-6), Sichuan Province Key Laboratory of Characteristic Biological Resources of Dry and Hot River Valley (no. GR-2022-C-04), Science & Technology Department of Sichuan Province (no. 2021YFN0101) and Panzhihua University (no. HJK2019-2020, no. SFKC2046, no. 2021YB001, and no. S202211360063).

References

- Cao W, Chang J, Qiao Y, Duan Z (2007) Fish Resources of Early Life History Stages in Yangtze River. China Water Power Press, Beijing, 34–38. [in Chinese]
- Di Rienzo A, Peterson AC, Garza JC, Valdes AM, Slatkin M, Freimer NB (1994) Mutational processes of simple sequence repeat loci in human populations. *Proceedings of the National Academy of Sciences of the United States of America* 91(8): 3166–3170. <https://doi.org/10.1073/pnas.91.8.3166>
- Ding R (1994) The Fishes of Sichuan, China. Sichuan Publishing House of Science and Technology, Chengdu, 111–112. [in Chinese]
- Evanno G, Regnaut S, Goudet J (2005) Detecting the number of clusters of individuals using the software STRUCTURE: A simulation study. *Molecular Ecology* 14(8): 2611–2620. <https://doi.org/10.1111/j.1365-294X.2005.02553.x>

- Excoffier L, Smouse P, Quattro J (1992) Analysis of molecular variance inferred from metric distances among DNA haplotypes: Application to human mitochondrial DNA restriction data. *Genetics* 131(2): 479–491. <https://doi.org/10.1093/genetics/131.2.479>
- Francis CY, Rong CY, Boyle T (1999) POPGENE, Microsoft Window based freeware for population genetic analysis. University of Alberta, Canada.
- Frankel OH (1983) The place of management in conservation. In: Schonewald-Cox CM, Chambers SM, MacBryde B, Thomas WL (Eds) *Genetics and Conservation: a reference for managing wild animal and plant Populations*. The Benjamin/Cumming Pub Company, Menlo Park, Canada, 434–436.
- Haxton T, Nienhuis S, Punt K, Baker T (2015) Assessing walleye movement among reaches of a large, fragmented river. *North American Journal of Fisheries Management* 35(3): 537–550. <https://doi.org/10.1080/02755947.2015.1012278>
- Kalinowski ST (2005) HP-RARE 1.0: A computer program for performing rarefaction on measures of allelic richness. *Molecular Ecology Notes* 5(1): 187–189. <https://doi.org/10.1111/j.1471-8286.2004.00845.x>
- Kimura M, Crow JW (1964) The number of alleles that can be maintained in a finite population. *Genetics* 49(4): 725–738. <https://doi.org/10.1093/genetics/49.4.725>
- Kimura M, Ohta T (1978) Stepwise mutation model and distribution of allelic frequencies in a finite population. *Proceedings of the National Academy of Sciences of the United States of America* 75(6): 2868–2872. <https://doi.org/10.1073/pnas.75.6.2868>
- Ku M, Wen X, Luo J, Liu W, Hu Y (1999) A Study on Transplantation and Culture of *Leptobotia microphthalmia*. *Journal of Hubei Agricultural College* 19: 146–148. [in Chinese]
- Li L, Wei QQ, Wu JM, Du H, Xie X (2015) Current status of fish assemblages in Yibin Reaches of the Yangtze River. *Resources Environment in the Yangtze Basin* 22: 1449–1457. [in Chinese]
- Liang H, Zhang X, Liang X (2009) Threatened fishes of the world: *Leptobotia elongata* (Bleeker, 1870) (Boridiidae). *Environmental Biology of Fishes* 85(4): 287–288. <https://doi.org/10.1007/s10641-009-9500-9>
- Liu D, Deng Y, Li Z, Li J, Song Z (2014a) Isolation and characterization of 14 tetranucleotide microsatellite DNA markers in the elongate loach *Leptobotia elongata* (Cypriniformes: Cobitidae) using 454 sequencing technology. *Conservation Genetics Resources* 6(1): 119–121. <https://doi.org/10.1007/s12686-013-0021-7>
- Liu D, Wu J, Deng L, Gan W, Du L, Song Z (2014b) Development of microsatellite markers for *Leptobotia elongata* (Cypriniformes: Cobitidae) using 454 sequencing and cross-species amplification. *Pakistan Journal of Zoology* 46: 1147–1151. <https://doi.org/10.1007/s12686-013-0021-7>
- Liu D, Hou F, Liu Q, Zhang X, Yan T, Song Z (2015) Strong population structure of *Schizopygopsis chengi* and the origin of *S. chengi baoxingensis* revealed by mtDNA and microsatellite markers. *Genetica* 143(1): 73–84. <https://doi.org/10.1007/s10709-015-9815-8>
- Liu D, Zhou Y, Yang K, Zhang X, Chen Y, Li C, Li H, Song Z (2018) Low genetic diversity in broodstocks of endangered Chinese sucker, *Myxocyprinus asiaticus*: Implications for artificial propagation and conservation. *ZooKeys* 792: 117–132. <https://doi.org/10.3897/zookeys.792.23785>

- Liu D, Li X, Song Z (2020) No decline of genetic diversity in elongate loach (*Leptobotia elongata*) with a tendency to form population structure in the upper Yangtze River. *Global Ecology and Conservation* 23: e01072. <https://doi.org/10.1016/j.gecco.2020.e01072>
- Liu D, Lan F, Xie S, Diao Y, Gong J (2021) Dynamic genetic diversity and population structure of *Coreius guichenoti*. *ZooKeys* 1055: 135–148. <https://doi.org/10.3897/zookeys.1055.70117>
- Peakall R, Smouse PE (2006) Genalex 6: Genetic analysis in Excel. Population genetic software for teaching and research. *Molecular Ecology Notes* 6(1): 288–295. <https://doi.org/10.1111/j.1471-8286.2005.01155.x>
- Pritchard JK, Stephens M, Donnelly P (2000) Inference of population structure using multilocus genotype data. *Genetics* 155(2): 945–959. <https://doi.org/10.1093/genetics/155.2.945>
- Ruzich J, Turnquist K, Nye N, Rowe D, Larson WA (2019) Isolation by a hydroelectric dam induces minimal impacts on genetic diversity and population structure in six fish species. *Conservation Genetics* 20(6): 1421–1436. <https://doi.org/10.1007/s10592-019-01220-1>
- Shen SY, Tian HW, Liu SP, Chen DQ, Lv H, Wang DQ (2017) Genetic diversity of *Leptobotia microphthalmalma* in the upper Yangtze River inferred from mitochondrial DNA. *Chinese Journal of Ecology* 36: 2824–2830. [in Chinese]
- Valsecchi E, Amos W, Raga JA, Podesta M, Sherwin W (2004) The effects of inbreeding on mortality during a morbillivirus outbreak in the Mediterranean striped dolphin (*Stenella coeruleoalba*). *Animal Conservation* 7(2): 139–146. <https://doi.org/10.1017/S1367943004001325>
- Yue P, Chen Y (1998) *China Red Data Book of Endangered Animals*. Science Press, Beijing, 221–224. [in Chinese]
- Zhou J, Liang Y, Chen X, Li M (2007) Nursing techniques of *Leptobotia microphthalmalma* larvae. *Journal of Aquaculture* 28: 12–13. [in Chinese]

Taxonomical review of *Prosymna angolensis* Boulenger, 1915 (Elapoidea, Prosymnidae) with the description of two new species

Werner Conradie^{1,2,3}, Chad Keates^{2,3,4,5},
Ninda L. Baptista^{3,6,7,8,9}, Javier Lobón-Rovira^{7,8,9}

1 Port Elizabeth Museum (Bayworld), P.O. Box 13147, Humewood 6013, Gqeberha, South Africa **2** Department of Nature Conservation Management, Natural Resource Science and Management Cluster, Faculty of Science, George Campus, Nelson Mandela University, George, South Africa **3** National Geographic Okavango Wilderness Project, Wild Bird Trust, Sandton, South Africa **4** South African Institute for Aquatic Biodiversity (SALAB), Makhanda, South Africa **5** Department of Zoology and Entomology, Rhodes University, Makhanda, South Africa **6** Instituto Superior de Ciências da Educação da Huíla (ISCED-Huíla), Rua Sarmiento Rodrigues, Lubango, Angola **7** CIBIO-InBIO, Centro de Investigação em Biodiversidade e Recursos Genéticos, Laboratório Associado, Universidade do Porto, Campus Agrário de Vairão, Rua Padre Armando Quintas, 4485-661 Vairão, Portugal **8** Departamento de Biologia, Faculdade de Ciências, Universidade do Porto, 4099-002 Porto, Portugal **9** BIOPOLIS Program in Genomics, Biodiversity and Land Planning, CIBIO, Campus de Vairão, 4485-661 Vairão, Portugal

Corresponding author: Werner Conradie (werner@bayworld.co.za)

Academic editor: Robert Jadin | Received 22 April 2022 | Accepted 15 August 2022 | Published 15 September 2022

<https://zoobank.org/016D0A91-4E4A-4EF5-A41B-7DAD0A10B408>

Citation: Conradie W, Keates C, Baptista NL, Lobón-Rovira J (2022) Taxonomical review of *Prosymna angolensis* Boulenger, 1915 (Elapoidea, Prosymnidae) with the description of two new species. ZooKeys 1121: 97–143. <https://doi.org/10.3897/zookeys.1121.85693>

Abstract

African Shovel-snout snakes (*Prosymna* Gray, 1849) are small, semi-fossorial snakes with a unique compressed and beak-like snout. *Prosymna* occur mainly in the savanna of sub-Saharan Africa. Of the 16 currently recognised species, four occur in Angola: *Prosymna ambigua* Bocage, 1873, *P. angolensis* Boulenger, 1915, *P. frontalis* (Peters, 1867), and *P. visseri* FitzSimons, 1959. The taxonomical status and evolutionary relationships of *P. angolensis* have never been assessed due to the lack of genetic material. This species is known to occur from western Angola southwards to Namibia, and eastwards to Zambia, Botswana and Zimbabwe. The species shows considerable variation in dorsal colouration across its range, and with the lower ventral scales count, an ‘eastern race’ was suggested. In recent years, *Prosymna* material from different parts of Angola has been collected, and with phylogenetic analysis and High Resolution X-ray Computed Tomography, the taxonomic status of these populations can be reviewed. Strong phylogenetic evidence was found to include the *angolensis* subgroup as part of the larger *sundevalli* group, and the

existence of three phylogenetic lineages within the *angolensis* subgroup were identified, which each exhibit clear morphological and colouration differences. One of these lineages is assigned to the nominotypical *P. angolensis* and the other two described as new species, one of which corroborates the distinct eastern population previously detected. These results reinforce that a considerable part of Angolan herpetological diversity is still to be described and the need for further studies.

Keywords

Africa, Angola, cryptic species, fossorial, Kalahari, Serpentes

Resumo

As cobras-de-focinho-de-pá africanas (*Prosymna*) são pequenas cobras semi-fossoriais com um focinho único, achatado e em forma de bico, que ocorrem principalmente na savana da África subsaariana. Das 16 espécies actualmente reconhecidas, quatro existem em Angola: *Prosymna ambigua* Bocage, 1873, *P. angolensis* Boulenger, 1915, *P. frontalis* (Peters, 1867), e *P. visseri* FitzSimons, 1959. O estatuto taxonómico e as relações evolutivas de *P. angolensis* nunca foram avaliados devido à falta de material genético. A espécie ocorre desde o oeste de Angola, para sul até a Namíbia, e para este em direcção à Zâmbia, Botswana e Zimbábue. Na sua área de ocorrência, esta espécie tem variação principalmente na coloração dorsal, e com base no menor número de escamas ventrais, foi sugerida a existência de uma raça oriental. Recentemente foi amostrado material de *Prosymna* de várias partes de Angola, e com recurso a análises filogenéticas e a tomografia computadorizada de raios-X de alta resolução, foi possível rever o estatuto taxonómico destas populações. Encontrámos fortes evidências filogenéticas para incluir o subgrupo *angolensis* como parte do grupo *sundevalli*. Revelámos a existência de três linhagens filogenéticas no subgrupo *angolensis*. Atribuímos uma dessas linhagens ao *P. angolensis* nominotípico, e descrevemos as outras duas como espécies novas, uma das quais corrobora a população oriental previamente detectada. Estes resultados reforçam a ideia de que uma parte considerável da diversidade herpetológica angolana está ainda por descrever, e a necessidade de mais estudos.

Palavras-chave

África, Angola, espécies crípticas, fossorial, Kalahari, Serpentes

Introduction

African Shovel-snout snakes, belonging to the genus *Prosymna*, are small terrestrial snakes occurring in sub-Saharan Africa, mostly associated with semi-desert, savanna and miombo woodlands (Broadley 1980). They are characterised by a compressed skull with a depressed, upward pointing snout with a sharp horizontal edge, which allows them to live a semi-fossorial lifestyle (Broadley 1990; Branch 1998; Marais 2004; Spawls et al. 2018; Pietersen et al. 2021). The absent or anteriorly reduced dentary teeth, and the unique modified blade-like rear maxillary teeth allow them to slit open soft-shelled reptile eggs, on which they feed almost exclusively, although some species feed on hard-shelled gecko eggs (Broadley 1979, 1980; Heinicke et al. 2020). Due to this unusual skull compression, snout shape and modified maxillary teeth, the higher taxonomical level of these snakes has been in flux. However, modern phylogenetic analyses have allowed them to be assigned to their own family, Prosymnidae (superfamily Elapoidea), sister to the family Psammophiidae (Vidal et al. 2008; Kelly et al.

2009; Pyron et al. 2013; Figueroa et al. 2016; Zaher et al. 2019). Currently, *Prosymna* is represented by 16 species (Heinicke et al. 2020; Uetz et al. 2022), and recent phylogenetic work has shown that cryptic diversity may exist in the genus, especially within *P. ambigua*, *P. frontalis*, and *P. stuhlmanni* (Heinicke et al. 2020).

The first *Prosymna* recorded from Angola were documented by Bocage (1873). He assigned material collected from Mossamedes [= Moçâmedes] and Biballa [= Bibala] to *Prosymna frontalis* (Peters, 1867) and described *Prosymna ambiguus* Bocage, 1873 (= *P. ambigua*) from Duque de Bragança (= Calandula) based on the higher number of midbody scale rows (17 vs. 15), the shape of the rostral and the larger parietal scales when compared to *P. frontalis*. Later, Bocage (1882) once again noted that the Angolan specimens of *P. frontalis* did not fully agree morphologically with the original description provided by Peters (1867). Afterwards, he provided a more detailed account including additional material collected from Angola, reporting the morphological variation observed when compared to *P. frontalis* types (Bocage 1895). The main confusion that Bocage faced at the time was that the two type specimens (one adult and one juvenile) of *P. frontalis* represented two separate species: *P. frontalis* and *P. bivittata* (see Mertens 1955; Broadley 1980). His material agrees in part with the juvenile specimen (= *P. bivittata*) in the number of postoculars (= 1) and lower subcaudal scale count (< 25), while it differed from the larger specimen (= *P. frontalis* lectotype) in lower subcaudal scale count (50 vs. 17–25) and the number of postorbital scales (one vs. two). The only difference was that the internasal condition (single bandlike scale) of the Angolan material was in agreement with the *P. frontalis* lectotype and not with the juvenile of *P. bivittata*. Due to this confusion in the overlapping morphology with the original *P. frontalis* types, Bocage decided not to take any taxonomic actions and kept referring to material from Angola under the name *P. frontalis*. It should be noted that the Reptile Database (Uetz et al. 2022) states that *P. angolensis* is a *nomen novum* for '*P. frontalis* Bocage, 1895'. This is incorrect, as Bocage (1895) never described *P. frontalis* as a new species.

Boulenger (1915), with no proper justification, described the Angolan material previously assigned to *P. frontalis* by Bocage (1873, 1882, 1895) as a new species, i.e., *P. angolensis* Boulenger, 1915, stating only how it differed from the only other Angolan congener at the time, *P. ambigua*. Additional material under the names *P. ambigua* and *P. angolensis* were recorded from central and western Angola by Monard (1931, 1937), Mertens (1937, 1938) and Bogert (1940). Until the mid-19th century, this was the only species of *Prosymna* known to occur in Angola, until Charles Koch collected a specimen from south-western Angola, that was later described as a new species, *Prosymna visseri* FitzSimons, 1959. When Broadley (1980) reviewed the *Prosymna* genus, he documented nominotypical *P. frontalis* from Benguela, collected by Wulf Haacke in the 1970's. This brought the number of *Prosymna* species occurring in Angola to four (Branch 2018; Marques et al. 2018).

Over the decades, the relationship of *P. angolensis* to other *Prosymna* species was addressed on a morphological basis by several authors, being considered as more closely related to *P. sundevalli* (Boulenger 1894), *P. lineata* (Bocage 1895), *P. ambigua* (Bogert 1940), and *P. frontalis* (Mertens 1955). Finally, with the whole genus revision,

Broadley (1980) was the first to attempt grouping *Prosymna* species based on shared morphological characters. He identified three main species groups (the *ambigua* group = *ambigua*, *ornatissima*, *semifasciata*, *stuhlmanni*; the *meleagris* group = *greigerti*, *meleagris*, *ruspolli*, *somalica*; the *sundevalli* group = *bivittata*, *lineata*, *sundevalli*). Whilst he briefly mentioned it might be part of the *sundevalli* group, he could not confidently assign *P. angolensis* to any of these groupings. With the aid of phylogenetics, Heinicke et al. (2020) partly validated Broadley's groupings, but due to the lack of *P. angolensis* genetic material, its relationship to its congeners remained unclear.

Since the description of *P. angolensis*, only a handful of specimens have been recorded from Angola (Monard 1931, 1937; Mertens 1937; Bogert 1940; Hellmich 1957; Baptista et al. 2019; Ceriaco et al. 2021a; Conradie et al. 2021). Specimens from outside of Angola were documented from northern Namibia (Mertens 1955), the Zambezi Region (= Caprivi Strip) in north-eastern Namibia, western Zambia, northern Botswana (Broadley 1980), and north-eastern Zimbabwe (Broadley 1995) (see Fig. 1). However, the specimens from Zambia and the Zambezi Region differ from the nominotypical Angolan form in the number of ventral scales (121–129 vs. 134–142),

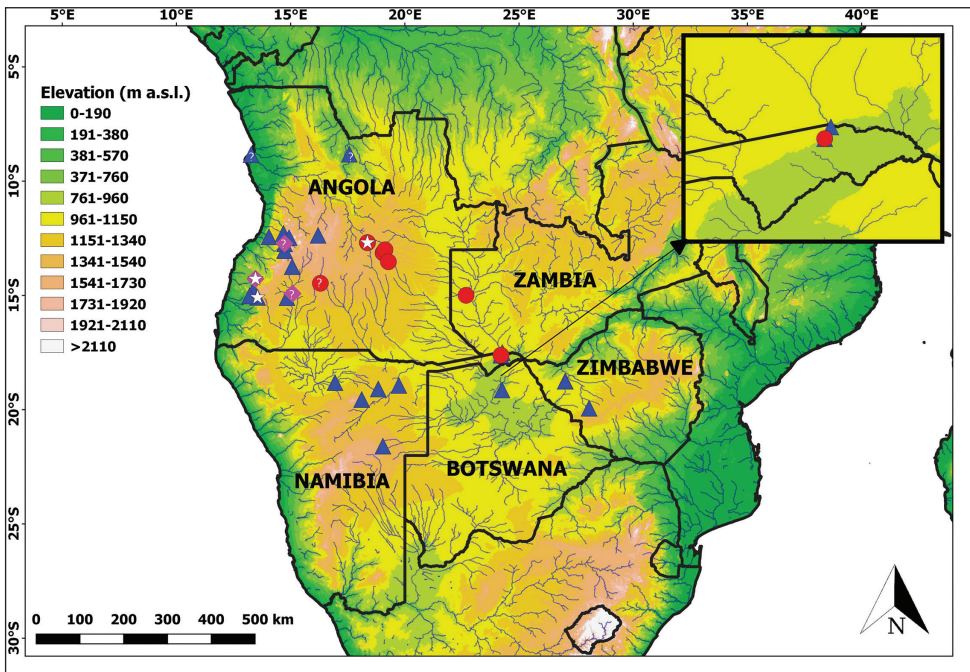


Figure 1. Geographic records of the *Prosymna angolensis* group, based on all literature records and newly examined material, including nominotypical *P. angolensis* (blue triangles), *Prosymna* ‘Eastern’ = *P. lisima* sp. nov. (red circles) and *Prosymna* ‘Coastal’ = *P. confusa* sp. nov. (purple diamonds). White stars represent respective type localities. Question marks represent material tentatively assigned to that species, but needs confirmation. Blue lines represent major river systems. Top right inset represents the eastern Zambezi Region, to show sympatry between *P. angolensis* and *Prosymna* ‘Eastern’ = *P. lisima* sp. nov.

number of postoculars (two vs. one), and dorsal colouration (large black confluent black blotches vs. mostly two dorsal rows of small paired black spots) (Broadley 1980). Interestingly, one specimen from Vila da Ponte (= Kuvango), in west/central Angola, exhibits the same combination of features (lower ventral scale counts, two postoculars and a dorsal pattern consisting of confluent black blotches posteriorly) (Monard 1937 fide Broadley 1980). Despite noticing these differences, Broadley (1980) did not make taxonomic changes, stating that a larger series was needed to clarify this issue.

Recent herpetological surveys undertaken in eastern and southwestern Angola led to the collection of several specimens assigned to *P. angolensis* (Branch 2018; Baptista et al. 2019; Conradie et al. 2021). The first was collected by William R. Branch from the coastal semi-arid lowlands in Namibe Province and was initially assigned to *P. ambigua* (Branch 2018). This identification was problematic because it had no morphological justification and was collected from a locality well outside the known range of that species. Upon re-examination of the specimen, it was concluded that it was a uniformly coloured *P. angolensis* (WC unpubl. data), another problematic identification, as it did not agree with the species description and this was the first record of *P. angolensis* from the more arid coastal plains of Angola. Nominotypical *P. angolensis*, which fully agrees with the original description, was collected from Bicular National Park in southwestern Angola (Baptista et al. 2019). Finally, during several expeditions to document the biodiversity of the headwaters of the Angolan Okavango-Cuando-Zambezi river basins in east-central Angola, a series of specimens was collected, and tentatively assigned to *P. angolensis* based on external morphology (Conradie et al. 2021), but they exhibited the same distinct characteristics reported from western Zambia and north-eastern Namibia specimens by Broadley (1980). This new material allowed us to revisit the taxonomical status and evolutionary relationships of *P. angolensis*, and investigate the morphological differences observed among these different populations using modern phylogenetic analysis and High Resolution X-ray Computed Tomography (HRCT).

Materials and methods

Sampling

At several sites during the 2016–2019 National Geographic Okavango Wilderness Project surveys, standard Y-shape intercept drift fence funnel trap arrays were deployed to passively collect specimens. Each Y-shaped trap array consisted of three drift fences (each 10 m long and 50 cm high) radiating from a central pitfall trap, with six one-way funnel traps placed on adjacent sides of each drift fence and three one-way funnels at the terminal ends of each drift fence. Trap arrays were installed in varied habitats to ensure the highest possible richness of captured species (Conradie et al. 2021). Consequently, a total of eight *Prosymna* individuals were captured. Snakes were euthanized by injecting them subcutaneously with tricaine methane sulfonate (MS222) solution (Conroy et al. 2009), after which they were formalin-fixed for 48 hours and

transferred to 70% ethanol for long-term storage. Prior to formalin fixing, tissue samples (liver) were preserved in 99% ethanol for subsequent genetic analysis. In addition, we included a recently collected specimen of nominotypical *P. angolensis* from Bicuar National Park (Baptista et al. 2019) and a specimen that was tentatively assigned to *P. ambigua* from southwestern Angola (Branch 2018), to complement the morphological and genetic analyses. Voucher specimens are held in the herpetological collection of Port Elizabeth Museum at Bayworld Complex (**PEM**), Gqeberha, South Africa and Coleção Herpetológica do Lubango (**CHL**), currently deposited in Instituto Superior de Ciências de Educação da Huíla (**ISCED-Huíla**), Lubango, Angola.

Additionally, *Prosymna angolensis* material examined by Broadley (1980) from the following institutions was included in this study:

AMNH	American Museum of Natural History, New York, USA;
CAS	California Academy of Sciences, Los Angeles, USA;
MBL	Museu Bocage, Lisbon, Portugal;
MCZ	Museum Comparative Zoology, Harvard, USA;
NMW	Naturhistorisches Museum zu Wien, Vienna, Austria;
NMZB/UM	National Museum of Zimbabwe, Bulawayo, Zimbabwe;
SAM	South African Museum (now Iziko Museums of South Africa), Cape Town, South Africa;
SMF	Forschungsinstitut und Natur-Museum Senckenberg, Frankfurt-am-Main, Germany;
TM	Transvaal Museum (now Ditsong National Museum of Natural History Northern Flagship Institute);
USBN	National Museum of Natural History, Washington, USA.

The original datasheets were made available to the authors by Sheila Broadley. Photographs of the following material were examined by WC: AMNH R50504, MCZ R-32468, NMW 19275.2 and SAM ZR16574.

DNA extraction, amplification, and sequencing

A standard salt extraction method (Bruford et al. 1992) was used to isolate DNA from the tissue sample using ATL lysis and AE elution buffers. Standard PCR procedures were utilised to amplify one partial mitochondrial ribosomal gene (ribosomal ribonucleic acid [*16S*]), two partial mitochondrial genes (cytochrome b [*cyt-b*] and NADH-dehydrogenase subunit 2 [*ND2*]) and one partial nuclear gene (oocyte maturation factor [*c-mos*]). The specific primer pairs used can be found in Table 1. Each amplification was conducted with a PCR mixture to the total volume of 25 µl containing 12.5 µl TopTaq Mastermix (Ampliqon; containing 2× master mix, 1.5 mM MgCl₂, 0.4 mM dNTPs, and Ampliqon Taq DNA polymerase), 2 µl forward primer (10 µM), 2 µl reverse primer (10 µM), 6.5 µl de-nucleated water and 2 µl genomic DNA (20–50 ng/µl). The cycling profile for all the genes was as follows: initial denaturing step at 94 °C for 5 min,

Table 1. Primers and PCR protocols used to generate sequences for the study.

Gene	Primer	Source	Annealing temperature (°C)
<i>16S</i>	L2510: 5'—CGCCTGTTTATCAAAAACAT—3'	Palumbi (1996)	50
	H3080: 5'—CCGGTCTGAACCTCAGATCACGT-3'		
<i>cyt-b</i>	WWF: 5'—AAAYCAYCGTTGTWATTCAACTAC—3'	Whiting et al. (2003)	52
	Cytb-R2: 5'—GGGTGRAAKGGRATTTTATC—3'		
<i>ND2</i>	ND2-F1-METF1: 5'—AAGCTTTCGGGCCCATACC—3'	Heinicke et al. (2014)	56
	ND2-R1-TRPR3: 5'—TTTAGGGCTTTGAAGGC—3'		
<i>c-mos</i>	S77: 5'—CAT GGACTGGGATCAGTTATG—3'	Slowinski and Lawson (2002)	52
	S78: 5'—CCTTGGGTGTGATTTTCT CACCT—3'		

followed by 35 cycles of 94 °C for 30 s, 50–60 °C for 45 s, and 72 °C for 45 s, with a final extension at 72 °C for 8 min. The prepared PCR products were purified and sequenced at MacroGen Corp. (Amsterdam, Netherlands) with the forward primers only.

Phylogenetic analyses

The phylogenetic placement of the newly collected *Prosymna* samples were estimated by comparing them with the sequenced data from Heinicke et al. (2020). In addition to the ingroup taxa (12 of the 16 currently recognised *Prosymna* species), the dataset was supplemented with sequences from closely related genera that were obtained from GenBank and used as outgroups (Appendix 1: Table A1).

The sequence trace files were checked using BioEdit Sequence Alignment Editor v. 7.2.5 (Hall 1999) and aligned with accessioned GenBank sequences using MEGA v.6.0 (Tamura et al. 2013) and the ClustalW alignment method. Four individual alignments were created (*16S*, *ND2*, *cyt-b*, *c-mos*) and added to the existing dataset from Heinicke et. al (2020), along with two additional nuclear markers (*RAG1* and *ENC-1*) from the same paper, which were used to resolve the deeper nodes. The congruency of the individual genes was tested using the homogeneity test implemented in PAUP4 v. 4.0a (Swofford 2003). All six gene alignments were not significantly different from one another allowing the creation of a concatenated dataset.

DAMBE v. 6.4.67 (Xia 2013) was used to test for saturation using the individual as well as the combined first and second codon positions of each gene. Saturation was absent from every marker, so a gene-partitioned dataset was created for the phylogenetic reconstruction. The optimal partition scheme and best-fitting models of molecular evolution were selected using ModelFinder implemented in IQ-TREE v.2.1.2 (Minh et al. 2021). The following settings were used: -p partition file (each partition has own evolution rate), a greedy strategy and the FreeRate heterogeneity model excluded (only invariable site and Gamma rate heterogeneity considered) (Chernomor et al. 2016; Kalyaanamoorthy et al. 2017). The best-fitting model scheme selected included the following three partitions and models of evolution: TIM2+I+G (*16S*); GTR+I+G (*cyt-b*, *ND2*); TN+G (*c-mos*, *RAG1*, *ENC-1*). MrBayes v.3.2.7a (Ronquist et al. 2012) and BEAST2 v.2.6.6 (Bouckaert et al. 2019) were not able to implement TIM2 or TN, so the next best alternative (GTR) was used in their place.

Phylogenetic reconstruction

Maximum likelihood (**ML**) analysis was conducted using IQ-TREE v.2.1.2 (Nguyen et al. 2015). A random starting tree was used using the gene-partitioned scheme mentioned above, the ultrafast bootstrap approximation (**UFBoot**) method (Hoang et al. 2018) and 1000 bootstrap replicates. Bayesian inference (**BI**) analysis was implemented using MrBayes v. 3.2.7a (Ronquist et al. 2012) and BEAST2 v. 2.6.6 (Drummond and Rambaut 2007; Suchard and Rambaut 2009) on the CIPRES Science Gateway XSEDE online resource (<http://www.phylo.org>; Miller et al. 2010; Tamura et al. 2013) using the gene-partitioned scheme mentioned above. For MrBayes, two parallel runs of 20 million generations were performed, with trees being sampled every 1000 generations using BEAGLE (high performance likelihood calculation library). Twenty percent of the generations were discarded as burn-in. For BEAST2, the analysis was run for 50 million generations and sampled every 10,000 generations. Ten percent of the sampled generations were discarded as burn-in. Using Tracer v. 1.6.0. (Rambaut and Drummond 2007), the effective sample size (**ESS**) was more than 200 for all parameters and the runs reached convergence, indicating that the burn-in for both BI phylogenies was adequate.

Species delimitation

Species delimitation was used to elucidate whether the putative Angolan taxa identified in the phylogenetic tree constituted separate species. Outgroup taxa were removed, leaving only members of *Prosymna* for single locus species delimitation. The *16S* and *cyt-b* genes were chosen as they had the best representation. The following species delimitation analyses were used: Automatic Barcode Discovery (**ABGD**), Assemble Species by Automatic Partitioning (**ASAP**), Poisson Tree Processes (**PTP**), and Bayesian Poisson Tree Processes (**bPTP**).

Firstly, a *16S* and *cyt-b* alignment were prepared and uploaded onto the ABGD web interface (abgd web (mnhn.fr), web version 07 July 2022) and the ASAP Web Interface (ASAP web (mnhn.fr), web version 07 July 2022). For ABGD, the followings settings were used: standard p-distance metrics, minimum barcode gap width (1), intraspecific divergence minima (0.001) and maxima (0.1) (Puillandre et al. 2012). For ASAP, the Simple Distance (p-distances) substitution model was used (Puillandre et al. 2021).

Secondly, a *16S* and *cyt-b* ML tree were created in IQTREE, both using the GTR + I + G substitution model and the same settings implemented in the multi-locus phylogeny. The phylogenies were rendered as newick files and uploaded unrooted onto the bPTP web server (<http://species.h-its.org/ptp/>; Zhang et al. 2013) for PTP and bPTP analysis. The individual gene trees were then rendered, using Figtree v.1.4.2 (Rambaut 2014), and the results from the different single-locus species delimitation analyses were overlaid.

Pairwise distance analysis

Pairwise distance analysis was implemented in MEGA X (Kumar et al. 2018) using the individual *16S* and *cyt-b* alignments, from the phylogenetic reconstruction. Sequences

were trimmed to reduce missing data from the datasets and sequences that still had more than 10% data were removed from the alignments to ensure the most accurate p-distance values were attained. For the *16S* alignment, the hyper-variable region was retained. Sequences were grouped according to species and pairwise distance analysis was conducted using the following settings: uniform rates, pairwise deletion and 500 bootstrap replicates.

Morphology

Morphological data was gathered from 39 *Prosymna angolensis* sensu lato (Table 2). Snout-vent length (SVL, measured from the tip of the snout to the posterior end of the cloacal scale or vent opening) and tail length (TL, measured from the cloacal opening to the tip of the tail) were measured to the nearest 1 mm using a flexible ruler or a tape measure. We also expressed the TL as a percentage of the total length (SVL + TL). The following scale counts were recorded using a Nikon SMZ1270 binocular stereo microscope: number of middorsal scale rows (counted one head length behind head, at midbody, and one head length anterior to the cloacal scale), number of preoculars, number of postoculars, the temporal scale arrangement, number of supralabials and the number of supralabials entering orbit, number of infralabials and number of infralabials in contact with 1st sublinguals, the presence of loreal, the number of ventral scales (Dowling 1951a), number of subcaudal scales (counted from anterior cloaca, excluding the terminal spine) and cloacal scale condition (divided or entire). Scale row reduction was also recorded (Dowling 1951b).

Table 2. Summary of morphological features and measurements for *Prosymna angolensis* group. For abbreviations see Materials and methods. Notes: * including data on the Ebanga (Monard 1937) and Capelongo (Bogert 1940) specimens.

	<i>P. angolensis</i>		<i>P. lisima</i> sp. nov.		<i>P. confusa</i> sp. nov.*
	Males	Females	Males	Females	Females
Sample size	6	21	7	3	3
SVL (mm)	160–248 (208.7 ± 29.8)	127–305 (224.7 ± 51.1)	138–198 (180.7 ± 20.5)	168–275 (214.3 ± 54.9)	231–240 (235.5 ± 6.4)
TL (mm)	22–30 (26.5 ± 2.7)	12–27 (29.9 ± 3.7)	17.0–28.9 (24.6 ± 3.7)	19.3–28.0 (22.6 ± 4.7)	23–29 (26.0 ± 4.2)
TL/total length ratio (%)	10.1–13.3 (11.40 ± 1.2)	6.5–9.4 (7.9 ± 0.9)	11.0–13.0 (12.0 ± 0.8)	8.8–10.9 (9.7 ± 1.1)	9.1–108 (9.9 ± 1.2)
Ventral scales	126–155 (138.1 ± 10.4)	134–163 (147.5 ± 8.3)	116–124 (120.2 ± 3.1)	117–129 (122.3 ± 6.1)	143–155 (149.7 ± 6.1)
Subcaudal scales	22–28 (25.4 ± 1.8)	16–25 (18.9 ± 2.5)	22–26 (23.7 ± 1.9)	18–24 (20.0 ± 3.5)	17–26 (21.0 ± 4.6)
Midbody scale rows	17-15-15 (rarely 19-15-15)		17-15-15		17-15-15
Cloacal scale	Entire		Entire		Entire
Preoculars	1		1 (rarely 2)		1
Postoculars	1 (rarely 0 or 2)		2		1
Temporals	1+2 (rarely 2+2, 2, 3)		1+2 (rarely 1+2+3)		1+5
Supralabials (contacting eye)	6 (3,4) [rarely 5 (2,3) or 7 (3,4)]		6 (3,4) [rarely 5 (2,3)]		5–6 (3, 4)
Infralabials (in contact with 1 st chin shield)	7 (3) [rarely 8 (3)]		7 (3)		7 (3)
Loreal	Present		Present		Present

For morphological comparison we preassigned material into three distinct groups based on the shared morphological and colouration differences observed by Broadley (1980) and our personal observations: 1) the nominotypical group which includes material (6 males; 21 females) from west/central Angola, northern Namibia, northern Botswana and north-eastern Zimbabwe (hereafter referred to as *P. angolensis* sensu stricto), 2) a group which includes material (7 males and 3 females) from eastern Angola, western Zambia and north-eastern Namibian (hereafter refer to as *Prosymna* ‘Eastern’), and a single female specimen from the coastal Angolan lowlands (PEM R24013) (hereafter refer to as *Prosymna* ‘Coastal’). We could not include the latter group in significant testing due to that we only had one confirmed sample.

To test if the ventral and subcaudal scale counts differs significantly between *Prosymna* ‘Eastern’ and *P. angolensis* sensu stricto as reported by Broadley (1980), we first corrected for size by dividing the ventral scale counts by the SVL and the subcaudal scale counts by the TL. The data was then separated by sex for further analyses. Due to our small sample size, we conducted a Shapiro-Wilk normality test and found that our data is not normally distributed and thus we proceed in conducting a non-parametric Wilcoxon test. We display the results using standard boxplots. All above-mentioned quantitative statistical comparisons were conducted using R v.4.1.0 (R Core Team 2021).

Skull osteology

In order to identify diagnostic osteological characters and evaluate cranial variability within this group, we compared High Resolution X-ray Computed Tomography (HRCT) of newly collected material from Angola with *Prosymna* data provided by Heinicke et al. (2020), and two additional species (*P. janii* and *P. cf. frontalis*) not included in the previous study. We generated and analysed HRCT of three newly collected specimens from Angola (PEM R23512 [male], PEM R23510 [male] and PEM R24013 [female]), one specimen of *P. angolensis* (SAM ZR16574 [female]), one *P. cf. frontalis* (PEM R17997 [male]) and one *P. janii* (PEM R08679 [male]) at Stellenbosch University CT Scanner Facility using a General Electric Nanotom S system, using the settings specified in Appendix 1: Table A2. All specimens were regarded as adults. Three-dimensional segmentation models were generated for the articulated skull in Avizo Lite 2020.2 (Thermo Fisher Scientific 2020). To facilitate visualization, individual bone units for skulls and jaws were coloured following the same colour palette as Lobón-Rovira and Bauer (2021). All rendered files (*.ply) of premaxilla, palatine and maxilla, were analysed in Mesh Lab (2020.2) for colour processing and stacking of reconstructed in lateral, dorsal, ventral or medial views. Annotations were made in Adobe Illustrator CC 22.0.1 (Adobe Systems Incorporated 2017) following the anatomical terminology of Heinicke et al. (2020) and Broadley (1980). CT-scan raw data (.tiff files) have been deposited in MorphoSource (www.morphosource.org; Project ID 435270, Appendix 1: Table A2).

Mapping

To enable the production of up-to-date occurrence maps for the *Prosymna angolensis* group, data were sourced from published datasets (e.g., Broadley 1980, 1995; Marques et al. 2018) and museum databases. Online virtual museum platforms (<http://www.inaturalist.org>, <http://vmus.adu.org.za>, <http://www.the-eis.com/atlas/>; all accessed 31 July 2022) were also consulted and only a single record from the Namibian Atlas project was found that agreed with the diagnostic features identified by Broadley (1980) for *P. angolensis*. We gathered a total of 55 records that were assignable to *Prosymna angolensis* sensu lato. The online GeoNames gazetteer (<http://www.geonames.org/>) or GEOLocate Web Application (<https://www.geo-locate.org/web/WebGeoref.aspx>) were used to georeference all historical data. Distribution data were mapped in QGIS v. 3.2 (<http://qgis.org>).

Results

Phylogenetic analyses

Maximum likelihood (bootstrap support [BS]) and both Bayesian Inference analyses (MrBayes posterior probability [MBPP]; BEAST posterior probability [BPP]) showed strong support for the monophyly of *Prosymna* (BS 100%, MBPP 1.0, BPP 1.0). (Fig. 2). The genus was characterised by four clades, identical to those found in Heinicke et al. (2020): *meleagris* group, south-western taxa, *ambigua* group, and *sundevalli* group. Whilst the inter-group structuring lacked support across the different algorithms, most of the relationships between sister species within the four groups were well supported.

The newly sequenced *P. angolensis* sensu lato material (hereafter '*angolensis* subgroup') formed a monophyletic group, that was recovered within the *sundevalli* group by all three algorithms (BS 100%, MBPP 1.0, BPP 1.0). All three algorithms also retrieved identical topological sub-structuring within the *sundevalli* group, with strong support for the sister relationship between *P. lineata* and the rest of the species in the group. The sister relationship between *P. sundevalli* + *P. bivittata* and the *angolensis* subgroup was however not supported by any of the algorithms. Whilst all the phylogenies recovered the *angolensis* subgroup as monophyletic, they differed in their sub-structuring, with ML (BS 100%) and BEAST (BPP 1.0) recovering *Prosymna* 'Coastal' as sister to *Prosymna* 'Eastern' + *P. angolensis* sensu stricto and MrBayes (MBPP 1.0) recovering *P. angolensis* sensu stricto as sister to *Prosymna* 'Coastal' + *Prosymna* 'Eastern'. All three algorithms recovered similar sub-structuring within the *Prosymna* 'Eastern' lineage with a specimen from Quembo River bridge camp (PEM R27381, Appendix 1: Table A1) being recovered as sister to the rest of the samples (BS 100%, MBPP 1.0, BPP 1.0).

The single locus ML phylogenies (Fig. 2b) produced similar topological structuring to the concatenated dataset, albeit with markedly lower support. Where the topologies do differ, the nodes lack support. Although inter-group support is low, the intra-group support is high and is similar to that observed in multi-locus phylogeny (Fig. 2a). Simi-

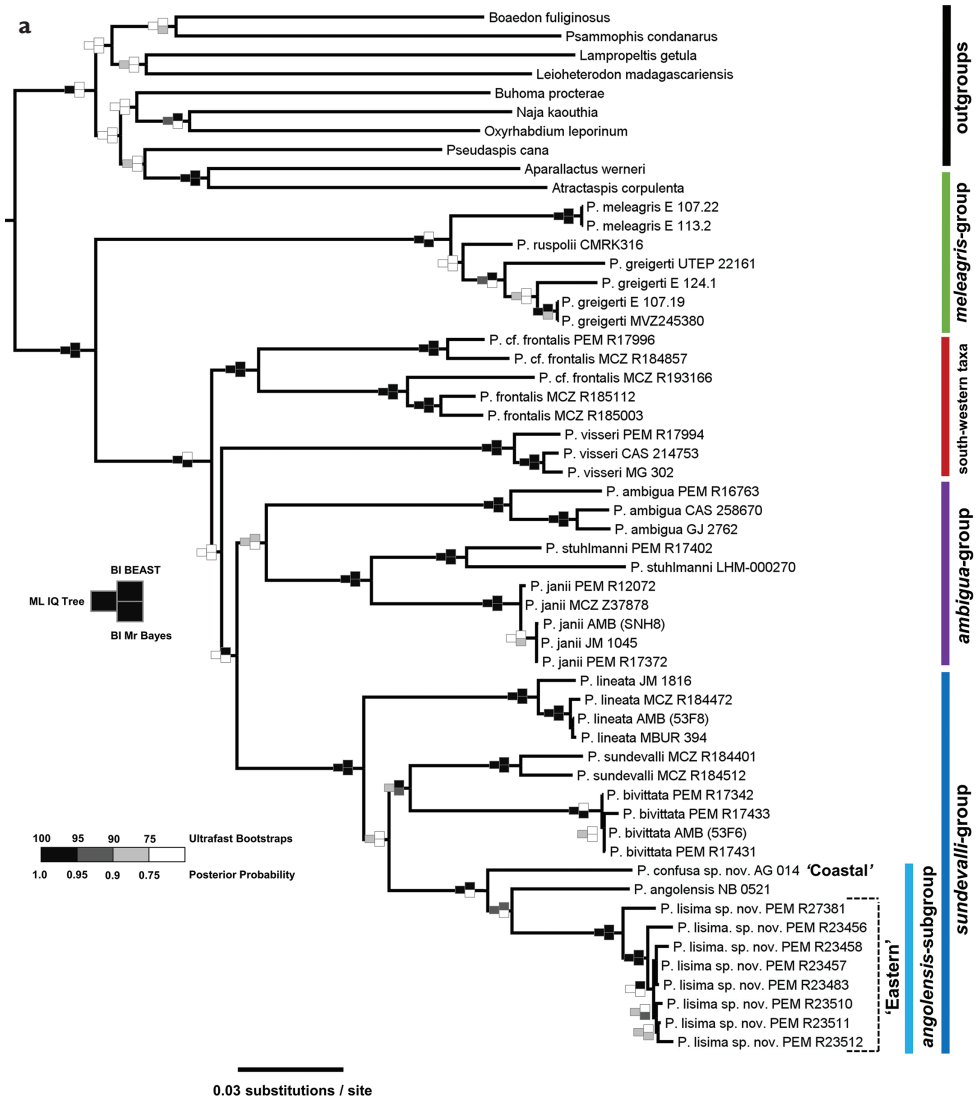


Figure 2. a Maximum likelihood (IQTREE) concatenated phylogeny with BI BEAST and BI MrBayes support overlain. Each of the species groups are demarcated by coloured vertical bars at the right margin **b** maximum likelihood (IQTREE) phylogenies (*16S* and *cyt-b*) with gene-specific single-locus species delimitation analyses results overlain. The bars to the right of the phylogeny represent the putative taxa assignments for each analysis and the values beneath the bars denote the total number of putative taxa for each analysis.

lar to the multi-locus phylogeny (Fig. 2a), the novel Angolan specimens were recovered as a monophyletic clade with both *16S* (BS 100%) and *cyt-b* (BS 100%) recovering *Prosymna* ‘Coastal’ as sister to *Prosymna* ‘Eastern’+ *P. angolensis* sensu stricto.

The species delimitation analyses employed across both the *16S* and *cyt-b* phylogenies recovered a substantial amount of putative taxa, with vastly different estimates

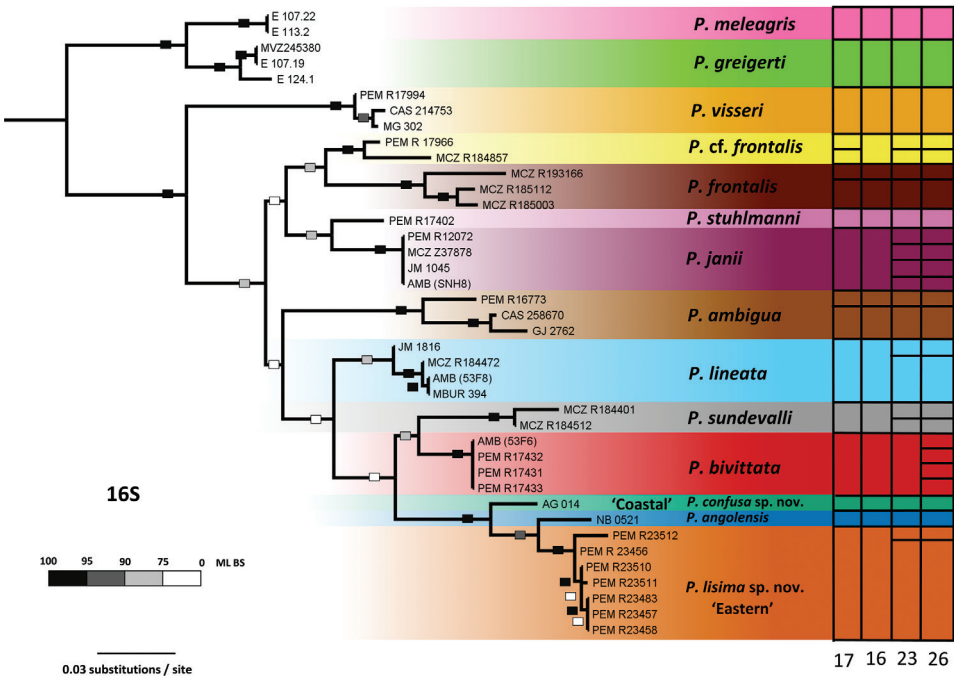
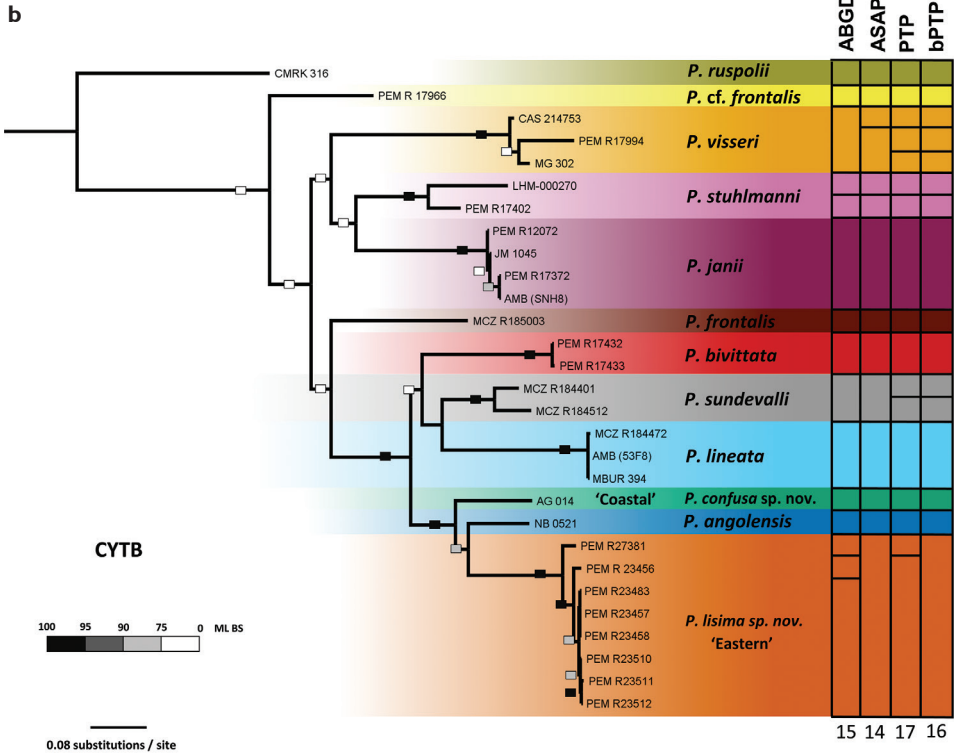


Figure 2. Continued.

between the different analyses. Across both phylogenies, ABGD and ASAP were more conservative and PTP and bPTP were more liberal with the number of putative taxa. Whilst the differential sampling afforded to the different gene phylogenies resulted in differing numbers of putative taxa, it must be noted that all four species delimitation methods recognised *Prosymna* ‘Eastern’, *Prosymna* ‘Coastal’ and *P. angolensis* sensu stricto as independent species when using both the *16S* and *cyt-b* marker. While not the focus of this study, notable cryptic speciation was also recovered in *P. frontalis*, *P. ambigua*, and *P. stuhlmanni* when using either the *16S* or *cyt-b* marker.

The average *16S* pairwise divergence separating species within the genus was 8.11% ($\pm 0.23\%$ s.e. – standard error) when the *angolensis* subgroup is considered a single species (Table 3). While the average pairwise divergences separating the three lineages of the *angolensis* subgroup from the rest of the genus varies from 6.99% ($\pm 0.52\%$ s.e.) to 7.99% ($\pm 0.67\%$ s.e.). Although the *angolensis* subgroup is well delineated from the rest of the genus, when these lineages are compared to one another, the *angolensis* subgroup was characterised by relatively low pairwise divergences. *Prosymna angolensis* sensu stricto was separated from *Prosymna* ‘Eastern’ material by an average

Table 3. Sequence divergence (uncorrected pairwise distance values) for *16S* and *cyt-b* separating the species of *Prosymna*. Numbers in the diagonal (in bold) denote intraspecific divergences, numbers below the diagonal denote interspecific divergences and numbers above the diagonal denote the standard error of the interspecific divergences. NA–Not Available.

		<i>16S</i>												
		1	2	3	4	5	6	7	8	9	10	11	12	13
1	<i>P. ambigua</i>	3.02	1.28	1.19	1.23	1.07	1.28	1.15	1.03	1.36	1.31	1.13	1.22	1.19
2	<i>P. angolensis</i>	8.58	NA	1.19	0.89	1.08	1.37	1.21	1.21	0.75	1.39	1.23	1.16	1.30
3	<i>P. bivittata</i>	7.28	6.26	0	1.00	1.12	1.39	1.35	1.09	1.28	1.41	1.23	0.95	1.31
4	<i>P. confusa</i> sp. nov. ‘Coastal’	8.34	3.75	5.07	NA	1.11	1.28	1.29	1.15	0.99	1.30	1.25	1.01	1.32
5	<i>P. frontalis</i>	8.11	7.71	8.01	8.14	5.28	1.22	1.01	0.99	1.15	1.23	0.93	1.08	1.13
6	<i>P. greigerti</i>	9.55	9.96	10.44	8.82	9.84	1.55	1.28	1.30	1.38	0.64	1.34	1.36	1.28
7	<i>P. janii</i>	7.51	7.32	8.63	7.96	6.75	8.35	0	1.02	1.30	1.24	0.93	1.29	1.23
8	<i>P. lineata</i>	6.50	6.73	5.87	6.39	6.93	9.44	5.78	0.69	1.22	1.27	0.92	1.07	1.20
9	<i>P. lisima</i> sp. nov. ‘Eastern’	10.06	2.92	7.53	4.76	8.56	10.85	8.53	7.36	0.63	1.40	1.30	1.25	1.27
10	<i>P. meleagris</i>	9.62	10.11	10.31	9.16	10.26	2.82	8.39	9.47	11.03	2.52	1.28	1.39	1.32
11	<i>P. stuhlmanni</i>	7.58	7.76	7.51	7.52	6.16	9.24	3.96	5.07	8.37	9.31	NA	1.20	1.25
12	<i>P. sundevalli</i>	8.56	7.63	4.97	5.63	7.85	11.11	8.92	6.32	8.16	11.68	8.04	1.54	1.28
13	<i>P. visseri</i>	7.88	8.38	8.01	8.36	8.01	9.07	7.40	7.90	7.76	9.49	7.77	8.64	0.74
		<i>cyt-b</i>												
		1	2	3	4	5	6	7	8	9	10	11		
1	<i>P. angolensis</i>	NA	1.43	1.40	1.38	1.58	1.56	1.31	1.67	1.70	1.39	1.64		
2	<i>P. bivittata</i>	15.76	0.33	1.41	1.32	1.60	1.55	1.57	1.70	1.72	1.40	1.64		
3	<i>P. confusa</i> sp. nov. ‘Coastal’	13.25	16.35	NA	1.38	1.62	1.60	1.47	1.70	1.72	1.32	1.74		
4	<i>P. frontalis</i>	19.95	19.72	19.28	17.97	1.44	1.45	1.44	1.49	1.35	1.34	1.47		
5	<i>P. janii</i>	19.64	21.50	19.91	20.17	1.08	1.59	1.57	1.72	1.62	1.51	1.67		
6	<i>P. lineata</i>	18.92	17.84	18.36	20.18	20.16	0.22	1.55	1.82	1.73	1.38	1.66		
7	<i>P. lisima</i> sp. nov. ‘Eastern’	13.90	18.73	15.55	21.38	19.75	17.67	1.58	1.71	1.69	1.39	1.58		
8	<i>P. ruspolii</i>	23.86	24.05	23.75	23.45	24.40	25.26	23.81	NA	1.80	1.67	1.69		
9	<i>P. stuhlmanni</i>	20.75	20.92	20.83	18.79	17.97	20.52	20.68	23.47	NA	1.45	1.65		
10	<i>P. sundevalli</i>	15.99	16.08	14.63	19.51	18.97	15.39	17.61	23.70	17.52	6.49	1.59		
11	<i>P. visseri</i>	21.87	22.29	22.38	21.27	20.33	22.57	21.73	25.04	19.56	20.49	3.09		

pairwise distance of 2.92% ($\pm 0.75\%$ s.e.) and from the *Prosymna* 'Coastal' sample by 3.75% ($\pm 0.89\%$ s.e.), while the *Prosymna* 'Eastern' and *Prosymna* 'Coastal' material were separated by 4.76% ($\pm 0.99\%$ s.e.).

For the *cyt-b* gene, the average pairwise divergence separating species of the genus was 20.60% ($\pm 0.42\%$ s.e.) (Table 3). The average pairwise divergences separating the three lineages of the *angolensis* subgroup from the rest of *Prosymna* varies from 18.39% ($\pm 1.11\%$ s.e.) to 19.08% ($\pm 0.95\%$ s.e.). Like the *16S* gene, the *angolensis* subgroup was characterised by lower pairwise divergences when these three lineages were compared to each other, albeit relatively higher than what was found when using the *16S* gene. *Prosymna angolensis* sensu stricto was separated from *Prosymna* 'Eastern' material by a pairwise distance of 13.90% ($\pm 1.31\%$ s.e.) and from *Prosymna* 'Coastal' material by a pairwise distance of 13.25% ($\pm 1.40\%$ s.e.), while eastern *Prosymna* 'Coastal' material is separated from the *Prosymna* 'Eastern' specimen by 15.55% ($\pm 1.47\%$ s.e.).

Morphology

There was a degree of overlap in most morphological features (measurements and scale counts) for all the material examined (Table 2). Although *Prosymna* 'Eastern' has lower number of ventral scales (116–129 [average 121] compared to *Prosymna angolensis* sensu stricto (126–163 [average 145])), the results of the non-parametric Wilcoxon test showed that there are no significant differences in the ventral and subcaudal scale counts when corrected for size for both sexes (Fig. 3). The only other consistent scalation differences between the *P. angolensis* sensu stricto and *Prosymna* 'Eastern' material, was the number of postoculars: predominantly has one postocular (only 4 of 31 had two postoculars) vs. always have two postoculars ($n = 10$), respectively. Due to small sample size, the morphology of the single specimen of *Prosymna* 'Coastal' could not be statistically compared with the other two lineages. It exhibited similar scalation to *P. angolensis* sensu stricto (i. e., presence of a higher ventral scales count and presence of a single postocular) (Table 2), but differ in dorsal colouration (see below).

Colouration

The colouration of *P. angolensis* sensu stricto (24 out of 28 examined) varied from pale grey to yellow-brown with a large black bar behind the head and a series of smaller paired black spots along the back, similar to *P. sundevalli*. In some cases (2 out of 28 examined), these black spots are very faint and disappear anteriorly or form continuous faint paravertebral stripes (2 out of 28 examined), similar to *P. lineata* (Fig. 4). On the other hand, all material from *Prosymna* 'Eastern' ($n = 10$) exhibited a golden yellow dorsum colouration with a large black bar behind the head, followed by fused irregular black blotches along the back continuing onto the tail (Fig. 5). The only subadult male collected had smaller paired dorsal black spots, similar to the main population but more defined (Fig. 5D). Although we could not statistically compare the morphology of the *Prosymna* 'Coastal' specimen, it has uniform dark grey dorsum with a very faint black bar behind the head (Fig. 6).

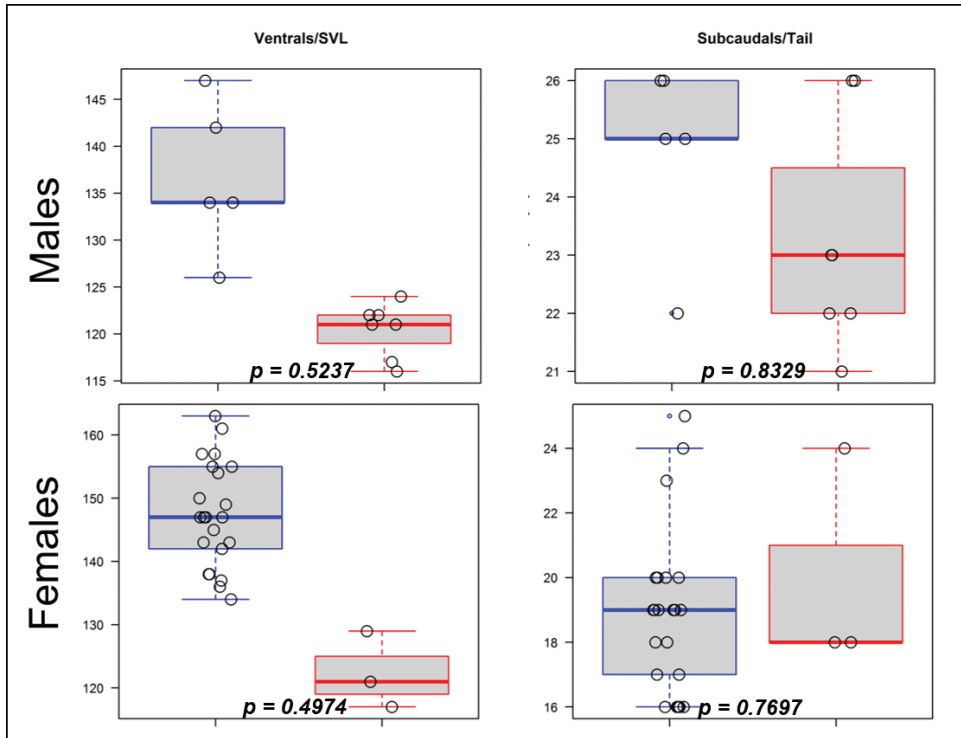


Figure 3. Summary boxplots (top whisker–maximum value; lower whisker–minimum value; dark horizontal line–median; box–1st and 3rd quartiles, open circles–data points) comparing ventral and subcaudal scales corrected for size among the species of *Prosymna* separated by sex: *Prosymna angolensis* (blue) and *Prosymna lisima* sp. nov. (red); *p*-value of non-parametric Wilcoxon test is indicated at bottom of each boxplot. *Prosymna confusa* sp. nov. is not included due to small sample size.

Skull osteology (Figs 7–9)

The osteological analysis has shown that material within the *angolensis* subgroup presents the same common features shared across *Prosymna*: a compact and rigid skull, anterior reduction of the maxilla, enlargement of the posterior maxillary teeth and reduced palatine, and a unique tooth loci formula with seven reduced tooth loci and four or five posterior lancet-shaped and enlarged tooth loci (see Heinicke et al. 2020). Some specimens in the *angolensis* subgroup had more than four frontal foramina present, such as in *P. angolensis* sensu stricto and *Prosymna* 'Eastern', vs. one or two in *Prosymna* 'Coastal'.

The *angolensis* subgroup shares some cranial features with the rest of the *sundevalli* group, such as an elongated maxillary process, with the premaxilla being in contact with the maxilla and the lack of a postorbital bone (except *Prosymna* 'Eastern', see below). It differs from the *sundevalli* group by the absence of partial or total fusion between the braincase and the parietal bone and the absence of lateral tubercles in the premaxilla in *angolensis* subgroup (vs. present in *sundevalli* group).

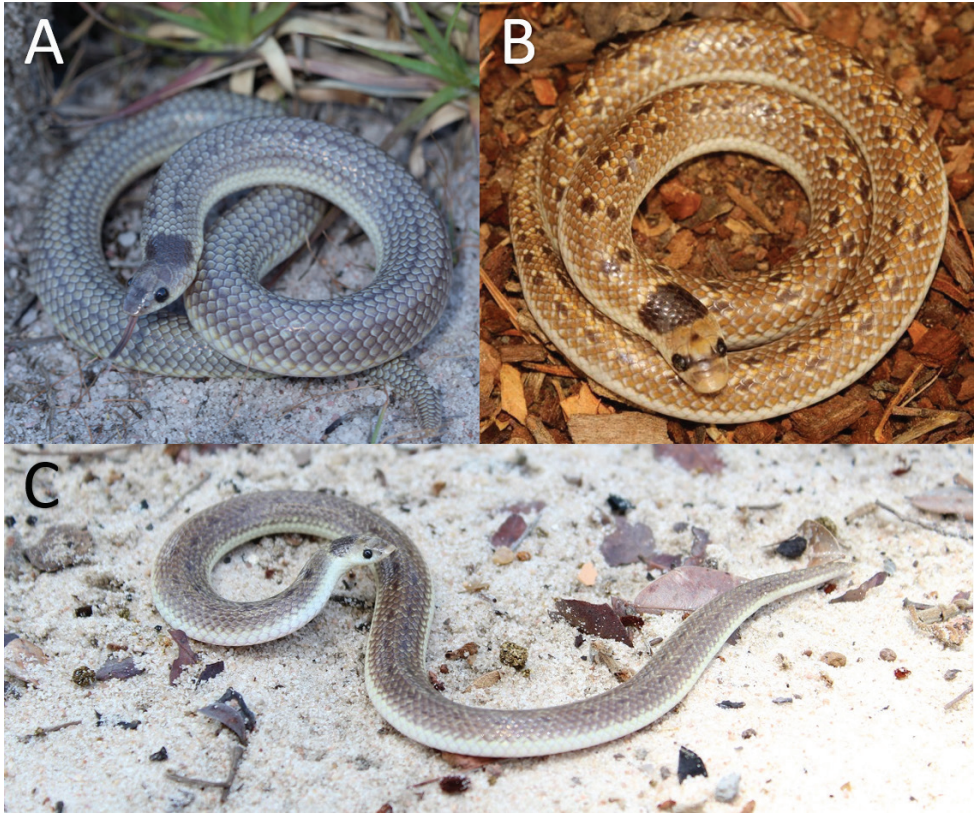


Figure 4. Variation in dorsal colouration of nominotypical *Prosymna angolensis* **A** Tundavala, Huíla Province, Angola (Photo: Justin R. Nicolau) **B** Grootfontein, Namibia (Photo: Francois Theart) **C** Bicuar National Park (CHL 0521), Huíla Province, Angola (Photo: Ninda L. Baptista).

The *Prosymna* ‘Eastern’ material is unique in possessing a well-developed postorbital bone, which is shared with *P.* cf. *frontalis* (although much more reduced) and the *ambigua* group (well developed, including here corroborated for *P. janii*). Two of the *angolensis* subgroup lineages (*P. angolensis* sensu stricto and *Prosymna* ‘Eastern’) present an unfused braincase (only known to be present in *ambigua* group, here corroborated for *P. janii*); however, the *Prosymna* ‘Coastal’ specimen presents a fused braincase.

Finally, the osteological comparison demonstrated the presence of unique diagnostic features between the three lineages from the *angolensis* subgroup, i.e., presence/absence of postorbital bone, fused/unfused braincases, and the number of palatine teeth and frontal foramina, which are addressed in more detail below.

Systematics

Based on the genetic, morphological, and colouration differences discussed above, we recognise all three lineages within the *angolensis* subgroup as independently evolving

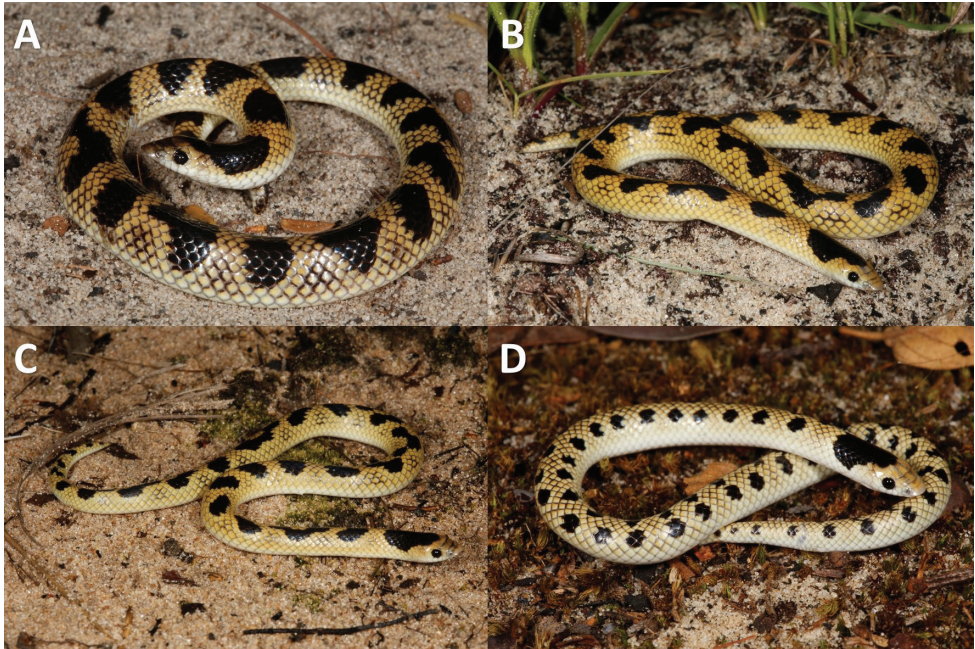


Figure 5. Photos of live *P. lisima* sp. nov. from eastern Angola **A** PEM R23457 from Quembo River Source, Moxico Province, Angola **B** PEM R23483 from Cuando River Source, Moxico Province, Angola **C** PEM R23512 from Cuito Source Lake, Moxico Province, Angola **D** PEM R27381 from Quembo River bridge camp, Moxico Province, Angola.



Figure 6. Live *P. confusa* sp. nov. (PEM R24013) from 20 km west of Lola on the road northwest to Camacuio and on the edge of Bentiaba River, Namibe Province, Angola (Photo: Bill Branch).

lineages and describe two (*Prosymna* ‘Eastern’ and *Prosymna* ‘Coastal’) of them as new species. We follow the general lineage-based species concept (de Queiroz 1998).

Reptilia: Squamata: Prosymnidae

Prosymna angolensis Boulenger, 1915

Figs 4, 7–9, 10

Common names: Angolan Shovel-snout snake (English); Cobra-de-focinho-de-pá-de-Angola (Portuguese).

Chresonymy.¹

Prosymna frontalis: Bocage 1873: 218, 1882: 288, 1895: 98; Boulenger 1894: 248, 1896: 641.

Prosymna ambigua: Monard 1931: 104, 1937: 123; Mertens 1937: 13.

Prosymna ambigua ambigua: Mertens 1938: 439; Loveridge 1958: 151.

Prosymna angolensis: Boulenger 1915: 208; Chabanaud 1916: 439; Monard 1937: 114, 122; Bogert 1940: 59; Mertens 1955: 94, 1971: 86; Hellmich 1957: 66; Loveridge 1958: 149; FitzSimons 1962: 161, 1966: 53, 1970: 104; Isemonger 1968: 129; Broadley 1980: 512, 1990: 227, 1995: 48; Auerbach 1987: 178; Branch 1998: 84, 2018: 64; Broadley et al. 2003: 187 (in part); Marais 2004: 236; Broadley and Blaylock 2013: 219; Herrmann and Branch 2013: 8; Wallach et al. 2014: 568; Baptista et al. 2019: 118; Chippaux and Jackson 2019: 283, Ceriaco et al. 2021a: 16 (in part).

When Boulenger (1915) described *P. angolensis*, he did not designate a precise type locality nor a type specimen for that matter. Later, Loveridge (1958) proposed designating Huíla as the type locality, but it was Broadley (1980) that finally restricted the type locality to Caconda by designating a lectotype of the material he examined on his visit to Museu Bocage, Lisbon (MBL), Portugal in 1968. The reasons for this change in the proposed type locality, were that the Huíla specimen was unaccounted for, as well as the Caconda material was in the best overall condition to represent the species. He initially designated MBL 1606b as the lectotype, but with the destruction of the MBL collection, he designated one of the remaining Caconda specimens in Naturhistorischen Museums in Wien (NMW 19275b) as the replacement neotype (see Gemel et al. 2019).

Material examined. *Neotype* (Fig. 10). NHMW 19275:2, collected from Caconda (approx. -13.73537, 15.06720, 1662 m a.s.l.), Huíla Province, Angola. Neotype designated by Donald Broadley (1980). **Additional material.** MBL 1609, Angola (no precise locality), Angola; MBL 1605a, Bibala, Angola; MBL 1605b, Bibala, Angola; CHL 0521, Bicular NP, Angola; NMW 19275:1, Caconda, Angola; NMW 19275:2, Caconda, Angola; MBL 1606a, Caconda, Angola; MBL 1606b (original lectotype), Caconda, Angola; MBL 1606c, Caconda, Angola; MBL 1608, Caconda, Angola; USBN 20035, Luanda, Angola; CAS 84181, Luanda, 3 mile S of airport, Angola;

1 Broadley (1980) listed Werner (1929: 142) as chresonymy of *Prosymna angolensis*, but we have removed it in this work as it refers to *Psammophis angolensis* (Bocage, 1872).

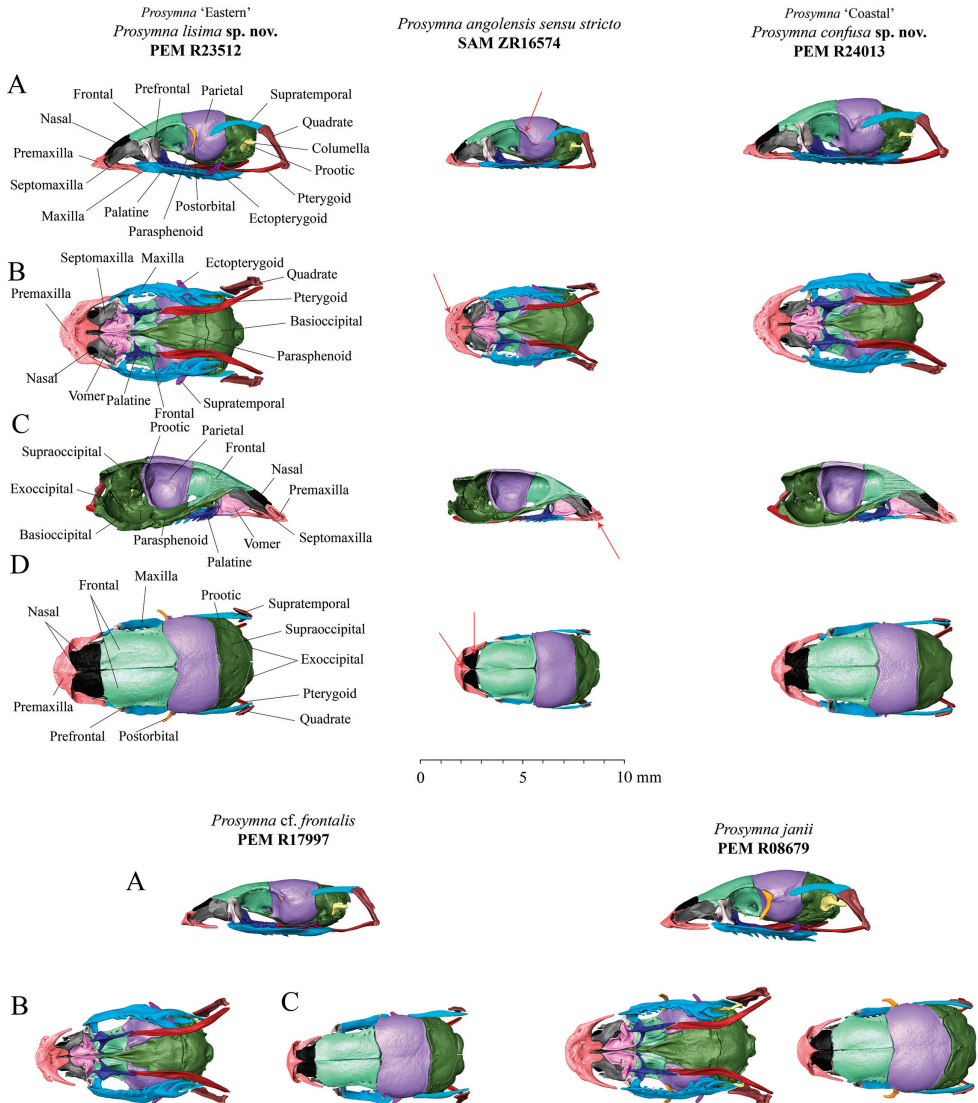


Figure 7. **A** lateral **B** ventral **C** medial **D** dorsal views of skulls of *Prosymna angolensis* subgroup. Red arrows depict variation characters between the *P. lisima* sp. nov., *P. angolensis*, *P. confusa* sp. nov., *P. cf. frontalis*, and *P. janii*.

MBL 1607, Maconjo = Maconge, Angola; MCZ 32468, Missão do Dondi Bela Vista, Angola; MBL 1604, interior of Mossamedes, Angola; UM 20178, Goeverega, Botswana; UM 21271, 15 km WSW of Katima Mulilo, Namibia; SMF 46614, Karakuwisa, Kavango, Namibia; TM 55043, Katima Mulilo, Namibia; UM 24204, Katima Mulilo, Namibia; SAM ZR16574, Namutoni, Namibia; NMZB 9532, NE of Waterberg, Namibia; NMZB 13953, Inyokene, Nyamandhlovo, Zimbabwe; NMZB 13787, Malinbdi Siding, Hwange, Zimbabwe; NMZB 13788, Malinbdi Siding, Hwange, Zimbabwe.

General description. See Table 2 for summarised meristic data. Dorsal scales smooth, arranged in 17-15-15 (rarely 19-15-15) rows at midbody, scale row reduction takes place between ventral scales 16–20 (males) and 14–49 (females); one (sometimes two or three on supracaudal scales) apical pits; 126–163 (126–155 males, 134–163 females) smooth ventral scales; 16–28 (22–28 males, 16–25 females) paired subcaudal scales; rostral is acutely angular horizontally; internasal is single and bandlike; 1 preocular; 1 (rarely 0 or 2) postocular; temporals mostly 1+2 (rarely 2+2, 2+3); mostly 6 supralabials, with 3rd and 4th entering the orbit (rarely 5 (2, 3) or 7 (3, 4)); 7 infralabials, with first 3 in contact with the chin shield (rarely 8 (3)), cloacal scale entire.

Skull osteology and teeth (Figs 7–9). Based on the examination of a single female specimen (SAM ZR16574, Namutoni, Namibia), *P. angolensis* presents a compact and rigid skull, which is common among *Prosymna* species. It has an unfused braincase and nasal bones. Parietals are fused and the fronto-lateral portion presents a sharp edge that forms the edge of the orbital rim. Postorbital bone is absent. Premaxilla has a reduced ascending nasal process with a small groove between the ascending process and frontal portion of the bone. Premaxilla lies between the ventral laminae of nasals with a high profile of the anterior portion which curves shapely to finish on a convex profile. Maxilla and premaxilla are in contact. Nasal bones are reduced and display a wing-shape with a narrower anterior portion. Septomaxilla is a well-developed bone, in broad contact with the premaxilla, frontal, vomer, prefrontal and frontal bones. Vomer well developed with perforated dorsolateral portion of the bone. Maxilla reduced anteriorly with an elongated pick-shaped palatine process, with seven or eight laterally reduced curved tooth loci, followed by four enlarged and lancet-shaped tooth loci. Palatine with three reduced teeth and an enlarged dorsal and curved vomerine process that reinforces the internal portion of the orbit. Pterygoid is a thin elongated bone. Supratemporal is an enlarged bone in broad contact with the quadrate and participates in the lateral movement of the lower jaw. The lower jaw consists of compound, splenial, coronoid, and dentary bones. Coronoid and splenial bones are reduced, almost vestigial. Dentary with eight or nine small sharp tooth loci, with first third clear of any teeth.

Colouration in life (Fig. 4). The head is yellowish-brown with variable darker black markings that can be absent. Most commonly there is an anterior black band across the frontal, followed by a pair of black blotches around the orbits, supraoculars and parietals. A distinct black nuchal spot or collar is often present. The dorsal colouration varies from having mostly small paired black longitudinal vertebral spots (similar to *P. sundevalli*) to a speckled pattern (similar to *P. lineata*) on a pale yellowish-brown to grey ground colour. Ventrums and outermost two or three dorsal scale rows yellowish white.

Hemipenis. Short hemipenis with a length that reaches the 9–10th ventral scales (Broadley 1980).

Size. Males vary from 160–248 (208.7 ± 29.8) mm SVL and 22–30 (26.5 ± 2.7) mm TL, with the largest male measuring 248+28 = 276 mm (NMZB 9532, NE of Waterberg, Namibia). Females vary from 127–305 (224.7 ± 51.1) mm SVL and 12–27 (19.9 ± 3.7) mm TL, with the largest female measuring 305+22 = 327 mm (SMF 32541,

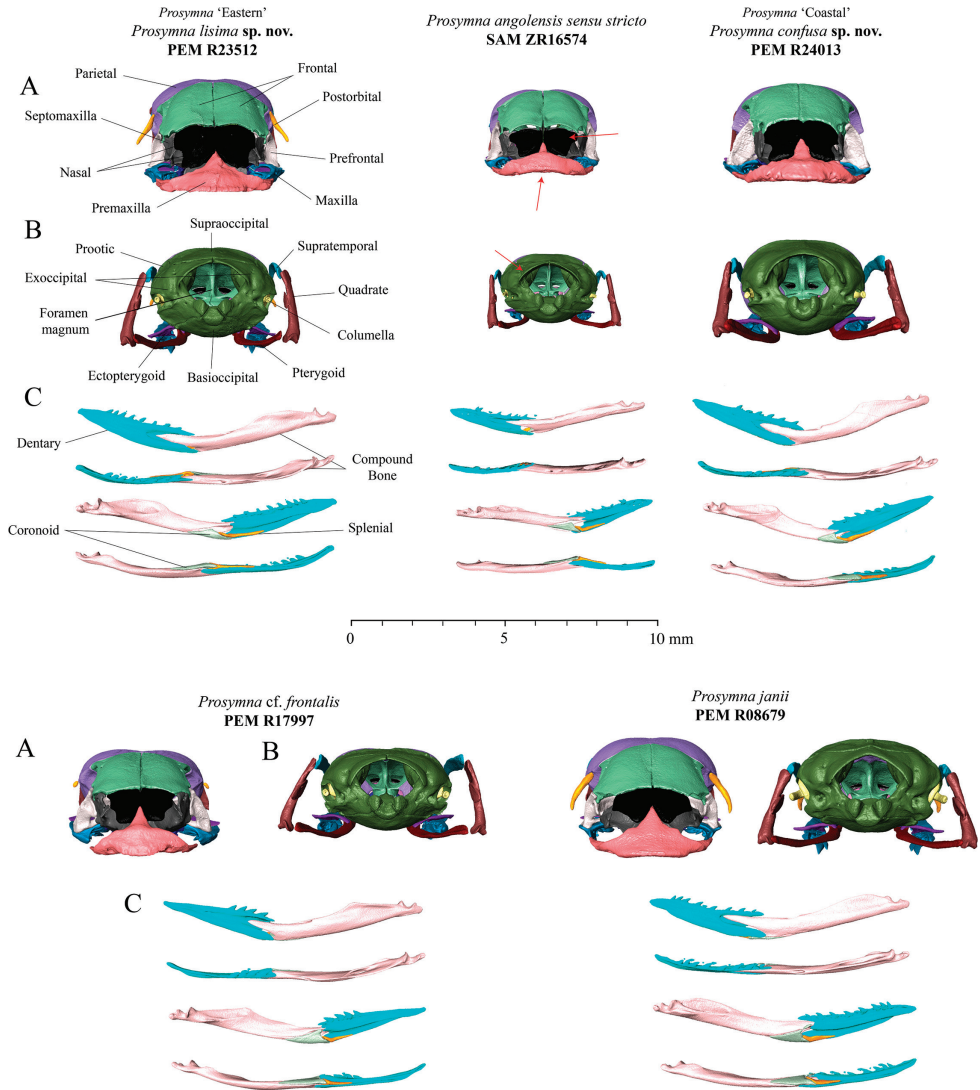


Figure 8. **A** Frontal and **B** posterior views of skulls, and **C** lateral, dorsal, medial and ventral view of jaw of *Prosymna angolensis* subgroup. Red arrows depict variation in characters between the *P. lisima* sp. nov., *P. angolensis*, *P. confusa* sp. nov., *P. cf. frontalis*, and *P. janii*.

Cubal, Angola). Bocage (1895) mentioned an unsexed individual (probably a female) that measured 331+29 = 360 mm, but this specimen was unaccounted for in MBL.

Natural history. This is a semi-fossorial species that feeds exclusively on reptile eggs, using its blade-like rear maxillary teeth to puncture the eggs, similar to other *Prosymna* species.

Distribution and habitat. Currently the species is known to occur in three main geographic clusters: west-central Angola, north-central Namibia and isolated records

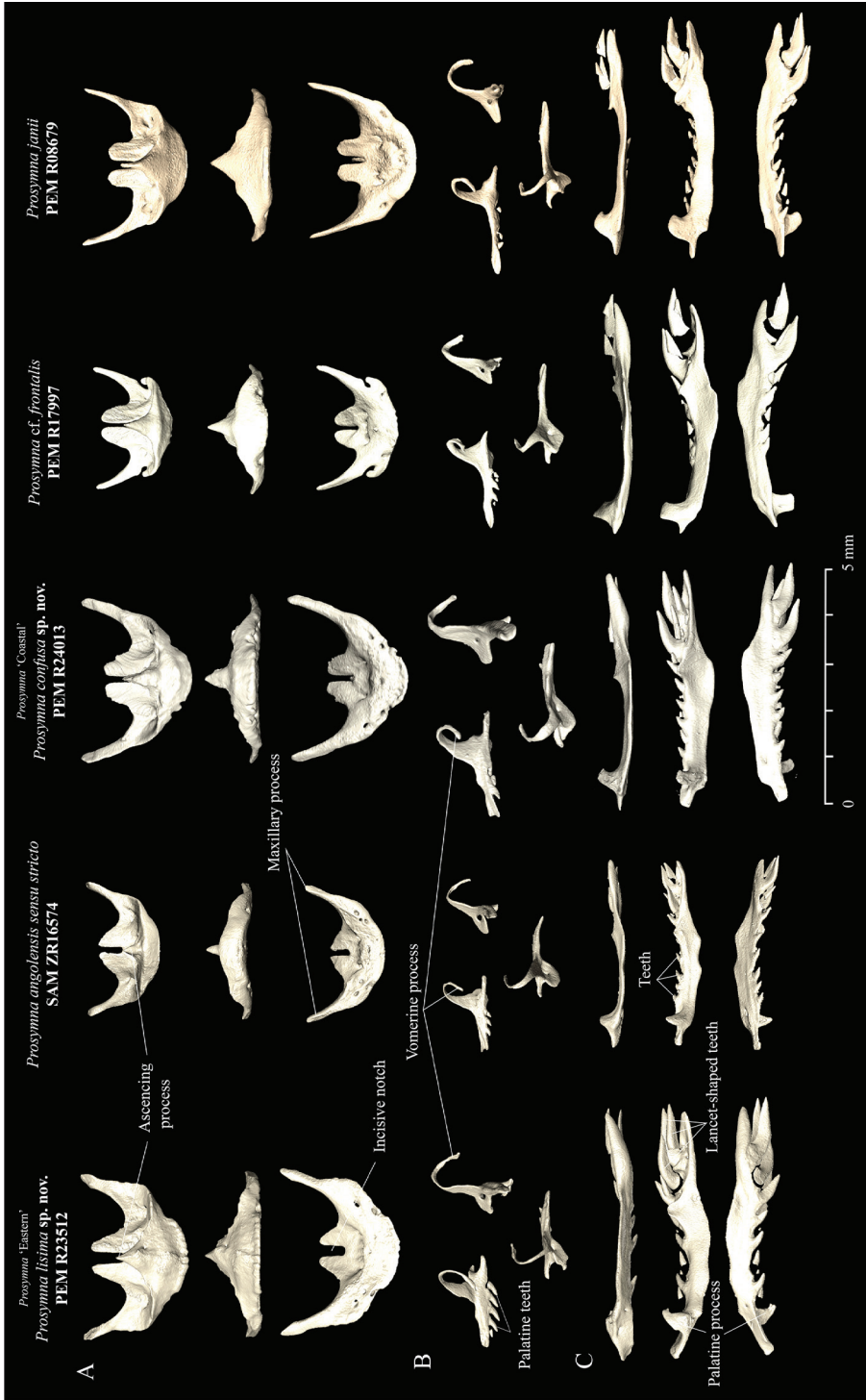


Figure 9. **A** Dorsal, frontal and ventral view of premaxillae **B** medial, posterior and dorsal views of palatine; and **C** lateral, dorsal, and ventral view of maxilla in *P. lisima* sp. nov., *P. angolensis*, *P. confusa* sp. nov., *P. cf. frontalis* and *P. janii* (from left to right).

from the Zambezi Region in north-eastern Namibia, northern Botswana and north-western Zimbabwe (Fig. 2). However, it is possible that this distribution might be more continuous, given this is a rarely observed species that mostly emerges to the surface only after good rains (Heinicke et al. 2020). The records from Luanda (USBN 20035 and CAS 84181) and northern Angola (IICT/R 14-1957) require verification. This species is associated with savanna with an annual rainfall of 500–1200 mm (Broadley 1980). In southwestern Angola it has been found in miombo woodland in sandy soils (Baptista et al. 2019). In the eastern Zambezi Region and northern Botswana, the species is associated with drier savanna in deep Kalahari sands (Broadley 1980).

Localities. ANGOLA: Bela-Vista (Missão do Dondi), -12.36667, 16.20000 (Hellmich 1957: 66); interior of Benguela (Bocage 1895: 98); Bibala, -14.76667, 13.36667 (Bocage 1873: 218); Bicuar National Park, Woodland trapline 1, -15.09441, 14.83831 (Baptista et al. 2019: 118); Caconda, -13.73537, 15.06720 (Bocage 1895: 151); Cubal, -13.03333, 14.73333 (Mertens 1938: 439); Ebanga, -12.73333, 14.73333 (Monard 1937: 123); Huíla, -15.08333, 13.55000 (Bocage 1895: 98); Luanda and ‘Luanda, 3 mi S of airport’, -8.83333, 13.26667 (Broadley 1980: 515); Maconjo, -15.016667, 13.2000 (Bocage



Figure 10. Neotype of *Prosymna angolensis* (NMW 19275:2) from Caconda, Huíla Province, Angola (Photos: Alice Schumacher, Natural History Museum Vienna).

1895: 98); interior of Mossamedes (Bocage 1873: 218); Quibula, -12.28333, 14.68333 (Bocage 1895: 98); Posto do Milando (-8.81667, 17.56667) (Ceríaco et al. 2021a: 16). Quindumbo, -12.46667, 14.93333 (Bocage 1895: 98); Quissange, -12.43333, 14.05000 (Bocage 1895: 98); Tundavala, -14.82018, 13.404217 (Justin Nicolau photo). **BOTSWANA:** Joverega (Geoverega), -19.13333, 24.25 (Broadley 1980: 515). **NAMIBIA:** Grootfontein, -19.55012, 18.10965 (Francois Theart photo); Karakuwisa, -18.933333, 19.733333 (Mertens 1955: 94); Katima Mulilo, -17.5, 24.266667 (Broadley 1980: 515); Namutoni, -18.807624, 16.940288 (FitzSimons 1962: 161); 15 km WSW of Katima Mulilo, -17.61448, 24.205932 (Broadley 1980: 515); Otjozondjupa Region, -19.08800, 18.83300 (http://www.the-eis.com/atlas/?q=details/snake-record&occurrence_id=654386). **ZIMBABWE:** Malindi Siding, Hwange, -18.74885, 27.01852 (Broadley 1995: 48); Inyokene, Nyamandlovu, -19.93333, 28.06667 (Broadley 1995: 48).

***Prosymna lisima* sp. nov.**

<https://zoobank.org/70A338BA-ED44-440B-AE3B-863E84B3AFBE>

Figs 5, 7–9, 11, 12

Common names: Kalahari Shovel-snout snake (English); Cobra-de-focinho-de-pá-do-kalahari (Portuguese).

Chresonymy.

Prosymna angolensis: Broadley 1971: 82, 1980: 512 (in part); Broadley et al. 2003: 187 (in part); Pietersen et al. 2021: 97, fig.; Conradie et al. 2021: 265.

Material examined. *Holotype* (male). PEM R23512, collected from Cuito River source lake (-12.68866, 18.36025, 1426 m a.s.l.), Moxico Province, Angola by Werner Conradie and James Harvey on 26 November 2016. *Paratypes* (five males). PEM R27381, collected from Quembo River lower bridge (-13.526579, 19.278096, 1248 m a.s.l.), Moxico Province, Angola by Werner Conradie, Chad Keates and Timóteo Júlio on 27 November 2019; PEM R23457–8, collected from Quembo River source (-13.13586, 19.04709, 1368 m a.s.l.), Moxico Province, Angola by Werner Conradie on 3 November 2016; PEM R23483, Cuando River source (-13.00164, 19.1296, 1372 m a.s.l.) Moxico Province, Angola by Werner Conradie and James Harvey on 17 November 2016; PEM R23510, collected from Cuito River source lake (-12.68866, 18.36025, 1426 m a.s.l.), Moxico Province, Angola by Werner Conradie and James Harvey on 26 November 2016. *Paratypes* (two females). PEM R23456, collected from Quembo River source (-13.13586, 19.04709, 1368 m a.s.l.), Moxico Province, Angola by Werner Conradie on 3 November 2016; PEM R23511, Cuito River source lake (-12.68866, 18.36025, 1426 m a.s.l.), Moxico Province, Angola by Werner Conradie and James Harvey on 26 November 2016.

Additional material assigned to the new species. NMZB-UM 10096, Kalabo (approx. -14.99391, 22.67795), Zambia; NMZB-UM 21272, 15 km WSW of Katima Mulilo (approx. -17.61448, 24.20593), Namibia. A specimen from Kuvangu [= Vila-da-Ponte], -14.46667, 16.3000 (Monard 1937: 123) has two postoculars and the

characteristic confluent blotched dorsal pattern and might belong to this new species, but this needs verification and is thus tentatively referred to the new species.

Diagnosis. The new species differs from other *Prosymna* in the following characters: rostral sharply depressed and angular (vs. rounded in *P. visseri*); presences of a single band-like internasals (vs. paired internasals in *P. somalica*, *P. bivittata*, *P. sudevalli*, *P. lineata*); dorsal scales smooth (keeled in *P. janii*); midbody scale rows 15–17 (vs. 19–21 in *P. pitmani*); 6 supralabials, with 3rd and 4th entering orbit (vs. 5 supralabials, with 2nd and 3rd entering orbit in *P. meleagris* and *P. greigerti*); single apical pits on dorsal scales (vs. paired apical pits in *P. ruspolii*); lower number of ventral scales in both sexes (116–129 vs. 153–199 in *P. frontalis*); dorsum with dark black spots (vs. scarlet head and dark body in *P. ornatissima*; uniform dark brown to grey in *P. ambigua* and *P. stublmanni*). It further differs from its closest congener, *P. angolensis*, in having two post oculars (vs. one), dorsal large black blotches mostly fused (vs. mostly small paired dorsal grey to black spots), postorbital bone present (vs. absent) and by the presence of four to five well-developed palatine teeth (vs. three reduced teeth).

Etymology. The name *lisima* is derived from the locally spoken Luchaze language in the region of the type locality meaning ‘source’. The full phrase used, ‘*Lisima Lwa Mwondo*’, is translated as “source of life”. This is a reference to central Angola, a high rainfall area where some of the most important rivers in Angola arise. This water makes it its way to the Okavango Delta, sustaining wildlife and local communities in Angola, Namibia and Botswana.

Description of holotype (Fig. 11). See Table 4 for further details and meristic data for the holotype. The body is cylindrical and elongated, tapering gradually to a

Table 4. Morphological features and measurements for the type series of *Prosymna lisima* sp. nov. (SVL = snout-vent length, τ = truncated).

Catalogue number	PEM R23512	PEM R23456	PEM R23457	PEM R23458	PEM R23483	PEM R23510	PEM R23511	PEM R27381
Type status	Holotype	Paratype	Paratype	Paratype	Paratype	Paratype	Paratype	Paratype
Sex	Male	Female	Male	Male	Male	Male	Female	Male
SVL+TL = total length mm	193+28.9 = 221.9	200+19.3 = 219.3	194+25.8 = 219.8	198+24.6 = 222.6	181+23.8 = 204.8	186+26.3 = 212.3	168+20.6 = 188.6	138+17τ = 155
TL/total length ratio (%)	13.0	8.8	11.7	11.1	11.6	12.4	10.9	11.0
Midbody scale rows	17-17-15	17-17-15	17-15-15	17-17-15	17-15-15	17-17-15	17-15-15	17-15-15
Ventral scales	122	121	117	124	121	116	117	122
Subcaudal scales	26	18	22	23	22	23	24	21τ
Cloacal Scale	Entire	Entire						
Preoculars	1/2	1	2	1	1	2	1	1
Postoculars	2	2	2	2	2	2	2	2
Temporals	1+2	1+2	1+2	1+2	1+2	1+2	1+2	1+2+3
Supralabials (contacting eye)	6 (3,4)	6 (3,4)	6 (3,4)	6 (3,4)	5 (2,3)/6 (3,4)	6 (3,4)	6 (3,4)	6 (3,4)
Infralabials (in contact with 1 st chin shield)	7 (3)	7 (3)	7 (3)	7 (3)	7 (3)	7 (3)	7 (3)	7 (3)
Loreal	Yes	Yes						
Dorsal colouration	26 fused blotches	30 fused blotches	21 fused blotches	31 fused blotches	22 fused blotches	26 fused blotches	27 fused blotches	36 paired blotches

very short tail, 13% total length, tail tip with a prominent spike. Dorsal scales smooth with single apical pits (some suprasubcaudal scales have two apical pits) in 17-15-15 scale rows, scale row reduction from 17 to 16 take place at ventral number 17 with the fusion of 3rd and 4th dorsal scale rows on left side and from 16 to 15 at ventral 23 with the fusion of 3rd and 4th dorsal scale rows on right side; 122 ventral scales; cloaca entire; 13 paired subcaudal scales. Head in dorsal view (Fig. 11B): head narrow and rounded, barely wider than 'neck'; rostral clearly visible from above, much broader than long (3.39×1.06 mm); a single narrow internasal, which is much longer than wide (2.73×0.67 mm) and in broad contact with the rostral anteriorly, posteriorly in broad contact with prefrontal and laterally with nasals; single band-like prefrontal which is longer than wide (3.70×1.30 mm), in contact laterally with loreal, and posteriorly with the frontal and supraocular scales; frontal pentangular, almost as long as wide (3.09×3.00 mm), nearly equal distance to snout (3.30 mm), shorter than prefrontals (3.0 vs. 3.70 mm), but nearly equal in length to the parietal scales (3.00 vs. 3.04 mm), in contact laterally with narrow supraoculars, and posteriorly with two very large pari-

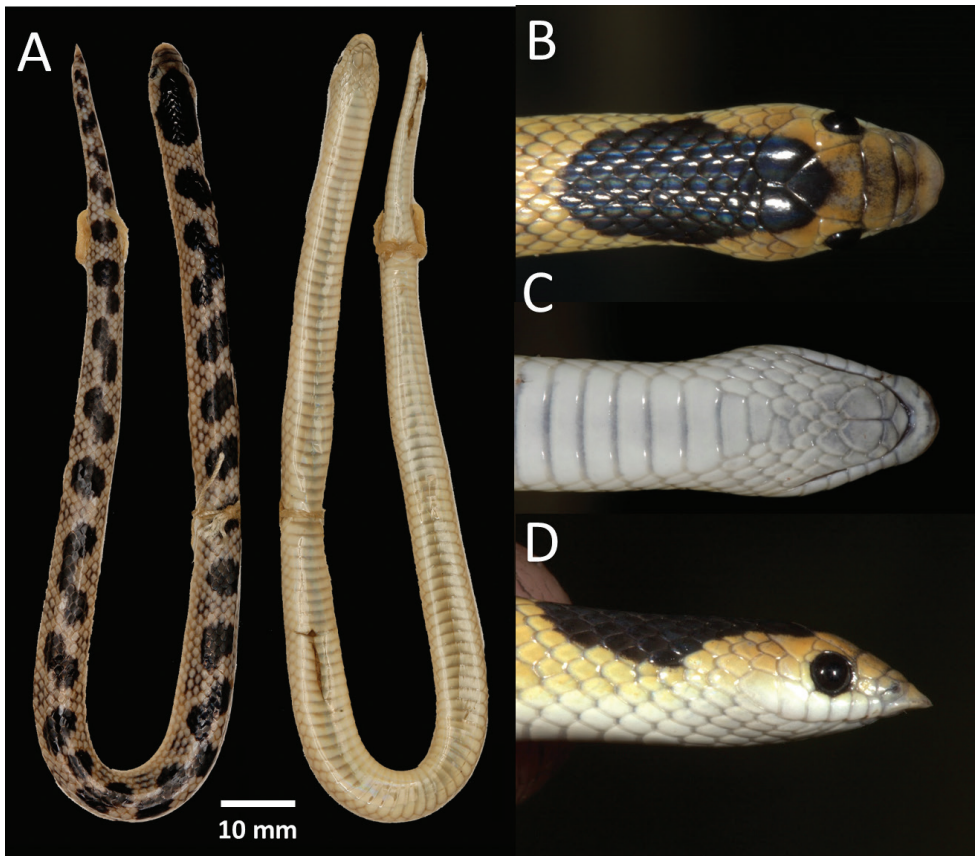


Figure 11. Holotype of *Prosymna lisima* sp. nov. (PEM R23512) from Cuito River source, Moxico Province, Angola **A** dorsal and ventral full body **B** dorsal head **C** ventral head **D** lateral head.

etals; paired parietals as wide as long (3.04×3.04 mm), in contact posteriorly with each other and laterally with temporals. Head in ventral view (Fig. 11C): rostral clearly visible from below, protruding well past jawline; mental small, triangular; infralabials seven, first three in contact with single paired chin shields, 1st infralabials in contact with each other; additional three or four rows of smaller gular scales present before start of ventral scales. Head in lateral view (Fig. 11D): snout sharply pointed, longer than the horizontal diameter of eye ($ED/SL = 0.49$); rostral large with acutely horizontal angular edge, excavated below; nostril is oval shaped, piercing a fully-divided nasal, and directed backwards; nasal scale longer than wide, with anterior part in full contact with rostral, posterior lower corner in contact with 1st supralabial and above with internasal scale and prefrontal; nasal suture present and intersecting 1st supralabial in uppermost corner; single small loreal as long as wide (0.7×0.7 mm), in contact below with 1st and 2nd supralabial, above with prefrontal, anteriorly with nasal and posteriorly with single preocular; a single preocular on the right side and two on the left side in contact anteriorly with loreal and prefrontal and above with supraocular, posteriorly protruding of loreal overlap with preoculars to create a small flap; eye large 19.36% headlight, vertical diameter (1.47 mm) two thirds as deep as distance between eye and lip (0.99 mm); pupil round; two postoculars, the lower one largest and in contact with 4th and 5th supralabials, first temporal scale and parietal, the upper smaller in contact with both supraocular and parietal; temporals 1+2 on both sides; narrow elongated supraocular in contact anteriorly with preocular, posteriorly with upper postocular and parietal and above with frontal; six supralabials, 3rd and 4th contacting eye, 5th and 6th supralabial the largest.

Colouration. In life (Figs 5C, 11B–D). Dorsum bright yellow-brown with 27 irregular fused black blotches that extend along the back from the nape onto the tail. Each dorsal scale has a darker edge giving it a faint reticulated pattern. Dorsolaterally, between the black vertebral blotches, there is a cluster of 2–4 scales with black edges. The large black nape blotch originates at the posterior margin of the frontal and runs through the parietal onto the dorsal scales, and is approximately nine scale rows deep and eleven scale rows wide. Each vertebral black blotch varies from 4–8 scale rows deep and 3–7 scale row wide. Some of the blotches are fused to form a continuous zig-zag pattern. Frontal and prefrontal sutures have a dark edge forming a pale grey crossbar. Eyes black. Ventrums cream-white, with the two outermost dorsal scale rows same colour as ventrum. In preservative (Fig. 11A). Same as in life, but yellow-brown colouration faded and the dark edges became more noticeable. Ventrums beige.

Paratype and additional material variation. See Table 2 and 4 for full meristic data. Dorsal scales smooth and in 17-17-15 rows at midbody; 116–124 (116–124 males, 117–129 females) smooth ventral scales; 18–26 (22–26 males, 18–24 females) paired subcaudal scales; one (rarely two) preoculars; two postoculars; temporals mostly 1+2; mostly six supralabials, with 3rd and 4th entering the orbit; seven infralabials, with first three in contact with the chin shield, cloacal scale entire; 21–36 fused dark dorsal spots. Largest female: 275+28 mm (NMZ UM 21272: 15 km WSW of Katima Mulilo); largest male: 198+25 mm (PEM R23458: Quembo River source). The col-

ouration of the type material is in general in agreement with the holotype, except that the dorsal fused blotches vary in size, number and arrangement (Fig. 5A–C). The nape black blotch always originates at the anterior part of the frontal extending through the parietals to 7–9 dorsal scale rows deep, 11–15 scales wide and start from the 3rd–5th lateral dorsal scale row. The dorsum consists of 21–36 confluent black blotches that are 7–11 scales wide and three to four scales deep. One specimen (PEM R23456) exhibits a distinct dark interorbital band and internasal band. The only juvenile collected (PEM R27381, Fig. 5C) has small paired black blotches (two scales deep and four scales wide) on a lighter yellow ground colour, large head blotch starts at posterior frontal through parietals, seven scales wide.

Skull osteology and teeth (Figs 7–9). This species presents a compact and rigid skull, common among *Prosymna* species with unfused braincase and nasal bones. Parietals are fused. Postorbital bone is present and contributes to the posterior edge of the orbital rim. Premaxilla has a short but robust ascending nasal process that lies between the ventral laminae of the nasals with low profile of the anterior portion which gradually slope ending in a moderate narrow tip and two elongated maxillary processes. Maxilla and premaxilla are in contact. Nasal bones are medium large bones in contact with frontal and premaxilla. Septomaxilla is a well-developed bone, in broad contact with the premaxilla, frontal, vomer, prefrontal and frontal bones. Vomer is well developed with a perforated dorsolateral portion. Maxillary is reduced anteriorly with an elongated pick-shaped palatine process with five or six laterally reduced curved tooth loci, followed by four to five enlarged lancet-shaped tooth loci, on same disposition. Palatine with four to five well developed teeth and an enlarged dorsal curved vomerine process. Pterygoid is a thin elongated bone. Supratemporal is in broad contact with the quadrate and participates in the lateral movement of the lower jaw. The lower jaw presents a compound bone, splenial, coronoid and dentary. Coronoid and splenial are reduced, almost vestigial. Dentary with eight tooth loci.

Hemipenis. Short simple structure, only reaching the 6–9th ventral scale. Single non-bifurcated sulcus. Ornamentation is flounced. Proximal third is smooth. Distal portion with four to five flounces that starts at the sulcal fold and encircle the whole organ, the most proximal often branched, forming a pocket of which the edges is smooth, tapering into a distal point. Retractor muscle is straight.

Natural history notes. All specimens were caught in late November during the rainy season. At this time, many adult lacertids, *Ichnotropis capensis* and *I. cf. grandiceps*, were also observed mating in the same habitat. *Prosymna* are well known to prey on soft-shell lizard eggs, and *P. lisima* sp. nov. may actively seek out these lacertids' eggs. Only two of the females had stomach contents, while all the males had empty stomachs. The largest female (PEM R23456) had three empty lizard egg shells in the hind gut, three empty egg shells at the rear end of the stomach, and four undigested lizard eggs in the main stomach (Fig. 12). Another female (PEM R23511) had four undigested lizard eggs in the main stomach. All eggs measured ~ 11.0 mm in length and each had a lateral cut. The eggs in the main stomach also all had a lateral cut but still maintained their shape and were surrounded by calcified leaked yolk (due to the pres-

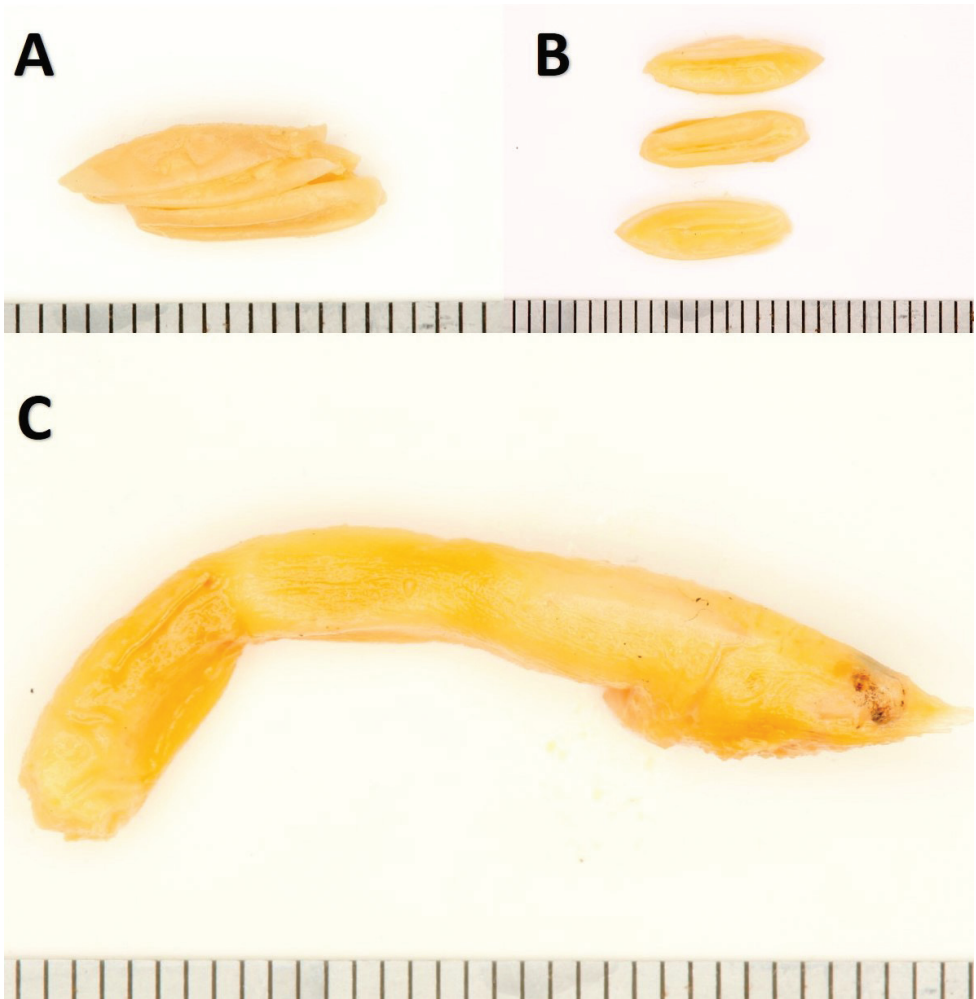


Figure 12. Stomach and gut contents of *Prosymna lisima* sp. nov. (PEM R23456) consisting of lizard egg shells. Scale bar: 1 mm.

ervation process). The eggs at the rear and the hindgut were all undecomposed and compressed. One of the paratype females (PEM R23456) was gravid, and had three eggs in early developmental stages (16.8×4.2 mm). Interestingly, on two different occasions, three specimens (two males and one female) were caught on the same night in the same trap array. This may indicate that males were following females to breed.

Distribution and habitat. Currently only known from east-central Angola, western Zambia and the Zambezi Region of north-eastern Namibia. In the region of Katima Mulilo (eastern Zambezi Region, Namibia) it occurs in sympatry with its sister species, *P. angolensis* (Fig. 2). The tentative assigned material from Kuvango (Monard 1931) needs verification, but it agrees in colouration and morphology to the new species. This species is expected to be much more widely distributed in the Kalahari basin,

as it seems to be associated with the deep Kalahari sands. The Angolan material occurs in Angolan moist miombo woodland, while the Zambian and Namibian material occurs in dry miombo woodland. The elevation ranges between 950 and 1450 m a.s.l. All newly collected specimens were captured in trap arrays set in sandy areas next to river source lakes or main rivers in eastern Angola (Conradie et al. 2021).

***Prosymna confusa* sp. nov.**

<https://zoobank.org/A4E2E3E8-A658-4007-B5F4-46D875457EA1>

Figs 6–9, 13

Common names: Plain Shovel-snout Snake (English); Cobra-de-focinho-de-pá-lisa (Portuguese).

Chresonymy.

Prosymna angolensis: Bogert 1940: 59; Monard 1937: 123 (in part); Broadley 1980: 152 (in part).

Prosymna ambigua: Branch 2018: 64, fig. 24; Pietersen et al. 2021: 96, fig.

Monard (1937) was the first to document a uniformly grey specimen from Ebanga. This was followed by Bogert (1940) who documented a specimen from Capelongo (AMNH R50504) that also exhibited a uniform pale brown dorsum with small white spots (similar to *P. meleagris* pattern). This uniform dorsum colouration is in agreement with the new specimen collected from coastal Angola (Branch 2018) and this colouration is very distinct from the other two species, yellowish grey with paired small black dorsum spots in *P. angolensis* and bright yellow with fused black blotches in *P. lisima* sp. nov.

Material examined. Holotype (female). PEM R24013, collected from 20 km west of Lola on the road northwest to Camacuio, on the edge of Bentiaba River (-14.27583, 13.45806, 791 m a.s.l.), Namibe Province, Angola by William R. Branch, Pedro Vaz Pinto and João S. de Almeida on 2 November 2015.

Additional material tentatively assigned to the new species. AMNH 50504, Capelongo, approx. -14.46645, 16.29241, Huíla Province, Angola (Bogert 1940: 59); Ebanga, approx. -12.73333, 14.73333, Benguela Province, Angola (Monard 1937: 123).

Diagnosis. The new species differs from other *Prosymna* species in the following characters: rostral sharply depressed and angular (vs. rounded in *P. visseri*); presence of a single band-like internasal (vs. paired internasals in *P. somalica*, *P. bivittata*, *P. sundevalli*, *P. lineata*); dorsal scales smooth (keeled in *P. jani*); midbody scale rows 15–17 (vs. 19–21 in *P. pitmani*); six supralabials, with 3rd and 4th entering orbit (vs. five supralabials, with 2nd and 3rd entering orbit in *P. meleagris* and *P. greigerti*); single apical pits on dorsal scales (vs. paired apical pits in *P. ruspolii*); lower number of ventral scales in both sexes (116–129 vs. 153–199 in *P. frontalis*); dorsum uniform dark grey (vs. scarlet head and dark body in *P. ornatissima*). It further differs from its closest congeners in the *angolensis* group: one postocular (vs. two in *P. lisima* sp. nov.), dorsum uniform grey (vs. dorsum with large mostly fused black blotches in *P. lisima* sp. nov.).

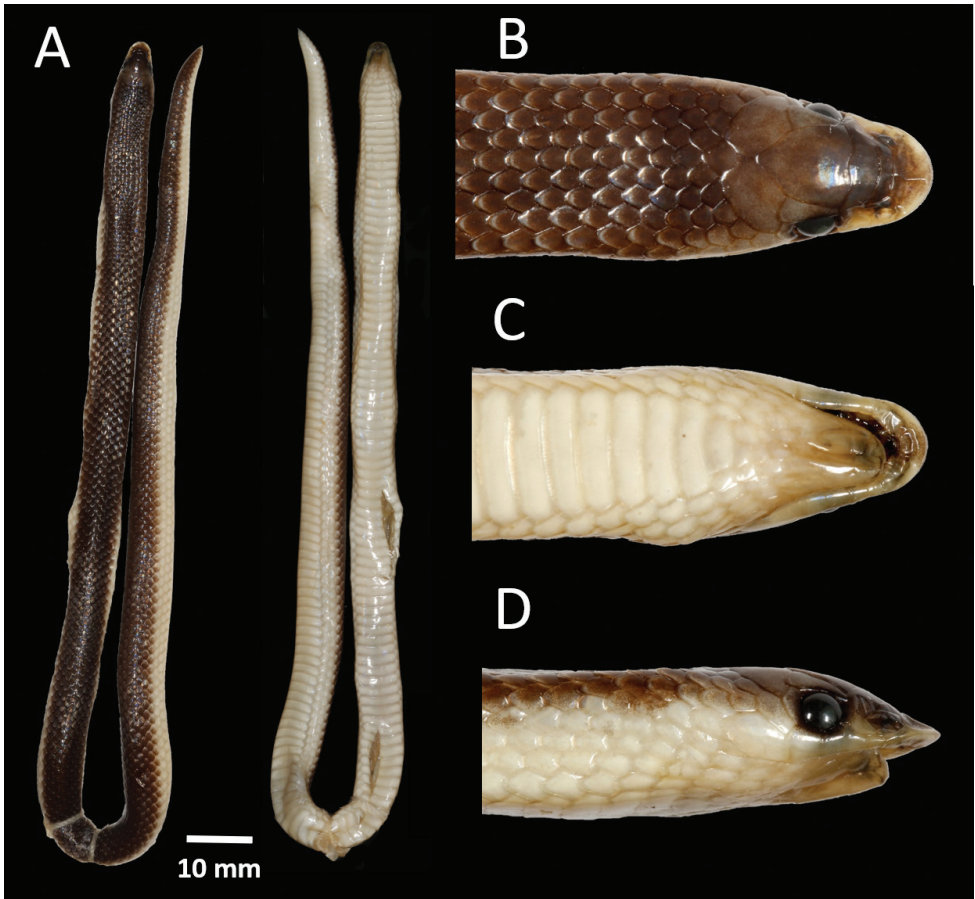


Figure 13. Holotype of *Prosymna confusa* sp. nov. (PEM R24013) from 20 km west of Lola on the road northwest to Camacuio and on the edge of Bentiaba River, Namibe Province, Angola **A** dorsal and ventral full body **B** dorsal head **C** ventral head **D** lateral head.

and mostly smaller paired longitudinal rows of grey to black spots in *P. angolensis*), postorbital bone absence (vs. present in *P. lisima* sp. nov.), presence of two well-developed palatine teeth (vs. four to five in *P. lisima* sp. nov. and three reduced teeth in *P. angolensis*), fused braincase (vs. unfused in *P. angolensis* and *P. lisima* sp. nov.) and two frontal foramina (vs. three to four in *P. angolensis* and *P. lisima* sp. nov.).

Etymology. When the late Bill Branch collected the holotype, he was unsure of its identification and referred to it as an unusual specimen that could not be assigned to any known species from Angola. He later referred to it as *P. ambigua* (Branch 2018), presumably based on its uniform grey colouration. The name *confusa* is a reflection of the confusion this specimen has caused and of the general confusion in the *P. angolensis* group.

Description of holotype (Fig. 13). Adult female measuring 240 mm SVL+29 mm TL = 269 mm total length. The body is cylindrical and elongated, tapering gradu-

ally to a very short tail, 10.8% total length, tail tip with prominent spike. Dorsal scales smooth, with single apical pits, in 17-15-15 scale rows, scale row reduction from 17 to 16 take place at ventral number 29 with the fusion of 3rd and 4th dorsal scale row on right side and from 16 to 15 at ventral 32 with the fusion of 3rd and 4th dorsal scale row on left side; 151 ventral scales; cloaca entire; 26 subcaudal scales. Head in dorsal view (Fig. 13B): head narrow and rounded, barely wider than 'neck'; rostral clearly visible from above, much broader than long (2.84 × 1.47 mm); a single narrow internasal, which is much longer than wide (2.40 × 0.57 mm) and in broad contact with the rostral anteriorly, posteriorly in broad contact with prefrontal and laterally with nasals; single band-like prefrontal which is longer than wide (3.71 × 1.25 mm), in contact laterally with loreal and posteriorly with the frontal and supraocular scales; frontal pentangular, almost as long as wide (2.97 × 3.14 mm), nearly equal in length to the distance to snout (2.91 mm), more than double than prefrontal width (3.14 vs. 1.25 mm), and three quarters the length of the parietals (3.14 vs. 2.43 mm), in contact laterally with narrow supraoculars, and posteriorly with two very large parietals; paired parietals longer than wide (2.28 × 2.43 mm), in contact posteriorly with each other and laterally with temporals. Head in ventral view (Fig. 13C): rostral clearly visible from below, protruding well past jawline; mental small, triangular; infralabials eight on right side and nine on left side, first three in contact with single paired chin shields, 1st infralabials in contact with each other; additional three rows of smaller gular scales present before the start of ventral scales. Head in lateral view (Fig. 13D): snout sharply pointed, longer than the horizontal diameter of eye (ED/SL = 0.45); rostral large with acutely horizontal angular edge, excavated below; nostril is oval shaped, piercing divided nasal, and directed backwards; nasal scale longer than wide, with anterior part in full contact with rostral, posterior lower corner in contact with 1st supralabial, upper section in contact with internasal scale and prefrontal and posteriorly with loreal and prefrontal; nasal suture present and intersecting loreal; single small loreal as long as wide (0.84 × 0.84 mm), in contact below with 1st and 2nd supralabial, above with prefrontal, anteriorly with nasal and posteriorly with single preocular; single preocular on both sides in contact anteriorly with loreal and above with supraocular and prefrontal, posteriorly with loreal; eye large 16.50% HL, vertical diameter (1.53 mm), two thirds as deep as distance between eye and lip (0.42); pupil round; one postoculars, in contact with 4th upperlabial, 1st temporal scale, supraocular, and parietal; temporals 1+2; narrow elongated supraocular in contact anteriorly with preocular and prefrontal, posteriorly with the postocular and above with frontal; five supralabials on both sides with 3rd and 4th in contact with eye on right and 2nd, 3rd and 4th on left, 5th and 6th supralabial the largest.

Colouration. In life (Fig. 6). Dorsum uniform grey with the anterior edges of scales with a white spot, outermost two to three scale rows white, with only the first outermost scale row of tail white. Nape with a faint collar that is three scale rows wide. The prefrontal and internasal black compared to the rest of the head being grey. Eye black. Ventrums white. In preservative (Fig. 13). Same as in life, but the grey faded and became brown. Ventrums beige.



Figure 14. A specimen (AMNH 50504) from Capelongo, approx. -14.46645, 16.29241; Huíla Province, Angola, assignable to the new species, *P. confusa* sp. nov. (Photos: Lauren Vonnahme, American Museum of Natural History).

Additional material variation. See Table 2 for summarised meristic data. Only data of three females were available, but the assignment of historical material to *P. confusa* sp. nov. still requires confirmation. Dorsal scales smooth and in 17-17-15 rows at midbody; 143–155 smooth ventral scales; 17–26 paired subcaudal scales; one preoculars; one postoculars; temporals 1+2; five or six supralabials, with 3rd and 4th entering the orbit; seven infralabials, with first three in contact with the 1st chin shield, cloacal scale entire. Largest female: 240+29 mm (holotype PEM R24013). The colouration is similar to the holotype, except that in the Capelongo specimen (AMNH R50504) the white spots are much more conspicuous (Fig. 14). The specimen from Ebanga is unaccounted for (Broadley 1980), but Monard (1937) described the colouration as uniform grey above.

Skull osteology and teeth (Figs 7–9). The holotype presents a compact and rigid skull common among *Prosymna* species with fused braincase, fused parietal, and unfused frontal and nasal bones. Postorbital bone is absent. Parietal with a fronto-lateral sharp edge that participates virtually as posterior edge of the orbital rim. Premaxilla has a well-developed and robust ascending nasal process that lies between the ventral laminae of the nasals with low profile of the anterior portion which gradually slope to a narrow tip and two elongated maxillary process in contact with the maxilla. Nasal bones are medium large bones in contact with frontal and premaxilla. Septomaxilla is a well-developed bone, in broad contact with premaxilla, frontal, vomer, prefrontal and frontal bone. The vomer is well developed with performed dorsolateral portion of the bone. Maxillary is reduced anteriorly with an elongated pick-shaped palatine process with six to seven laterally reduced curved tooth loci, followed by four to five enlarged lancet-shaped tooth loci. Palatine with two well developed teeth and an enlarged dorsal and curved vomerine process. Pterygoid is a thin elongated bone. Supratemporal is in broad contact with the quadrate and participates in the lateral movement of the lower jaw. The

lower jaw is comprised of compound, splenial, coronoid, and dentary bones. Coronoid and splenial bones are reduced, almost vestigial. Dentary bone with six tooth loci.

Hemipenis. Unknown. Bogert (1940) suggested it to be similar to *P. ambigua*. However, *Prosymna ambigua* is unique in having a very long 'telescopic' hemipenis that is longer than the tail, which is not present in the *sundevalli* group (Broadley 1980). The latter group, to which *P. confusa* sp. nov. belongs, is characterised by its short hemipenes (8–10th ventral scales long vs. longer than tail in *P. ambigua*), low number of flounces (5–6 vs. more than 50 in *P. ambigua*) and straight retractor muscle (telescopic in *P. ambigua*). *Prosymna frontalis* shares a similar hemipenile structure with *P. ambigua*.

Natural history notes. The holotype was found actively moving around near a large rock outcrop during the day.

Distribution and habitat. This species is endemic to southwestern Angola (Fig. 2), and appears to be associated with mopane woodlands, dry savannas, and semi-desert shrublands (Barbosa 1970). The new specimen was found in sandy plains with scattered low granite outcrops, with varying degrees of short grass cover and scattered bushes. Vegetation included *Colophospermum mopane*, *Ficus* sp., *Senegalia* (= *Acacia*) *mellifera*, *Commiphora* sp., *Boscia foetida*, and *Salvadora persica*. The two additional historical specimens from Ebanga and Capelongo that are tentatively assigned to this species occurred in similar dry habitat.

Discussion

The taxonomic status of *Prosymna angolensis* has been the subject of debate by several researchers over time. Thanks to the access to new material, we are able to describe two new species and provide the first phylogenetic placement of *P. angolensis*. Our work recovered a similar topology to that of Heinicke et al. (2020), with four clades characterising Prosymnidae. The addition of the new Angolan samples did not help resolve the alpha taxonomy or provide better support for deeper relationships between and within groups, as in Heinicke et al. (2020). However, our sampling does allow for a broader understanding of the phylogenetic relationships in the *sundevalli* group.

While the phylogenetic placement between lineages within the *angolensis* subgroup remains unresolved (particularly *P. angolensis* sensu stricto) and species pairwise distances are below those of their congeners; the topological support offered by ML and BEAST coupled with species delimitation analyses lends support for the distinctiveness of the two novel taxa at a genetic level. A single, near topotypical, sample of *P. angolensis* was available for molecular analysis and, based on the disjunct distribution between the populations of Angola and Namibia, Botswana, and Zimbabwe of *P. angolensis*, cryptic diversity is expected and worth further investigation.

Whilst our phylogeny lacks the resolution necessary to resolve the inter-specific relationships within the *sundevalli* group, which is likely a product of incomplete taxon sampling, it is clear that the *angolensis* subgroup is within the larger *sundevalli* group, as suggested by Broadley (1980). Our work further identified two new lineages within

the *angolensis* subgroup, one of which agrees with differences in morphology and colouration previously reported from western Zambia and the Zambezi Region (Broadley 1980). Although the ‘eastern race’ was partly defined based on the lower ventral scale counts (Broadley 1980), we show here that the differences are not significant and that these might be related to the sizes of the animals collected. Studies have shown positive correlation between ventral and subcaudal scales and body size, and that caution should be taken when used as a diagnostic feature (Lindell 1994; Lee et al. 2016). Based on the clear morphological (head scalation and osteology), dorsal colouration, and genetic differences reported in this study, we here describe these two lineages as *P. lisima* sp. nov. and *P. confusa* sp. nov. This raises the total number of *Prosymna* species to 18, with six species occurring in Angola. This number is, however, expected to grow as further cryptic diversity has been identified in *P. frontalis*, *P. ambigua*, and *P. stuhlmanni* (Heinicke et al. 2020) that may warrant taxonomic re-evaluation.

Because we only compared a small series of skulls for the osteological characterisation (one or two scans per species), further intra-specific variation may exist, thus the osteological differences observed should be taken with caution. That said, there were some striking differences among the groups, as mentioned by Heinicke et al. (2020). The postorbital was only recorded in *P. ambigua* and *P. stuhlmanni* and suggested as vestigial in *P. greigerti* by Heinicke et al. (2020). Here we confirm the presence of a well-developed postorbital bone in *P. janii*, the only remaining member of the *ambigua* group. Additionally, we recorded the presence of a postorbital bone in two additional species, *P. lisima* sp. nov. and *P. cf. frontalis*, being almost absent in the latter. This shows that the postorbital bone development is not restricted to the *ambigua* group but rather, present in the south-western taxa and the *sundevalli* group. This bone was present at a well-developed state in the *ambigua* group (reaching the maxilla) and *P. lisima* sp. nov. (slightly reduced, only reaching midway to the maxilla), but being small, almost absent in *P. cf. frontalis*. The purpose of the postorbital bone is currently unknown, but it may be associated with additional muscle attachment points to aid in feeding or crushing lizard eggs. This may suggest that the postorbital bone has been lost several times from its ancestral trait as a consequence of diet specialisation. Therefore, we recommend further research along this line, to shed light on the evolutionary history of this group.

In *Prosymna cf. frontalis*, the anterior portion of the maxilla has no teeth, similar to that in *P. visseri*. Heinicke et al. (2020) speculated, based on the fact that *P. frontalis* is also more rupicolous than its fossorial relatives, they may also have lost these anterior maxillae to allow them to feed on more hard-shelled gecko eggs which are found sympatrically. Although *P. confusa* sp. nov. may occur in similar habitat to *P. cf. frontalis*, it does not share the same maxillary tooth arrangement, which may indicate a different feeding strategy, such as feeding on sympatrically occurring soft-shelled lacertid eggs (e.g., *Heliobolus* sp. and *Pedioplanis* sp.). *Prosymna confusa* sp. nov. shares similar dentary development to *P. cf. frontalis*, in that the most anterior section of the dentary bone is free of teeth, compared to other species where they extend almost to the tip of the dentary.

The descriptions of two new species, *P. confusa* sp. nov., endemic from dry habitats in southwestern Angola, and *P. lisima* sp. nov., associated to the Kalahari sands from

Angola to neighbouring countries to the east, are an indication of how much diversity is likely still to be described from these regions. In the last decade a renewed interest in the Angolan herpetofauna has led to numerous expeditions to remote areas. Consequently, the number of species recorded from the country, has increased considerably (Conradie et al. 2012a, 2012b, 2013, 2020; Stanley et al. 2016; Ceriaco et al. 2018, 2020a, 2020b, 2020c, 2021b; Branch et al. 2019, 2021; Marques et al. 2019a, 2019b, 2020, 2022a, 2022b; Hallermann et al. 2020; Nielsen et al. 2020; Baptista et al. 2021; Lobón-Rovira et al. 2021; Parrinha et al. 2021; Wagner et al. 2021). Among these are four new species of snakes (Conradie et al. 2020; Hallermann et al. 2020). The addition of two new species of *Prosymna* brings the number of recorded snake species from Angola to ca. 135. This is approximately 69% of the known squamate diversity recorded from the country. As more research is conducted on Angolan herpetofauna, many more new species descriptions and additions are expected. Finally, we raise the importance of further surveys in this poorly studied region of Africa, with the aim of collecting recent material that will allow us to clarify the taxonomic placement of several species' complexes and poorly understood species.

Acknowledgements

We thank the Wild Bird Trust, which administrates the National Geographic Okavango Wilderness Project (2015–2019 National Geographic Society grant). Material was collected and exported under the following export permits issued by the Angolan Ministry of Environment Institute of Biodiversity (MINAMB): 31/GGPCC/2016, 151/INBAC/MINAMB/2019). Fieldwork in Bicular National Park was carried out in the framework of the Southern African Science Service Centre for Climate Change and Adaptive Land Management (SASSCAL) project, sponsored by the German Federal Ministry of Education and Research (BMBF) under promotion number 01LG1201M. The genetic component of this work was funded through the Wild Bird Trust grant to WC (grant WBT01 and OWP017). We would also like to acknowledge the use of infrastructure and equipment provided by the NRF-SAIAB Aquatic Genomics Research Platform and the funding channeled through the NRF-SAIAB Institutional Support System. We thank Luke Verburgt, James Harvey, Timóteo Júlio, Pedro Vaz Pinto, and the late Bill Branch for field assistance or collecting valuable specimens. Francois Theart and Justin Nicolau kindly provided comparative photographs from Namibia and Angola, respectively. We thank Enviro-Insight for constructing and donating the drift fences required for the trapping animals. WC thanks the Eastern Cape Province Department of Sport, Recreation, Arts and Culture (DSRAC) and Port Elizabeth Museum (Bayworld) for granting special leave to take part in these surveys. JLR and NLB are currently supported by Fundação para a Ciência e Tecnologia (FCT) contracts PD/BD/140808/2018 and PD/BD/140810/2018, respectively. Ethical clearance for the study was obtained from the Port Elizabeth Museum (Bayworld) ethics committee (Ethical Clearance no. 2013 & 2017-2). We thank Sheila Broadley who kindly made available Don Broadley's data on the *Prosymna angolensis* group. Photos of key museum specimens was kindly provided by

Georg Gassner and Alice Schumacher (Natural History Museum Vienna), Jose Rosado, Breda Zimkus, and Joseph Martinez (Museum of Comparative Zoology, Harvard University), Lauren Vonnahme (American Museum of Natural History), and Jofred Opperman (Iziko Museums of South Africa). We also further thank Jofred Opperman (Iziko Museums of South Africa) for facilitating the loan of specimens to be CT-scanned. We thank Muofhe Tshibalanganda (Central Analytic Facilities, Stellenbosch University) for performing the CT-scanning. We further want to express our gratitude to the two reviewers, Krystal Tolley and Luís Ceríaco, whose edits helped to improve the paper.

References

- Auerbach RD (1987) The Amphibians and Reptiles of Botswana. Mokwepa Consultants, Gaborone, Botswana, 295 pp.
- Baptista NL, Vaz Pinto P, Keates C, Edwards S, Roedel M-O, Conradie W (2021) A new species of red toad, *Schismaderma* Smith, 1849 (Anura: Bufonidae), from central Angola. *Zootaxa* 5081(3): 301–332. <https://doi.org/10.11646/zootaxa.5081.3.1>
- Baptista NL, António T, Branch WR (2019) The herpetofauna of Bicuar National Park and surroundings, southwestern Angola: a preliminary checklist. *Amphibian & Reptile Conservation* 13(2)[Special Section]: 96–130[e203].
- Barbosa LAG (1970) Carta Fitogeográfica de Angola. Instituto de Investigação Científica de Angola, Luanda, Angola, 323 pp.
- Bocage JVB (1873) Mélanges erpétologiques. II. Sur quelques Reptiles et Batraciens nouveaux, rares ou peu connus d'Afrique occidentale. *Jornal de Sciencias Mathematicas, Physicas e Naturaes* 4: 209–227.
- Bocage JVB (1882) Notícia acerca de alguns reptis d'Angôche que existem no Museu Nacional de Lisboa. *Jornal de Sciencias Mathematicas, Physicas e Naturaes. Academia Real das Sciencias de Lisboa VIII(32):* 286–290.
- Bocage JVB (1895) Herpétologie d'Angola et du Congo. Ministério da Marinha e das Colónias, Lisbonne, Portugal, 203 pp. [20 pls]
- Bogert CM (1940) Herpetological Results of the Vernay Angola expedition. *Bulletin of the American Museum of Natural History* 77: 1–107.
- Bouckaert R, Vaughan TG, Barido-Sottani J, Duchêne S, Fourment M, Gavryushkina A, Heled J, Jones G, Kühnert D, De Maio N, Matschiner M, Mendes FK, Müller NE, Ogilvie HA, du Plessis L, Popinga A, Rambaut A, Rasmussen D, Siveroni I, Suchard MA, Wu C-H, Xie D, Zhang C, Stadler T, Drummond AJ (2019) BEAST 2.5: An advanced software platform for Bayesian evolutionary analysis. *PLoS Computational Biology* 15(4): e1006650. <https://doi.org/10.1371/journal.pcbi.1006650>
- Boulenger GA (1894) Catalogue of the snakes in the British Museum (Natural History). Volume II. Containing the conclusion of the Colubriæ Aglyphæ. British Museum (Natural History), London, [xi,] 382 pp.
- Boulenger GA (1896) Catalogue of the snakes in the British Museum (Natural History). Volume III. Containing the Families Colubridæ (Opisthoglyphæ and Proteroglyphæ), Amblycephalidæ, and Viperidæ. British Museum (Natural History), London, [xiv,] 727 pp.

- Boulenger GA (1915) A list of the snakes of the Belgian and Portuguese Congo, northern Rhodesia, and Angola. *Proceedings of the Zoological Society of London* 1915(2): 193–223. <https://doi.org/10.1111/j.1469-7998.1915.tb07411.x>
- Branch WR (1998) *Field Guide to the Snakes and other Reptiles of Southern Africa*. Revised Edition. Struik Publishers, Cape Town, 399 pp.
- Branch WR (2018) Snakes of Angola: An annotated checklist. *Amphibian & Reptile Conservation* 12(2)[General Section]: 41–82[e159].
- Branch WR, Conradie W, Vaz Pinto P, Tolley KA (2019b) Another Angolan Namib endemic species: a new *Nucras* Gray, 1838 (Squamata: Lacertidae) from southwestern Angola. *Amphibian & Reptile Conservation* 13(2): 82–95.
- Branch WR, Schmitz A, Lobón-Rovira J, Baptista NL, António T, Conradie W (2021) Rock island melody: A revision of the *Afroedura bogerti* Loveridge, 1944 group, with descriptions of four new endemic species from Angola. *Zoosystematics and Evolution* 87(1): 55–82. <https://doi.org/10.3897/zse.97.57202>
- Broadley DG (1971) The reptiles and amphibians of Zambia. *The Puku* 6: 1–143.
- Broadley DG (1979) Predation on Reptile Eggs by African Snakes of the Genus *Prosymna*. *Herpetologica* 35: 338–341.
- Broadley DG (1980) A revision of the African snake genus *Prosymna* Gray (Colubridae). *Occasional papers of the National Museums of Rhodesia, Series B. Nature and Science* 6: 481–556.
- Broadley DG (1990) *FitzSimons' Snakes of southern Africa*. Revised Edition. Jonathan Ball and Ad. Donker Publishers, Parklands, 376 pp.
- Broadley DG (1995) Geographical Distribution - *Prosymna angolensis*. *African Herp News* 23: 48.
- Broadley D, Blaylock R (2013) *The Snakes of Zimbabwe and Botswana*. Chimaira, Frankfurt, 387 pp.
- Broadley DG, Doria CT, Wigge J (2003) *Snakes of Zambia. An Atlas and Field Guide*. Edition Chimaira, Frankfurt, 280 pp.
- Bruford MW, Hanotte M, Brookfield JFY, Burke T (1992) “Single locus and multilocus DNA fingerprint” in *Molecular Genetic Analysis of Populations: A Practical Approach*. IRL Press, Oxford, 225–270.
- Ceríaco LMP, Marques MP, Bandeira S, Agarwal I, Stanley EL, Bauer AM, Heinicke MP, Blackburn DC (2018) A new earless species of *Poyntonophrynus* (Anura, Bufonidae) from the Serra da Neve Inselberg, Namibe Province, Angola. *ZooKeys* 780: 109–136. <https://doi.org/10.3897/zookeys.780.25859>
- Ceríaco LMP, Agarwal I, Marques MP, Bauer AM (2020a) A review of the genus *Hemidactylus* Goldfuss, 1820 (Squamata: Gekkonidae) from Angola, with the description of two new species. *Zootaxa* 4746(1): 1–71. <https://doi.org/10.11646/zootaxa.4746.1.1>
- Ceríaco LMP, Heinicke MP, Parker KL, Marques MP, Bauer AM (2020b) A review of the African snake-eyed skinks (Scincidae: *Panaspis*) from Angola, with the description of a new species. *Zootaxa* 4747(1): 77–112. <https://doi.org/10.11646/zootaxa.4747.1.3>
- Ceríaco LMP, Agarwal I, Marques MP, Bauer AM (2020c) A correction to a recent review of the genus *Hemidactylus* Goldfuss, 1820 (Squamata: Gekkonidae) from Angola, with the description of two additional species. *Zootaxa* 4861(1): 92–106. <https://doi.org/10.11646/zootaxa.4861.1.6>

- Ceríaco LMP, Parrinha D, Marques MP (2021a) Saving collections: Taxonomic revision of the herpetological collection of the Instituto de Investigação Científica Tropical, Lisbon (Portugal) with a protocol to rescue abandoned collections. *ZooKeys* 1052: 85–156. <https://doi.org/10.3897/zookeys.1052.64607>
- Ceríaco LMP, Santos BS, Marques MP, Bauer AM, Tiutenko A (2021b) Citizen science meets specimens in old formalin filled jars: A new species of Banded Rubber Frog, genus *Phrynomantis* (Anura: Microhylidae) from Angola. *Alytes* 38(1–4): 18–48.
- Chabanaud P (1916) Revision du genre *Prosymna* Gray. *Bulletin du Muséum National d'Histoire Naturelle* 1916: 433–440.
- Chernomor O, Von Haeseler A, Minh BQ (2016) Terrace Aware Data Structure for Phylogenomic Inference from Supermatrices. *Systematic Biology* 65(6): 997–1008. <https://doi.org/10.1093/sysbio/syw037>
- Chippaux J-P, Jackson K (2019) *Snakes of Central and Western Africa*. Johns Hopkins University Press, Baltimore, 448 pp.
- Conradie W, Branch W, Measey GJ, Tolley KA (2012a) A new species of *Hyperolius* Rapp, 1842 (Anura: Hyperoliidae) from the Serra da Chela mountains, southwestern Angola. *Zootaxa* 3269(1): 1–17. <https://doi.org/10.11646/zootaxa.3269.1.1>
- Conradie W, Measey GJ, Branch WR, Tolley KA (2012b) Revised phylogeny of African sand lizards (*Pedioplanis*), with the description of two new species from southwestern Angola. *African Journal of Herpetology* 61(2): 91–112. <https://doi.org/10.1080/21564574.2012.676079>
- Conradie W, Branch WR, Tolley KA (2013) Fifty shades of grey: giving colour to the poorly known Angolan Ashy reed frog (Hyperoliidae: *Hyperolius cinereus*), with the description of a new species. *Zootaxa* 3635(3): 201–223. <https://doi.org/10.11646/zootaxa.3635.3.1>
- Conradie W, Deepak V, Keates C, Gower DJ (2020) Kissing cousins: a review of the African genus *Limmnophis* Günther, 1865 (Colubridae: Natricinae), with the description of a new species from north-eastern Angola. *African Journal of Herpetology* 69(1): 79–107. <https://doi.org/10.1080/21564574.2020.1782483>
- Conradie W, Baptista NL, Verburgt L, Keates C, Harvey J, Júlio T, Neef G (2021) Contributions to the herpetofauna of the Angolan Okavango-Cuando-Zambezi river drainages. Part 1: Serpentes (snakes). *Amphibian & Reptile Conservation* 15(2)[General Section]: 244–278[e292].
- Conroy CJ, Papenfuss T, Parker J, Hahn NE (2009) Use of Tricaine Methanesulfonate (MS222) for Euthanasia of Reptiles. *Journal of the American Association for Laboratory Animal Science [JAALAS]* 48: 28–32.
- de Queiroz K (1998) The general lineage concept of species, species criteria, and the process of speciation: A conceptual unification and terminological recommendations. In: Howard DJ, Berlocher SH (Eds) *Endless forms: Species and speciation*. Oxford University Press, Oxford, UK, 470 pp.
- Dowling HG (1951a) A proposed standard system of counting ventral scales in snakes. *British Journal of Herpetology* 5: 97–99. <https://doi.org/10.2307/1437542>
- Dowling HG (1951b) A proposes method of expressing scale reductions in snakes. *Copeia* 2(2): 131–134. <https://doi.org/10.2307/1437542>
- Drummond AJ, Rambaut A (2007) BEAST: Bayesian evolutionary analysis by sampling trees. *BMC Evolutionary Biology* 7(1): e214. <https://doi.org/10.1186/1471-2148-7-214>

- Figueroa A, McKelvy AD, Grismer LL, Bell CD, Lailvaux SP (2016) A species-level phylogeny of extant snakes with description of a new colubrid subfamily and genus. *PLoS ONE* 11(9): e0161070. <https://doi.org/10.1371/journal.pone.0161070>
- FitzSimons VFM (1962) *Snakes of southern Africa*. Purnell and Sons, Cape Town, South Africa, 424 pp.
- FitzSimons VFM (1966) A check-list, with synoptic keys, to the snakes of southern Africa. *Annals of the Transvaal Museum* 25: 25–79.
- FitzSimons VFM (1970) *A field guide to the snakes of southern Africa*. Collins, London, 231 pp.
- Gemel R, Gassner G, Schweiger S (2019) Katalog der Typen der Herpetologischen Sammlung des Naturhistorischen Museums Wien–2018. *Annalen des Naturhistorischen Museums in Wien, Serie B* 121: 33–248.
- Hall TA (1999) BioEdit, a user-friendly biological sequence alignment editor and analysis program for Windows 95/98/NT. *Nucleic Acids Symposium Series* 41: 95–98.
- Hallermann J, Ceriaco LMP, Schmitz A, Ernst R, Conradie W, Verburgt L, Marques MP, Bauer AM (2020) A review of the Angolan House snakes, genus *Boaedon* Duméril, Bibron and Duméril (1854) (Serpentes: Lamprophiidae), with description of three new species in the *Boaedon fuliginosus* (Boie, 1827) species complex. *African Journal of Herpetology* 69(1): 29–78. <https://doi.org/10.1080/21564574.2020.1777470>
- Heinicke MP, Daza J, Greenbaum E, Jackman TF, Bauer AM (2014) Phylogeny, taxonomy and biogeography of a circum-Indian Ocean clade of leaf-toed geckos (Reptilia: Gekkota), with a description of two new genera. *Systematics and Biodiversity* 12(1): 23–42. <https://doi.org/10.1080/14772000.2013.877999>
- Heinicke MP, Titus-McQuillan JE, Daza JD, Kull EM, Stanley EL, Bauer AM (2020) Phylogeny and evolution of unique skull morphologies in dietary specialist African shovel-snouted snakes (Lamprophiidae: *Prosymna*). *Biological Journal of the Linnean Society. Linnean Society of London* 131(1): 136–153. <https://doi.org/10.1093/biolinnean/blaa076>
- Hellmich W (1957) Die reptilienausbeute der Hamburgischen Angola Expedition. *Mitteilungen aus dem Hamburgischen Zoologischen Museum und Institut* 55: 39–80.
- Herrmann H-W, Branch WR (2013) Fifty years of herpetological research in the Namib Desert and Namibia with an updated and annotated species checklist. *Journal of Arid Environments* 93: 94–115. <https://doi.org/10.1016/j.jaridenv.2012.05.003>
- Hoang DT, Chernomor O, Von Haeseler A, Minh BQ, Vinh LS (2018) UFBoot2: Improving the ultrafast bootstrap approximation. *Molecular Biology and Evolution* 35(2): 518–522. <https://doi.org/10.1093/molbev/msx281>
- Isemonger RM (1968) *Snakes of Africa*. 1st Edn. Books of Africa, Cape Town, 263 pp.
- Kalyaanamoorthy S, Minh BQ, Wong TKF, Von Haeseler A, Jermiin LS (2017) ModelFinder: Fast model selection for accurate phylogenetic estimates. *Nature Methods* 14(6): 587–589. <https://doi.org/10.1038/nmeth.4285>
- Kelly CMR, Barker NP, Villet MH, Broadley DG (2009) Phylogeny, biogeography, and classification of the snake superfamily Elapoidea: A rapid radiation in the late Eocene. *Cladistics* 25(1): 38–63. <https://doi.org/10.1111/j.1096-0031.2008.00237.x>
- Kumar S, Stecher G, Li M, Knyaz C, Tamura K (2018) MEGA X: Molecular Evolutionary Genetics Analysis across Computing Platforms. *Molecular Biology and Evolution* 35(6): 1547–1549. <https://doi.org/10.1093/molbev/msy096>

- Lee JL, Thompson A, Mulcahy DG (2016) Relationships between numbers of vertebrae, scale counts, and body size, with implications for taxonomy in Nightsnakes (Genus: *Hypsiglena*). *Journal of Herpetology* 50(4): 616–620. <https://doi.org/10.1670/15-066>
- Lindell LE (1994) The evolution of vertebral number and body size in snakes. *Functional Ecology* 8(6): 708–719. <https://doi.org/10.2307/2390230>
- Lobón-Rovira J, Bauer AM (2021) Bone-by-bone: A detailed skull description of White-headed dwarf gecko *Lygodactylus picturatus* (Peters, 1870). *African Journal of Herpetology* 70(2): 1–20. <https://doi.org/10.1080/21564574.2021.1980120>
- Lobón-Rovira J, Conradie W, Iglesias DB, Ernst R, Veríssimo L, Baptista N, Vaz Pinto P (2021) Between sand, rocks and branches: An integrative taxonomic revision of Angolan *Hemidactylus* Goldfuss, 1820, with description of four new species. *Vertebrate Zoology* 71: 465–501. <https://doi.org/10.3897/vz.71.e64781>
- Loveridge A (1958) Revision of five African snake genera. *Bulletin of Comparative Zoology* 1191: 1–198.
- Marais J (2004) *A Complete Guide to the Snakes of Southern Africa*, 2nd edn. Struik Publishers, Cape Town, 312 pp.
- Marques P, Ceriáco LMP, Blackburn DC, Bauer AM (2018) Diversity and Distribution of the Amphibians and Terrestrial Reptiles of Angola - Atlas of Historical and Bibliographic Records (1840–2017). *Proceedings of the California Academy of Science (Series 4)* 65: 1–501 [Supplement II].
- Marques MP, Ceriáco LMP, Bandeira S, Pauwels OSG, Bauer AM (2019a) Description of a new long-tailed skink (Scincidae: *Trachylepis*) from Angola and the Democratic Republic of the Congo. *Zootaxa* 4568(1): 51–68. <https://doi.org/10.11646/zootaxa.4568.1.3>
- Marques MP, Ceriáco LMP, Stanley EL, Bandeira SA, Agarwal I, Bauer AM (2019b) A new species of Girdled Lizard (Squamata: *Cordylidae*) from the Serra da Neve Inselberg, Namibe Province, southwestern Angola. *Zootaxa* 4668(4): 503–524. <https://doi.org/10.11646/zootaxa.4668.4.4>
- Marques MP, Ceriáco LMP, Buehler MD, Bandeira SA, Janota JM, Bauer AM (2020) A revision of the Dwarf Geckos, genus *Lygodactylus* (Squamata: Gekkonidae), from Angola, with the description of three new species. *Zootaxa* 4853(3): 301–352. <https://doi.org/10.11646/zootaxa.4853.3.1>
- Marques MP, Parrinha D, Santo BS, Bandeira S, Butler BO, Sousa CAN, Bauer AM, Wagner P (2022a) All in all it's just another branch in the tree: A new species of *Acanthocercus* Fitzinger, 1843 (Squamata: Agamidae), from Angola. *Zootaxa* 5099(2): 221–243. <https://doi.org/10.11646/zootaxa.5099.2.4>
- Marques MP, Ceriáco LMP, Heinicke MP, Chehour RM, Conradie W, Tolley KA, Bauer A (2022b) The Angolan Bushveld Lizards, genus *Heliobolus* Fitzinger, 1843 (Squamata: Lacertidae): integrative taxonomy and the description of two new species. *Vertebrate Zoology* [in press].
- Mertens R (1937) Reptilien und Amphibien aus dem südlichen Inner-Afrika. *Abhandlungen der Senckenbergischen Naturforschenden Gesellschaft* 20: 425–443.
- Mertens R (1938) Amphibien und Reptilien aus Angola gesammelt von W. Shack. *Senckenbergiana* 20: 425–443.
- Mertens R (1955) Die Amphibien und Reptilien Südwestafrikas. Aus den Ergebnissen einer im Jahre 1952 ausgeführten Reise. *Abhandlungen der Senckenbergischen Naturforschenden Gesellschaft* 490: 1–172.

- Mertens R (1971) Die Herpetofauna Südwest-Afrikas. Abhandlungen der Senckenbergischen Naturforschenden Gesellschaft 529: 1–110.
- Miller MA, Pfeiffer W, Schwartz T (2010) Creating the CIPRES Science Gateway for Inference of Large Phylogenetic Trees. In: 2010 Gateway Computing Environments Workshop (GCE), New Orleans, LA, 1–8. <https://doi.org/10.1109/GCE.2010.5676129>
- Minh BQ, Lanfear R, Trifinopoulos J, Schrempf D, Schmidt HA (2021) IQ-TREE version 2.1.2: Tutorials and Manual Phylogenomic software by maximum likelihood. <http://www.iqtree.org/doc/iqtree-doc.pdf> [accessed 21 March 2022]
- Monard A (1931) Mission scientifique Suisse dans l'Angola. Résultats scientifiques. Reptiles. Bulletin de la Société Neuchâtoise des sciences Naturelles 33: 89–111.
- Monard A (1937) Contribution à l'Herpétologie d'Angola. Arquivos do Museu Bocage 8: 19–154.
- National Geographic Okavango Wilderness Project (2017) Initial Findings from Exploration of the Upper Catchments of the Cuito, Cuanavale, and Cuando Rivers, May 2015 to December 2016. Unpublished report, 368 pp.
- Nguyen LT, Schmidt HA, Von Haeseler A, Minh BQ (2015) IQ-TREE: A fast and effective stochastic algorithm for estimating maximum-likelihood phylogenies. *Molecular Biology and Evolution* 32(1): 268–274. <https://doi.org/10.1093/molbev/msu300>
- Nielsen SV, Conradie W, Ceriáco LMP, Bauer AM, Heinicke MP, Stanley EL, Blackburn DC (2020) A new species of Rain Frog (Brevicipitidae, *Breviceps*) endemic to Angola. *ZooKeys* 979: 133–160. <https://doi.org/10.3897/zookeys.979.56863>
- Palumbi SR (1996) The polymerase chain reaction. In: Hillis D, Moritz C, Mable B (Eds) *Molecular Systematics*. 2nd Edn. Sinauer Associates, Sunderland, 205–247.
- Parrinha D, Marques MP, Heinicke MP, Khalid F, Parker KL, Tolley KA, Childers JL, Conradie W, Bauer AM, Ceriáco LMP (2021) A revision of Angolan species in the genus *Pedioplanis* Fitzinger (Squamata: Lacertidae), with the description of a new species. *Zootaxa* 5032(1): 001–046. <https://doi.org/10.11646/zootaxa.5032.1.1>
- Peters WCH (1867) Über eine Sammlung von Flederthieren und Amphibien aus Otjimbingue in Südwest-afrika, welche Hr. Missionär Hahn dem zoologischen museum zugesandt hat. *Monatsberichte der Königlichen Preussische Akademie der Wissenschaften zu Berlin* 4: 133–138.
- Pietersen DW, Verburgt L, Davies J (2021) Snakes and other reptiles of Zambia and Malawi. Struik Nature, Cape Town, 376 pp.
- Puillandre N, Lambert A, Brouillet S, Achaz GJME (2012) ABGD, Automatic Barcode Gap Discovery for primary species delimitation. *Molecular Ecology* 21(8): 1864–1877. <https://doi.org/10.1111/j.1365-294X.2011.05239.x>
- Puillandre N, Brouillet S, Achaz G (2021) ASAP: Assemble species by automatic partitioning. *Molecular Ecology Resources* 21(2): 609–620. <https://doi.org/10.1111/1755-0998.13281>
- Pyron RA, Burbrink FT, Wiens JJ (2013) A phylogeny and revised classification of Squamata, including 4161 species of lizards and snakes. *BMC Evolutionary Biology* 13(1): e93. <https://doi.org/10.1186/1471-2148-13-93>
- R Core Team (2021) R: A language and environment for statistical computing. R Foundation for Statistical Computing, Vienna. <https://www.R-project.org/>
- Rambaut A (2014) FigTree. Tree Figure Drawing Tool Version 1.4.4. [Available from:] <http://tree.bio.ed.ac.uk/>
- Rambaut A, Drummond AJ (2009) Tracer. [Available at:] <http://beast.bio.ed.ac.uk/Tracer>

- Ronquist F, Teslenko M, Van Der Mark P, Ayres DL, Darling A, Hohna S, Larget B, Liu L, Suchard MA, Huelsenback JP (2012) MrBayes 3.2: Efficient Bayesian Phylogenetic Inference and Model Choice Across a Large Model Space. *Software for Systematic and Evolution* 61(3): 539–542. <https://doi.org/10.1093/sysbio/sys029>
- Slowinski JB, Lawson R (2002) Snake phylogeny: Evidence from nuclear and mitochondrial genes. *Molecular Phylogenetics and Evolution* 24(2): 194–202. [https://doi.org/10.1016/S1055-7903\(02\)00239-7](https://doi.org/10.1016/S1055-7903(02)00239-7)
- Spawls S, Howell K, Hinkel H, Menegon M (2018) *Field guide to East African reptiles*. Bloomsbury, London, 624 pp.
- Stanley EL, Ceriaco LMP, Bandeira S, Valerio H, Bates MF, Branch WR (2016) A review of *Cordylus machadoi* (Squamata: Cordylidae) in southwestern Angola, with the description of a new species from the Pro-Namib desert. *Zootaxa* 4061(3): 201–226. <https://doi.org/10.11646/zootaxa.4061.3.1>
- Suchard MA, Rambaut A (2009) Many-core algorithms for statistical phylogenetics. *Bioinformatics (Oxford, England)* 25(11): 1370–1376. <https://doi.org/10.1093/bioinformatics/btp244>
- Swofford DL (2003) PAUP* Phylogenetic Analysis Using Parsimony (*and other methods). Version 4.0a 169 Sinauer Associates. <https://doi.org/10.1002/0471650129.dob0522>
- Tamura K, Stecher G, Peterson D, Filipski A, Kumar S (2013) MEGA6: Molecular Evolutionary Genetics Analysis Version 6.0. *Molecular Biology and Evolution* 30(12): 2725–2729. <https://doi.org/10.1093/molbev/mst197>
- Thermo Fisher Scientific (2020) Thermo Fisher Scientific Reports Fourth Quarter and Full Year 2020 Results.
- Uetz P, Freed P, Hošek J [Eds] (2022) The Reptile Database. <http://www.reptile-database.org> [accessed 11 April 2021]
- Vidal N, Branch WR, Pauwels OSG, Hedges SB, Broadley DG, Wink M, Cruaud C, Joger U, Nagy ZT (2008) Dissecting the major African snake radiation: A molecular phylogeny of the Lamprophiidae Fitzinger (Serpentes, Caenophidia). *Zootaxa* 1945(1): 51–66. <https://doi.org/10.11646/zootaxa.1945.1.3>
- Wagner P, Butler BO, Ceriaco LM, Bauer AM (2021) A new species of the *Acanthocercus atricolis* (Smith, 1849) complex (Squamata, Agamidae). *Salamandra (Frankfurt)* 57: 449–463.
- Wallach V, Williams KL, Boundy J (2014) *Snakes of the World: A catalogue of living and extinct species*. [type catalogue] CRC Press, Florida, 1237 pp.
- Werner F (1929) Übersicht der Gattungen und Arten der Schlangen der Familie Colubridae. III. *Zoologische Jahrbucher. Abteilung für Systematik, Geographie und Biologie der Tiere* 57: 1–481.
- Whiting AS, Bauer AM, Sites JW (2003) Phylogenetic relationships and limb loss in sub-Saharan African scincine lizards (Squamata: Scincidae). *Molecular Phylogenetics and Evolution* 29(3): 582–598. [https://doi.org/10.1016/S1055-7903\(03\)00142-8](https://doi.org/10.1016/S1055-7903(03)00142-8)
- Xia X (2013) DAMBE5: A comprehensive software package for data analysis in Molecular Biology and Evolution. *Molecular Biology and Evolution* 30(7): 1720–1728. <https://doi.org/10.1093/molbev/mst064>
- Zaher H, Murphy RW, Arredondo JC, Graboski R, Machado-Filho PR, Mahlow K, Montingelli GG, Quadros AB, Orlov NL, Wilkinson M, Zhang Y-P, Grazziotin F (2019) Large-scale molecular phylogeny, morphology, divergence-time estimation, and the fossil record of

advanced caenophidian snakes (Squamata: Serpentes). PLoS ONE 14(5): e0216148. <https://doi.org/10.1371/journal.pone.0216148>

Zhang J, Kapli P, Pavlidis P, Stamatakis A (2013) A general species delimitation method with applications to phylogenetic placements. Bioinformatics 29(22): 2869–2876. <https://doi.org/10.1093/bioinformatics/btt499>

Appendix I

Table A1. List of samples used in this study and their associated metadata. NA–Not Available.

Species	Voucher ID	Locality	Molecular Markers					
			<i>16S</i>	<i>ND2</i>	<i>cyt-b</i>	<i>c-mos</i>	<i>RAG1</i>	<i>ENC-1</i>
Ingroup								
<i>Prosymna angolensis</i>	NB 0521/ CHL 0521	Bicuar National Park, Huila, Angola	OP288036	OP289543	OP289533	OP289553	NA	NA
<i>P. confusa</i> sp. nov. 'Coastal'	AG 014/ PEM R24013	20 km W Lola, road northwest to Camacuio, Namibe, Angola	OP288044	OP289552	OP289542	OP289562	NA	NA
<i>P. lisima</i> sp. nov. 'Eastern'	WC-4694/ PEM R23456	Quembo River Source, Moxico, Angola	OP288037	OP289544	OP289534	OP289554	NA	NA
<i>P. lisima</i> sp. nov. 'Eastern'	WC-4696/ PEM R23457	Quembo River Source, Moxico, Angola	OP288038	OP289545	OP289535	OP289555	NA	NA
<i>P. lisima</i> sp. nov. 'Eastern'	WC-4706/ PEM R23458	Quembo River Source, Moxico, Angola	OP288039	OP289546	OP289536	OP289556	NA	NA
<i>P. lisima</i> sp. nov. 'Eastern'	WC-4810/ PEM R23483	Cuando River Source, Moxico, Angola	OP288040	OP289547	OP289537	OP289557	NA	NA
<i>P. lisima</i> sp. nov. 'Eastern'	WC-4870/ PEM R23510	Cuito Source Lake, Moxico, Angola	OP288041	OP289548	OP289538	OP289558	NA	NA
<i>P. lisima</i> sp. nov. 'Eastern'	WC-4863/ PEM R23511	Cuito Source Lake, Moxico, Angola	OP288042	OP289549	OP289539	OP289559	NA	NA
<i>P. lisima</i> sp. nov. 'Eastern'	WC-4862/ PEM R23512	Cuito Source Lake, Moxico, Angola	OP288043	OP289550	OP289540	OP289560	NA	NA
<i>P. lisima</i> sp. nov. 'Eastern'	WC-6844/ PEM R27381	Quembo River bridge camp, Moxico, Angola	NA	OP289551	OP289541	OP289561	NA	NA
<i>P. ambigua</i>	CAS 258670	Cangandala NP, Malanje, Angola	MT453136	MT460633	NA	MT460596	MT460655	NA
<i>P. ambigua</i>	GJ 2762	Malanje, Angola	MT453137	MT460634	NA	MT460597	MT460656	NA
<i>P. ambigua</i>	PEM R16763	Gnimeiti River, Klein's Camp, Loliondo Game Controlled Area, Mara, Tanzania	MT453112	NA	NA	MT460579	MT460635	NA
<i>P. bivittata</i>	AMB (53F6)	NA	MT453113	MT460610	NA	NA	NA	NA
<i>P. bivittata</i>	PEM R17431	Mkhuze Falls Private Game Reserve, KwaZulu-Natal, South Africa	MT453114	MT460611	NA	NA	MT460636	NA

Species	Voucher ID	Locality	Molecular Markers					
			16S	ND2	cyt-b	c-mos	RAG1	ENC-1
<i>P. bivittata</i>	PEM R17432	Mkhuze Falls Private Game Reserve, KwaZulu-Natal, South Africa	MT453115	MT460612	MT482412	MT460580	MT460637	MT460598
<i>P. bivittata</i>	PEM R17433	Mkhuze Falls Private Game Reserve, KwaZulu-Natal, South Africa	MT453116	MT460613	MT482413	MT460581	MT460638	NA
<i>P. cf. frontalis</i>	MCZ R193166	Farm Omandumba, Erongo, Namibia	MT453117	MT460614	NA	NA	MT460639	NA
<i>P. cf. frontalis</i>	PEM R17996	Espinheira, Namibe, Angola	MT453118	MT460615	MT482414	MT460582	MT460640	MT460599
<i>P. cf. frontalis</i>	MCZ R184857	Hobatere Lodge, Namibia	MT453119	NA	NA	NA	MT460641	NA
<i>P. frontalis</i>	MCZ R185112	Farm Oas, Karas, Namibia	MT453120	MT460616	NA	NA	NA	NA
<i>P. frontalis</i>	MCZ R185003	Geister Schlucht, Klein Aus Vista, Karas, Namibia	MT453121	MT460617	KR814693	KR814680	MT460642	
<i>P. greigerti</i>	E 107.19	NA	JF340124	NA	NA	NA	NA	NA
<i>P. greigerti</i>	E 124.1	NA	JF340125	NA	NA	NA	NA	NA
<i>P. greigerti</i>	UTEP 22161	Pian Upe Wildlife Reserve, Hyena Hill, Northern Region, Uganda	NA	MT460632	NA	MT460595	MT460654	NA
<i>P. janii</i>	JM 1045	KwaZulu-Natal, South Africa	MT453122	MT460618	MT482415	NA	MT460643	NA
<i>P. janii</i>	MCZ Z37878	KwaZulu-Natal, South Africa	MT453123	NA	NA	NA	NA	NA
<i>P. janii</i>	AMB (SNH8)	KwaZulu-Natal, South Africa	MT453124	MT460620	MT482417	MT460583	MT460644	MT460601
<i>P. janii</i>	PEM R12072	Madlangula, Kosi Bay Nature Reserve, KwaZulu-Natal, South Africa	FJ404222	NA	FJ404319	FJ404293	NA	NA
<i>P. janii</i>	PEM R17372	uMkhuze, Greater St. Lucia Wetland Park, KwaZulu-Natal, South Africa	NA	MT460619	MT482416	NA	NA	MT460600
<i>P. lineata</i>	MCZ R184472	7.5 km E of Musina on Tishipe Rd., Limpopo, South Africa	MT453126	MT460622	MT482419	MT460585	MT460646	MT460602
<i>P. lineata</i>	JM 1816	Khamai, Limpopo, South Africa	MT453127	MT460623	NA	MT460586	MT460647	NA
<i>P. lineata</i>	MBUR 394	Makgabeng area, Limpopo, South Africa	MT453128	MT460624	MT482420	NA	NA	MT460603
<i>P. lineata</i>	AMB (53F8)	Blouberg, Limpopo, South Africa	MT453125	MT460621	MT482418	MT460584	MT460645	NA
<i>P. meleagris</i>	E 107.22	NA	JF340122	NA	NA	NA	NA	NA
<i>P. meleagris</i>	E 113.2	NA	JF340123	NA	NA	NA	NA	NA
<i>P. meleagris</i>	MVZ245380	Shai Hills, Greater Accra Region, Ghana	MT453135	MT460631	NA	MT460594	MT460653	NA
<i>P. ruspolii</i>	CMRK316	Tanzania	NA	NA	DQ486347	DQ486171	NA	NA
<i>P. stubmanni</i>	LHM-000270	3.2 km W of Lesheba Wilderness Reserve, Limpopo, South Africa	NA	MT460625	MT482421	MT460587	NA	NA

Species	Voucher ID	Locality	Molecular Markers					
			<i>16S</i>	<i>ND2</i>	<i>cyt-b</i>	<i>c-mos</i>	<i>RAG1</i>	<i>ENC-1</i>
<i>P. stuhlmanni</i>	PEM R17402	Mkhuze Game Reserve, KwaZulu-Natal, South Africa	MT453129	MT460626	MT482422	MT460588	MT460648	MT460604
<i>Psundeavalli</i>	MCZ R184401	Farm Newstead, Eastern Cape, South Africa	MT453130	MT460627	MT482423	MT460589	MT460649	MT460605
<i>Psundeavalli</i>	MCZ R184512	23.9 km NE Vaalwater on Rd. to Melkrivier, Limpopo, South Africa	MT453131	MT460628	MT482424	MT460590	MT460650	MT460606
<i>P. visseri</i>	CAS 214753	Opuwo Dist. ca 2 km N of Sesfontein, Kunene Region, Namibia	MT453132	MT460629	MT482425	MT460591	MT460651	MT460607
<i>P. visseri</i>	PEM R17994	Espinheira, Namibe, Angola	MT453133	MT460630	MT482426	MT460592	MT460652	MT460608
<i>P. visseri</i>	MG 302	Farm Kaross, Kunene Region, Namibia	MT453134	NA	MT482427	MT460593	NA	MT460609
Outgroup								
<i>Psammophis condanarius</i>	NA	NA	Z46479	AY058991	AF471075	AF471104	NA	NA
<i>Pseudaspis cana</i>	NA	NA	AY611898	AY058992	AY612080	AY611989	NA	NA
<i>Aparallactus werneri</i>	NA	NA	AY188045	NA	AF471035	AF471116	NA	JN881241
<i>Atractaspis corpulenta</i>	NA	NA	AY611837	NA	AY612020	AY611929	NA	JN881242
<i>Boaedon fuliginosus</i>	NA	NA	KX249802	NA	KM519712	AF544686	KM519725	JN881267
<i>Buboma proctenae</i>	NA	NA	AY611818	NA	AY612001	AY611910	NA	NA
<i>Lampropeltis getula</i>	NA	NA	KX694649	MG672874	MG672798	KX694811	MG673016	JN881266
<i>Leioheterodon madagascariensis</i>	NA	NA	AY188061	AY059010	AY188022	AF544685	NA	NA
<i>Naja kaouthia</i>	NA	NA	KX277260	AY059008	AF217835	AY058938	JF412633	JN881273
<i>Oxyrhabdium leporinum</i>			NA	NA	AF471029	DQ112081	NA	NA

Table A2. High Resolution X-ray Computed Tomography (HRCT) parameters used to scan *Prosymna* skulls.

Species	Catalogue Number	Voxel (mm)	Voltage (kV)	Current (µA)	Exposure Time (secs)	MorphoSource
<i>Prosymna angolensis</i>	SAM ZR16574	0.00499991	60	300	0.5	https://doi.org/10.17602/M2/M435305
<i>Prosymna confusa</i> sp. nov.	PEM R24013	0.00799991	90	100	0.5	https://doi.org/10.17602/M2/M435274
<i>Prosymna lisima</i> sp. nov.	PEM R23512	0.00699991	60	300	0.5	https://doi.org/10.17602/M2/M435310
<i>Prosymna lisima</i> sp. nov.	PEM R23510	0.00699991	60	300	0.5	https://doi.org/10.17602/M2/M435343
<i>Prosymna</i> cf. <i>frontalis</i>	PEM R17997	0.00699991	100	80	0.5	https://doi.org/10.17602/M2/M435295
<i>Prosymna jani</i>	PEM R08679	0.00699991	90	80	0.5	https://doi.org/10.17602/M2/M435300

Description of three new species previously identified as *Stolephorus bengalensis* (Dutt & Babu Rao, 1959) or *Stolephorus insularis* Hardenberg, 1933 and a re-description of *S. bengalensis* (Chordata, Osteichthyes, Clupeiformes, Engraulidae)

Harutaka Hata¹, Sébastien Lavoué², Hiroyuki Motomura³

1 National Museum of Natural History, Smithsonian Institution, 10th and Constitution Ave, NW Washington, DC 20560, USA **2** School of Biological Sciences, Universiti Sains Malaysia, 11800, Penang, Malaysia **3** The Kagoshima University Museum, 1-21-30 Korimoto, Kagoshima 890-0065, Japan

Corresponding author: Hata Harutaka (k2795502@kadai.jp)

Academic editor: Tihomir Stefanov | Received 22 March 2022 | Accepted 22 August 2022 | Published 15 September 2022

<https://zoobank.org/1D6F2518-F6B7-4BEE-A41F-86F417DBD423>

Citation: Hata H, Lavoué S, Motomura H (2022) Description of three new species previously identified as *Stolephorus bengalensis* (Dutt & Babu Rao, 1959) or *Stolephorus insularis* Hardenberg, 1933 and a re-description of *S. bengalensis* (Chordata, Osteichthyes, Clupeiformes, Engraulidae). ZooKeys 1121: 145–173. <https://doi.org/10.3897/zookeys.1121.84171>

Abstract

Examination of numerous specimens characterised by predorsal scute, long maxilla, indented preopercle and pelvic scute lacking a spine and previously identified as *Stolephorus bengalensis* (Dutt & Babu Rao, 1959) or *Stolephorus insularis* Hardenberg, 1933, revealed four distinct species, true *S. bengalensis* (distributed from the Bay of Bengal to Pakistan) and three new species, viz., *Stolephorus eldorado* **sp. nov.** (Taiwan to Java, Indonesia), *Stolephorus diabolus* **sp. nov.** (Strait of Malacca, from Penang, Malaysia, to Singapore) and *Stolephorus eclipsis* **sp. nov.** (Bintan Island, Riau Archipelago, Indonesia). Characters separating the four species include numbers of gill rakers on each gill arch and vertebrae and pelvic fin and dorsal-fin ray lengths. Two molecular markers (mitochondrial cytochrome *b* and cytochrome oxidase I genes) demonstrated the distinction of three of the species examined morphologically and enabled a reconstruction of their phylogenetic relationships. Each species was genetically divergent from the others by 3.5%–7.7% mean uncorrected distance in the mitochondrial cytochrome oxidase I gene.

Keywords

Actinopterygii, Clupeomorpha, phylogenetics, *Stolephorus tri*, taxonomy

Introduction

The anchovy genus *Stolephorus* Lacepède, 1803 (Teleostei: Clupeiformes: Engraulidae), diagnosed by the presence of prepelvic scutes and an embedded urohyal and lack of postpelvic scutes, currently includes 37 valid species that preferentially inhabit marine and/or estuarine waters in the Indo-Pacific region (Wongratana 1983, 1987a, b; Whitehead et al. 1988; Wongratana et al. 1999; Kimura et al. 2009; Hata and Motomura 2018a, b, c, d, e, 2021a, b, c, 2022; Hata et al. 2019, 2020a, b, 2021; Gangan et al. 2020). Amongst them, species with a predorsal scute, paired dark lines on the dorsum behind the dorsal fin, a long maxilla (posterior tip well beyond the preopercle posterior margin), the preopercle posterior margin concave and pelvic scute without a posteriorly projecting spine (Fig. 1) are regarded as *Stolephorus insularis* Hardenberg, 1933 by Whitehead et al. (1988), who reviewed the genus. Hata et al. (2019) revised the taxonomy of seven nominal species of *Stolephorus*, treating Whitehead et al.'s (1988) *S. insularis* as *Stolephorus bengalensis* (Dutt & Babu Rao, 1959) and regarding the nominal species *S. insularis* as a junior synonym of *Stolephorus tri* (Bleeker, 1852). However, subsequent re-examination of specimens, identified as *S. bengalensis*, in fact revealed the presence of four species.

The aim of this study is to re-describe *S. bengalensis* and describe three new species of *Stolephorus* from specimens previously regarded as *S. insularis* or *S. bengalensis*. In addition to the morphological comparisons, complete mitochondrial cytochrome *b* gene and partial mitochondrial cytochrome oxidase I (COI) gene sequences from 31 specimens were used to estimate the genetic distinction of three of the latter (the fourth species unavailable) plus one unidentified, but related species from Segara Anakan Lagoon, Central Java, Indonesia (Nuryanto et al. 2017).

Materials and methods

Counts and proportional measurements followed Hata and Motomura (2017). Counts of fin rays and vertebrae followed Hubbs and Lagler (1947), the last two rays of dorsal and anal fins being counted separately, unless they originated from the same base, in which case they were counted as one ray. Vertebrae counts includes urostyle. All measurements were made with digital calipers to the nearest 0.01 mm. “Pelvic scute” refers to a scute joined to the pelvic girdle and “prepelvic scute”, “postpelvic scute” and “predorsal scute” to hard spine-like scutes anterior to the pelvic fin, posterior to the pelvic fin and just anterior to the dorsal-fin origin, respectively. Osteological characters, including vertebral counts, were determined from radiographs of 32, 2, 14 and 45 specimens of *S. bengalensis*, *S. diabolus* sp. nov., *S. eclipsis* sp. nov. and *S. eldorado* sp. nov., respectively. Abbreviations are as follows – SL: standard length; HL: head length; and UGR, LGR and TGR: rakers on upper limb, lower limb and total gill rakers, respectively, with associated numbers indicating the specific gill arch. Institutional codes generally follow Sabaj (2020). USMFC stands for Universiti Sains Malaysia Fish Collection, School of Biological Sciences, Penang, Malaysia.

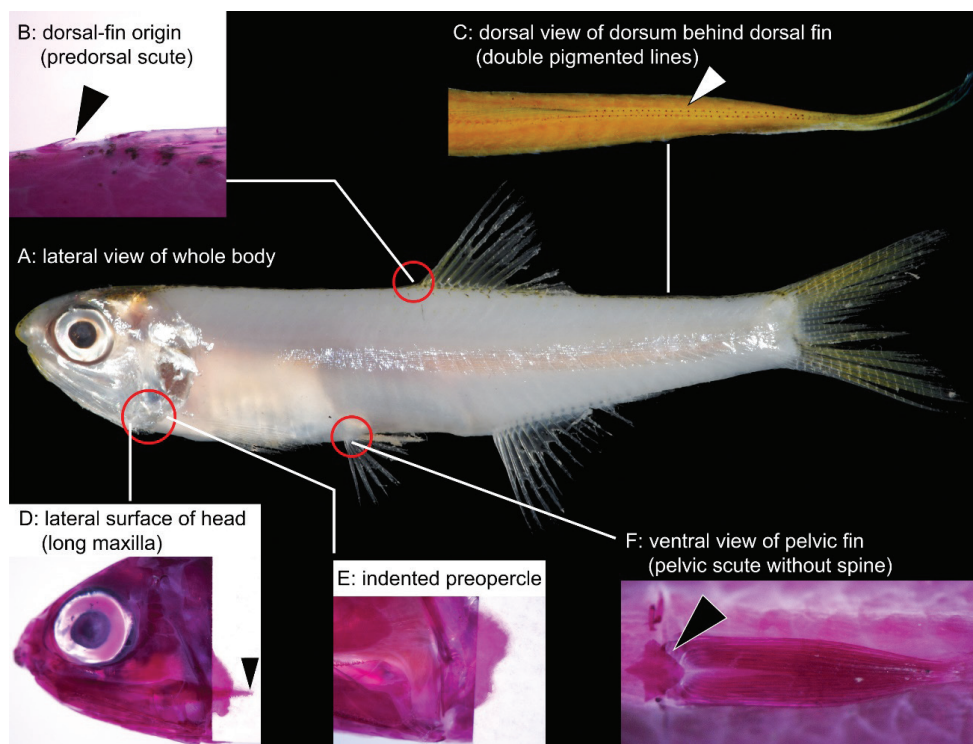


Figure 1. Diagnostic characters of species previously identified as *Stolephorus bengalensis* **A** lateral view of whole body **B** dorsal-fin origin (triangle indicates predorsal scute, located just anterior to dorsal-fin origin) **C** dorsal view of dorsum behind dorsal fin (triangle indicates paired dark lines) **D** lateral surface of head (triangle indicates posterior tip of maxilla, posteriorly well beyond posterior margin of pre-opercle) **E** preopercle with concave posterior margin (supramaxilla removed) and **F** ventral view of pelvic fin (triangle indicates pelvic scute, lacking spine) (**A** KAUM-I. 94521, paratype of *S. eldorado* sp. nov. in fresh condition, 43.4 mm SL, Ha Long Bay, northern Vietnam **B**, **E**, **F** KAUM-I. 113148, paratype of *S. eldorado* sp. nov., 55.3 mm SL, Ke-tzu-liao, south-western Taiwan **C** ZUMT 62056, paratype of *S. diabolus* sp. nov., 38.4 mm SL, Singapore **D** KAUM-I. 94509, paratype of *S. eldorado* sp. nov., 41.4 mm SL, Ha Long Bay, northern Vietnam) (**B**, **D**, **E** and **F** alizarin stain).

The mitochondrial genotypes of 31 specimens comprising three (out of four) species of *Stolephorus* examined in this study, plus one closely related, but unidentified species, were compared using the complete (1140 base pairs [bp]) cytochrome *b* gene and partial (648 bp) COI gene. The cytochrome *b* gene sequences were published in Hata et al (2019; 2020b) and are available in GenBank (Table 1). The COI gene was newly sequenced for 19 specimens of *S. eldorado*, including the holotype and several paratypes (Table 1) and the resulting data combined with COI sequences (available in GenBank) of *S. diabolus* (two specimens from West Peninsular Malaysia, including the holotype), *S. bengalensis* (eight specimens from India), *S. eldorado* (one specimen from China; Pang et al. 2019) and a single specimen of an unidentified *Stolephorus* species (from Segara Anakan Lagoon, Central

Table 1. Taxonomic treatment and molecular marker sampling of 32 specimens of *Stolephorus* examined in the molecular section of the present study. “-” indicates corresponding sequence not determined. Bold accession numbers indicate sequences determined during the study. (Abbreviations: Cytb, cytochrome b; COI, cytochrome oxidase I; Gb, GenBank; “***”, holotype; “*”, paratype).

Species	Voucher	Origin	Cytb	COI
<i>S. eldorado</i>	KAUM-I. 94509*	Ha Long Bay, northern Vietnam	MH380318	OM672421
sp. nov.	KAUM-I. 94517**	Ha Long Bay, northern Vietnam	MH380319	OM672422
	KAUM-I. 94519*	Ha Long Bay, northern Vietnam	MH380320	OM672423
	KAUM-I. 94520*	Ha Long Bay, northern Vietnam	MH380321	OM672424
	KAUM-I. 94521*	Ha Long Bay, northern Vietnam	MH380322	OM672425
	KAUM-I. 113142*	off Dong-gang, Pingtung, Taiwan	MH380323	OM672426
	KAUM-I. 113143*	off Dong-gang, Pingtung, Taiwan	MH380324	OM672427
	KAUM-I. 113144*	off Dong-gang, Pingtung, Taiwan	MH380325	OM672428
	KAUM-I. 113145*	off Dong-gang, Pingtung, Taiwan	MH380326	OM672417
	KAUM-I. 113146*	off Dong-gang, Pingtung, Taiwan	MH380327	OM672418
	KAUM-I. 113147*	off Dong-gang, Pingtung, Taiwan	MH380328	OM672419
	KAUM-I. 113148*	off Dong-gang, Pingtung, Taiwan	MH380329	OM672429
	KAUM-I. 113149*	off Dong-gang, Pingtung, Taiwan	MH380330	OM672420
	KAUM-I. 113150*	off Dong-gang, Pingtung, Taiwan	MH380331	OM672430
	KAUM-I. 113151*	off Dong-gang, Pingtung, Taiwan	MH380332	OM672431
	NTUM12426 (Bgk15)	Bangkok, Thailand	MH380652	OM672414
	NTUM12426 (Bgk17)	Bangkok, Thailand	MH380653	OM672415
	- (Bgk39)	Bangkok, Thailand	MH380333	OM672416
	- (HK01)	Hong Kong	MH380334	OM672413
	20180725PZ25	Zhangzhou city, China (24.26N, 118.11°E) (Gb)	MH732976	OM672413
<i>S. diabolus</i>	IPMB-I 13.00001**	Telok Bahang, Penang Island, Malaysia	MT080882	MT080410
sp. nov.	- (larvae not preserved)	Klang Strait, West Peninsular Malaysia (Gb)	-	MH673948
<i>S. bengalensis</i>	-	off Kochi, Kerala, India (9.97°N, 76.28°E) (Gb)	-	KU871055
(Dutt &	-	off Kochi, Kerala, India (9.97°N, 76.28°E) (Gb)	-	KU871061
Babu Rao,	-	off Kochi, Kerala, India (9.97°N, 76.28°E) (Gb)	-	KU894592
1959)	-	off Kochi, Kerala, India (9.97°N, 76.28°E) (Gb)	-	KU894597
	-	off Kochi, Kerala, India (9.97°N, 76.28°E) (Gb)	-	KU894598
	-	off Kochi, Kerala, India (9.97°N, 76.28°E) (Gb)	-	KU894599
	-	off Kochi, Kerala, India (9.97°N, 76.28°E) (Gb)	-	KU894600
	-	off Kochi, Kerala, India (9.97°N, 76.28°E) (Gb)	-	KU894601
<i>Stolephorus</i>	- (larvae not preserved)	Segara Anakan lagoon, Central Java (Gb)	-	KY944580
sp.				
Outgroup:				
<i>S. andhraensis</i>	NTUM12328 (Bg14)	Bangkok, Thailand	MH380656	MH380744
Babu Rao,				
1966				

Java) (Table 1). One specimen of *Stolephorus acinaces* Hata, Lavoué & Motomura, 2020 was selected as the outgroup.

DNA was extracted from ethanol-preserved tissue samples. Polymerase chain reaction (PCR) amplification and sequencing of the COI gene followed standard protocols (Ward et al. 2005), with annealing at 55 °C. Amplification of the partial COI gene used the following primers: forward COI_FishF1 (5'-TCA ACC AAC CAC AAA GAC ATT GGC AC-3') and reverse COI_FishR2 (5'-ACT TCA GGG TGA

CCG AAG AAT CAG AA-3') (Ward et al. 2005). PCR products were purified and sequenced in both directions by Sanger Sequencing technology using the same PCR primers. Sequences generated in this study have been deposited in the GenBank database (accession numbers given in Table 1).

Alignments of the cytochrome *b* and COI sequences were determined separately by eye, requiring neither insertions nor deletions. The final alignment combining the two genes (for 31 specimens plus one outgroup) comprised 1788 nucleotide positions. Uncorrected pairwise genetic distances (i.e. p-distances) amongst species were calculated with MEGA X (Stecher et al. 2020). The relationships between specimens were inferred by the Maximum Likelihood (ML) method of phylogenetic reconstruction using the general time-reversible model of nucleotide substitution with rate heterogeneity following a discrete gamma distribution (GTR + Γ), using the software RAxML-NG (Kozlov et al. 2019) as implemented in the graphical interface raxmlGUI 2.0 (Edler et al. 2020). The tree was rooted using a specimen of *S. acinaces* and the robustness of each node determined by bootstrap support (500 replicates).

Results and discussions

Stolephorus bengalensis (Dutt & Babu Rao, 1959)

[English name: Hardenberg's Anchovy]

Figs 2, 3; Tables 2–4

Anchoviella baganensis bengalensis Dutt & Babu Rao, 1959: 160 [original locality: Waltair and Kakinada, Andhra Pradesh, east coast of India; type locality: Kilakarai, Gulf of Mannar, India, based on the neotype designated by Hata et al. (2019)].

Stolephorus baganensis macrops (lapsus memoriae for *Stolephorus megalops*) (not of Delsman): Whitehead 1967 (in part): 18 (Bay of Bengal).

Stolephorus insularis (not of Delsman): Whitehead et al. 1988 (in part): 413 (northern part of Indian Ocean); Young et al. 1994: 222, fig. 7 (Wangkun and Fangliao, Taiwan); Wongratana et al. 1999 (in part): 1736 (northern part of Indian Ocean); Gangan et al. 2020: 562, fig. 5 (Kochi, Kerala State, India).

Stolephorus bengalensis: Hata et al. 2019 (in part): 24, fig. 12 (Pakistan and India; neotype designation).

Neotype. USNM 276476, 45.8 mm SL, Kilakarai, Gulf of Mannar, India, 20 Feb 1964, J. W. Reintjes and P. S. B. R. James.

Non-type specimens. 46 specimens, 30.8–58.7 mm SL. **INDIA:** BMNH 1969.5.30.34–45, 12 specimens, Chennai, Tamil Nadu State; OCF-P 10435, 4 specimens, 30.8–38.1 mm SL, estuary of Hooghly River, West Bengal State (purchased in fish market in Kolkata, West Bengal State); USNM 204227, 21 specimens, 42.7–51.8 mm SL, Sassan Docks, Mumbai, Maharashtra State. **PAKISTAN:** KAUM–I. 69286, 50.0 mm SL, KAUM–I. 69287, 58.7 mm SL, KAUM–I. 69288, 50.5 mm SL,



Figure 2. **A** lateral **B** dorsal and **C** ventral views of neotype of *Stolephorus bengalensis* (USNM 276476, 45.6 mm SL, Gulf of Mannar, India). Scale bars indicate 2 mm.

KAUM-I. 69289, 54.4 mm SL, KAUM-I. 69290, 49.0 mm SL, KAUM-I. 69291, 53.1 mm SL, KAUM-I. 69292, 47.3 mm SL, KAUM-I. 69294, 58.6 mm, KAUM-I. 69295, 58.6 mm, West Wharf, Karachi.

Diagnosis. A species of *Stolephorus* with the following combination of characters: 1UGR 16–19 (modally 18), 1LGR 23–27 (25), 1TGR 40–45 (44); 2UGR 11–15 (13), 2LGR 21–25 (23), 2TGR 33–39 (36); 3UGR 10–12 (11), 3LGR 13–15 (13), 3TGR 23–27 (24); 4UGR 7–9 (8), 4LGR 10–12 (11), 4TGR 17–21 (19); prepelvic scutes 5–7 (6); total vertebrae 40 or 41 (40); long maxilla, posterior tip just reaching or slightly short of posterior margin of opercle; predorsal scutes present; pelvic scute without spine; body scales deciduous; posterior border of pre-opercle concave, indented; paired dark patch on parietal area with little following pigmentation; distinct double pigment lines along dorsum posterior to dorsal fin; black spots below eye and on lower-jaw tip absent; anal-fin base long, 19.0–21.3% (20.2%) of SL; maximum orbit diameter 7.3–8.6% (8.1%) of SL; third dorsal-fin ray long, 18.5–19.9% (19.0%) of SL; pelvic fin rather long, 9.4–11.0% (10.2%) of SL, its posterior tip not reaching to vertical through dorsal-fin origin when depressed in specimens > 50 mm SL; distance between posterior ends of supramaxilla and maxilla 5.3–6.6% (5.8%) of SL.

Description. Data for neotype presented first, followed by data for non-type specimens in parentheses (if different). Counts and measurements, expressed as percentages of SL or HL, given in Tables 2 and 3. Body laterally compressed, elongate, deepest at

Table 2. Meristics of specimens of *Stolephorus bengalensis* and *Stolephorus eldorado* sp. nov.

	<i>Stolephorus bengalensis</i>			<i>Stolephorus eldorado</i> sp. nov.		
	Neotype of <i>Anchoviella</i> <i>baganensis</i> <i>bengalensis</i>	Non- types		Holotype	Paratypes	
	USNM 276476	<i>n</i> = 46		KAUM-I. 94517	<i>n</i> = 57	
Standard length (mm)	45.8	30.8–58.7	Modes ± SD	44.4	37.5–58.8	Modes ± SD
Dorsal-fin rays (unbranched)	3	3	3 ± 0	3	3	3 ± 0
Dorsal-fin rays (branched)	12	11–14	13 ± 0.7	13	11–14	13 ± 0.6
Anal-fin rays (unbranched)	3	3	3 ± 0	3	3*	3 ± 0.1
Anal-fin rays (branched)	18	16–20	18 ± 0.9	18	16–19	18 ± 0.6
Pectoral-fin rays (unbranched)	1	1	1 ± 0	1	1	1 ± 0
Pectoral-fin rays (branched)	11	10–12	11 ± 0.7	12	9–13	11 ± 0.8
Pelvic-fin rays (unbranched)	1	1	1 ± 0	1	1	1 ± 0
Pelvic-fin rays (branched)	6	6	6 ± 0	6	6	6 ± 0
Gill rakers on 1 st gill arch (upper)	16	17–19	18 ± 0.8	18	16–21	18 ± 1.1
Gill rakers on 1 st gill arch (lower)	24	23–27	25 ± 1.1	26	23–28	25 ± 1.0
Gill rakers on 1 st gill arch (total)	40	40–45	44 ± 1.5	44	40–47	42 ± 1.7
Gill rakers on 2 nd gill arch (upper)	13	11–15	13 ± 0.8	12	10–14	13 ± 0.8
Gill rakers on 2 nd gill arch (lower)	22	21–25	23 ± 0.9	24	20–24	23 ± 1.0
Gill rakers on 2 nd gill arch (total)	35	33–39	36 ± 1.5	36	30–38	36 ± 1.5
Gill rakers on 3 rd gill arch (upper)	10	10–12	11 ± 0.6	10	8–12	10 ± 0.8
Gill rakers on 3 rd gill arch (lower)	13	13–15	13 ± 0.6	13	12–14	13 ± 0.6
Gill rakers on 3 rd gill arch (total)	23	23–27	24 ± 1.1	23	20–26	23 ± 1.1
Gill rakers on 4 th gill arch (upper)	9	7–9	8 ± 0.6	8	7–10	8 ± 0.7
Gill rakers on 4 th gill arch (lower)	10	10–12	11 ± 0.5	11	9–12	11 ± 0.8
Gill rakers on 4 th gill arch (total)	19	17–21	19 ± 1.0	19	16–22	18 ± 1.3
Gill rakers on posterior face of 3 rd gill arch	6	4–7	5 ± 0.7	5	4–7	5 ± 0.7
Prepelvic scutes	7	5–7	6 ± 0.5	6	5–7	6 ± 0.6
Scale rows in longitudinal series	35	34–36	35 ± 0.7	34	34–36	35 ± 0.7
Transverse scales	8	8	8 ± 0	8	8–9	8 ± 0.3
Pseudobranchial filaments	broken	13–18	16 ± 1.3	17	14–18	16 ± 1.2
Total vertebrae	40	40–41	40 ± 0.4	39	38–40	39 ± 0.7

*one specimen with 4 unbranched anal-fin rays.

dorsal-fin origin. Dorsal profile of head and body slightly convex from snout tip to dorsal-fin origin, gently lowering to uppermost point of caudal-fin base. Ventral profile of head and body slightly convex from lower jaw tip to pelvic-fin insertion, thereafter, slowly rising to lowermost point of caudal-fin base. Single spine-like scute just anterior to dorsal-fin origin. Abdomen somewhat rounded, covered with seven (four to seven) spine-like prepelvic scutes. Pelvic scute without spine. Postpelvic scutes absent. Anus just anterior to anal-fin origin. Snout tip rounded; snout length less than eye diameter. Mouth large, inferior, ventral to body axis, extending backwards beyond posterior margin of eye. Maxilla long, its posterior tip pointed, just reaching (or slightly short of) opercle posterior margin. Lower jaw slender. Single row of conical teeth on both jaws

Table 3. Morphometrics of specimens of *Stolephorus bengalensis* and *Stolephorus eldorado* sp. nov.

	<i>Stolephorus bengalensis</i>			<i>Stolephorus eldorado</i> sp. nov.		
	Neotype of <i>Anchoviella baganensis bengalensis</i>		Non-types Means ± SD	Holotype	Paratypes	
	USNM 276476	n = 46			KAUM-I. 94517	n = 57
Standard length (mm)	45.8	30.8–58.7	Means ± SD	44.4	37.5–58.8	Means ± SD
As % SL						
Head length	25.8	23.0–26.1	24.7 ± 0.8	26.1	22.8–27.8	25.7 ± 1.3
Body depth	20.7	19.8–22.9	21.5 ± 0.7	17.9	17.3–22.0	20.3 ± 1.3
Pre-dorsal-fin length	56.8	52.3–57.1	54.5 ± 1.3	53.7	51.6–56.5	54.0 ± 1.2
Snout tip to pectoral-fin insertion	29.0	25.1–27.9	26.4 ± 0.8	28.0	22.5–29.2	26.9 ± 1.6
Snout tip to pelvic-fin insertion	47.6	42.4–49.4	45.1 ± 1.3	45.4	43.9–48.6	46.1 ± 1.2
Snout tip to anal-fin origin	66.3	61.3–66.5	64.2 ± 1.2	61.4	61.3–66.5	63.6 ± 1.2
Dorsal-fin base length	13.4	13.3–15.6	14.5 ± 0.6	14.3	13.2–15.7	14.6 ± 0.5
Anal-fin base length	20.8	19.0–21.3	20.2 ± 0.6	20.4	19.0–22.3	20.4 ± 0.8
Caudal-peduncle length	17.4	16.0–20.0	18.0 ± 1.1	18.1	16.4–19.8	18.2 ± 1.0
Caudal-peduncle depth	10.0	9.3–11.2	10.3 ± 0.4	9.3	8.7–10.9	9.7 ± 0.6
D–P1	37.2	33.9–38.1	35.9 ± 1.1	34.7	34.2–39.6	36.3 ± 1.2
D–P2	23.0	21.3–25.9	23.8 ± 1.0	20.4	19.1–26.1	23.2 ± 1.7
D–A	22.0	21.3–24.2	22.7 ± 0.8	20.2	19.2–23.2	21.6 ± 1.1
P1–P2	22.1	17.3–22.2	19.3 ± 1.4	19.6	16.9–23.8	20.3 ± 1.8
P2–A	19.7	15.9–20.3	18.6 ± 1.1	17.3	16.1–20.3	18.2 ± 1.0
Pectoral-fin length	broken	15.9–16.9	16.4 ± 0.4	18.0	14.9–18.5	16.5 ± 0.8
Pelvic-fin length	broken	9.4–11.0	10.2 ± 0.4	10.6	9.1–11.0	10.0 ± 0.5
Maxilla length	broken	19.7–22.3	21.0 ± 0.7	21.5	19.6–22.9	21.4 ± 0.9
Lower-jaw length	17.1	15.3–17.6	16.3 ± 0.5	17.3	14.6–17.9	16.7 ± 0.7
Supramaxilla end to maxilla end	broken	5.3–6.6	5.8 ± 0.3	5.1	5.0–6.3	5.6 ± 0.4
Maximum orbit diameter	8.5	7.3–8.6	8.1 ± 0.3	9.3	8.2–9.9	8.9 ± 0.4
Eye diameter	6.9	6.1–7.6	6.9 ± 0.3	8.0	6.4–8.6	7.5 ± 0.5
Snout length	4.4	3.4–4.0	3.7 ± 0.2	3.7	3.1–4.3	3.7 ± 0.3
Interorbital width	6.74	5.2–6.3	5.9 ± 0.3	5.8	4.9–6.2	5.8 ± 0.3
Postorbital length	12.8	11.8–14.1	13.0 ± 0.5	12.3	11.6–14.9	12.9 ± 0.7
1 st dorsal-fin ray length	0.9	0.9–2.1	1.5 ± 0.3	1.9	0.9–2.2	1.5 ± 0.3
2 nd dorsal-fin ray length	7.3	6.6–8.9	7.7 ± 0.6	broken	5.9–8.1	7.3 ± 0.6
3 rd dorsal-fin ray length	18.8	18.5–19.9	19.0 ± 0.4	broken	15.9–18.6	17.4 ± 0.8
1 st anal-fin ray length	1.9	1.0–2.0	1.6 ± 0.3	1.5	0.8–2.2	1.6 ± 0.3
2 nd anal-fin ray length	5.2	4.6–6.3	5.4 ± 0.5	6.5	4.1–6.5	5.2 ± 0.8
3 rd anal-fin ray length	13.0	14.0–16.5	15.0 ± 0.8	14.4	13.3–15.5	14.1 ± 1.8

Abbreviations: D–P1 (distance from dorsal-fin origin to pectoral-fin insertion); D–P2 (distance from dorsal-fin origin to pelvic-fin insertion); D–A (distance between origins of dorsal and anal fins); P1–P2 (distance between insertions of pectoral and pelvic fins); P2–A (distance between pelvic-fin insertion and anal-fin origin).

and palatine. Patch of fine conical teeth on pterygoid. Several distinct conical teeth on vomer. Several rows of conical teeth on upper edges of basihyal and basibranchial. Eye large, round, covered with adipose eyelid, positioned laterally on head dorsal to horizontal through pectoral-fin insertion, visible in dorsal view. Pupil round. Orbit elliptical. Nostrils close to each other, anterior to orbit. Posterior margin of pre-opercle

Table 4. Frequency distribution of total vertebral numbers of *Stolephorus bengalensis*, *Stolephorus diabolus* sp. nov., *Stolephorus eclipis* sp. nov. and *Stolephorus eldorado* sp. nov.

		Total vertebrae			
		38	39	40	41
<i>Stolephorus bengalensis</i>	<i>n</i> = 32			27	5
<i>Stolephorus diabolus</i> sp. nov.	<i>n</i> = 2		2		
<i>Stolephorus eclipis</i> sp. nov.	<i>n</i> = 14	6	8		
<i>Stolephorus eldorado</i> sp. nov.	<i>n</i> = 45	11	24	10	

concave, indented. Subopercle and opercle with smoothly rounded posterior margins. Gill membrane without serrations. Interorbital space flat, width less than eye diameter. Pseudobranchial filaments present, length of longest filament less than eye diameter. Gill rakers long, slender, rough, visible from side of head when mouth opened. Single row of asperities on anterior surface of gill rakers. Isthmus muscle long, reaching anteriorly to posterior margin of gill membranes. Urohyal hidden by isthmus muscle, not visible without dissection. Gill membrane on each side joined distally, most of isthmus muscle exposed, not covered by gill membrane. Scales on lateral surface of body thin, cycloid, deciduous, those on lateral body surface with several centrally continuous vertical grooves and several longitudinal striae anteriorly (Fig. 3). Head scales absent. Fins scaleless, except for broad triangular sheath of scales on caudal fin. Dorsal-fin origin posterior to vertical through base of last pelvic-fin ray, slightly posterior to middle of body. Dorsal and anal fins with three anteriormost rays unbranched. First dorsal and anal-fin rays minute. Anteriormost three rays of both dorsal and anal fins closely spaced. Anal-fin origin just below base of tenth (ninth to eleventh) dorsal-fin ray. Posterior tip of depressed anal fin not reaching caudal-fin base. Uppermost pectoral-fin ray unbranched, inserted below body axis. Posterior tip of pectoral fin not reaching to pelvic fin insertion. Dorsal, ventral and posterior margins of pectoral fin nearly linear. Pelvic fin shorter than pectoral fin, insertion anterior to vertical through dorsal-fin origin. Posterior tip of depressed pelvic fin not reaching to vertical through dorsal-fin origin. Caudal fin forked, posterior tips pointed.

Colour of preserved specimens. Body uniformly pale ivory. A pair of distinct dark patches on parietal region, with little pigmentation on occipital area. Double pigmented lines dorsally posterior to dorsal fin. A few melanophores scattered anteriorly on snout. No black spots below eye and on lower-jaw tip. Melanophores scattered along bases of dorsal and anal fins. All fins transparent, melanophores scattered along fin rays of caudal fin and anterior parts of dorsal and anal fins.

Distribution. *Stolephorus bengalensis* is distributed in the northern Indian Ocean from Pakistan to the Bay of Bengal (Fig. 4). It is abundantly landed and marketed along the coast of the Bay of Bengal.

Morphological comparisons. *Stolephorus bengalensis* has been considered conspecific with the three new species described herein, the four species being easily separable from all other congeners, except for *Stolephorus acinaces*, *Stolephorus andhraensis* Babu Rao, 1966, *Stolephorus carpentariae* (De Vis, 1882), *Stolephorus hindustanensis* Hata & Motomura, 2022, *Stolephorus holodon* (Boulenger, 1900),

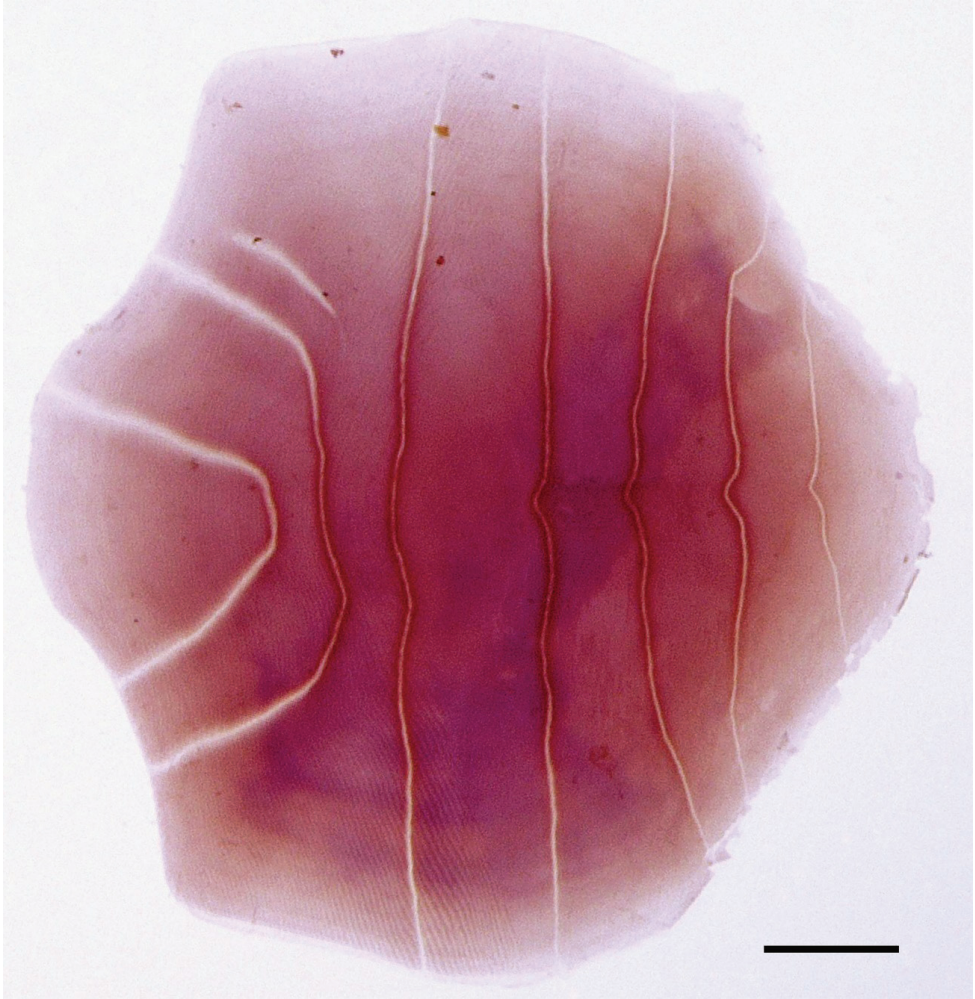


Figure 3. Stained scale removed from right side of mid-body (above anal fin) of *Stolephorus bengalensis*, BMNH 1969.5.30.34–45, 47.8 mm SL, Chennai, India (left-right inverted; scale bar indicates 0.5 mm).

Stolephorus ronquilloi Wongratana, 1983 and *Stolephorus tamilensis* Gangan, Pavan-Kumar, Jahageerdar & Jaiswar, 2020, the former having a concavely indented pre-opercular margin and lacking a spine on the pelvic scute (Whitehead et al. 1988; Wongratana et al. 1999; Kimura et al. 2009; Hata and Motomura 2018a, b, c, d, e, 2021a, b, c, 2022; Hata et al. 2019, 2020a, b, 2021; Gangan et al. 2020). However, the former four species are distinguished from the other seven by having a predorsal scute (vs. absent in the latter) and double dark lines on the dorsum posterior to the dorsal fin (vs. no lines on the dorsum, except in *S. hindustanensis* and *S. ronquilloi*). Moreover, *S. carpentariae* also differs from *S. bengalensis* and the three new species in having 19 or 20 branched anal-fin rays [16–18 (rarely 19 or 20) in the remaining five species] and the anal-fin origin located below the origin of the second to sixth dorsal-

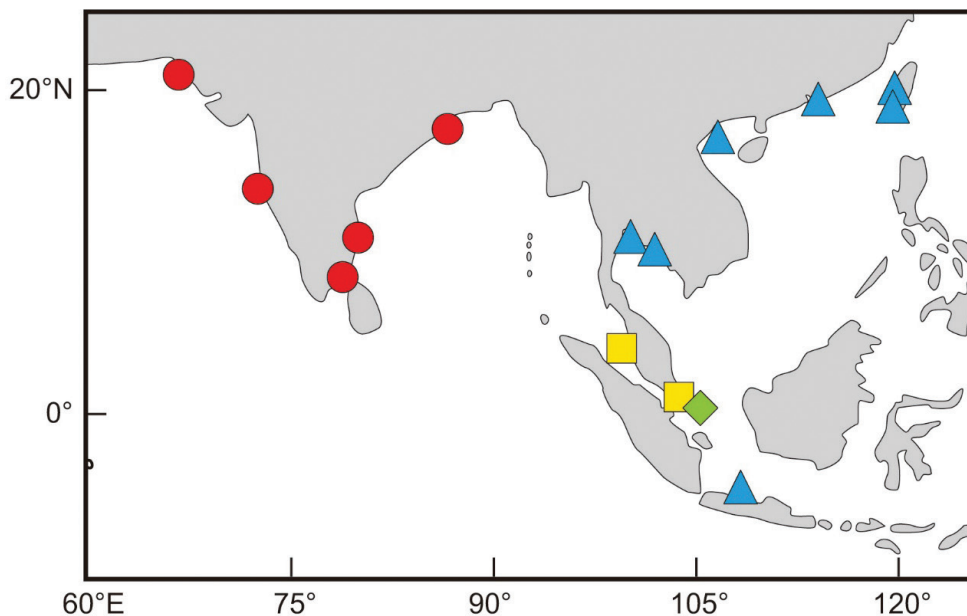


Figure 4. Map of the northern part of the Indo-West Pacific region showing distributional records of *Stolephorus bengalensis* (red circles), *S. diabolus* (yellow squares) sp. nov., *S. eclipsis* (green diamond) sp. nov. and *S. eldorado* (blue triangles) sp. nov., based on specimens examined in this study. Land masses outlined with black lines.

fin ray (vs. eighth to eleventh) (Whitehead et al. 1988; Wongratana et al. 1999; Gangan et al. 2020; Hata et al. 2020b). *Stolephorus bengalensis*, *S. diabolus* sp. nov., *S. eclipsis* sp. nov. and *S. eldorado* sp. nov. resemble *Stolephorus baganensis* Delsman, 1931, *Stolephorus dubiosus* Wongratana, 1983 and *Stolephorus tri* (Bleeker, 1852) in having a predorsal scute and double pigment lines on the dorsum behind the dorsal fin, but differ in having deciduous body scales (vs. body scales not deciduous) and lacking a spine on the pelvic scute (pelvic scute with a hard posteriorly projecting spine) (Whitehead et al. 1988; Wongratana et al. 1999; Hata et al. 2019). Comparisons of *S. bengalensis* with *S. diabolus* sp. nov., *S. eclipsis* sp. nov. and *S. eldorado* sp. nov. are given in “Comparisons” under each new species.

Molecular comparisons. *Stolephorus bengalensis*, *S. diabolus* sp. nov. and *S. eldorado* sp. nov. were divergent from each other by at least 3.5% COI-based mean uncorrected genetic distance (min-max = 3.5–7.7%) (Fig. 5). In contrast, each species was genetically uniform, with intraspecific differentiation not exceeding 1% (note: *Stolephorus* sp. represented by a single specimen – see below), forming clear intraspecific versus interspecific genetic gaps. The ML phylogenetic tree using COI and cytochrome *b* markers (Fig. 5) was fully resolved, with interspecific relationships supported by bootstrap values above 80%. Each species formed a well-supported monophyletic group, in agreement with their genetic distinction, thereby confirming their taxonomic status, which was further supported by the morphological observations. The COI se-

quence of an unidentified larva collected from the Segara Anakan Lagoon, Central Java (Nuryanto et al. 2017), indicated either a range extension of *S. eclipsis* sp. nov. or the presence of an unidentified species of *Stolephorus*, related to *S. bengalensis*.

***Stolephorus diabolus* sp. nov.**

<https://zoobank.org/09515D76-5020-4C13-9391-7F325335C74C>

[New English name: Demon Anchovy]

Figs 1C, 6; Tables 4–6

Stolephorus bengalensis (not of Dutt and Babu Rao): Hata et al. 2022: (in part) 34 (Singapore).

Holotype. IPMB-I 13.00001, 49.7 mm SL, Teluk Bahang, Penang, Malaysia.

Paratypes. 14 specimens, 28.5–43.7 mm SL. USMFC 82-0017, 43.7 mm SL, collected with the holotype; USMFC 82-0057, 4 specimens, 40.1–41.1 mm SL, estuary of Merbok River, Jeti Semeling, Malaysia; ZUMT 62056, 5 specimens, 28.5–38.4 mm SL, KAUM-I. 163702, 36.3 mm SL, KAUM-I. 163703, 36.4 mm SL, NSMT-P 143554, 36.4 mm SL, NSMT-P 143555, 36.6 mm SL, Singapore.

Diagnosis. A species of *Stolephorus* with the following combination of characters: 1UGR 14–16 (modally 16), 1LGR 20–23 (22), 1TGR 35–38 (38); 2UGR 10 or 11 (11), 2LGR 19 or 20 (20), 2TGR 30 or 31 (31); 3UGR 8 or 9 (9), 3LGR 11 or 12 (12), 3TGR 20 or 21 (21); 4UGR 6 or 7 (7), 4LGR 9 or 10 (9), 4TGR 15–17 (17); prepelvic scutes 5–7 (6); total vertebrae 39; long maxilla, posterior tip just reaching or slightly short of posterior margin of opercle; predorsal scute present; pelvic scute without spine; body scales deciduous; posterior border of pre-opercle concave, indented; paired dark patch on parietal area with little following pigmentation; distinct double pigment lines along dorsum posterior to dorsal fin; black spots below eye and on lower-jaw tip absent; anal-fin base long, 19.8–22.3% (mean 20.7%) of SL; maximum orbit diameter 8.1–8.7% (8.3%) of SL; third dorsal-fin ray short, 17.0–18.5% (18.0%) of SL; pelvic fin rather long, 9.6–11.3% (10.0%) of SL, its posterior tip not reaching to vertical through dorsal-fin origin when depressed in specimens > 40 mm SL; distance between posterior ends of supramaxilla and maxilla 5.7–6.4% (6.1%) of SL.

Description. Data for holotype presented first, followed by data for paratypes in parentheses (if different). Counts and measurements, expressed as percentages of SL or HL, given in Tables 5 and 6. Body laterally compressed, elongate, deepest at dorsal-fin origin. Dorsal profile of head and body slightly convex from snout tip to dorsal-fin origin, gently lowering to uppermost point of caudal-fin base. Ventral profile of head and body slightly convex from lower jaw tip to pelvic-fin insertion, thereafter, slowly rising to lowermost point of caudal-fin base. Single spine-like scute just anterior to dorsal-fin origin. Abdomen somewhat rounded. Scutes on ventrum broken in holotype (five to seven spine-like prepelvic scutes on ventrum in paratypes). Pelvic scute without spine. Postpelvic scutes absent. Anus just anterior to anal-fin origin. Snout

Table 5. Meristics of specimens of *Stolephorus diabolus* sp. nov. and *Stolephorus eclipsis* sp. nov.

	<i>Stolephorus diabolus</i> sp. nov.			<i>Stolephorus eclipsis</i> sp. nov.		
	Holotype	Paratypes		Holotype	Paratypes	
	IPMB-I 13.00001	n = 14		MZB 26452	n = 28	
Standard length (mm)	49.7	28.5–43.7	Modes ± SD	40.3	32.0–43.7	Modes ± SD
Dorsal-fin rays (unbranched)	3	3	3 ± 0	3	3	3 ± 0
Dorsal-fin rays (branched)	12	12–13	13 ± 0.5	12	11–13	12 ± 0.4
Anal-fin rays (unbranched)	3	3	3 ± 0	3	3	3 ± 0
Anal-fin rays (branched)	16	16–18	17 ± 0.7	17	16–18	17 ± 0.7
Pectoral-fin rays (unbranched)	1	1	1 ± 0	1	1	1 ± 0
Pectoral-fin rays (branched)	11	10–13	11 ± 0.8	10	10–12	11 ± 0.6
Pelvic-fin rays (unbranched)	1	1	1 ± 0	1	1	1 ± 0
Pelvic-fin rays (branched)	6	6	6 ± 0	6	6	6 ± 0
Gill rakers on 1 st gill arch (upper)	16	14–16	16 ± 0.6	20	19–21	20 ± 0.7
Gill rakers on 1 st gill arch (lower)	22	20–23	22 ± 0.7	28	26–30	28 ± 0.8
Gill rakers on 1 st gill arch (total)	38	35–38	38 ± 1.0	48	47–51	47 ± 1.1
Gill rakers on 2 nd gill arch (upper)	10	11	11 ± 0.2	13	13–16	14 ± 0.7
Gill rakers on 2 nd gill arch (lower)	20	19–20	20 ± 0.4	25	24–27	25 ± 0.8
Gill rakers on 2 nd gill arch (total)	30	30–31	31 ± 0.4	38	37–42	39 ± 1.4
Gill rakers on 3 rd gill arch (upper)	9	8–9	9 ± 0.2	11	10–13	12 ± 0.7
Gill rakers on 3 rd gill arch (lower)	12	11–12	12 ± 0.5	14	14–16	15 ± 0.6
Gill rakers on 3 rd gill arch (total)	21	20–21	21 ± 0.5	25	25–28	27 ± 1.1
Gill rakers on 4 th gill arch (upper)	7	6–7	7 ± 0.4	8	8–11	9 ± 0.9
Gill rakers on 4 th gill arch (lower)	9	9–10	9 ± 0.5	11	11–13	12 ± 0.5
Gill rakers on 4 th gill arch (total)	16	15–17	17 ± 0.8	19	19–24	21 ± 1.2
Gill rakers on posterior face of 3 rd gill arch	3	3–5	4 ± 0.5	4	4–7	5 ± 0.7
Prepelvic scutes	broken	5–7	6 ± 0.5	6	5–7	6 ± 0.5
Scale rows in longitudinal series	34	34–35	35 ± 0.5	35	35–36	35 ± 0.4
Transverse scales	8	8–9	8 ± 0.2	8	8	8 ± 0
Pseudobranchial filaments	broken	14–16	15 ± 0.7	14	14–18	15 ± 1.2
Total vertebrae	39	39	39 ± 0	38	38–39	39 ± 0.5

tip rounded; snout length less than eye diameter. Mouth large, inferior, ventral to body axis, extending backwards beyond posterior margin of eye. Maxilla long, its posterior tip broken in holotype (posterior pointed, just reaching or slightly short of opercle posterior margin in paratypes). Lower jaw slender. Single row of conical teeth on both jaws and palatine. Patch of fine conical teeth on pterygoid. Several distinct conical teeth on vomer. Several rows of conical teeth on upper edges of basihyal and basibranchial. Eye large, round, covered with adipose eyelid, positioned laterally on head dorsal to horizontal through pectoral-fin insertion, visible in dorsal view. Pupil round. Orbit elliptical. Nostrils close to each other, anterior to orbit. Posterior margin of pre-opercle concave, indented. Subopercle and opercle with smoothly rounded posterior margins. Gill membrane without serrations. Interorbital space flat, width less than eye diameter. Pseudobranchial filaments present, length of longest filament less than eye diameter. Gill rakers long, slender, rough, visible from side of head when mouth opened. Single row of asperities on anterior surface of gill rakers. Isthmus

Table 6. Morphometrics of specimens of *Stolephorus diabolus* sp. nov. and *Stolephorus eclipsis* sp. nov.

	<i>Stolephorus diabolus</i> sp. nov.			<i>Stolephorus eclipsis</i> sp. nov.		
	Holotype	Paratypes	Means ± SD	Holotype	Paratypes	Means ± SD
	IPMB-I 13.00001	n = 14		MZB 26452	n = 28	
Standard length (mm)	49.7	28.5–43.7		40.3	32.0–43.7	
As % SL						
Head length	24.8	25.0–25.9	25.4 ± 0.3	25.4	23.6–26.7	24.8 ± 0.8
Body depth	21.7	19.8–21.9	20.9 ± 0.7	20.6	18.4–20.8	19.6 ± 0.6
Pre-dorsal-fin length	51.8	51.3–52.9	52.1 ± 0.5	52.8	51.3–54.9	53.4 ± 1.0
Snout tip to pectoral-fin insertion	25.7	26.2–28.4	27.2 ± 0.6	26.8	24.8–28.5	26.5 ± 0.9
Snout tip to pelvic-fin insertion	48.2	45.8–49.0	47.2 ± 0.8	47.0	44.8–47.3	46.2 ± 0.7
Snout tip to anal-fin origin	65.4	63.0–66.0	64.4 ± 0.9	63.1	62.8–65.8	64.1 ± 0.9
Dorsal-fin base length	15.0	13.9–16.6	15.0 ± 0.7	13.6	13.1–14.5	13.8 ± 0.4
Anal-fin base length	19.8	19.9–22.3	20.7 ± 0.8	19.3	17.6–19.3	18.6 ± 0.5
Caudal-peduncle length	18.8	16.4–19.4	17.8 ± 0.9	17.4	14.7–18.5	17.1 ± 0.9
Caudal-peduncle depth	9.8	9.4–10.3	9.8 ± 0.2	9.9	9.2–10.6	9.8 ± 0.4
D–P1	36.5	33.8–36.4	35.3 ± 0.8	38.0	34.0–38.8	36.5 ± 1.3
D–P2	23.5	21.9–24.5	23.4 ± 0.6	24.1	21.0–23.9	22.5 ± 0.8
D–A	22.6	20.7–23.1	22.2 ± 0.8	21.3	20.0–21.9	20.9 ± 0.5
P1–P2	24.1	19.4–20.0	21.0 ± 1.1	21.3	19.3–22.8	21.0 ± 0.9
P2–A	18.0	16.3–19.5	18.0 ± 0.9	18.5	17.5–20.6	19.0 ± 0.8
Pectoral-fin length	16.2	15.4–17.1	16.2 ± 0.5	16.4	15.5–17.7	16.7 ± 0.6
Pelvic-fin length	9.8	9.6–11.3	10.0 ± 0.4	8.7	8.8–9.9	9.4 ± 0.3
Maxilla length	broken	20.9–21.9	21.4 ± 0.3	20.7	19.9–22.5	21.1 ± 0.7
Lower-jaw length	16.2	16.2–17.5	16.6 ± 0.3	16.4	15.8–17.7	16.6 ± 0.5
Supramaxilla end to maxilla end	broken	5.7–6.4	6.1 ± 0.2	5.2	4.7–5.4	5.1 ± 0.2
Maximum orbit diameter	8.2	8.1–8.7	8.3 ± 0.2	8.8	7.9–9.6	8.7 ± 0.4
Eye diameter	6.5	6.1–7.7	6.9 ± 0.5	6.8	6.7–8.3	7.3 ± 0.4
Snout length	3.7	3.6–4.2	3.8 ± 0.2	4.0	3.4–4.2	3.8 ± 0.2
Interorbital width	5.6	5.5–5.9	5.7 ± 0.2	5.7	5.5–6.2	5.8 ± 0.2
Postorbital length	12.8	12.9–14.2	13.4 ± 0.4	12.1	11.5–12.9	12.1 ± 0.4
1 st dorsal-fin ray length	1.5	0.8–2.2	1.6 ± 0.4	1.5	1.0–2.2	1.5 ± 0.3
2 nd dorsal-fin ray length	broken	7.0–9.8	8.1 ± 0.7	broken	5.1–5.7	7.6 ± 0.6
3 rd dorsal-fin ray length	broken	17.0–18.5	18.0 ± 0.5	17.1	16.5–18.8	17.6 ± 0.7
1 st anal-fin ray length	1.6	0.9–2.2	1.5 ± 0.4	1.9	1.2–2.2	1.7 ± 0.3
2 nd anal-fin ray length	5.3	4.8–7.2	5.5 ± 0.6	5.2	5.1–5.7	5.3 ± 0.2
3 rd anal-fin ray length	broken	14.6–16.0	15.4 ± 0.4	14.4	13.4–15.0	14.2 ± 0.5

Abbreviations: D–P1 (distance from dorsal-fin origin to pectoral-fin insertion); D–P2 (distance from dorsal-fin origin to pelvic-fin insertion); D–A (distance between origins of dorsal and anal fins); P1–P2 (distance between insertions of pectoral and pelvic fins); P2–A (distance between pelvic-fin insertion and anal-fin origin).

muscle long, reaching anteriorly to posterior margin of gill membranes. Urohyal hidden by isthmus muscle, not visible without dissection. Gill membrane on each side joined distally, most of isthmus muscle exposed, not covered by gill membrane. Body scales deciduous, completely lacking on specimens, except for prepelvic scutes. Head

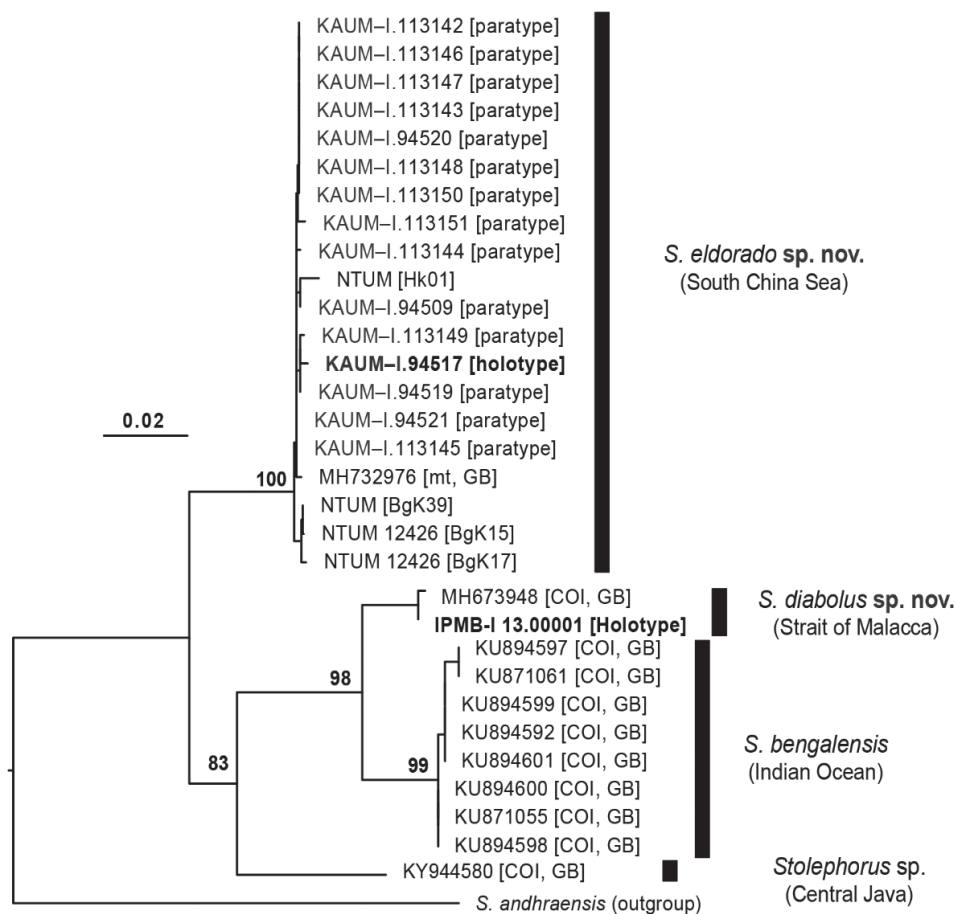


Figure 5. Maximum-likelihood phylogenetic tree of four species of *Stolephorus* related to *S. bengalensis*, based on the cytochrome *b* and cytochrome oxidase I genes (total: 1,788 base pairs) of 31 specimens, each species forming a monophyletic group. Each specimen identified by Museum Registration Number or GenBank number (see text and Table 1 for details). Type status (either holotype or paratype), specimen code, gene used (mt or COI) and sequence origin (GB) are indicated in brackets where necessary. Tree rooted by a specimen of *Stolephorus andhraensis*. Branch lengths proportional to number of substitutions. Bootstrap proportions indicated at nodes.

scales absent. Fins scaleless, except for broad triangular sheath of scales on caudal fin. Dorsal-fin origin posterior to vertical through base of last pelvic-fin ray, slightly posterior to middle of body. Dorsal and anal fins with three anteriormost rays unbranched. First dorsal- and anal-fin rays minute. Anteriormost three rays of both dorsal and anal fins closely spaced. Anal-fin origin just below base of eighth (eighth to eleventh) dorsal-fin ray. Posterior tip of depressed anal fin not reaching caudal-fin base. Uppermost pectoral-fin ray unbranched, inserted below body axis. Posterior tip of pectoral fin not reaching to pelvic fin insertion. Dorsal, ventral and posterior margins of pectoral fin nearly linear. Pelvic fin shorter than pectoral fin, insertion anterior to vertical through



Figure 6. **A** lateral **B** dorsal and **C** ventral views of preserved holotype of *S. diabolus* sp. nov., IPMB-I 13.00001, 49.7 mm SL, Teluk Bahang, Penang, Malaysia **D** lateral view of preserved paratype of *S. diabolus* sp. nov., ZUMT 62056, 37.3 mm SL, Singapore. Scale bars: 2 mm.

dorsal-fin origin. Posterior tip of depressed pelvic fin not reaching to vertical through dorsal-fin origin (reaching to vertical through first to sixth dorsal-fin ray origin in some paratypes smaller than 40 mm SL). Caudal fin forked, posterior tips pointed.

Colour of preserved specimens. Body uniformly pale white. A pair of distinct dark patches on parietal region, with little pigmentation on occipital area. No black spots below eye and on lower-jaw tip. Melanophores scattered on posterior margins of scale pockets on dorsum. Double pigmented lines dorsally posterior to dorsal fin. Melanophores scattered along bases of dorsal and anal fins. All fins transparent, melanophores scattered along fin rays of caudal fin and anterior parts of dorsal and anal fins.

Distribution. *Stolephorus diabolus* sp. nov. is currently known only from the western coast of the Peninsular Malaysia (Merbok River Estuary and Penang) and Singapore (Fig. 4).

Etymology. The specific name “*diabolus*” is derived from Latin meaning “demon”, in reference to the hard spine on the dorsum of the species.

Comparisons. The new species is distinguished from *S. bengalensis*, *S. eclipsis* and *S. eldorado* by lower gill raker counts: 1TGR, 35–38 in *S. diabolus* (vs. 40 or more in the other three species); 2TGR, 30 or 31 in *S. diabolus* [vs. 33 or more (rarely 30 or 31 in *S. eldorado*)]; 3TGR, 20 or 21 in *S. diabolus* [vs. 22 or more in the other three

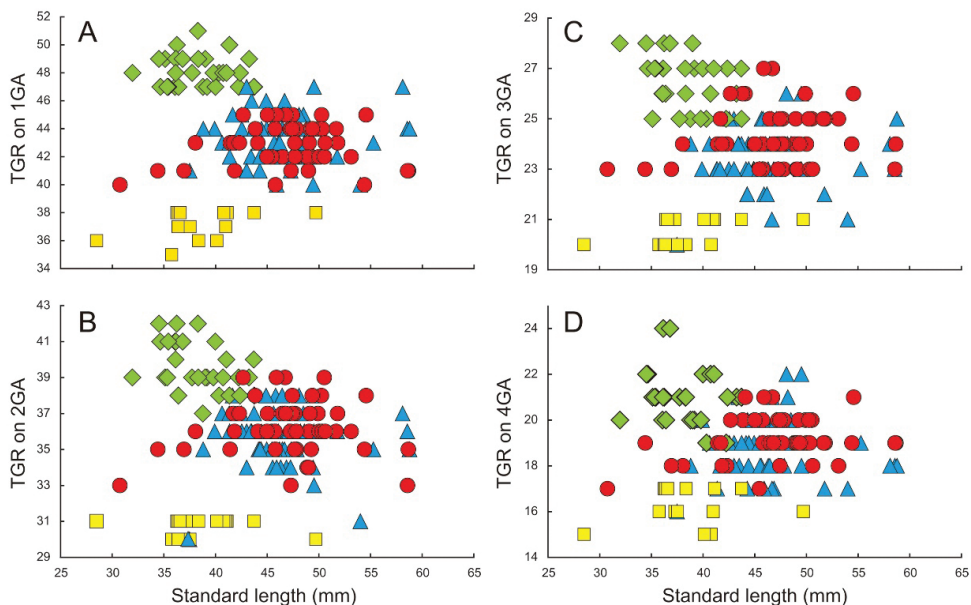


Figure 7. Relationships of total gill raker numbers (TGR) on **A** first gill arch (1GA) **B** second gill arch (2GA) **C** third gill arch (3GA) and **D** fourth gill arch (4GA) to standard length in *Stolephorus bengalensis* (red circles), *S. diabolus* sp. nov. (yellow squares), *S. eclipsis* sp. nov. (green diamonds) and *S. eldorado* sp. nov. (blue triangles).

species (rarely 21 in *S. eldorado*]; and 4TGR, 15–17 in *S. diabolus* (vs. 17 or more) (Fig. 7). Moreover, *S. diabolus* has a shorter orbit diameter than *S. eldorado* [maximum orbit diameter 8.1–8.7% (mean 8.3%) of SL in *S. diabolus* vs. 8.2–9.9% (8.9%) in *S. eldorado*; Fig. 8A]. Furthermore, *S. diabolus* is distinguished from *S. bengalensis* by having a shorter third dorsal-fin ray [17.0–18.5% (mean 18.0%) of SL in *S. diabolus* vs. 18.5–19.9% (19.0%) in *S. bengalensis* (Fig. 8B)] and lower total vertebral numbers [39 vs. 40 or 41 (modally 40) (Table 4)]. Detailed comparisons of *S. diabolus* with *S. eclipsis* and *S. eldorado* are given in “Comparisons” under each species.

Stolephorus eclipsis sp. nov.

<https://zoobank.org/1556E6AA-0531-4361-874E-3FE6DB1FEA10>

[New English name: Eclipse Anchovy]

Fig. 9; Tables 4–6

Holotype. MZB 26452, 40.3 mm SL, Bintan Island, Riau Archipelago, Indonesia.

Paratypes. 28 specimens, 32.0–43.7 mm SL. LBRC-F 5039, 35.4 mm SL, LBRC-F 5040, 35.3 mm SL, LBRC-F 5041, 36.1 mm SL, Tanjungpinang, Bintan Island, Riau Archipelago, Indonesia; MZB 26440, 32.0 mm SL, MZB 26441, 36.1 mm SL, MZB 26442, 35.1 mm SL, MZB 26443, 34.7 mm SL, MZB 26444, 34.5 mm SL,

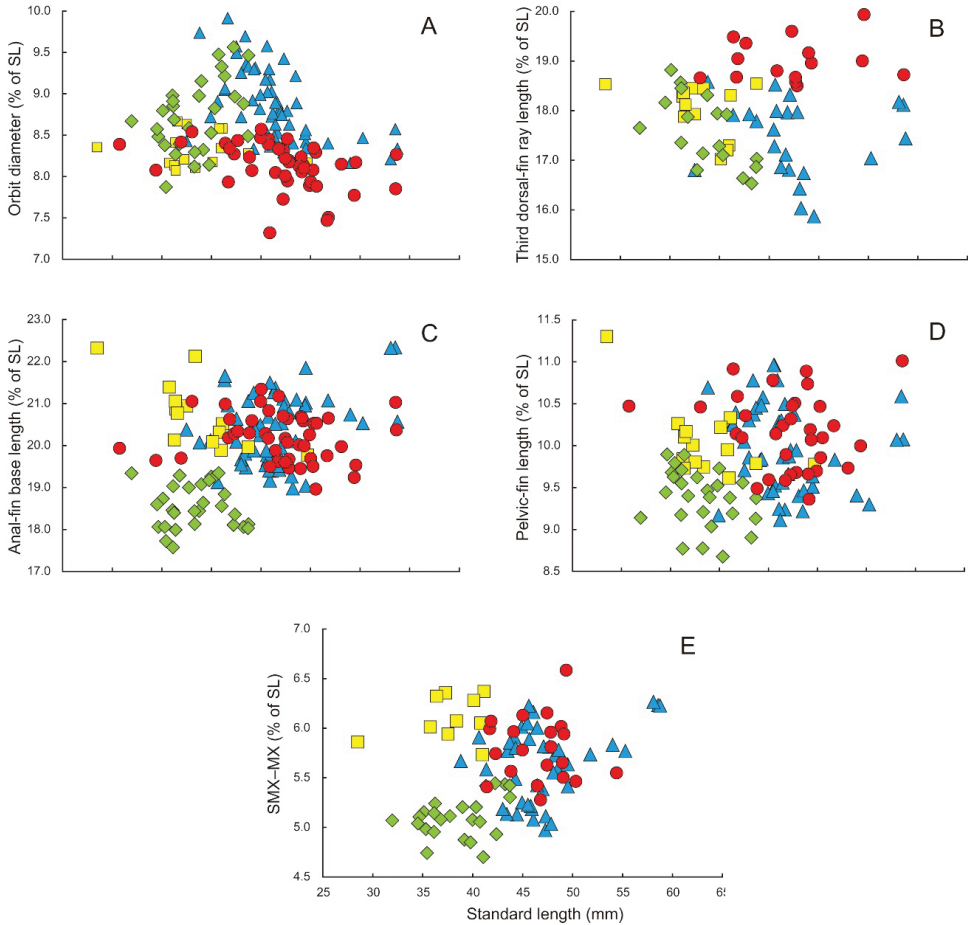


Figure 8. Relationships of **A** orbit diameter (as % of standard length; SL) **B** third dorsal-fin ray length (as % of SL) **C** anal-fin base length (as % of SL) **D** pelvic-fin length (as % of SL) and **E** distance between posterior ends of supramaxilla and maxilla (SMX–MX) in *Stolephorus bengalensis* (red circles), *S. diabolus* sp. nov. (yellow squares), *S. eclipsis* sp. nov. (green diamonds) and *S. eldorado* sp. nov. (blue triangles).

MZB 26445, 36.3 mm SL, MZB 26446, 36.2 mm SL, MZB 26447, 38.8 mm SL, MZB 26448, 39.2 mm SL, MZB 26449, 37.7 mm SL, MZB 26450, 40.0 mm SL, MZB 26451, 36.8 mm SL, 26453, 36.4 mm SL, MZB 26454, 39.0 mm SL, MZB 26455, 41.3 mm SL, MZB 26456, 43.7 mm SL, MZB 26457, 39.8 mm SL, MZB 26458, 40.7 mm SL, MZB 26459, 43.2 mm SL, MZB 26460, 43.7 mm SL, MZB 26461, 5 specimens, 38.3–42.4 mm SL, collected with the holotype.

Diagnosis. A species of *Stolephorus* with the following combination of characters: 1UGR 19–21 (modally 20), 1LGR 26–30 (28), 1TGR 47–51 (47); 2UGR 13–16 (14), 2LGR 24–27 (25), 2TGR 37–42 (39); 3UGR 10–13 (12), 3LGR 14–16 (15), 3TGR 25–28 (27); 4UGR 8–11 (9), 4LGR 11–13 (12), 4TGR 19–24 (21); prepelvic scutes 5–7 (6); total vertebrae 38–39 (39); long maxilla, posterior tip just reaching or slightly



Figure 9. **A** lateral **B** dorsal and **C** ventral views of preserved holotype of *S. eclipsis* sp. nov., MZB 26452, 40.3 mm SL, Bintan Island, Riau Archipelago, Indonesia. Scale bars indicate 2 mm.

short of posterior margin of opercle; predorsal scute present; pelvic scute without spine; body scales deciduous; posterior border of pre-opercle concave, indented; paired dark patch on parietal area with little following pigmentation; distinct double pigment lines along dorsum posterior to dorsal fin; black spots below eye and on lower-jaw tip absent; anal-fin base short, 17.6–19.3% (mean 18.6%) of SL; third dorsal-fin ray 16.5–18.8% (17.6%) of SL; pelvic fin short, 8.7–9.9% (9.4%) of SL, its posterior tip usually not reaching to vertical through dorsal-fin origin when depressed; distance between posterior ends of supramaxilla and maxilla 4.7–5.4% (5.1%) of SL; pre-dorsal-fin length 51.3–54.9% (53.4%) of SL; dorsal-fin base short, 13.1–14.5% (13.8%) of SL.

Description. Data for holotype presented first, followed by data for paratypes in parentheses (if different). Counts and measurements, expressed as percentages of SL or HL, given in Tables 5 and 6. Body laterally compressed, elongate, deepest at dorsal-fin origin. Dorsal profile of head and body slightly convex from snout tip to dorsal-fin origin, gently lowering to uppermost point of caudal-fin base. Ventral profile of head and body slightly convex from lower jaw tip to pelvic-fin insertion, thereafter, slowly rising to lowermost point of caudal-fin base. Single spine-like scute just anterior to dorsal-fin origin. Abdomen somewhat rounded, covered with six (five to seven) spine-like prepelvic scutes. Pelvic scute without spine. Postpelvic scutes absent. Anus just anterior to anal-fin origin. Snout tip rounded; snout length less than eye diameter. Mouth large, inferior, ventral to body axis, extending backwards beyond posterior margin of eye. Maxilla long, its posterior tip pointed, just reaching (or slightly short of) opercle posterior margin. Lower jaw slender. Single row of conical teeth on both jaws and palatine. Patch of fine conical teeth on pterygoid. Several distinct conical teeth on vomer. Several rows of conical teeth on upper edges of basihyal and basibranchial. Eye large, round, covered with adipose eyelid, positioned laterally on head dorsal to

horizontal through pectoral-fin insertion, visible in dorsal view. Pupil round. Orbit elliptical. Nostrils close to each other, anterior to orbit. Posterior margin of pre-opercle concave, indented. Subopercle and opercle with smoothly rounded posterior margins. Gill membrane without serrations. Interorbital space flat, width less than eye diameter. Pseudobranchial filaments present, length of longest filament less than eye diameter. Gill rakers long, slender, rough, visible from side of head when mouth opened. Single row of asperities on anterior surface of gill rakers. Isthmus muscle long, reaching anteriorly to posterior margin of gill membranes. Urohyal hidden by isthmus muscle, not visible without dissection. Gill membrane on each side joined distally, most of isthmus muscle exposed, not covered by gill membrane. Body scales deciduous, completely lacking on specimens, except for prepelvic scutes. Head scales absent. Fins scaleless, except for broad triangular sheath of scales on caudal fin. Dorsal-fin origin posterior to vertical through base of last pelvic-fin ray, slightly posterior to middle of body. Dorsal and anal fins with three anteriormost rays unbranched. First dorsal- and anal-fin rays minute. Anteriormost three rays of both dorsal and anal fins closely-spaced. Anal-fin origin just below base of eighth (eighth to eleventh) dorsal-fin ray. Posterior tip of depressed anal fin not reaching caudal-fin base. Uppermost pectoral-fin ray unbranched, inserted below body axis. Posterior tip of pectoral fin not reaching to pelvic fin insertion. Dorsal, ventral and posterior margins of pectoral fin nearly linear. Pelvic fin shorter than pectoral fin, insertion anterior to vertical through dorsal-fin origin. Posterior tip of depressed pelvic fin not reaching to vertical through dorsal-fin origin (reaching to vertical through first to third dorsal-fin ray origin in some paratypes). Caudal fin forked, posterior tips pointed.

Colour of preserved specimens. Body uniformly pale ivory. A pair of distinct dark patches on parietal region, with little pigmentation on occipital area. Double pigmented lines dorsally posterior to dorsal fin. A few melanophores scattered anteriorly on snout. No black spots below eye and on lower-jaw tip. Melanophores scattered along bases of dorsal and anal fins. All fins transparent, melanophores scattered along fin rays of caudal fin and anterior parts of dorsal and anal fins.

Distribution. *Stolephorus eclipsis* sp. nov. is currently known only from Bintan Island, Riau Archipelago, Indonesia (Fig. 4).

Etymology. The specific name “*eclipsis*” refers to eclipse, reminiscent of the concave pre-opercle of the new species.

Comparisons. The new species differs from *S. bengalensis*, *S. diabolus* and *S. eldorado* in having higher gill raker counts [1TGR, 47–51 or more in *S. eclipsis* (vs. 47 or fewer in the other three species); 2TGR, 37–42 in *S. eclipsis* (vs. 39 or fewer); 3TGR, 25–28 in *S. eclipsis* (vs. 27 or fewer); and 4TGR, 19–24 in *S. eclipsis* (vs. 22 or fewer) (Fig. 7)], a shorter anal-fin base (17.6–19.3% of SL in *S. eclipsis* vs. 19.0–21.3% in *S. bengalensis*, 19.8–22.3% in *S. diabolus* and 19.0–22.3% in *S. eldorado*; Fig. 8C) and pelvic fin [8.7–9.9% (mean 9.4%) of SL in *S. eclipsis* vs. 9.4–11.0% (10.2%) in *S. bengalensis*, 9.6–11.3% (10.0%) in *S. diabolus* and 9.1–11.0% (10.0%) in *S. eldorado*; Fig. 8D) and shorter distance between the posterior ends of the supramaxilla and maxilla [4.7–5.4% (5.1%) of SL in *S. eclipsis* vs. 5.3–6.6% (5.8%) in *S. bengalensis*, 5.7–6.4% (6.1%)

in *S. diabolus* and 5.0–6.3% (5.6%) in *S. eldorado*; Fig. 8E]. *Stolephorus eclipsis* also differs from *S. bengalensis* in having a shorter third dorsal-fin ray (16.5–18.8% of SL in *S. eclipsis* vs. 18.5–19.9% in *S. bengalensis*; Fig. 8B) and lower total vertebral number [38–39 (modally 39) vs. 40 or 41 (40) (Table 4)]. Moreover, *S. eclipsis* is distinguished from *S. diabolus* by a greater pre-dorsal-fin distance [51.3–54.9% (mean 53.4%) of SL in *S. eclipsis* vs. 51.3–52.9% (52.1%) in *S. diabolus*; Fig. 10A] and shorter dorsal-fin base (13.1–14.5% of SL vs. 13.9–16.6%; Fig. 10B) and postorbital head length (11.5–12.9% of SL vs. 12.8–14.2%; Fig. 10C).

***Stolephorus eldorado* sp. nov.**

<https://zoobank.org/0A916EDA-E70A-4EAF-85C2-7AC51C588BC4>

[New English name: El Dorado Anchovy]

Figs 1A, B, D, E, F, 11; Tables 2–4

Stolephorus insularis (not of Delsman): Whitehead et al. 1988 (in part): 413 unnumbered fig. (Taiwan to Java Sea); Young et al. 1999: 222, fig. 7 (western coast of Taiwan); Wongratana et al. 1999 (in part): 1736, unnumbered fig. (Taiwan to Java Sea); Hata 2018: 41, unnumbered figs (Ha Long Bay, northern Vietnam).

Stolephorus tri (not of Bleeker): Zhang 2001: 129, fig. II-59 (Beihai City, Guangxi Province, China).

Stolephorus bengalensis (not of Dutt and Babu Rao): Hata et al. 2019 (in part): 24, fig. 12a, b (Taiwan; Hainan Island, China; Ha Long Bay, Vietnam; Gulf of Thailand; Songkhla, Thailand; Kuala Terengganu, Terengganu, Malaysia); Hata 2019: 206, unnumbered figs (Ke-tzu-liao, Ziguan District, Kaohsiung, Taiwan); Hata et al. 2022: (in part) 34 (Wenzhou City, Zhejiang Province, China).

Holotype. KAUM–I. 94517, 44.4 mm SL, Ha Long Bay, Ha Long City, Quang Ninh District, Vietnam (purchased at fish market in Ha Long City), 24 Oct 2016; coll. by H. Hata and M. Matsunuma.

Paratypes. 57 specimens, 37.5–58.8 mm SL. **TAIWAN:** ASIZP 73957, 51.8 mm SL, Fangyan, Changhua (23°57'42.8"N, 120°17'39.8"E); KAUM–I. 110282, 49.5 mm SL, KAUM–I. 113142, 54.0 mm SL, KAUM–I. 113143, 45.5 mm SL, KAUM–I. 113144, 44.3 mm SL, KAUM–I. 113145, 46.3 mm SL, KAUM–I. 113146, 37.5 mm SL, KAUM–I. 113147, 47.3 mm SL, KAUM–I. 113148, 55.3 mm SL, KAUM–I. 113149, 49.4 mm SL, KAUM–I. 113150, 45.9 mm SL, KAUM–I. 113151, 47.3 mm SL, off Ke-tzu-liao, Ziguan District, Kaohsiung. **CHINA:** BMNH 1965.4.1.981–983, 3 specimens, 58.1–58.8 mm SL, Stanley, Hong Kong. **VIETNAM:** FRLM 49725, 46.9 mm SL, KAUM–I. 67322, 46.7 mm SL, KAUM–I. 67405, 45.6 mm SL, KAUM–I. 94509, 41.4 mm SL, KAUM–I. 94518, 43.7 mm SL, KAUM–I. 94519, 38.8 mm SL, KAUM–I. 94520, 41.7 mm SL, KAUM–I. 94521, 43.4 mm SL, Ha Long Bay, Ha Long, Quang Ninh Province. **THAILAND:** CAS 46931, 8 specimens, 44.4–46.7 mm SL, between Bangsaen and Chol Buri, Chol Buri, Gulf of Thailand; CAS 230414,

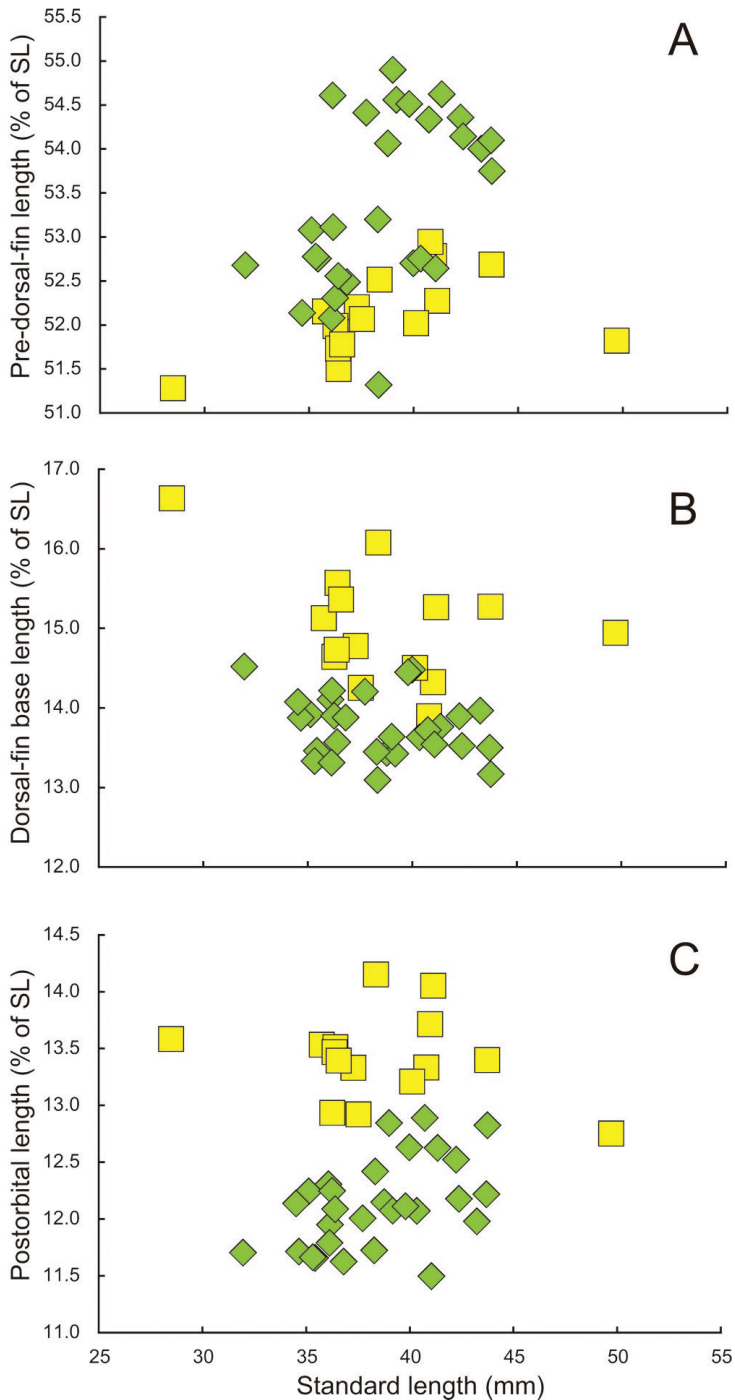


Figure 10. Relationships of **A** pre-dorsal-fin length (as % of standard length; SL) **B** dorsal-fin base length (as % of SL), and **C** postorbital length (as % of SL) in *Stolephorus diabolus* sp. nov. (yellow squares) and *S. eclipsis* sp. nov. (green diamonds).

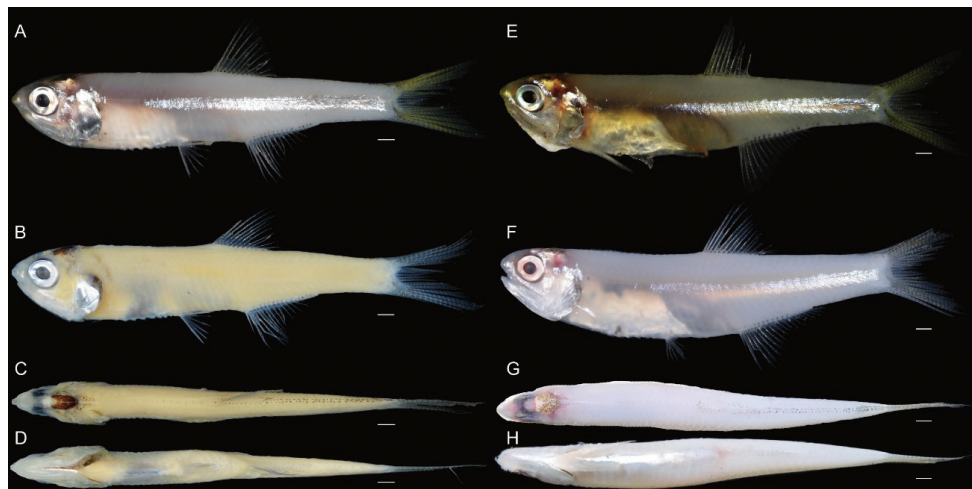


Figure 11. Holotype of *S. eldorado* sp. nov. (KAUM-I. 94517, 44.4 mm SL, Ha Long Bay, northern Vietnam) **A** lateral view (fresh) **B** lateral **C** dorsal, and **D** ventral views (preserved); paratypes of *S. eldorado* sp. nov. (KAUM-I. 67322, 46.7 mm SL, Ha Long Bay, northern Vietnam) **E** lateral view (fresh), (KAUM-I. 110282, 49.5 mm SL, Ke-tzu-liao, southwestern Taiwan) **F** lateral **G** dorsal, and **H** ventral views (fresh). Scale bars indicate 2 mm.

4 specimens, 39.9–45.8 mm SL, Lem Nam Point, south tip of Lem Nam Peninsula, Gulf of Thailand (12°02'55"N, 102°35'35"E), approx. 0.6 m depth; KAUM-I. 23190, 48.2 mm SL, Gulf of Thailand (obtained at fish market in Mahachai, Samut Prakan Province), trawl; NSMT-P 142790, 47.9 mm SL, Ko Maeo Island, off Songkhla; URM-P 12398, 3 specimens, 43.0–45.5 mm SL, Song Khula; URM-P 13635, 11 specimens, 46.2–49.5 mm SL, Ang Sila. **INDONESIA:** BMNH 1965.10.20.42–47, 6 specimens, 40.6–43.5 mm SL, 20 miles (approx. 32 km) east of Tegal, Java.

Diagnosis. A species of *Stolephorus* with the following combination of characters: 1UGR 16–21 (modally 18), 1LGR 23–28 (25), 1TGR 40–47 (42); 2UGR 10–14 (13), 2LGR 20–24 (23), 2TGR 33–38 (rarely 30) (modally 36); 3UGR 8–12 (modally 10), 3LGR 12–14 (13), 3TGR 20–26 (23); 4UGR 7–10 (8), 4LGR 9–12 (11), 4TGR 16–22 (18); prepelvic scutes 5–7 (6); total vertebrae 38–40 (39); long maxilla, posterior tip just reaching or slightly short of posterior margin of opercle; predorsal scutes present; pelvic scute without spine; body scales deciduous; posterior border of pre-opercle concave, indented; paired dark patch on parietal area with little following pigmentation; distinct double pigment lines along dorsum posterior to dorsal fin; black spots below eye and on lower-jaw tip absent; anal-fin base long, 19.0–22.3% (20.4%) of SL; orbit rather long, 8.2–9.9% (8.9%) of SL; third dorsal-fin ray short, 15.9–18.6% (17.4%) of SL; pelvic fin rather long, 9.1–11.0% (10.0%) of SL, its posterior tip usually not reaching to vertical through dorsal-fin origin when depressed in individuals > 50 mm SL; distance between posterior ends of supramaxilla and maxilla 5.0–6.3% (5.6%) of SL.

Description. Data for holotype presented first, followed by data for paratypes in parentheses (if different). Counts and measurements, expressed as percentages of SL or HL, given in Tables 2 and 3. Body laterally compressed, elongate, deepest at dorsal-fin origin. Dorsal profile of head and body slightly convex from snout tip to dorsal-fin origin, gently lowering to uppermost point of caudal-fin base. Ventral profile of head and body slightly convex from lower jaw tip to pelvic-fin insertion, thereafter, slowly rising to lowermost point of caudal-fin base. Single spine-like scute just anterior to dorsal-fin origin. Abdomen somewhat rounded, covered with six (five to seven) spine-like prepelvic scutes. Pelvic scute without spine. Postpelvic scutes absent. Anus just anterior to anal-fin origin. Snout tip rounded; snout length less than eye diameter. Mouth large, inferior, ventral to body axis, extending backwards beyond posterior margin of eye. Maxilla long, its posterior tip pointed, just reaching (or slightly short of) opercle posterior margin. Lower jaw slender. Single row of conical teeth on both jaws and palatine. Patch of fine conical teeth on pterygoid. Several distinct conical teeth on vomer. Several rows of conical teeth on upper edges of basihyal and basibranchial. Eye large, round, covered with adipose eyelid, positioned laterally on head dorsal to horizontal through pectoral-fin insertion, visible in dorsal view. Pupil round. Orbit elliptical. Nostrils close to each other, anterior to orbit. Posterior margin of pre-opercle concave, indented. Subopercle and opercle with smoothly rounded posterior margins. Gill membrane without serrations. Interorbital space flat, width less than eye diameter. Pseudobranchial filaments present, length of longest filament less than eye diameter. Gill rakers long, slender, rough, visible from side of head when mouth opened. Single row of asperities on anterior surface of gill rakers. Isthmus muscle long, reaching anteriorly to posterior margin of gill membranes. Urohyal hidden by isthmus muscle, not visible without dissection. Gill membrane on each side joined distally, most of isthmus muscle exposed, not covered by gill membrane. Body scales deciduous, completely lacking on all specimens, except for prepelvic scutes. Head scales absent. Fins scaleless, except for broad triangular sheath of scales on caudal fin. Dorsal-fin origin posterior to vertical through base of last pelvic-fin ray, slightly posterior to middle of body. Dorsal and anal fins with three anteriormost rays unbranched. First dorsal- and anal-fin rays minute. Anteriormost three rays of both dorsal and anal fins closely spaced. Anal-fin origin just below base of ninth (eighth to tenth) dorsal-fin ray. Posterior tip of depressed anal fin not reaching caudal-fin base. Uppermost pectoral-fin ray unbranched, inserted below body axis. Posterior tip of pectoral fin not reaching to pelvic fin insertion. Dorsal, ventral and posterior margins of pectoral fin nearly linear. Pelvic fin shorter than pectoral fin, insertion anterior to vertical through dorsal-fin origin. Posterior tip of depressed pelvic fin not reaching to vertical through dorsal-fin origin (reaching to vertical through first to fourth dorsal-fin ray origin in some paratypes smaller than 50 mm SL). Caudal fin forked, posterior tips pointed.

Colour of fresh specimens. (based on colour photographs of KAUM–I. 67322, 46.7 mm SL, KAUM–I. 67405, 45.6 mm SL, KAUM–I. 94517, 44.4 mm SL, KAUM–I. 94521, 43.4 mm SL and KAUM–I. 110282, 49.5 mm SL). Body yellowish milky-white, a silver longitudinal band, of width slightly less than pupil diameter, extending from just above posterior tip of pectoral fin to caudal-fin base. Caudal fin yellow with black posterior margin. Melanophores scattered along caudal-fin rays, ventral surface of caudal pe-

duncle and bases of dorsal and anal fins. Fin rays of dorsal and anal fins yellow. A few melanophores scattered on snout and fin rays of anterior part of dorsal fin. Fin rays and fin membrane of pectoral and pelvic fins transparent whitish, lacking melanophores. A pair of dark patches on parietal region, with little pigmentation on occipital area. Distinct double pigment lines on dorsum from end of dorsal-fin base to caudal-fin base. Body wholly yellowish when freshly caught (Fig. 11E), quickly becoming white after death (Figs 11F–H).

Colour of preserved specimens. Body uniformly pale white. A pair of distinct dark patches on parietal region, with little pigmentation on occipital area. Melanophores scattered on posterior margins of scale pockets on dorsum. Double pigmented lines dorsally posterior to dorsal fin. A few melanophores scattered anteriorly on snout. No black spots below eye and on lower-jaw tip. Melanophores scattered along bases of dorsal and anal fins. All fins transparent, with melanophores scattered along fin rays of caudal fin and anterior parts of dorsal and anal fins.

Distribution. *Stolephorus eldorado* sp. nov. is distributed in the western Pacific from Taiwan to Java, Indonesia (Fig. 4). The species is abundantly caught by trawl and marketed fresh in northern Vietnam. It is a set net bycatch in south-western Taiwan.

Etymology. The specific name “*eldorado*”, referring to the mythical city of gold, reflects the bright yellow colouration of the new species.

Morphological comparisons. *Stolephorus eldorado* sp. nov. has been previously identified as *S. insularis* or *S. bengalensis* (together with *S. bengalensis*, *S. diabolus* and *S. eclipsis* as recognised here) (e.g. Whitehead et al. 1988; Wongratana et al. 1999; Hata et al. 2019). However, *S. eldorado* is distinguished from *S. diabolus* and *S. eclipsis* by having an intermediate number of gill rakers on each gill arch (Table 2; Fig. 7). More detailed comparisons of *S. eldorado* with the latter two species are given in “Comparisons” under each species.

Although *S. eldorado* sp. nov. closely resembles *S. bengalensis* in having very similar numbers of gill rakers on each gill arch, the former differs from the latter in having a greater orbit diameter [maximum orbit diameter 8.2–9.9% (mean 8.9%) of SL vs. 7.3–8.6% (8.1%) in *S. bengalensis* (Fig. 8A)], shorter third dorsal-fin ray [15.9–18.6% (mean 17.4%) of SL vs. 18.5–19.9% (19.0%)] (Fig. 8B) and fewer total vertebrae [38–40 (modally 39) vs. 40 or 41 (40)] (Table 4).

Key to species previously identified as *Stolephorus insularis* by Whitehead et al. (1988) or *Stolephorus bengalensis* by Hata et al. (2019)

- 1 1TGR \leq 38.....
*S. diabolus* (western coast of Malay Peninsula to Singapore)
 – 1TGR \geq 41 2
 2 1TGR \geq 47; anal-fin base short, less than 19.3% of SL; pelvic fin short,
 8.7–9.9% of SL; distance between posterior ends of supramaxilla and maxilla
 less than 5.4% of SL*S. eclipsis* (Bintan Island, Indonesia)
 – 1TGR \leq 47; anal-fin base rather long, more than 19.0% of SL; pelvic fin
 rather long, 9.1–10.1% of SL; distance between posterior ends of supramax-
 illa and maxilla more than 5.0% of SL..... 3

- 3 Third dorsal-fin ray short, 15.9–18.6% (mean 17.5%) of SL; maximum orbit diameter 8.2–9.9% (8.9%) of SL..... ***S. eldorado* (Taiwan to Java)**
- Third dorsal-fin ray long, 18.5–19.9% (mean 19.0%) of SL; maximum orbit diameter 7.3–8.6% (8.1%) of SL.....
..... ***S. bengalensis* (Pakistan to Bay of Bengal)**

Acknowledgements

We thank K.-T. Shao and S.-P. Huang (ASIZP), O. Crimmen, J. Maclaine and N. Martin (BMNH), D. Catania and M. Hoang (CAS), S. Kimura (FRLM), T. Peristywady (LBRC), K. Wibowo and G. Wahyudewantoro (MZB), K. Matsuura, G. Shinohara and M. Nakae (NSMT), K. Miyamoto (OCF), M. Manjaji-Matsumoto, A. A. Flora and S. R. M. Shaleh (Universiti Malaysia Sabah), K. Koeda (URM) J. Williams, K. Murphy, S. Raredon and D. Pitassy (USNM) and M. Aizawa, K. Sakamoto and R. Ueshima (ZUMT) for opportunities to examine specimens of *Stolephorus*. We also thank Y. Haraguchi and other volunteers and students of KAUM and NSMT for their curatorial assistance and G. Hardy (Ngunguru, New Zealand), for reading the manuscript and providing help with English. Vietnamese specimens were collected with the support of the Institute of Marine Environment and Resources (Haiphong) and the Ha Long Bay Management Department (Ha Long), with permission for the use of specimens granted by the Biodiversity Conservation Agency, Ministry of Natural Resources and Environment (Hanoi). Pakistan specimens were collected by the Marine Fisheries Department (MFD), Government of Pakistan, Karachi and donated from MFD via P. N. Psomadakis (Fisheries and Aquaculture Department, FAO, Rome) (permission no: MFD/UTF/Field guide/2014/J-1). Finally, we thank two anonymous reviewers and the editor for their insightful comments which helped to improve the manuscript. This study was supported in part by JSPS Overseas Research Fellowships (202160519), JSPS KAKENHI Grant Number 19K23691, JSPS Fellows (DC2: 29-6652) and the Sasakawa Scientific Research Grant from the Japan Science Society (28–745) to HH; JSPS KAKENHI Grant Numbers 20H03311 and 21H03651; the JSPS Core-to-core CREPSUM JPJSCCB2020009; and “Establishment of Glocal Research and Education Network in the Amami Islands” project of Kagoshima University adopted by the Ministry of Education, Culture, Sports, Science and Technology, Japan to HM; and short term research grant 304/PBIOLOGI/6315400 from Universiti Sains Malaysia to SL.

References

- Babu Rao M (1966) A new species of *Stolephorus* Lacépède from the east coast of India (Pisces: Engraulidae). *Annals & Magazine of Natural History* 13(9): 101–110. <https://doi.org/10.1080/00222936608651641>
- Bleeker P (1852) Bijdrage tot de kennis der Haringachtige visschen van den Soenda-Molukschen Archipel. *Verhandelingen van het Bataviaasch Genootschap van Kunsten en Wetenschappen* 24(8): 1–52.

- Boulenger GA (1900) Descriptions of new fishes from the Cape of Good Hope. Marine Investigations in South Africa 8: 10–12[+ pls. 1–3].
- De Vis CW (1882) Description of three new fishes of Queensland. Proceedings of the Linnean Society of New South Wales 7(3): 318–320. <https://doi.org/10.5962/bhl.part.22754>
- Dutt S, Babu Rao M (1959) Occurrence of *Anchoviella baganensis* Hardenberg off east coast of India. Current Science 28: 160–161.
- Edler D, Klein J, Antonelli A, Silvestro D (2020) raxmlGUI 2.0: A graphical interface and toolkit for phylogenetic analyses using RAxML. Methods in Ecology and Evolution 12(2): 373–377. <https://doi.org/10.1111/2041-210X.13512>
- Gangan SS, Pavan-Kumar A, Jahageerdar S, Jaiswar AK (2020) A new species of *Stolephorus* (Clupeiformes: Engraulidae) from the Bay of Bengal. Zootaxa 4743(3): 561–574. <https://doi.org/10.11646/zootaxa.4743.4.6>
- Hardenberg JDF (1933) New *Stolephorus* species of the Indo-Australian seas. Natuurkundig Tijdschrift voor Nederlandsch Indië 93: 258–263.
- Hata H (2018) *Stolephorus insularis* Hardenberg, 1933. In: Kimura S, Imamura H, Quan NV, Duong PT (Eds) Fishes of Ha Long Bay, the World Natural Heritage Site in Northern Vietnam. Fisheries Research Laboratory, Mie University, Shima, 41.
- Hata H (2019) Family Engraulidae. In: Koeda K, Ho H-C (Eds) Fishes of southern Taiwan. National Museum of Marine Biology & Aquarium, Pingtung, 199–210.
- Hata H, Motomura H (2017) A new species of anchovy, *Encrasicholina auster* (Clupeiformes: Engraulidae), from Fiji, southwestern Pacific Ocean. New Zealand Journal of Zoology 44(2): 122–128. <https://doi.org/10.1080/03014223.2016.1268177>
- Hata H, Motomura H (2018a) *Stolephorus continentalis*, a new anchovy from the north-western South China Sea and redescription of *Stolephorus chinensis* (Günther 1880) (Clupeiformes: Engraulidae). Ichthyological Research 65(3): 374–382. <https://doi.org/10.1007/s10228-018-0621-z>
- Hata H, Motomura H (2018b) First record of the anchovy, *Stolephorus teguhi* (Engraulidae) from the Philippines. Philippine Journal of Systematic Biology 11: 20–24. <https://doi.org/10.26757/pjsb.2017b11017>
- Hata H, Motomura H (2018c) Additional specimens of the poorly known anchovy *Stolephorus multibranchus* (Clupeiformes: Engraulidae) from Kosrae, Caroline Islands. Biogeography 20: 78–84.
- Hata H, Motomura H (2018d) Redescription and distributional range extension of the poorly known anchovy *Stolephorus nelsoni* (Clupeiformes: Engraulidae). Acta Ichthyologica et Piscatoria 48(4): 381–386. <https://doi.org/10.3750/AIEP/02501>
- Hata H, Motomura H (2018e) *Stolephorus insignis*, a new anchovy from the western Pacific, and redescription of *Stolephorus apiensis* (Jordan and Seale 1906) (Clupeiformes: Engraulidae). Ichthyological Research 66(2): 280–288. <https://doi.org/10.1007/s10228-018-00675-5>
- Hata H, Motomura H (2021a) Two new species of *Stolephorus* (Teleostei: Clupeiformes: Engraulidae) from the western Pacific. The Raffles Bulletin of Zoology 69: 109–117. <https://doi.org/10.26107/RBZ-2021-0009>
- Hata H, Motomura H (2021b) *Stolephorus grandis*, a new anchovy (Teleostei: Clupeiformes: Engraulidae) from New Guinea and Australia. Zootaxa 5004(3): 481–489. <https://doi.org/10.11646/zootaxa.5004.3.5>

- Hata H, Motomura H (2021c) A new species of the anchovy genus *Stolephorus* Lacepède 1803 from North Sumatra, Indonesia, and redescription of *Stolephorus pacificus* Baldwin 1984 and *Stolephorus teguhi* Kimura, Hori and Shibukawa 2009 (Teleostei: Clupeiformes: Engraulidae). *Zoological Studies* 60: 65. <https://doi.org/10.6620/ZS.2021.60-65>
- Hata H, Motomura H (2022) Redescription of *Stolephorus ronquilloi* Wongratana, 1983 and description of *Stolephorus hindustanensis*, new anchovy from the western coast of India (Teleostei: Clupeiformes: Engraulidae). *Taxonomy* 2(1): 124–135. <https://doi.org/10.3390/taxonomy2010010>
- Hata H, Lavoué S, Motomura H (2019) Taxonomic status of seven nominal species of the anchovy genus *Stolephorus* described by Delsman (1931), Hardenberg (1933), and Dutt and Babu Rao (1959), with redescription of *Stolephorus tri* (Bleeker 1852) and *Stolephorus waitei* Jordan and Seale 1926 (Clupeiformes: Engraulidae). *Ichthyological Research* 67(1): 7–38. <https://doi.org/10.1007/s10228-019-00697-7>
- Hata H, Lavoué S, Motomura H (2020a) *Stolephorus babarani*, a new species of anchovy (Teleostei: Clupeiformes: Engraulidae) from Panay Island, central Philippines. *Zootaxa* 4178(4): 509–520. <https://doi.org/10.11646/zootaxa.4718.4.5>
- Hata H, Lavoué S, Motomura H (2020b) *Stolephorus acinaces*, a new anchovy from the northern Borneo, and redescription of *Stolephorus andhraensis* (Babu Rao 1966) (Clupeiformes: Engraulidae). *Marine Biodiversity* 50(6): 102. <https://doi.org/10.1007/s12526-020-01115-2>
- Hata H, Lavoué S, Motomura H (2021) Taxonomic status of nominal species of the anchovy genus *Stolephorus* previously regarded as synonyms of *Stolephorus commersonii* Lacepède 1803 and *Stolephorus indicus* (van Hasselt 1823), and descriptions of three new species (Clupeiformes: Engraulidae). *Ichthyological Research* 68(3): 327–372. <https://doi.org/10.1007/s10228-020-00792-0>
- Hata H, Koeda K, Aizawa M, Sakamoto K, Ueshima R (2022) A list of Clupeiformes (Actinopterygii: Teleostei) specimens deposited in the Department of Zoology, The University Museum, The University of Tokyo. *The University Museum, The University of Tokyo. Bulletin* 128: 17–58.
- Hubbs CL, Lagler JF (1947) *Fishes of the Great Lakes region*. Cranbrook Institute of Science Bulletin 26: [i–xi +]1–186.
- Kimura K, Hori K, Shibukawa K (2009) A new anchovy, *Stolephorus teguhi* (Clupeiformes: Engraulidae) from North Sulawesi, Indonesia. *Ichthyological Research* 56(3): 292–295. <https://doi.org/10.1007/s10228-009-0103-4>
- Kozlov AM, Darriba D, Flouri T, Morel B, Stamatakis A (2019) RAxML-NG: A fast, scalable and user-friendly tool for maximum likelihood phylogenetic inference. *Bioinformatics* 35(21): 4453–4455. <https://doi.org/10.1093/bioinformatics/btz305>
- Nuryanto A, Pramono H, Sastranegara MH (2017) Molecular Identification of Fish Larvae from East Plawangan of Segara Anakan, Cilacap, Central Java, Indonesia. *Biosaintifika* 9(1): 33–40. <https://doi.org/10.15294/biosaintifika.v9i1.9191>
- Pang Z, Liu L, Liu B, Gong L, Jiang L, Lü Z (2019) The complete mitochondrial genome of *Stolephorus insularis* (Clupeiformes: Engraulidae) and phylogenetic studies of Engraulidae. *Mitochondrial DNA Part B* 4(1): 921–922. <https://doi.org/10.1080/23802359.2018.1536470>

- Sabaj MH (2020) Codes for natural history collections in Ichthyology and Herpetology. *Copeia* 108(3): 593–669. <https://doi.org/10.1643/ASIHCODONS2020>
- Stecher G, Tamura K, Kumar S (2020) Molecular Evolutionary Genetics Analysis (MEGA) for macOS. *Molecular Biology and Evolution* 37(4): 1237–1239. <https://doi.org/10.1093/molbev/msz312>
- Ward RD, Zemlak TS, Innes BH, Last PR, Hebert PDN (2005) DNA barcoding Australia's fish species. *Philosophical Transactions of the Royal Society B Biological Sciences* 360: 1847–1857. <https://doi.org/10.1098/rstb.2005.1716>
- Whitehead PJP (1967) Indian Ocean anchovies collected by the Anton Bruun and Te Vega, 1963–1964. *Journal of the Marine Biological Association of India* 9: 13–37.
- Whitehead PJP, Nelson GJ, Wongratana T (1988) FAO species catalogue. Vol. 7. Clupeoid fishes of the world (suborder Clupeoidei). An annotated and illustrated catalogue of the herrings, sardines, pilchards, sprats, shads, anchovies and wolf-herrings. Pt 2 – Engraulidae. FAO Fisheries Synopsis No 125 7(2):[i–viii +] 305–579.
- Wongratana T (1983) Diagnoses of 24 new species and proposal of a new name for a species of Indo-Pacific clupeoid fishes. *Japanese Journal of Ichthyology* 29: 385–407.
- Wongratana T (1987a) Four new species of clupeoid fishes (Clupeidae and Engraulidae) from Australian waters. *Proceedings of the Biological Society of Washington* 100: 104–111.
- Wongratana T (1987b) Two new species of anchovies of the genus *Stolephorus* (Engraulidae), with a key to species of *Engraulis*, *Encrasicholina*, and *Stolephorus*. *American Museum Novitates* 2876: 1–8.
- Wongratana T, Munroe TA, Nizinski MS (1999) Order Clupeiformes. Engraulidae. Anchovies. In: Carpenter KE, Niem VH (Eds) FAO species identification guide for fishery purposes. The living marine resources of the western central Pacific. Vol. 3. Batoid fishes, chimaeras and bony fishes pt 1 (Elopidae to Linophrynidae). FAO, Rome, 1698–1753.
- Young S-S, Chiu T-S, Shen S-C (1994) A revision of the family Engraulidae (Pisces) from Taiwan. *Zoological Studies* 33(3): 217–227.
- Zhang S (2001) Fauna Sinica Osteichthyes. Acipenseriformes, Elopiformes, Clupeiformes, Gonorhynchiformes. Science Press, Beijing, 209 pp.

Leaving no stone unturned: three additional new species of *Atractus* ground snakes (Serpentes, Colubridae) from Ecuador discovered using a biogeographical approach

Alejandro Arteaga¹, Amanda Quezada¹, Jose Vieira², Juan M. Guayasamin³

1 Biodiversity Field Lab (BioFL), Khamai Foundation, Quito, Ecuador **2** ExSitu, Quito, Ecuador **3** Laboratorio de Biología Evolutiva, Instituto Biósfera, Colegio de Ciencias Biológicas y Ambientales COCIBA, Universidad San Francisco de Quito USFQ, Quito, Ecuador

Corresponding author: Alejandro Arteaga (alejandro@khamai.bio)

Academic editor: Robert Jadin | Received 27 June 2022 | Accepted 21 August 2022 | Published 15 September 2022

<https://zoobank.org/15C9C77E-6888-49BB-BC57-F7500EF2E06C>

Citation: Arteaga A, Quezada A, Vieira J, Guayasamin JM (2022) Leaving no stone unturned: three additional new species of *Atractus* ground snakes (Serpentes, Colubridae) from Ecuador discovered using a biogeographical approach. ZooKeys 1121: 175–210. <https://doi.org/10.3897/zookeys.1121.86539>

Abstract

The genus *Atractus* includes 146 species of cryptozoic snakes occurring from Panama to northeastern Argentina. Here, a molecular phylogeny of this genus is presented, which encompasses 29% (= 42; six are included here for the first time) of the species currently recognized. Morphological and phylogenetic support is found for three new species of ground snakes, which are described here based on their unique combination of molecular, meristic, and color pattern characteristics. The name *A. arangoi* Prado, 1939 is revalidated for a Colombian snake species previously subsumed under *A. major* Boulenger, 1894 based on new material collected in Ecuador. Reidentifications are provided for *Atractus* voucher specimens and sequences deposited in GenBank. With these changes, the number of *Atractus* reported in Ecuador increases from 27 to 31 species. Finally, attention is given to the importance of using a biogeographical framework that includes molecular data and a comprehensive geographic sampling when proposing species limits in complex taxonomic groups.

Keywords

Biodiversity, biogeography, Colubridae, fossorial, phylogeny, new species, taxonomy

Introduction

Atractus Wagler, 1828 is the most speciose snake genus in the world (Uetz et al. 2022). There are 146 known species, and these numbers are likely to rise with the exploration of remote mountain ranges, the use of molecular tools in *Atractus* systematics, and the application of a biogeographical framework when establishing limits between species.

In Ecuador, the exploration of remote mountain ranges (e.g., the Cordillera de Guacamayos, Sumaco Volcano, and the Cordillera del Cóndor) within the last two decades has resulted in the discovery of at least six species of *Atractus*, including the most heavy-bodied and strikingly colored in the genus (Myers and Schargel 2006; Schargel et al. 2013; Arteaga et al. 2017; Passos et al. 2018; Melo-Sampaio et al. 2021). Unlike other snake genera inhabiting the same mountain ranges (e.g., *Dipsas*; see Arteaga et al. 2018), snakes in the genus *Atractus* inhabiting remote cloud forests and inter-Andean valleys are generally considered rare. Some are known only from their type localities (e.g., *A. cerberus* Arteaga et al., 2017) whereas for some species the males (e.g., *A. atlas* Passos et al., 2018) or juveniles (e.g., *A. touzeti* Schargel et al., 2013) have not yet been reported. All of this suggests that *Atractus* in general, with the exception of some locally abundant species (e.g., *A. marthae* Meneses-Pelayo & Passos, 2019), are difficult to find. Thus, species inhabiting poorly visited areas may remain undetected without long-term projects focused on cryptozoic herpetofauna (Myers 2003).

The use of molecular tools in *Atractus* systematics is also likely to increase the rate at which new species in this genus are detected and described. Only seven species of *Atractus* have been described using molecular data in addition to meristic and color pattern characteristics (Arteaga et al. 2017; Melo-Sampaio et al. 2019; Melo-Sampaio et al. 2021). Some of these new species were previously considered to be widespread, polychromatic, and difficult to diagnose (Savage 1960). Therefore, they probably would have never been detected using meristics and other morphological data alone. Furthermore, only approximately 30% of the current known diversity of the genus has been included in published phylogenetic analyses (i.e., Arteaga et al. 2017; Passos et al. 2022), and even a smaller percentage of the included species have been thoroughly sampled throughout their range. This lack of information presents both a challenge and an opportunity to uncover further cryptic diversity within the genus.

Finally, a mention should be made about the importance of using a biogeographical framework that includes molecular data and species distribution models (when the number and quality of locality records is sufficient for these analyses; see van Proosdij et al. 2015) when defining species limits within *Atractus*. Finding ground snakes along the Andes has showed us (Arteaga et al. 2013, 2017) and other authors (Savage 1955, 1960; Cisneros-Heredia 2005; Salazar-Valenzuela et al. 2014) that snakes in this genus have lower dispersal capacity than other colubrids and many species are endemic to a single mountain range or restricted to an isolated inter-Andean valley. Thus, the presence of the same *Atractus* species in two geographically isolated areas that are climatically and floristically distinct and are separated from each other by tens or even hundreds of kilometers of discontinuous habitat is unlikely. An example of this scenario

is *A. gigas* Myers & Schargel, 2006, a species previously considered to be endemic to the Pacific slopes of the Andes in Ecuador (Myers and Schargel 2006; Tolhurst et al. 2010; Arteaga et al. 2013), but later reported on the Amazonian slopes of the Andes in Peru (Passos et al. 2010). Although specimens from both localities may resemble each other in lepidosis, they differ in coloration, ecological requirements, and phylogenetic affinities. More recently, without explanation, but probably based on similarities in meristics, Passos et al. (2022) proposed the reidentification of 15 specimens of *Atractus* having sequences deposited in GenBank. Given that some of these reidentifications involve type series and the majority of them were done without providing an explanation, their validity is evaluated in this work.

To help clear the waters of *Atractus* taxonomy, in this work we present a curated phylogeny of the genus, reidentify *Atractus* sequences in GenBank, present the description of three new species, and provide the revalidation of a taxon previously subsumed under *A. major*.

Materials and methods

Ethics statement

This study was carried out in strict accordance with the guidelines for use of live amphibians and reptiles in field research (Beaupre et al. 2004) compiled by the American Society of Ichthyologists and Herpetologists (**ASIH**), the Herpetologists' League (**HL**) and the Society for the Study of Amphibians and Reptiles (**SSAR**). All procedures with animals (see below) were reviewed by the Ministerio del Ambiente, Agua y Transición Ecológica (**MAATE**) and specifically approved as part of obtaining the following field permits for research and collection: MAE-DNB-CM-2015-0017 (granted to Universidad Tecnológica Indoamérica), MAE-DNB-CM-2018-0105 and MAATE-DBI-CM-2022-0245 (granted to Universidad San Francisco de Quito), and 004-AIC-DPC-B-MAE-18 (granted to Universidad del Azuay). Specimens were euthanized with 20% benzocaine, fixed in 10% formalin or 90% ethanol, and stored in 70% ethanol. Museum vouchers were deposited at Museo de Zoología de la Universidad Tecnológica Indoamérica (**MZUTI**), Museo de Zoología de la Universidad San Francisco de Quito (**ZSFQ**), Museo de Zoología de la Universidad del Azuay (**MZUA**), and the herpetology collection at Bioparque Amaru (**AMARU**). Specimens labeled JMG were also deposited at ZSFQ.

Common names

Criteria for common name designation are as proposed by Caramaschi et al. (2006) and Coloma and Guayasamin (2011–2017), reviewed by Arteaga et al. (2019). These are as follows (in order of importance): (i) the etymological intention (implicit or explicit) that the authors used when naming the species (specific epithet); (ii) a common

name that is already widely used in the scientific literature; (iii) a common name that has an important ancestral or cultural meaning; (iv) a common name based on any distinctive aspect of the species (distribution, morphology, behavior, etc.).

Morphological data

Our terminology for *Atractus* cephalic shields follows Savage (1960), diagnoses and descriptions generally follow Passos et al. (2009a), and ventral and subcaudal counts follow Dowling (1951). We examined comparative alcohol-preserved specimens from the herpetology collections at MZUTI, MZUA, ZSFQ, American Museum of Natural History (AMNH), Museo de Zoología de la Pontificia Universidad Católica del Ecuador (QCAZ), and Muséum National d'Histoire Naturelle (MNHN) (Table 1). Morphological measurements were taken with measuring tapes to the nearest 1 mm, or with digital calipers to the nearest 0.1 mm. Abbreviations are as follows: snout-vent length (SVL); tail length (TL). Sex was determined by establishing the presence/absence of hemipenes through a subcaudal incision at the base of the tail unless hemipenes were everted.

Sampling

Tissue samples from 12 individuals representing seven species (including the three new species described here) were obtained in Ecuador. All specimens included in the genetic analyses were morphologically identified according to Savage (1960), Arteaga et al. (2017), Melo-Sampaio et al. (2021), and Arteaga et al. (2022). We generated sequence data for samples marked with an asterisk under Appendix I, which includes museum vouchers at MZUTI, MZUA, and ZSFQ.

Laboratory techniques

Genomic DNA was extracted from 96% ethanol-preserved tissue samples (liver, muscle tissue, or scales) using either a guanidinium isothiocyanate extraction protocol (Peñafiel et al. 2020), or a modified salt precipitation method based on the Puregene DNA purification kit (Gentra Systems). The nucleotide sequences of the primers and the PCR conditions applied to each primer pair are detailed in Appendix II. PCR products were cleaned with either ExoSAP-IT (Affymetrix, Cleveland, OH), or Exonuclease I and Alkaline Phosphatase (Illustra ExoProStar by GE Healthcare) before they were sent to Macrogen Inc (Seoul, South Korea) for sequencing. All PCR products were sequenced in both forward and reverse directions with the same primers that were used for amplification. The edited sequences were deposited in GenBank (Appendix I).

DNA phylogenetic analyses

A total of 274 DNA sequences were used to build a phylogenetic tree of the genus *Atractus*, of which 32 were generated during this work and 242 were downloaded from GenBank, most of which were produced by Arteaga et al. (2017), Melo-Sampaio et al. (2021), and

Table 1. Locality data for specimens examined in this study. Coordinates represent actual GPS readings taken at the locality of collection or georeferencing attempts from gazetteers under standard guidelines, although some variation from the exact collecting locality will be present. Similarly, elevations are taken from Google Earth and may not exactly match the elevations as originally reported.

Species	Voucher	Country	Province	Locality	Latitude, Longitude	Elev. (m)
<i>A. arangoi</i>	DHMECN 8343	Ecuador	Sucumbíos	Bloque 27	0.32271, -76.19300	264
<i>A. arangoi</i>	ZSFQ 4947	Ecuador	Napo	Jatun Sacha Biological Station	-1.06633, -77.61640	423
<i>A. arangoi</i>	ZSFQ 4948	Ecuador	Napo	Jatun Sacha Biological Station	-1.06633, -77.61640	423
<i>A. discovery</i> sp. nov.	MZUA.RE.0466	Ecuador	Morona Santiago	Campamento Arenales	-2.59253, -78.56507	2057
<i>A. discovery</i> sp. nov.	ZSFQ 4936	Ecuador	Azuay	Amaluza	-2.61583, -78.56538	2002
<i>A. discovery</i> sp. nov.	ZSFQ 4937	Ecuador	Azuay	Amaluza	-2.61583, -78.56538	2002
<i>A. major</i>	MNHN 0.6149	Ecuador	—	—	—	—
<i>A. major</i>	QCAZ 11565	Ecuador	Orellana	Tambococha	-0.97839, -75.42569	194
<i>A. major</i>	QCAZ 11587	Ecuador	Orellana	Tambococha	-1.03981, -75.44849	210
<i>A. major</i>	QCAZ 11596	Ecuador	Orellana	Tambococha	-0.97839, -75.42569	194
<i>A. major</i>	QCAZ 11809	Ecuador	Pastaza	Campo Villano B	-1.45745, -77.44455	331
<i>A. major</i>	QCAZ 4691	Ecuador	Pastaza	Río Sarayakillo	-1.72754, -77.48048	434
<i>A. major</i>	QCAZ 4895	Ecuador	Orellana	Vía Pompeya Sur-Iro	-0.99307, -76.24904	246
<i>A. major</i>	QCAZ 7881	Ecuador	Sucumbíos	Pañacocha	-0.44791, -76.07097	240
<i>A. major</i>	QCAZ 7896	Ecuador	Orellana	Vía Pompeya Sur-Iro	-0.99320, -76.24907	246
<i>A. major</i>	QCAZ 8040	Ecuador	Napo	Comunidad Garenó	-1.04856, -77.37742	334
<i>A. major</i>	QCAZR 11744	Ecuador	Pastaza	Lorocachi	-1.65567, -75.96886	212
<i>A. major</i>	ZSFQ 4955	Ecuador	Morona Santiago	Macas-Riobamba	-2.25674, -78.16797	1148
<i>A. michaelsabini</i> sp. nov.	AMNH 18325	Ecuador	El Oro	El Chiral	-3.63825, -79.59723	1841
<i>A. michaelsabini</i> sp. nov.	AMNH 22110	Ecuador	El Oro	La Chonta	-3.56585, -79.85144	1025
<i>A. michaelsabini</i> sp. nov.	AMNH 22111	Ecuador	El Oro	La Chonta	-3.56585, -79.85144	1025
<i>A. michaelsabini</i> sp. nov.	DHMECN 7644	Ecuador	Azuay	Reserva Yunguilla	-3.22684, -79.27520	1748
<i>A. michaelsabini</i> sp. nov.	DHMECN 7645	Ecuador	Azuay	Reserva Yunguilla	-3.22684, -79.27520	1748
<i>A. michaelsabini</i> sp. nov.	QCAZ 7887	Ecuador	El Oro	Guanazán	-3.44139, -79.49417	2596
<i>A. michaelsabini</i> sp. nov.	QCAZ 7902	Ecuador	El Oro	Guanazán	-3.44668, -79.49051	2663
<i>A. michaelsabini</i> sp. nov.	QCAZ 9643	Ecuador	El Oro	El Panecillo	-3.46753, -79.48248	2775
<i>A. michaelsabini</i> sp. nov.	QCAZ 9652	Ecuador	El Oro	El Panecillo	-3.46753, -79.48248	2775
<i>A. michaelsabini</i> sp. nov.	ZSFQ 4938	Ecuador	Azuay	Corraleja	-3.38740, -79.22785	2660
<i>A. michaelsabini</i> sp. nov.	ZSFQ 4939	Ecuador	El Oro	Guanazán	-3.46753, -79.48248	2750
<i>A. pachacamac</i>	ZSFQ 4954	Ecuador	Morona Santiago	Macas-Riobamba	-2.24087, -78.27632	1644
<i>A. resplendens</i>	ZSFQ 4953	Ecuador	Tungurahua	Montañas de San Antonio	-1.43413, -78.40726	2655
<i>A. resplendens</i>	ZSFQ 4952	Ecuador	Tungurahua	Montañas de San Antonio	-1.43413, -78.40726	2655
<i>A. resplendens</i>	ZSFQ 4951	Ecuador	Tungurahua	Montañas de San Antonio	-1.43413, -78.40726	2655
<i>A. roulei</i>	MNHN 1906.0243	Ecuador	Chimborazo	Alausí	-2.20636, -78.84611	2400
<i>A. roulei</i>	MZUA.RE.0080	Ecuador	Azuay	Míguir, 10 km E of	-2.78771, -79.37132	2596
<i>A. roulei</i>	MZUTI 5107	Ecuador	Bolívar	Above Balzapamba	-1.83601, -79.13322	2026
<i>A. roulei</i>	QCAZ 6256	Ecuador	Azuay	Hierba Mala	-2.70430, -79.43367	2427
<i>A. roulei</i>	ZSFQ 4943	Ecuador	Chimborazo	Tixán	-2.16174, -78.81227	2892
<i>A. roulei</i>	ZSFQ 4944	Ecuador	Chimborazo	Tixán	-2.16174, -78.81227	2892
<i>A. roulei</i>	ZSFQ 4942	Ecuador	Chimborazo	Tixán	-2.16174, -78.81227	2892
<i>A. roulei</i>	ZSFQ 4941	Ecuador	Chimborazo	Tixán	-2.16174, -78.81227	2892
<i>A. roulei</i>	ZSFQ 4940	Ecuador	Chimborazo	Tixán	-2.16174, -78.81227	2892
<i>A. roulei</i>	ZSFQ 4945	Ecuador	Chimborazo	Tixán	-2.16174, -78.81227	2892
<i>A. zgap</i> sp. nov.	ZSFQ 4946	Ecuador	Napo	Santa Rosa	-0.31004, -77.78591	1500
<i>A. zgap</i> sp. nov.	QCAZ 12666	Ecuador	Napo	Borja, 1 km NE of	-0.40954, -77.84005	1703
<i>A. zgap</i> sp. nov.	QCAZ 5183	Ecuador	Napo	Bosque La Cascada	-0.14572, -77.49593	1460

Passos et al. (2022). Of these, 85 sequences are 367–516 bp long fragments of the 16S gene, 66 are 578–1,079 bp long fragments of the CYTB gene, 69 are 567–849 bp long fragments of the ND4 gene, 18 are 513–573 bp long fragments of the C-MOS gene, 19 are 386–516 bp long fragments of the NT3 gene, and 17 are 736 bp long fragments of the RAG-1 gene. New sequences were edited and assembled using the program Geneious Pro™ 2021.1.1 (Drummond et al. 2021) and aligned with those downloaded from GenBank (Appendix I) using MAFFT v.7 (Katoh and Standley 2013) under the default parameters in Geneious Pro™ 2021.1.1. Genes were combined into a single matrix with 16 partitions, one per non-coding gene and three per protein coding gene corresponding to each codon position. The best partition strategies along with the best-fit models of evolution were obtained in PartitionFinder 2.1.1 (Lanfear et al. 2016) under the Bayesian information criterion.

Phylogenetic relationships were assessed under both a Bayesian inference (**BI**) approach in MrBayes 3.2.0 (Ronquist and Huelsenbeck 2013) and a maximum likelihood (**ML**) approach in RAxML-NG v. 1.1.0 (Kozlov et al. 2019). For the ML analysis, nodal support was assessed using the *standard* bootstrapping algorithm with 1000 non-parametric bootstraps. For the BI analysis, four independent analyses were performed to reduce the chance of converging on a local optimum. Each analysis consisted of 6,666,667 generations and four Markov chains with default heating settings. Trees were sampled every 1,000 generations and 25% of them were arbitrarily discarded as “burn-in.” The resulting 5,000 saved trees per analysis were used to calculate posterior probabilities (PP) for each bipartition in a 50% majority-rule consensus tree. We used Tracer 1.7.2 (Rambaut et al. 2022) to assess convergence and effective sample sizes (ESS) for all parameters. Additionally, we verified that the average standard deviation of split frequencies between chains and the potential scale reduction factor (**PSRF**) of all the estimated parameters approached values of ≤ 0.01 and 1, respectively. Genetic distances between *Atractus roulei* Despax, 1910 and its sister species were calculated using the uncorrected distance matrix in Geneious Pro™ 2021.1.1. GenBank accession numbers are listed in Appendix I.

Distribution maps and ecological niche models

We present ranges of occurrence for five species of *Atractus*, including the three new species described here. Presence localities are derived from museum vouchers (Table 1), photographic records (iNaturalist), and the literature (all summarized under Suppl. material 1: Table S1). For three of the five species, a binary environmental niche model (ENM) accompanies the dot maps. These models estimate potential areas of distribution on the basis of observed presences and a set of environmental predictors (Elith and Leathwick 2009). To delimit the occupancy areas and the potential species distribution, we used the BAM diagram proposal (Soberón and Peterson 2005; Peterson et al. 2011). To create the models, we used presence localities listed under Suppl. material 1: Table S1, 19 bioclimatic variables from Worldclim 1.4 (Hijmans et al. 2005), and Maxent 3.4.1k, an algorithm based on the principle of maximum entropy (Phillips et al. 2006; Elith et al. 2011; Renner and Warton 2013).

For the first explorative exercise, we used the 19 climate layers from the WorldClim project and assessed which variables were the most important for the model,

according to the Jackknife test calculated in MaxEnt (Royle et al. 2012). Correlated environmental variables ($r < 0.8$) were identified using the PEARSON correlation test of PAST 3. In a second modelling exercise, we used the locality records for each species (Suppl. material 1: Table S1) and the variables identified in the first approach to generate the species distribution. 5,000 iterations were specified to the program with clamping and no extrapolation. All other parameters in MaxEnt were maintained at default settings. To create the binary environmental niche models, suitable areas were distinguished from unsuitable areas by setting a *minimum training presence* threshold value. The logistic format was used to obtain the values for habitat suitability (continuous probability from 0 to 1), which were subsequently converted to binary presence-absence values on the basis of the established threshold value, defined herein as *the minimum training presence*. The convergence threshold was set to 10^{-5} , maximum iterations to 500, and the regularization parameter to “auto”.

Results

Molecular phylogeny and taxonomic consequences

Selected partitions and models of evolution are presented in Table 2. We consider strong support for a clade when Bayesian analyses yield posterior probability values $> 95\%$, following Felsenstein (2004), or when bootstrap values are greater than 70%. The overall topology and support of the BI (Fig. 1) and ML (Suppl. material 2: Figure S1) analyses are similar to that of Arteaga et al. (2017) and Passos et al. (2022). Species of the *Atractus roulei* species group are sister to all other sampled *Atractus* in the BI analysis, a view contrary to the ML analysis and to Murphy et al. (2019), in which *A. trilineatus* Wagler, 1928 and *A. boimirim* Passos et al., 2016, respectively are recovered as sister to all other *Atractus*. Below, we outline some differences between our analysis and those published in Murphy et al. (2019) and Passos et al. (2022).

Atractus roulei is the strongly supported sister species of *A. carrioni* Parker, 1930, a relationship recovered in previous studies, but we found additional geographically structured genetic divergence within the former species (Figs 1, 2). We found moderate support for the placement of *A. trilineatus* as sister to *A. major* sensu Schargel et al. (2013), but strong support for the reciprocal monophyly between snakes assignable to *A. arangoi*, previously subsumed under *A. major*, and all other samples of *A. major*, including samples from throughout the species' area of distribution. Samples labeled *A. arangoi* in our phylogeny are not closely related to *A. torquatus* (Duméril, Bibron, & Duméril, 1854), a name that has been applied to Ecuadorian specimens of the former (see Maynard et al. 2017). Our sample of *A. touzeti* Schargel et al., 2013 from the type locality is strongly supported as sister to the sample of *A. atlas* Passos et al., 2018. We found strong support for the relationship between *A. resplendens* Werner, 1901 from near the type locality and a new species from southeastern Ecuador. Our included samples of *A. orcesi* Savage, 1955 form a strongly supported sister clade to *A. duboisi* (Boulenger,

Table 2. Partition scheme and models of evolution used in phylogenetic analyses. Numbers in parentheses indicate codon position.

Partition	Best model	Gene regions	Number of aligned sites
1	GTR+I+G	16S, cytb(3), ND4(1), NT3(1)	1202
2	HKY+I+G	cytb(1), ND4(2)	631
3	GTR+I+G	cytb(2), ND4(3)	630
4	JC	CMOS(1), NT3(3)	305
5	K80+I	CMOS(2), NT3(2), RAG1(2), RAG1(3)	794
6	HKY	CMOS(3), RAG1(1)	423

1880). A new species previously confused with *A. ecuadorensis* Savage, 1955, *A. orcesi*, and *A. resplendens* is not closely related to any of these species, but is recovered as the strongly supported sister species to a clade that contains *A. ukupacha* Melo-Sampaio et al., 2021, *A. pachacamac* Melo-Sampaio et al., 2021, *A. snethlageae* da Cunha & do Nascimento, 1983, *A. dapsilis* Melo-Sampaio et al., 2019, *A. schach* (Boie, 1827), and *A. trefauti* Melo-Sampaio et al., 2019. The latter two are sister species and their topological distance is smaller than intraspecific distances in other *Atractus* species sampled.

We find strong support for the relationship between members of the *Atractus iridescens* species group, which mirrors the results of Arteaga et al. (2017) and Murphy et al. (2019), and even those of Passos et al. (2022), although in the latter work some the terminals have been renamed. However, in the ML analysis (Suppl. material 2: Figure S1), *A. dunni* Savage, 1955 is weakly nested within *A. microrhynchus* Cope, 1868. Finally, we excluded *A. imperfectus* Myers, 2003 (voucher CH 9399) from the analyses as the short sequence available for comparison in GenBank (gene fragment 16S) represented a rogue taxon that assumed varying phylogenetic positions in the tree collection used to build the consensus tree.

Systematic accounts

We name or provide redescrptions only for species that are monophyletic in our molecular phylogeny and share diagnostic features of their coloration pattern and lepidosis. Based on these species' delimitation criteria, which follow the general species concept of de Queiroz (2007), we describe three new species of *Atractus*.

Atractus discovery sp. nov.

<https://zoobank.org/0343A95C-BC4B-4654-8333-55D8A34CD2EF>

Figs 3, 4, 5d

Proposed standard english name: Discovery Ground Snake.

Proposed standard spanish name: Culebra tierrera de Discovery.

Holotype. ZSFQ 4937 (Figs 3, 4), adult male collected by Alejandro Arteaga and Amanda Quezada at Amaluza, Azuay province, Ecuador (S2.61582, W78.56537; 2002 m).

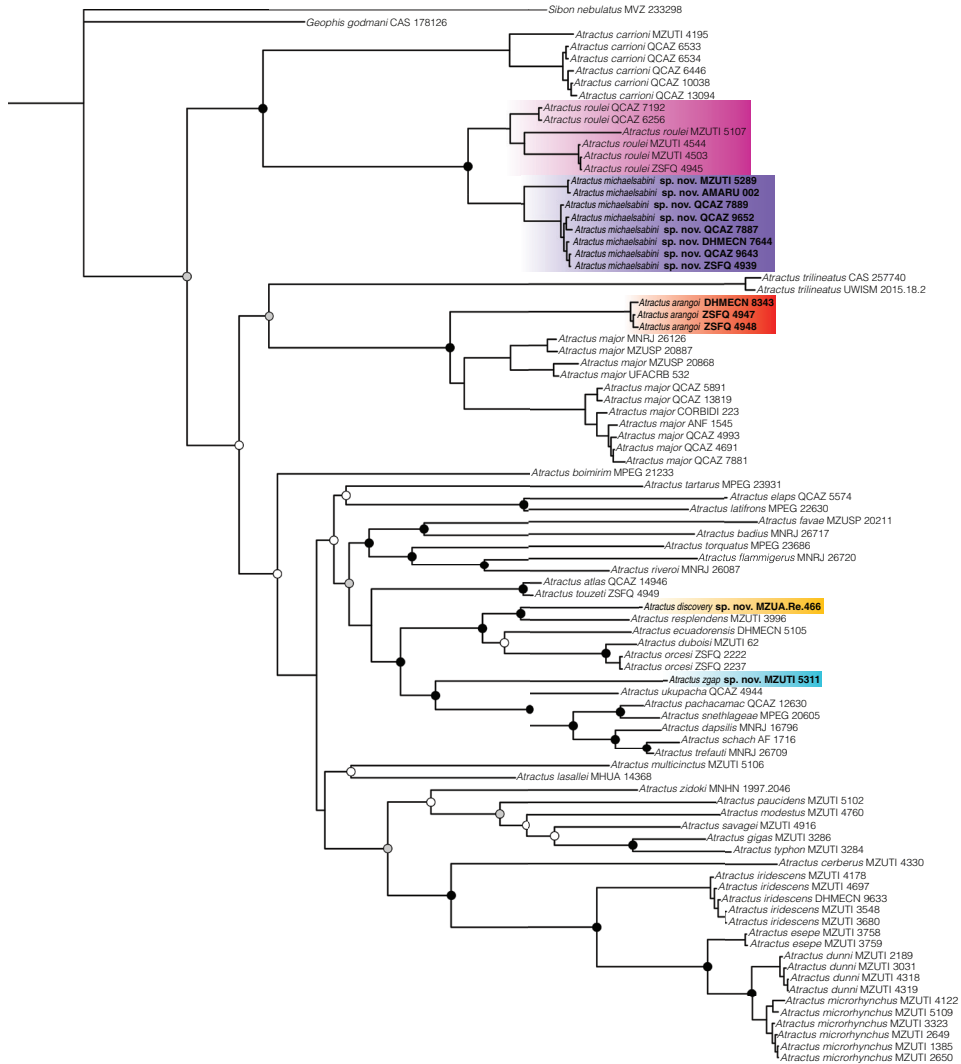


Figure 1. Phylogenetic relationships within *Atractus* inferred using a Bayesian inference and derived from analysis of 3,985 bp of DNA (gene fragments 16S, CYTB, ND4, C-MOS, NT3, and RAG1). Support values on intra-specific branches are not shown for clarity. Voucher numbers for sequences are indicated for each terminal. Black dots indicate clades with posterior probability values from 95–100%. Grey dots indicate values from 70–94%. White dots indicate values from 50–69% (values < 50% not shown). Colored clades correspond to the species’ distribution presented in the map of Fig. 2. New or resurrected species are indicated in bold type.

Paratypes. ZSFQ 4936 (Fig 5d), adult female collected by Alejandro Arteaga and Amanda Quezada at the type locality. MZUA.Re.466, adult female collected on 16 November 2018 at Campamento Arenales, Morona Santiago province, Ecuador (S2.59253, W78.56507; 2057 m).

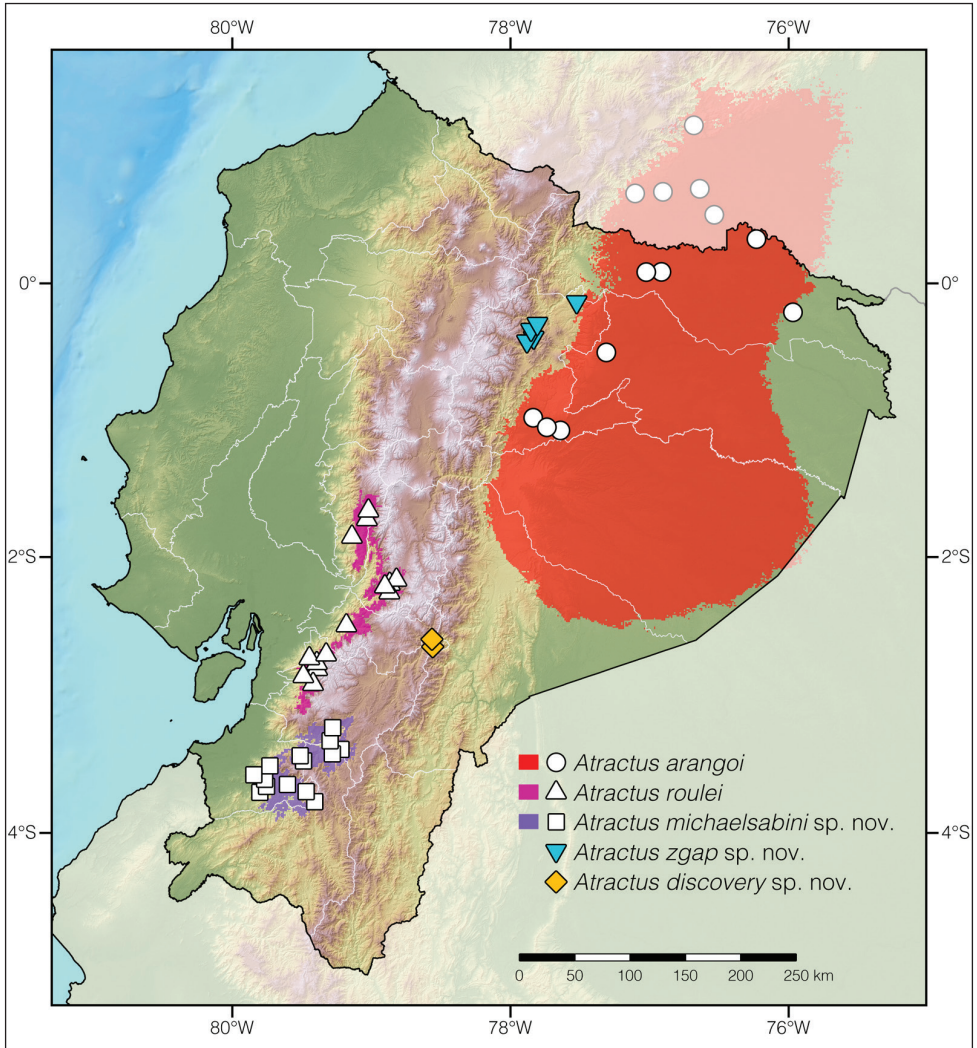


Figure 2. Distribution of *Atractus arangoi*, *A. roulei*, *A. michaelsabini* sp. nov., *A. zgap* sp. nov., and *A. discovery* sp. nov. in Ecuador and adjacent Colombia. White dots represent localities listed under Suppl. material 1. Each colored area is a geographic representation of the suitable environmental conditions for one of the clades recovered in the phylogeny of Fig. 1.

Diagnosis. *Atractus discovery* sp. nov. is placed in the genus *Atractus*, as diagnosed by Savage (1960), based on phylogenetic evidence (Fig. 1). The species is diagnosed based on the following combination of characters: (1) 17/17/17 smooth dorsals; (2) one postocular; (3) loreal 2.5–3 × longer than high; (4) temporals 1+2; (5) eight supralabials, fourth and fifth contacting orbit; (6) seven infralabials, first four contacting chinshields; (7) six or seven maxillary teeth; (8) one row of gular scales; (9) three preventrals; (10) 168 ventrals in the male holotype (Fig. 3b) and 170–172 ventrals in females; (11) 27 subcaudals in the male holotype and 17–18 subcaudals in females;

(12) dorsal ground color light brown with faint stippling of a darker shade (Figs 3a, 5d); (13) venter yellow with a brown ventral stripe (Fig. 3b); (14) 284 mm SVL in the male holotype and 308–328 mm SVL in females; (15) 28 mm TL in the male holotype and 19–24 mm TL in females.

Comparisons. *Atractus discovery* sp. nov. differs from most of its congeners by having a bright yellow belly with a conspicuous dark brown longitudinal stripe. This species is compared to other small brownish congeneric ground snakes distributed along the Amazonian slopes of the Andes (most of these are pictured in Fig. 5): *Atractus avernus* Passos et al., 2009b, *A. duboisi*, *A. ecuadorensis*, *A. zgap* sp. nov., *A. occipitoalbus* (Jan, 1862), *A. orcesi*, and *A. resplendens*. From *A. avernus*, *A. duboisi*, *A. occipitoalbus*, and *A. orcesi*, the new species differs in having 17/17/17 (instead of 15/15/15) dorsal scale rows. From *A. ecuadorensis*, *A. zgap* sp. nov., and *A. resplendens*, it differs in having a bright yellow belly with a conspicuous dark brown longitudinal stripe. From *A. ecuadorensis* and *A. zgap* sp. nov., it further differs by having one (instead of two) postocular scale (Fig. 4c).

Description of holotype. Adult male, SVL 284 mm, tail length 28 mm (9.9% SVL); body diameter 7.8 mm; head length 8.8 mm (3.1% SVL); head width 5.6 mm (2.0% SVL); interocular distance 3.4 mm; head slightly distinct from body; snout-orbit distance 3.4 mm; rostral 1.6 mm wide, ca. as broad as high; internasals 0.9 mm wide; prefrontals 2.1 mm wide; frontal 2.9 mm wide, with a curvilinear triangular shape in dorsal view; parietals 2.2 mm wide, $\sim 2 \times$ as long as wide; nasal divided; loreal 2.0 mm long, $\sim 3 \times$ longer than high; eye diameter 1.1 mm; pupil round; supraoculars 1.3 mm wide; one postocular; temporals 1+2, upper posterior temporal elongate; eight supralabials, fourth and fifth contacting orbit; symphyisial 1.0 mm wide, $\sim 2 \times$ as broad as long and separated from chinshields by first pair of infralabials; seven infralabials, first four contacting chinshields; chinshields $\sim 2 \times$ as long as broad, posterior chinshields absent; four rows of gular scales; dorsal scales arranged in 17/17/17 rows, smooth without apical pits; two preventrals; ventrals 168; anal plate single; 27 paired subcaudals.

Natural history. The three known specimens of *Atractus discovery* sp. nov. were found in open areas adjacent to cloud forest border. MZUA.Re.466 was crawling at ground level at around 7:30 pm. It was crossing a series of cement stairs. ZSFQ 4936 and ZSFQ 4937 were found during a cloudy day, buried 15–40 cm under soft soil at the border between the clearing of a graveyard, pastures, and remnants of native vegetation.

Distribution. *Atractus discovery* sp. nov. is known only from two localities (Arenales and Amaluza, listed under Suppl. material 1: Table S1) on each side of the Río Paute, in the Ecuadorian provinces Azuay and Morona Santiago, at elevations 2002–2057 m a.s.l. The airline distance between the two localities is 2.6 km (Fig. 2).

Etymology. The specific epithet *discovery* is used as a noun in apposition and honors ‘The Explorers Club Discovery Expedition Grants’ (<https://www.explorers.org/grants>) initiative, a program seeking to foster scientific understanding for the betterment of humanity and all life on Earth and beyond. The grant program supports researchers and explorers from around the world in their quest to mitigate climate change, prevent the extinction of species and cultures, and ensure the health of the Earth and its inhabitants. ‘The Explorers Club Discovery Expedition Grants’ program funded the expedition that resulted in the discovery of this new species of snake.

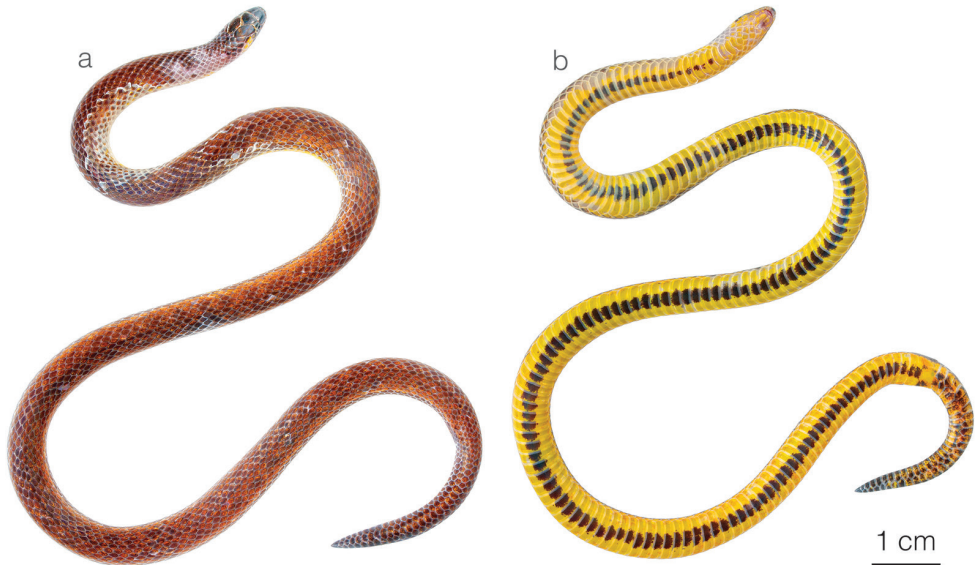


Figure 3. Adult male holotype of *Atractus discovery* sp. nov. ZSFQ 4937 in **a** dorsal and **b** ventral view.

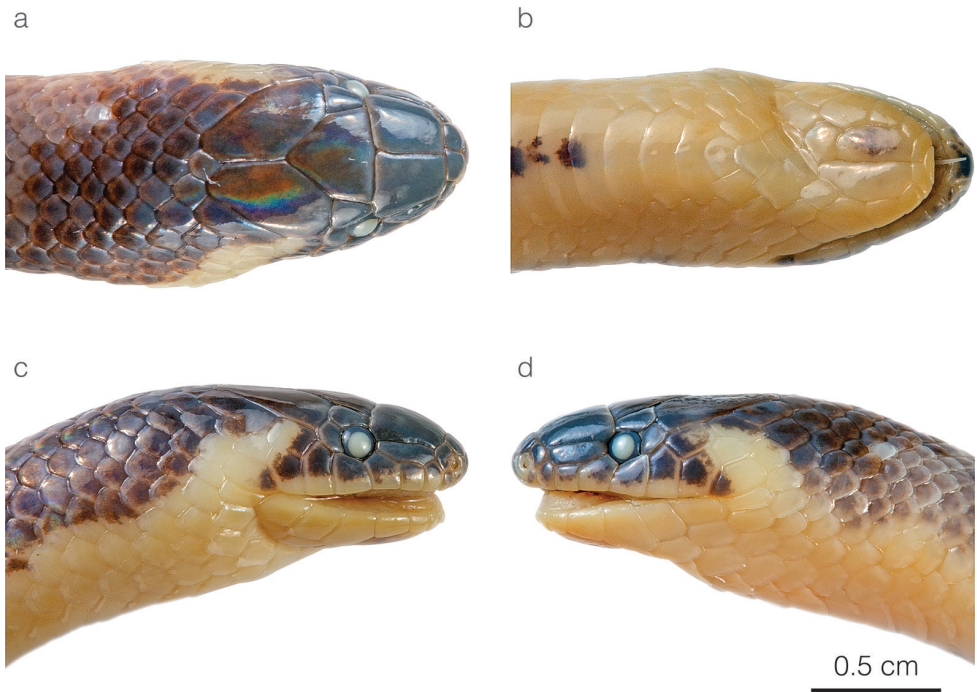


Figure 4. Head of the adult male holotype of *Atractus discovery* sp. nov. ZSFQ 4937 in **a** dorsal **b** ventral **c** lateral right, and **d** lateral left view.



Figure 5. Photographs of living specimens of brown-colored *Atractus* occurring along the Amazonian slopes of the Andes in Ecuador **a** *A. arangoi* ZSFQ 4948 from Jatun Sacha Biological Reserve, Napo province, Ecuador **b** *A. resplendens* ZSFQ 4953 from Montañas de San Antonio, Tungurahua province, Ecuador **c** *A. duboisi* from Orito Yacu, Napo province, Ecuador **d** *A. discovery* sp. nov. ZSFQ 4936 from Amaluzá, Azuay province, Ecuador **e** *A. orcesi* ZSFQ 2234 from El Higuerón, Sucumbíos province, Ecuador **f** *A. pachacamac* from Nangaritza, Zamora Chinchipe province, Ecuador **g** *A. zgap* sp. nov. ZSFQ 4946 from Santa Rosa, Napo province, Ecuador **h** *A. occipitoalbus* JMG-2077 from Macas, Morona Santiago province, Ecuador **i** *A. major* from Jatun Sacha Biological Reserve, Napo province, Ecuador; and **j** *A. major* from Reserva Natural Palmarí, Amazonas state, Brazil (photo by Sebastián Di Doménico).

Conservation status. We consider *Atractus discovery* sp. nov. to be Data Deficient, following IUCN Red List criteria, because the species belongs to a poorly studied genus of snakes and is known only from three specimens collected recently in a single river valley (Río Paute) in the Amazonian slopes of the Ecuadorian Andes. In addition to the presence of a system of major hydroelectric dams in this valley, most of the native cloud forest habitat in the segment between Amaluza and Arenales has been converted to pastures. However, we consider there is insufficient data to estimate whether this new snake species is restricted to the immediate environs of the type locality or if it is widely distributed along the unexplored cloud forests of the adjacent Sangay National Park.

***Atractus zgap* sp. nov.**

<https://zoobank.org/A9A58D40-CF58-4267-A691-B5E776B43C1B>

Figs 5g, 6, 7

Proposed standard English name: ZGAP Ground Snake.

Proposed standard Spanish name: Culebra tierrera de ZGAP.

Holotype. ZSFQ 4946 (Figs 5g, 6, 7), adult female collected by Diego Piñán at Santa Rosa, Napo province, Ecuador (S0.31004, W77.78591; 1500 m).

Paratypes. MZUTI 5311, adult female collected by Diego Piñán in February 2017 at El Chaco, Napo Province, Ecuador (S0.31004, W77.78591; 1500 m). QCAZ 12666, a juvenile collected by Pablo Medrano on 16 May 2014 at San Francisco de Borja, Napo province, Ecuador (S0.40953, W77.84005; 1703 m). QCAZ 5183, a juvenile collected by Patricia Bejarano on 13 November 2011 at Bosque Protector “La Cascada,” Napo province, Ecuador (S0.14572, W77.49593; 1460 m).

Diagnosis. *Atractus zgap* sp. nov. is placed in the genus *Atractus*, as diagnosed by Savage (1960), based on phylogenetic evidence (Fig. 1). The species is diagnosed based on the following combination of characters: (1) 17/17/17 smooth dorsals; (2) two postoculars; (3) loreal 2 × longer than high; (4) temporals 1+2; (5) seven supralabials, third and fourth contacting orbit; (6) seven infralabials, first three contacting chinshields; (7) seven maxillary teeth; (8) three rows of gular scales; (9) two or three prefrontals; (10) 173–177 ventrals in females; (11) 31 subcaudals in an uncollected male and 25–27 subcaudals in females; (12) dorsal ground color brown with faint dark longitudinal lines (Figs 5g, 6a); (13) venter yellow with fine brown stippling (Fig. 6b); (14) 376 mm SVL in the female holotype; (15) 37 mm TL in the female holotype.

Comparisons. *Atractus zgap* sp. nov. is compared to other small brownish congeneric ground snakes distributed along the Amazonian slopes of the Andes (most of these are illustrated in Fig. 5): *Atractus avernus*, *A. duboisi*, *A. discovery* sp. nov., *A. ecuadorensis*, *A. occipitoalbus*, *A. orcesi*, and *A. resplendens*. From *A. avernus*, *A. duboisi*, *A. occipitoalbus*, and *A. orcesi*, the new species differs in having 17/17/17 dorsal scale rows. From *A. discovery* sp. nov., the new species differs in having two postocular scales (Fig. 7c) and no dark ventral stripe. From *A. ecuadorensis*, the new species differs in



Figure 6. Adult female holotype of *Atractus zgap* sp. nov. ZSFQ 4946 in **a** dorsal and **b** ventral view.

having fewer (31 instead of 41) subcaudals in males, seven (instead of five or six) infralabials, a shorter ($2 \times$ instead of $3 \times$ longer than high) loreal, frontal longer than prefrontals, and five faint (instead of six or seven clearly defined) longitudinal black lines (Figs 5g, 6). From *A. resplendens*, the new species differs in having a shorter ($2 \times$ instead of $3 \times$ longer than high) loreal, two (instead of one) postoculars, and a brownish dorsum with faint longitudinal black lines, whereas in *A. resplendens* the dorsum is dark gray with fine yellow stippling (Fig. 5b).

Description of holotype. Adult female, SVL 376 mm, tail length 37 mm (9.8% SVL); body diameter 9.1 mm; head length 11.7 mm (3.1% SVL); head width 6.4 mm (1.7% SVL); interocular distance 4.3 mm; head slightly distinct from body; snout-orbit distance 3.8 mm; rostral 2.5 mm wide, ca. as broad as high; internasals 1.3 mm wide; prefrontals 2.5 mm wide; frontal 3.1 mm wide, with a curvilinear triangular shape in dorsal view; parietals 2.4 mm wide (56% length); nasal divided; loreal 1.6 mm long, $\sim 2 \times$ longer than high; eye diameter 1.7 mm; pupil round; supraoculars 1.2 mm wide; two postoculars; temporals 1+2; seven supralabials, third and fourth contacting orbit; symphyseal 1.7 mm wide, $\sim 2 \times$ as broad as long, separated from chinshields by first pair of infralabials; seven infralabials, first three contacting chin shields; chinshields $\sim 2 \times$ as long as broad, posterior chinshields absent; dorsal scales arranged in 17/17/17 rows, smooth without apical pits; two preventrals; ventrals 173; anal plate single; 25 paired subcaudals.

Natural history. Most individuals of *Atractus zgap* sp. nov. have been found during the day hidden under rocks, among herbs, or buried under soft soil in plantations and rural gardens close to remnants of native forest. At night, they have been seen crossing



Figure 7. Head of the adult female holotype of *Atractus zgap* sp. nov. ZSFQ 4946 in **a** dorsal **b** ventral **c** lateral right, and **d** lateral left view.

rural roads. Occasionally, during sunny days right after a rain, individuals have been seen crawling on the pavement or on gravel roads (Diego Piñán, pers. comm.).

Distribution. *Atractus zgap* sp. nov. is known only from five localities (See Suppl. material 1: Table S1) along the valley of the Río Quijos, Napo province, in the Amazonian slopes of the Andes in northeastern Ecuador, at elevations 1460–1703 m a.s.l. (Fig. 2).

Etymology. The specific epithet *zgap* is used as a noun in apposition and honors the ‘Zoological Society for the Conservation of Species and Populations’ (ZGAP) (<https://www.zgap.de>), a program seeking to conserve unknown but highly endangered species and their natural habitats throughout the world. The ZGAP grant program supports the fieldwork of young scientists who are eager to implement and start conservation projects in their home countries. Specifically, ZGAP has supported the work on endangered Andean reptiles in Ecuador conducted by AA and JV.

Conservation status. We consider *Atractus zgap* sp. nov. to be Endangered following the IUCN criteria B2a, b (i, iii) (IUCN 2001), because the species’ extent of occurrence is estimated to be less than 500 km² (Fig. 2) and its habitat is severely fragmented and declining in extent and quality due to deforestation. The valley of the Río Quijos formed the eastern frontier of the Incan Empire (1400–1532) and the cloud forest in the area suffered from intensive land-use even before European arrival (Loughlin et al. 2018). Today, this valley is one of the most important cattle farming areas along the

eastern slopes of the Andes and the majority of the forest along the Quijos river plains has been destroyed. Although *A. zgap* occurs in one protected area (Bosque Protector “La Cascada”) and its presence is expected in adjacent Parque Nacional Cayambe-Coca and Parque Nacional Sumaco Napo-Galeras, it has so far not been recorded in major protected areas.

***Atractus michaelsabini* sp. nov.**

<https://zoobank.org/E85C68A2-DAEF-4BC5-A6B3-6D1FEDEB9983>

Figs 8, 9, 10f–h

Proposed standard English name: Michael Sabin’s Ground Snake.

Proposed standard Spanish name: Culebra tierrera de Michael Sabin.

Atractus roulei Savage, 1960: 68 (part).

Atractus lehmanni Arteaga et al., 2017: 97.

Holotype. ZSFQ 4938 (Figs 8, 9, 10g), adult male collected by Jorge Luis Romero at Corraleja, Azuay province, Ecuador (S3.3874, W79.22785; 2660 m).

Paratypes. MZUTI 5289, adult female collected by Jorge Luis Romero at the type locality. AMARU 002 (Fig. 10f), adult female collected by Jorge Luis Romero at the type locality. ZSFQ 4939 (Fig. 10h), juvenile female collected by Jose Vieira and Amanda Quezada at El Panecillo, El Oro province, Ecuador (S3.46753, W79.48248; 2750 m). QCAZ 7887 and 7902, adult male and female collected by Silvia Aldás in December 2006 at Guanazán, El Oro province, Ecuador (S3.44667, W79.49051; 2663 m). QCAZ 9643 and 9652, adult females collected by Silvia Aldás in August 2009 at El Panecillo, El Oro province, Ecuador (S3.46753, W79.48248; 2775 m). DHMECN 7644–45, adult males collected by Mario Yáñez-Muñoz, Luis Oyagata, Patricia Bejarano, and Marco Altamirano in March 2010 at Reserva Biológica Yunguilla, Azuay province, Ecuador (S3.22684, W79.27520; 1748 m). AMNH 18325, adult female collected in July 1920 at El Chiral, El Oro province, Ecuador (S3.63825, W79.59723; 1841 m). AMNH 22110–11, collected in August 1921 at La Chonta, El Oro province, Ecuador (S3.56585, W79.85144; 1025 m).

Diagnosis. *Atractus michaelsabini* sp. nov. is placed in the genus *Atractus*, as diagnosed by Savage (1960), based on phylogenetic evidence (Fig. 1). The species is diagnosed based on the following combination of characters: (1) 15/15/15 smooth dorsals; (2) one postocular; (3) loreal 3 × longer than high; (4) temporals 1+2; (5) five or six supralabials, with (usually) third and fourth contacting orbit; (6) five or six infralabials, with (usually) first three contacting chinshields; (7) 9–13 maxillary teeth; (8) 1–3 rows of gular scales; (9) 1–3 preventrals; (10) 143–144 ventrals in males and 144–153 in females; (11) 24–31 subcaudals in males and 17–19 in females; (12) dorsal ground color golden yellow (Figs 8, 10f–g) to dark brown (Fig. 10h) with each scale outlined in black, forming a reticulation; (13) venter yellowish with various degrees of brown stippling (Fig. 8b); (14) 256–321 mm



Figure 8. Adult male holotype of *Atractus michaelsabini* sp. nov. ZSFQ 4938 in **a** dorsal and **b** ventral view.

SVL in males and 201–392 mm SVL in females; (15) 35–42 mm TL in males and 21–37 mm TL in females.

Comparisons. *Atractus michaelsabini* sp. nov. is compared to other members of the *A. roulei* species group: *Atractus carrioni* and *A. roulei*. From *A. carrioni*, the new species differs in having a loreal scale (Fig. 9c) (absent in *A. carrioni*). From *A. roulei* (Figs 10a–e), the new species differs in having a dorsal pattern in which each scale is outlined in a thin black line, thus creating a reticulation, and by having the prefrontal scale in broad contact with the postnasal (Fig. 9c) (not in contact or barely in contact in *A. roulei*). Furthermore, the existence of the bright golden yellow morph in adult individuals has so far been recorded only in *A. michaelsabini* sp. nov.; not in *A. roulei*, where adults are dark brown dorsally (Fig. 10a–e). In *A. roulei*, there is a black spot at the base of each dorsal scale, whereas in *A. michaelsabini* sp. nov. the spot is at the tip of each dorsal scale and is connected to the black reticulum. Genetic divergence in a 578 bp long fragment of the mitochondrial CYTB gene between *A. michaelsabini* sp. nov. and *A. roulei* is 6.5–7.2%, whereas intraspecific distances are 0–4.5% in *A. michaelsabini* sp. nov. and 0–4.8% in *A. roulei*.

Description of holotype. Adult male, SVL 256 mm, tail length 39 mm (15.2% SVL); body diameter 7.4 mm; head length 10.7 mm (3.1% SVL); head width 6.4 mm (2.5% SVL); interocular distance 3.7 mm; head slightly distinct from body; snout-orbit distance 3.5 mm; rostral 1.9 mm wide, ca. as broad as high; internasals 1.0 mm wide; prefrontals 2.0 mm wide; frontal 3.0 mm wide, with a curvilinear triangular shape in dorsal view; parietals 2.9 mm wide (65% length); nasal divided; loreal

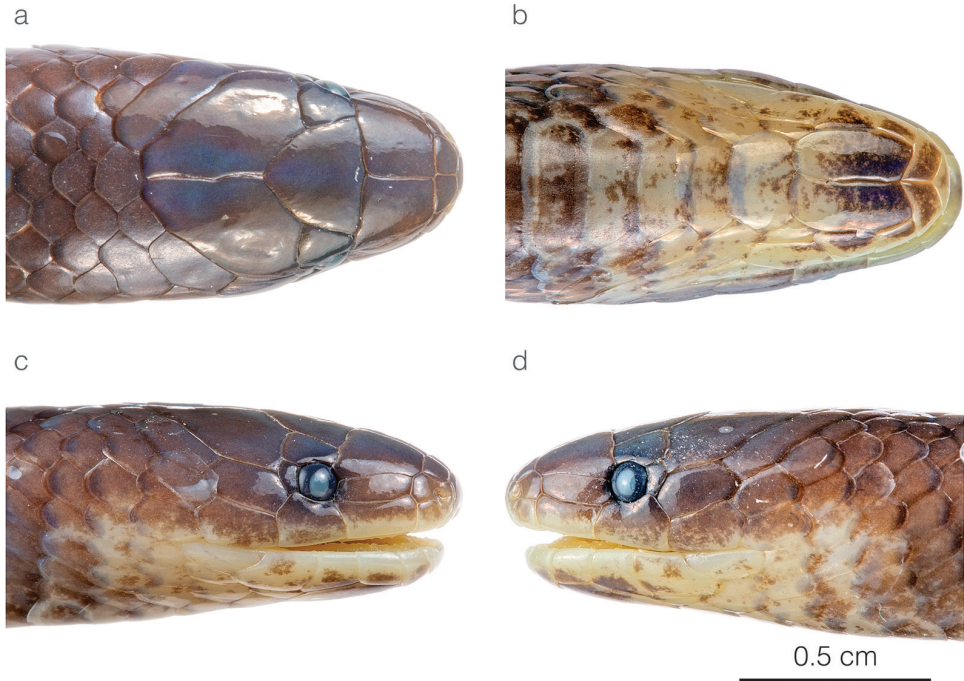


Figure 9. Head of the adult male holotype of *Atractus michaelsabini* sp. nov. ZSFQ 4938 in **a** dorsal **b** ventral **c** lateral right, and **d** lateral left view.

2.2 mm long, $\sim 3 \times$ longer than high; eye diameter 1.4 mm; pupil round; supraoculars 1.3 mm wide; one postocular; temporals 1+2; five supralabials, third contacting orbit; symphyseal 1.7 mm wide, $\sim 3 \times$ as broad as long, separated from chinshields by first pair of infralabials; five infralabials, first three contacting chinshields; chinshields $\sim 2 \times$ as long as broad, posterior chinshields absent; dorsal scales arranged in 15/15/15 rows, smooth without apical pits; no prefrontals; ventrals 143; anal plate single; 31 paired subcaudals.

Natural history. Most individuals of *Atractus michaelsabini* sp. nov. have been found during the day hidden under rocks, mats of rotten vegetation, or buried in soft soil in pastures and maize plantations close to remnants of native forest. At night, they have been seen crossing forest trails. At the type locality, clutches of three or four eggs have been found under soil (Jorge Luis Romero, pers. comm.). Anecdotal information suggests that these snakes are more active during the rainy months (February–May at the type locality; Jorge Luis Romero, pers. comm.).

Distribution. *Atractus michaelsabini* sp. nov. is endemic to an estimated 2,530 km² area along the Pacific slopes of the Andes in southwestern Ecuador. The species occurs in the xeric inter-Andean valley of the Río Jubones as well as on the slopes of the Cordillera de Chilla. *Atractus michaelsabini* sp. nov. is known from provinces Azuay, El Oro, and Loja, and has been recorded at elevations between 927 and 2922 a.s.l. (Fig. 2).



Figure 10. Photographs of living specimens of *Atractus roulei* and *A. michaelsabini* sp. nov. **a** *A. roulei* ZSFQ 4942 from Tixán, Chimborazo province, Ecuador **b** *A. roulei* ZSFQ 4944 from Tixán, Chimborazo province, Ecuador **c** *A. roulei* ZSFQ 4941 from Tixán, Chimborazo province, Ecuador **d** *A. roulei* ZSFQ 4945 from Tixán, Chimborazo province, Ecuador **e** *A. roulei* from Tixán, Chimborazo province, Ecuador **f** *A. michaelsabini* sp. nov. AMARU 002 from Corraleja, Azuay province, Ecuador **g** *A. michaelsabini* sp. nov. holotype ZSFQ 4938 from Corraleja, Azuay province, Ecuador and **h** *A. michaelsabini* sp. nov. ZSFQ 4939 from El Panecillo, El Oro province, Ecuador.

Etymology. The specific epithet *michaelsabini* is a patronym honoring a young nature lover, Michael Sabin, grandson of American philanthropist and conservationist Andrew “Andy” Sabin. The Sabin family is involved in conservation and field research of amphibians and reptiles and has protected over 264,365 acres of critical habitat throughout the world.

Conservation status. We consider *Atractus michaelsabini* sp. nov. to be Endangered following the IUCN criteria B1a, b (i, iii) (IUCN 2001), because the species’ extent of occurrence is estimated to be much less than 5,000 km² (Fig. 2) and its habitat is severely fragmented and declining in extent and quality due to deforestation. Although *A. michaelsabini* sp. nov. is present in two protected areas (private reserves Buenaventura and Yunguilla of Fundación Jocotoco), nine of the 14 localities where the species has been recorded (Suppl. material 1: Table S1) are in heavily human-modified areas. Based on maps of Ecuador’s vegetation cover (MAE 2012), we estimate that nearly 70% of the forest cover throughout the species’ potential distribution area has been destroyed, mostly due to the expansion of the agricultural frontier.

Distribution maps

Our resulting distribution maps increase the number of known localities of occurrence for the studied taxa (listed under Suppl. material 1: Table S1) and show a distinct geographical separation between *Atractus roulei* and *A. michaelsabini* sp. nov. (Fig. 2). The predicted area of suitable habitat for *A. michaelsabini* sp. nov. includes the upper watershed of the Río Jubones (a xeric inter-Andean valley) as well as both slopes of the Cordillera de Chilla (an area having vegetation classified as evergreen montane forest; see Sierra 1999). Likewise, the predicted area of suitable habitat for *A. roulei* includes evergreen montane forests along the Pacific slopes of the Andes as well as the xeric inter-Andean valley of the upper Río Chanchán. The predicted area of suitable habitat for *A. arangoi* includes almost the entire extent of Pastaza province, although we did not find records of this species from this province. Although we did not build binary environmental niche models for *A. discovery* sp. nov. and *A. zgap* sp. nov. (only two and six localities are available for these species), they are both known only from their corresponding river valleys and occur on both sides of the Río Paute and Río Quijos, respectively.

Revalidation of *Atractus arangoi*

Prado (1939) described *Atractus arangoi* from Colombia whereas Daniel (1949) reported this species in Puerto Asís, Putumayo department. Schargel et al. (2013) considered *A. arangoi* to be a junior synonym of *A. major* claiming that all the putative diagnostic characters for *A. arangoi* fall within the variation in *A. major* as defined in their work. In our phylogenetic tree of *Atractus* (Fig. 1), we included sequences of three snakes that fit the original description of *A. arangoi*. DHMECN 8343 (reported as *A. major* in Arteaga et al. 2017), ZSFQ 4947 (Fig. 11), and ZSFQ 4948 (Fig. 5a). These three specimens form a strongly supported clade sister to all other samples of *A. major*, which includes specimens from throughout the latter species’ area of distribution. Furthermore, we find

that these specimens, in addition to others reported in the literature as *A. torquatus* and *A. major* (see Duellman 1978; Maynard et al. 2017) can easily be separated from *A. major* based on differences in coloration, body size (compare Figs 5a and 5i, j), and ventral and subcaudal counts (summarized in Table 3), as originally suggested by Prado (1939). Thus, we formally remove *A. arangoi* from the synonymy of *A. major*, include this species in the herpetofauna of Ecuador, and provide a distribution map for this species (Fig. 2).

Presence of *Atractus gigas* in Peru

Passos et al. (2010) reported *Atractus gigas*, a snake species previously considered to be endemic to the cloud forests of northwestern Ecuador (Myers and Schargel 2006), on the Amazonian slopes of the Andes in Peru. The identification of the Peruvian specimens as *A. gigas* was based on their large size and the partial overlap in some characters of lepidosis with the Ecuadorian samples. However, these Peruvian snakes have a smaller number of subcaudals (25 or 26 instead of 31–37 in Ecuadorian specimens), a shorter loreal scale, first four infralabials contacting chinshields (instead of first three in Ecuadorian specimens), and a completely different color pattern in both juveniles and adults (for a figure depicting the variation among Ecuadorian individuals see Arteaga 2022). Juveniles of “*A. gigas*” from Peru have a black dorsum with short (one scale wide) reddish brown bands whereas juveniles of Ecuadorian *A. gigas* have a contrasting pattern of dark-brown to black rounded bands or blotches on a rosy white background color. Adults of “*A. gigas*” from Peru have a dorsal pattern in which each scale is dark brown distally but cream towards the base, forming a reticulation. Adults of *A. gigas* from Ecuador are uniformly rich dark brown or glossy black, and the skin between the scales is whitish (Arteaga 2022). QCAZ 14946, a specimen identified as *A. atlas* in Melo-Sampaio et al. (2021) from Reserva Biológica Cerro Plateado, just 7 km from the Peruvian border on the southeastern slopes of the Ecuadorian Andes, resembles Peruvian “*A. gigas*” as depicted in Passos et al. (2010) in having a short loreal, dorsal scales with a cream base, first four infralabials contacting chinshields, and fewer than 30 subcaudals. This specimen was included in our phylogeny (Fig. 1) and was recovered as the strongly supported sister taxon to a new sample of *A. touzeti* from this species’ type locality. Based on this evidence, we suggest that Peruvian specimens CORBIDI 877 and ZFMK 89147, as well as other *Atractus* specimens from Cajamarca labeled as *A. gigas*,

Table 3. Differences in coloration, scale counts, and size between *Atractus arangoi* and *A. major*. The range of each continuous variable is from our own sample, Prado (1939), and Maynard et al. (2017). The numbers in parentheses represent the sample size.

Variable character	<i>Atractus arangoi</i>		<i>Atractus major</i>	
	Absent		Present	
Dark brown or black nape stripe	Absent		Present	
Dorsal markings	Irregular dark blotches		Complete irregular dark bands anteriorly; blotches posteriorly	
Sex	Males (<i>n</i> = 2)	Females (<i>n</i> = 2)	Males (<i>n</i> = 7)	Females (<i>n</i> = 5)
Maximum SVL	309 mm	412 mm	533 mm	986 mm
Ventral scales	154–163	160–161	162–165	172–177
Subcaudal scales	38–39	29–32	36–45	34–37



Figure 11. Adult male of *Atractus arangoi* ZSFQ 4947 in **a** dorsal and **b** ventral view.

be reidentified as *A. atlas*, or at the very least, be considered as an undescribed species related to the latter. Thus, we suggest *A. gigas* be removed from the herpetofauna of Peru, a view that confirms this species as endemic to the cloud forests of northwestern Ecuador as originally suggested by Myers and Schargel (2006) and Arteaga et al. (2013).

Status of *Atractus occidentalis* and reidentification of specimens of *Atractus* of the *iridescens* group

In his unpublished BSc thesis, Mejía Guerrero (2018) used species distribution models, a comprehensive (based on 88 specimens) comparison of scale counts, and species delimitation analysis based on a combination of novel DNA sequences and those provided in Arteaga et al. (2017) to test species limits within the *Atractus iridescens* species group. He proposed that *A. occidentalis* Savage, 1955 is a junior synonym of *A. microrhynchus* and that some individuals identified as *A. dunnii* from Mindo are actually *A. microrhynchus*. The topology for the included members of the *A. iridescens* group in our BI phylogeny (Fig. 1) and that of Murphy et al. (2019), though not identical, agree with the proposal of Mejía Guerrero (2018). Based this evidence, we also consider *A. occidentalis* to be a junior synonym of *A. microrhynchus*. Recently, Passos et al. (2022) provided a list of reidentifications of 15 (not 17, because two are duplicates and MZUTI 4178 retained the same identification despite being listed in the table) *Atractus* specimens having sequences deposited in GenBank, notably among them the members of the *A. iridescens* species group deposited in MZUTI and DHMECN. In this work, one reidentification (that of the holotype of *A. pyroni*; MZUTI 5107) was backed up by ample evidence and two oth-

ers (ANF 2390, now MZUTI 5409; and GFM 307, now MPEG 21582) were substantiated in Melo-Sampaio et al. (2021), but the remaining were proposed without providing any evidence, either in the form of new phylogenetic relationships, new scale counts, or previously unsampled morphological features. Since these specimens are deposited at MZUTI and DHMECN, as well as their corresponding photo vouchers available in Arteaga et al. (2017), and their DNA sequences on GenBank, their identity can be tested by anyone. Although the reidentification of the remaining specimens provided by Passos et al. (2022) was unsubstantiated, not all of them were unwarranted (see Table 4). We agree that DHMECN 7644 (identified as *A. lehmanni* Boettger, 1898 in Arteaga et al. 2017) and IBSP 71932 (identified as *A. zebrinus* Jan, 1862 in Grazziotin et al. 2012) are misidentified, but their new identifications provided by Passos et al. (2022) are not correct either (see Table 4). DHMECN 7644 is a paratype of *A. michaelsabini* sp. nov., as defined herein, and IBSP 71932 is probably an *A. trihedrurus* Amaral, 1926, not an “*A. triherurus*.” Although the latter probably represents a typo and is a minor error, the problems with the remaining reidentifications are not trivial. For example, Passos et al. (2022) reidentified the same specimen, MZUTI 3758, as *A. iridescens* Peracca, 1896 and also as *A. cf. iridescens*. Additionally, these authors completely reidentified the type series of both *A. cerberus* and *A. esepe* Arteaga et al., 2017, probably without much confidence since this action is not explained elsewhere in their work and is not trivial. Since MZUTI 4330 and MZUTI 3758 are name-bearing specimens, reidentification of these holotypes as *A. iridescens*, *A. cf. iridescens*, or anything other than their original identification presented in Arteaga et al. (2017) implies that these species are not valid. Surprisingly, the fact that the taxonomic validity of these two species is not questioned elsewhere in Passos et al. (2022) suggests that some of these reidentifications were proposed carelessly. Thus, in Table 4, we evaluate these reidentifications and mention whether they are substantiated or warranted or neither. Finally, we propose the reidentification of an additional six *Atractus* specimens (Table 5) having sequences deposited in GenBank based on the results presented in Fig 1.

Table 4. Reidentification of *Atractus* specimens reidentified in Passos et al. 2022 based on direct examination of voucher specimens.

Voucher	Original identification (Arteaga et al. 2017)	Proposed reidentification (Passos et al 2022)	Reidentification warranted and substantiated	Identification
MZUTI 4330	<i>Atractus cerberus</i>	<i>Atractus</i> cf. <i>iridescens</i>	No	<i>Atractus cerberus</i>
MZUTI 1385, 2649–50, 3323	<i>Atractus occidentalis</i>	<i>Atractus dunni</i>	No	<i>Atractus microrhynchus</i>
MZUTI 3758–59	<i>Atractus esepe</i>	<i>Atractus</i> cf. <i>iridescens</i> and <i>A. iridescens</i>	No	<i>Atractus esepe</i>
MZUTI 4178	<i>Atractus iridescens</i>	<i>Atractus iridescens</i>	Identity remained the same, but listed as “reidentified”	<i>Atractus iridescens</i>
MZUTI 4122	<i>Atractus microrhynchus</i>	<i>Atractus iridescens</i>	No	<i>Atractus microrhynchus</i>
DHMECN 7644	<i>Atractus lehmanni</i>	<i>Atractus roulei</i>	Warranted at time of publication	<i>Atractus michaelsabini</i> sp. nov.
MZUTI 5109	<i>Atractus microrhynchus</i>	<i>Atractus dunni</i>	No	<i>Atractus microrhynchus</i>
MZUTI 5107	<i>Atractus pyroni</i>	<i>Atractus roulei</i>	Yes	<i>Atractus roulei</i>
ANF 2390	<i>Atractus touzeti</i>	<i>Atractus pachacamac</i>	Yes	<i>Atractus pachacamac</i>
GFM 307	<i>Atractus schach</i>	<i>Atractus snethlageae</i>	Yes	<i>Atractus snethlageae</i>
IBSP 71932	<i>Atractus zebrinus</i>	<i>Atractus triherurus</i>	Yes, but name misspelled	<i>Atractus trihedrurus</i>

Table 5. Reidentification of *Atractus* sequences available in GenBank based on direct examination of voucher specimens.

Voucher	GenBank accession numbers	Identity in GenBank	Identification
DHMECN 8343	KY610059, KY610105	<i>Atractus major</i>	<i>Atractus arangoi</i>
QCAZ 7887	MT507872, MT511989	<i>Atractus roulei</i>	<i>Atractus michaelsabini</i> sp. nov.
QCAZ 7889	MT507874, MT511990	<i>Atractus roulei</i>	<i>Atractus michaelsabini</i> sp. nov.
QCAZ 9643	MT507875, MT511981, MT511991	<i>Atractus roulei</i>	<i>Atractus michaelsabini</i> sp. nov.
QCAZ 9652	MT507876, MT511992	<i>Atractus roulei</i>	<i>Atractus michaelsabini</i> sp. nov.
MHUA 14368	GQ334664, GQ334581, GQ334558, GQ334480	<i>Atractus wagleri</i>	<i>Atractus lasallei</i>

Discussion

Atractus is perhaps the most taxonomically complex snake genus and the work needed to elucidate its evolutionary relationships is just starting. Achieving a comprehensive understanding of the real diversity within this cryptozoic group of snakes will require an approach combining three actions: 1) improving the taxon sampling available for comparison at the molecular level; 2) re-sampling type localities as well as exploring new remote areas; and 3) defining species boundaries among *Atractus* species using an integrative taxonomic approach, not only scale counts. Below, we discuss how our results help clear the waters in *Atractus* taxonomy and provide insights on where future research efforts might be most effective.

The molecular phylogenies presented here (Fig. 1 and Suppl. material 2: Fig. S1) include only approximately 30% of the total known diversity of the genus *Atractus*; thus, many higher-level relationships within species groups are still unknown. The placement of *A. trilineatus* as sister to a clade containing *A. arangoi* and *A. major*, rather than as an early divergent *Atractus* species (Murphy et al. 2019) is puzzling, but this relationship is moderately supported in both the BI and ML analyses and will likely benefit from an improved sampling of molecular characters. *Atractus arangoi* is supported as a valid species in our molecular analyses and is easily diagnosable from *A. major* based on body size, coloration, and lepidosis (Table 3), confirming its status as a valid species (Prado 1939; Daniel 1949). With the exception of the weakly placed *A. zidoki* Gasc & Rodrigues, 1979, we found that cis-Andean species of *Atractus* are more closely related to other cis-Andean species, whereas trans-Andean ground snakes are more closely related to other trans-Andean species. This finding may prove useful in understanding why the presence of the same *Atractus* species on both sides of the Andes, a scenario suggested for *A. gigas* by Passos et al. (2010), is unlikely.

There is a clade formed by the remaining Ecuadorian *Atractus* that were included in the phylogeny and are distributed along the Amazonian slopes of the Andes. The new species, *A. discovery* sp. nov. and *A. zgap* sp. nov., are included in this group. While the former is the strongly supported sister species to *A. resplendens*, it has a coloration pattern most similar to *A. orcesi* (Fig. 5e), a species not previously included in any phylogenetic analyses and characterized by having a yellow belly with a black ventral stripe. The black stripe on a yellow belly is a characteristic shared by *A. duboisi*, *A. discovery* sp. nov., and *A. orcesi*, but is absent from *A. resplendens* and *A. ecuadorensis* (the other two members of the group) and confirms this as a useful character in diagnosing species within this clade. In the ML analysis (Suppl. material 2: Figure S1), *A. dunni* is nested within

A. microrhynchus, a topology not recovered in the BI phylogeny or in previous analyses despite being based on the same DNA sequences. We believe this incongruence is the result of character sampling and methodological approach instead of these two species being conspecific. The phylogenetic position of *A. zgap* sp. nov., a snake most similar to *A. ecuadorensis* in size, coloration, and lepidosis, as sister to a clade of banded Amazonian *Atractus* rather than to *A. ecuadorensis* is puzzling. Although the placement of *A. zgap* sp. nov. in both the BI and ML analyses is strongly supported and is probably correct, we do not have as much confidence in the position of *A. ecuadorensis* and this may be explained by the fact that only one gene fragment (ND4) was available for the latter species (Appendix I). We found higher intraspecific topological distances between members of *A. carrioni*, *A. major*, and *A. roulei* than between the pair of species *A. trefauti*-*A. schach*. Therefore, attention should be given to reevaluating the validity of these species.

The binary environmental niche models (Fig. 2) for both *Atractus michaelsabini* sp. nov. and *A. roulei* include xeric inter-Andean valleys where populations of these snakes are known to occur, even though elsewhere these species inhabit humid areas where the dominant vegetation cover is evergreen montane forest (Sierra 1999). We found that the deep intraspecific genetic divergence found within both of these taxa corresponds to the sampling of populations distributed on different bioclimatic regimes (i.e., snakes of xeric habitats are genetically distinct from snakes of humid habitats). Although we did not find morphological differences that would allow the distinction of these subpopulations, we do not rule out the possibility that they correspond to cryptic species diversity.

In addition to creating a more robust phylogenetic tree of ground snakes, one of the most important actions in the quest towards a more clear, stable, and useful *Atractus* taxonomy is the correct identification of museum specimens. Based on our review of the reidentifications proposed in Passos et al. (2022), it is evident that reassigning the species identities of museum vouchers is not a trivial pursuit. On the contrary, it has consequences that go beyond taxonomy. For example, reidentifying the only known museum specimens of the Critically Endangered *A. cerberus* as *A. iridescens*, a Least Concern species, implies that the population of this species in the isolated Pacoche forest of west-central Ecuador is not as unique and worthy of conservation efforts. It also implies that the presence of a species endemic to the humid Chocó rainforest in an isolated mountain range belonging to another biogeographic province is likely.

The last point on biogeography deserves elaboration. The use of species distribution models can be used not only to discover and test biogeographical patterns but also to test species as hypotheses (Ahmadzadeh et al. 2013; Ortega-Andrade et al. 2015). The elaboration of distribution maps using ecological variables, in addition to the presentation of accurate color photographs of specimens and their corresponding genetic information as a part of an integrative taxonomic approach can greatly benefit *Atractus* taxonomy, a branch of herpetology in which diagnoses have largely been based only on meristics (Savage 1960; Passos et al. 2009c; Passos et al. 2010). Using this framework can help prevent *Atractus* species that are valid taxa and occur in distinct biogeographical provinces to be subsumed under the same name on the basis of overlapping scale counts. An example of this are the snakes *A. gigas* and *A. dunni*, two cloud forest species endemic to the Pacific slopes of the Andes in northwestern Ecuador. These snakes

present a biogeographic pattern of distribution shared by other co-occurring reptiles (Avila Pires 2001; Köhler et al. 2004; Arteaga et al. 2013; Torres-Carvajal and Lobos 2014; Arteaga et al. 2016). Given how narrow the climatic requirements of these two *Atractus* species are (Mejía Guerrero 2018; Mantilla Espinoza 2021), their presence on the Amazonian slopes of the Andes, or on the Chococoan lowlands, as suggested by Passos et al. (2010) and Passos et al. (2022), respectively, is unlikely. In this work, we presented evidence that supports the status of *A. gigas* and *A. dunni* as species endemic to the cloud forests of the Pacific slopes of the Andes in northwestern Ecuador.

Finally, although *Atractus* systematics have progressed greatly since Savage published his monograph on the Ecuadorian members of this genus in 1960, many “stones are still left unturned.” The Ecuadorian species *A. clarki* Dunn & Bailey, 1939, *A. collaris* Peracca, 1897, *A. gaigeae* Savage, 1955, and *A. occipitoalbus* have not been included in a phylogenetic work, and their status remains uncertain. Also, an overwhelming majority of *Atractus* diversity, both described and undescribed, is in Colombia (Uetz et al. 2022). Unfortunately, only one or two samples of *Atractus* coming from Colombia have been included in published phylogenetic trees of this genus (Arteaga et al. 2017; Murphy et al. 2019; Melo-Sampaio et al. 2021, Passos et al. 2022). Thus, we suggest that future work on *Atractus* be focused on unveiling the incredible diversity of this genus in Colombia.

Acknowledgements

This article was greatly improved by comments of Omar Entiauspe-Neto, Abel Batista, and Robert Jadin. For granting access to the protected forests under their care, we are grateful to Pedro Alvarado of CELEC EP, Martin Schaefer and David Agro of Fundación Jocotoco, and Alex Rosillo of Fundación Jatun Sacha. Special thanks to Eric Osterman, Gabriella Marcano, and María José Quiroz for their assistance and companionship in the field. For providing specimens, photos, and ecological information of *Atractus*, we are grateful to Diego Piñán and Jorge Luis Romero. For creating the image of the juvenile of *A. major*, we are grateful to Sebastián Di Doménico. Gabriela Gavilanes provided invaluable lab assistance in generating DNA sequence data. For granting access to specimens under their care, we are grateful to Christopher Raxworthy (AMNH), Sebastián Padrón (MZUA), and Ernesto Arbeláez (AMARU). Special thanks to Arne Schulze for encouraging AA to combine the discovery of *A. zgap* sp. nov. with a concrete plan for the conservation of this species. Fieldwork was made possible with the support of “The Explorers Club Discovery Expedition Grants”, The Zoological Society for the Conservation of Species and Populations (ZGAP), Khamai Foundation, Tropical Herping, Re:wild, Sabin Family Foundation, and Prefectura del Azuay. Laboratory work was carried out at USFQ. Sequencing was made possible with support of the Inedita Program from the Ecuadorian Science Agency SENESCYT (Respuestas a la Crisis de Biodiversidad: La Descripción de Especies como Herramienta de Conservación; INEDITA PIC-20-INE-USFQ-001). The project also benefited from funds granted by Universidad San Francisco de Quito (HUBI 5466, 5467, 16871).

References

- Ahmadzadeh F, Flecks M, Carretero MA, Mozaffari O, Böhme W, Harris DJ, Freitas S, Rödder D (2013) Cryptic speciation patterns in Iranian rock lizards uncovered by integrative taxonomy. *PLoS ONE* 8(12): e80563. <https://doi.org/10.1371/journal.pone.0080563>
- Amaral A (1926) Novos gêneros e espécies de ophidios brasileiros. *Archivos do Museu Nacional do Rio de Janeiro* 26: 1–27.
- Arévalo E, Davis SK, Sites JW (1994) Mitochondrial DNA-sequence divergence and phylogenetic relationships among eight chromosome races of the *Sceloporus grammicus* complex (Phrynosomatidae) in Central Mexico. *Systematic Biology* 43(3): 387–418. <https://doi.org/10.1093/sysbio/43.3.387>
- Arteaga A (2022) Giant Ground Snake (*Atractus gigas*). In: Arteaga A, Bustamante L, Vieira J, Guayasamin JM (Eds) Reptiles of Ecuador: Life in the middle of the world. <https://doi.org/10.47051/MNHT9360>
- Arteaga A, Bustamante L, Guayasamin JM (2013) The amphibians and reptiles of Mindo. Universidad Tecnológica Indoamérica, Quito, 257 pp.
- Arteaga A, Pyron RA, Peñafiel N, Romero-Barreto P, Culebras J, Bustamante L, Yáñez-Muñoz MH, Guayasamin JM (2016) Comparative phylogeography reveals cryptic diversity and repeated patterns of cladogenesis for amphibians and reptiles in northwestern Ecuador. *PLoS ONE* 11: e0151746. <https://doi.org/10.1371/journal.pone.0151746>
- Arteaga A, Mebert K, Valencia JH, Cisneros-Heredia DF, Peñafiel N, Reyes-Puig C, Vieira-Fernandes JL, Guayasamin JM (2017) Molecular phylogeny of *Atractus* (Serpentes, Dipsadidae), with emphasis on Ecuadorian species and the description of three new taxa. *ZooKeys* 661: 91–123. <https://doi.org/10.3897/zookeys.661.11224>
- Arteaga A, Salazar-Valenzuela D, Mebert K, Peñafiel N, Aguiar G, Sánchez-Nivicela JC, Pyron RA, Colston TJ, Cisneros-Heredia DF, Yáñez-Muñoz MH, Venegas PJ, Guayasamin JM, Torres-Carvajal O (2018) Systematics of South American snail-eating snakes (Serpentes, Dipsadini), with the description of five new species from Ecuador and Peru. *ZooKeys* 766: 79–147. <https://doi.org/10.3897/zookeys.766.24523>
- Arteaga A, Bustamante L, Vieira J, Tapia W, Guayasamin JM (2019) Reptiles of the Galápagos: life on the Enchanted Islands. Tropical Herping, Quito, 208 pp. <https://doi.org/10.47051/AQJU7348>
- Arteaga A, Bustamante L, Vieira J, Guayasamin JM (2022) Reptiles of Ecuador: life in the middle of the world. <https://doi.org/10.47051/MNHT9360>
- Avila-Pires TCS (2001) A new species of *Lepidoblepharis* (Reptilia: Squamata: Gekkonidae) from Ecuador, with a redescription of *L. grandis* Miyata, 1985. *Occasional Paper of the Sam Noble Oklahoma Museum of Natural History* 11: 1–11.
- Beaupre SJ, Jacobson ER, Lillywhite HB, Zamudio K (2004) Guidelines for use of live amphibians and reptiles in field and laboratory research. *American Society of Ichthyologists and Herpetologists, Lawrence*, 43 pp.
- Boettger O (1898) Katalog der Reptilien-Sammlung im Museum der Senckenbergischen Naturforschenden Gesellschaft in Frankfurt. II Teil (Schlangen). Gebrüder Knauer, Frankfurt, 160 pp.
- Boie F (1827) Bemerkungen über Merrem's Versuch eines Systems der Amphibien. *Isis von Oken* 20: 508–566.

- Boulenger GA (1880) Reptiles et Batraciens recueillis par M. Emile de Ville dans les Andes de l'Équateur. Bulletin de la Société Zoologique de France 5: 41–48.
- Boulenger GA (1894) Catalogue of the snakes in the British Museum. Taylor & Francis, London, 382 pp. <https://doi.org/10.5962/bhl.title.8316>
- Burbrink FT, Lawson R, Slowinski JB (2000) Mitochondrial DNA phylogeography of the polytypic North American rat snake (*Elaphe obsoleta*): A critique of the subspecies concept. Evolution 54(6): 2107–2188. <https://doi.org/10.1111/j.0014-3820.2000.tb01253.x>
- Caramaschi U, de Sá RO, Heyer WR (2006) *Leptodactylus*. Information bank for *Leptodactylus* frogs. <https://facultyhub.richmond.edu>
- Cisneros-Heredia D (2005) Rediscovery of the Ecuadorian snake *Atractus dunni* Savage, 1955 (Serpentes: Colubridae). Journal by the National Museum. Natural History Series 174: 87–114.
- Coloma LA, Guayasamin JM (2011–2017) Nombres vernáculos de anfibios de Ecuador. <http://www.anfibiosecuador.ec>
- Cope ED (1868) An examination of the Reptilia and Batrachia obtained by the Orton Expedition to Equador and the Upper Amazon, with notes on other species. Proceedings. Academy of Natural Sciences of Philadelphia 20: 96–140.
- da Cunha OR, do Nascimento FP (1983) Ofidios da Amazonia. XX. As especies de *Atractus* Wagler, 1828, na Amazonia oriental & Maranhao (Ophidia, Colubridae). Boletim do Museu Paraense Emílio Goeldi 123: 1–38.
- Daniel H (1949) Las serpientes en Colombia. Revista Facultad Nacional de Agronomía 9: 301–333.
- de Queiroz K (2007) Species concepts and species delimitation. Systematic Biology 56(6): 879–886. <https://doi.org/10.1080/10635150701701083>
- Despax R (1910) Mission géodésique de l'Équateur. Collections recueillies par M. le Dr. Rivet. Liste des Ophidiens et description des espèces nouvelles. Bulletin du Muséum National d'Histoire Naturelle 16: 368–376. <https://doi.org/10.5962/bhl.part.20432>
- Dowling HG (1951) A proposed standard system of counting ventrals in snakes. British Journal of Herpetology 1: 97–99.
- Drummond AJ, Ashton B, Buxton S, Cheung M, Cooper A, Heled J, Kearse M, Moir R, Stones-Havas S, Sturrock S, Thierer T, Wilson A (2021) Geneious version 2021.1. <https://www.geneious.com>
- Duellman WE (1978) The biology of an equatorial herpetofauna in Amazonian Ecuador. Publications of the Museum of Natural History, University of Kansas 65: 1–352.
- Duméril AMC, Bibron G, Duméril AHA (1854) Erpétologie générale ou Histoire Naturelle complète des Reptiles. Librairie Encyclopédique de Roret, Paris, 780 pp. <https://doi.org/10.5962/bhl.title.45973>
- Dunn ER, Bailey JR (1939) Snakes from the uplands of the Canal Zone and of Darien. Bulletin of the Museum of Comparative Zoology at Harvard College 86: 1–22.
- Elith J, Leathwick JR (2009) Species distribution models: Ecological explanation and prediction across space and time. Annual Review of Ecology, Evolution, and Systematics 40(1): 677–697. <https://doi.org/10.1146/annurev.ecolsys.110308.120159>
- Elith J, Phillips SJ, Hastie T, Dudík M, Chee YE, Yates CJ (2011) A statistical explanation of MaxEnt for ecologists. Diversity & Distributions 17(1): 43–57. <https://doi.org/10.1111/j.1472-4642.2010.00725.x>
- Felsenstein J (2004) Inferring phylogenies. Sinauer Associates, Sunderland, 664 pp.

- Gasc JP, Rodrigues MT (1979) Une nouvelle espèce du genre *Atractus* (Colubridae, Serpentes) de la Guyane Française. Bulletin du Muséum National d'Histoire Naturelle 2: 547–557.
- Grazziotin FG, Zaher H, Murphy RW, Scrocchi GJ, Benavides MA, Zhang YP, Bonatto SL (2012) Molecular phylogeny of the New World Dipsadidae (Serpentes: Colubroidea): a reappraisal. Cladistics 1(5): 1–223. <https://doi.org/10.1111/j.1096-0031.2012.00393.x>
- Hijmans RJ, Cameron SE, Parra JL, Jones PG, Jarvis A (2005) Very high resolution interpolated climate surfaces for global land areas. International Journal of Climatology 25(15): 1965–1978. <https://doi.org/10.1002/joc.1276>
- IUCN (2001) IUCN Red List categories and criteria: Version 3.1. IUCN Species Survival Commission, Gland and Cambridge, 30 pp.
- Jan G (1862) Enumerazione sistematico delle specie d'ofidi del gruppo Calamaridae. Archivio per la Zoologia, l'Anatomia e la Fisiologia 2: 1–76.
- Katoh K, Standley DM (2013) MAFFT multiple sequence alignment software version 7: Improvements in performance and usability. Molecular Biology and Evolution 30(4): 772–780. <https://doi.org/10.1093/molbev/mst010>
- Köhler G, Böhme W, Schmitz A (2004) A new species of *Echinosauro* (Squamata: Gymnophthalmidae) from Ecuador. Journal of Herpetology 38(1): 52–60. <https://doi.org/10.1670/164-02A>
- Kozlov AM, Darriba D, Flouri T, Morel B, Stamatakis A (2019) RAxML-NG: A fast, scalable and user-friendly tool for maximum likelihood phylogenetic inference. Bioinformatics 35(21): 4453–4455. <https://doi.org/10.1093/bioinformatics/btz305>
- Lanfear R, Frandsen PB, Wright AM, Senfeld T, Calcott B (2016) PartitionFinder 2: New methods for selecting partitioned models of evolution for molecular and morphological phylogenetic analyses. Molecular Biology and Evolution 34: 772–773. <https://doi.org/10.1093/molbev/msw260>
- Loughlin NJD, Gosling WD, Mothes P, Montoya E (2018) Ecological consequences of post-Columbian indigenous depopulation in the Andean-Amazonian corridor. Nature Ecology & Evolution 2(8): 1233–1236. <https://doi.org/10.1038/s41559-018-0602-7>
- MAE (2012) Línea base de deforestación del Ecuador continental. Ministerio del Ambiente del Ecuador, Quito, 30 pp.
- Mantilla Espinoza EF (2021) Áreas potenciales de conservación para serpientes del género *Atractus* por encima de los 2000 m.s.n.m. en el Ecuador. BSc thesis, Universidad Central del Ecuador, 59 pp.
- Maynard RJ, Lynch RL, Maier P, Hamilton P (2017) Reptiles of San José de Payamino, Orellana, Ecuador. Field guides of the Field Museum of Natural History, Chicago, 9 pp.
- Mejía Guerrero MA (2018) Revisión taxonómica de las serpientes tierraeras *Atractus* del grupo *iridescens* Arteaga et al. 2017. BSc thesis, Quito, Pontificia Universidad Católica del Ecuador, 67 pp.
- Melo-Sampaio PR, Passos P, Fouquet A, Da Costa Prudente AL (2019) Systematic review of *Atractus schach* (Serpentes: Dipsadidae) species complex from the Guiana Shield with description of three new species. Systematics and Biodiversity 17(3): 207–229. <https://doi.org/10.1080/14772000.2019.1611674>
- Melo-Sampaio PR, Passos P, Prudente ALC, Venegas PJ, Torres-Carvajal O (2021) Systematic review of the polychromatic ground snakes *Atractus snethlageae* complex reveals four new species from threatened environments. Journal of Zoological Systematics and Evolutionary Research 00(3): 1–30. <https://doi.org/10.1111/jzs.12453>

- Meneses-Pelayo E, Passos P (2019) New polychromatic species of *Atractus* (Serpentes: Dipsadidae) from the eastern portion of the Colombian Andes. *Copeia* 107(2): 250–261. <https://doi.org/10.1643/CH-18-163>
- Murphy JC, Salvi D, Braswell AL, Jowers MJ (2019) Phylogenetic position and biogeography of Three-Lined Snakes (*Atractus trilineatus*: Squamata, Dipsadidae) in the Eastern Caribbean. *Herpetologica* 75(3): 247–253. <https://doi.org/10.1655/D-18-00043>
- Myers CW (2003) Rare snakes – five new species from eastern Panama: reviews of northern *Atractus* and southern *Geophis* (Colubridae: Dipsadinae). *American Museum Novitates* 3391: 1–47. [https://doi.org/10.1206/0003-0082\(2003\)391<0001:RSFNSF>2.0.CO;2](https://doi.org/10.1206/0003-0082(2003)391<0001:RSFNSF>2.0.CO;2)
- Myers CW, Schargel WE (2006) Morphological extremes—two new snakes of the genus *Atractus* from northwestern South America (Colubridae: Dipsadinae). *American Museum Novitates* 3532(1): 1–13. [https://doi.org/10.1206/0003-0082\(2006\)3532\[1:MENSOT\]2.0.CO;2](https://doi.org/10.1206/0003-0082(2006)3532[1:MENSOT]2.0.CO;2)
- Ortega-Andrade MH, Rojas-Soto OR, Valencia JH, Espinosa de los Monteros A, Morrone JJ, Ron S, Cannatella DC (2015) Insights from integrative systematics reveal cryptic diversity in *Pristimantis* frogs (Anura: Craugastoridae) from the upper amazon basin. *PLoS ONE* 10(11): e0143392. <https://doi.org/10.1371/journal.pone.0143392>
- Palumbi SR, Martin A, Romano S, McMillan WO, Stice L, Grabowski G (1991) The simple fool's guide to PCR, version 2.0. University of Hawaii, Honolulu, 94 pp.
- Parker HW (1930) A new colubrine snake from Ecuador. *Annals & Magazine of Natural History* 5(26): 207–209. <https://doi.org/10.1080/00222933008673120>
- Passos P, Arredondo JC, Fernandes R, Lynch JD (2009a) Three new *Atractus* (Serpentes: Dipsadidae) from the Andes of Colombia. *Copeia* 2009(3): 425–436. <https://doi.org/10.1643/CH-08-063>
- Passos P, Chiesse A, Torres-Carvajal O, Savage JM (2009b) Testing species boundaries within the *Atractus occipitoalbus* complex (Serpentes: Dipsadidae). *Herpetologica* 65(4): 384–403. <https://doi.org/10.1655/08-024.1>
- Passos P, Mueses-Cisneros JJ, Lynch JD, Fernandes R (2009c) Pacific lowland snakes of the genus *Atractus* (Serpentes: Dipsadidae), with description of three new species. *Zootaxa* 2293(1): 1–34. <https://doi.org/10.11646/zootaxa.2293.1.1>
- Passos P, Dobyey M, Venegas PJ (2010) Variation and natural history notes on giant ground-snake, *Atractus gigas* (Serpentes: Dipsadidae). *South American Journal of Herpetology* 5(2): 73–82. <https://doi.org/10.2994/057.005.0201>
- Passos P, Prudente ALC, Lynch JD (2016) Redescription of *Atractus punctiventris* and description of two new *Atractus* (Serpentes: Dipsadidae) from Brazilian Amazonia. *Herpetological Monograph* 30(1): 1–20. <https://doi.org/10.1655/HERPMONOGRAPHS-D-14-00009>
- Passos P, Scanferla A, Melo-Sampaio PR, Brito J, Almendariz A (2018) A giant on the ground: another large-bodied *Atractus* (Serpentes: Dipsadinae) from Ecuadorian Andes, with comments on the dietary specializations of the goo-eaters snakes. *Anais da Academia Brasileira de Ciências* 91(suppl 1): e20170976. <https://doi.org/10.1590/0001-3765201820170976>
- Passos P, Melo-Sampaio PR, Ramos LO, Grazziotin FG, Fouquet A, Torres-Carvajal O (2022) When the tail shakes the snake: phylogenetic affinities and morphology of *Atractus badius* (Serpentes: Dipsadidae), reveals some current pitfalls on the snake's genomic age. *Annals of the Brazilian Academy of Sciences* 94(1): e20191254. <https://doi.org/10.1590/0001-3765202220191254>

- Peñafiel N, Flores DM, Rivero De Aguilar J, Guayasamin JM, Bonaccorso E (2020) A cost-effective protocol for total DNA isolation from animal tissue. *Neotropical Biodiversity* 5(1): 69–74. <https://doi.org/10.1080/23766808.2019.1706387>
- Peracca MG (1896) Sopra alcuni Ofidii nuovi o poco noti dell'America meridionale. *Bollettino dei Musei di Zoologia e di Anatomia Comparata della Università di Torino* 11: 1–4. <https://doi.org/10.5962/bhl.part.4563>
- Peracca MG (1897) Intorna ad una piccola raccolta di Rettili di Cononacco (Perù orientale). *Bollettino dei Musei di Zoologia e di Anatomia Comparata della Università di Torino* 12: 1–7. <https://doi.org/10.5962/bhl.part.4563>
- Peterson AT, Soberon JR, Pearson RG, Anderson RP, Martínez-Meyer E, Nakamura M, Bastos Araújo M (2011) *Ecological niches and geographic distributions*. Princeton University Press, Princeton, 328 pp. <https://doi.org/10.23943/princeton/9780691136868.003.0003>
- Phillips SJ, Anderson RP, Schapire RE (2006) Maximum entropy modeling of species geographic distributions. *Ecological Modelling* 190(3–4): 231–259. <https://doi.org/10.1016/j.ecolmodel.2005.03.026>
- Prado A (1939) Cinco especies novas de serpentes colombianas do genero *Atractus* Wagler. *Memorias do Instituto Butantan* 13: 1–9.
- Rambaut A, Suchard M, Drummond AJ (2022) Tracer version 1.7.1 <http://www.beast.community>
- Renner IW, Warton DI (2013) Equivalence of MAXENT and poisson point process models for species distribution modeling in ecology. *Biometrics* 69(1): 274–281. <https://doi.org/10.1111/j.1541-0420.2012.01824.x>
- Ronquist F, Huelsenbeck JP (2013) MrBayes 3: Bayesian phylogenetic inference under mixed models. *Bioinformatics* 19(12): 1572–1574. <https://doi.org/10.1093/bioinformatics/btg180>
- Royle JA, Chandler RB, Yackulic C, Nichols JD (2012) Likelihood analysis of species occurrence probability from presence-only data for modelling species distributions. *Methods in Ecology and Evolution* 3(3): 545–554. <https://doi.org/10.1111/j.2041-210X.2011.00182.x>
- Salazar-Valenzuela D, Torres-Carvajal O, Passos P (2014) A new species of *Atractus* (Serpentes: Dipsadidae) from the Andes of Ecuador. *Herpetologica* 70(3): 350–363. <https://doi.org/10.1655/HERPETOLOGICA-D-13-00045>
- Savage JM (1955) Descriptions of new colubrid snakes, genus *Atractus*, from Ecuador. *Proceedings of the Biological Society of Washington* 68: 11–20.
- Savage JM (1960) A revision of the Ecuadorian snakes of the Colubrid genus *Atractus*. *Miscellaneous Publications, Museum of Zoology, University of Michigan* 112: 1–184.
- Schargel WE, Lamar WW, Passos P, Valencia JH, Cisneros-Heredia DF, Campbell JA (2013) A new giant *Atractus* (Serpentes: Dipsadidae) from Ecuador, with notes on some other large Amazonian congeners. *Zootaxa* 3721(5): 455–474. <https://doi.org/10.11646/zootaxa.3721.5.2>
- Sierra R (1999) Propuesta preliminar de un sistema de clasificación de vegetación para el Ecuador continental. *EcoCiencia, Quito*, 174 pp.
- Soberón J, Peterson TA (2005) Interpretation of models of fundamental ecological niches and species' distributional areas. *Biodiversity Informatics* 2(0): 1–10. <https://doi.org/10.17161/bi.v2i0.4>

- Tolhurst B, Peck M, Morales JN, Cane T, Recchio I (2010) Extended distribution of a recently described dipsadine colubrid snake: *Atractus gigas*. *Herpetology Notes* 3: 73–75.
- Torres-Carvajal O, Lobos SE (2014) A new species of *Alopoglossus* lizard (Squamata, Gymnophthalmidae) from the tropical Andes, with a molecular phylogeny of the genus. *ZooKeys* 410: 105–120. <https://doi.org/10.3897/zookeys.410.7401>
- Uetz P, Freed P, Hošek J (2022) The Reptile Database. <http://www.reptile-database.org> [accessed 12 Jun 2022]
- van Proosdij ASJ, Sosef MSM, Wieringa JJ, Raes N (2015) Minimum required number of specimen records to develop accurate species distribution models. *Ecography* 39(6): 542–552. <https://doi.org/10.1111/ecog.01509>
- Wagler J (1828) Auszüge aus seinem Systema Amphibiorum. *Isis von Oken* 21: 740–744.
- Werner F (1901) Ueber Reptilien und Batrachier aus Ecuador und Neu-Guinea. *Verhandlungen der Kaiserlich-Königlichen Zoologisch-Botanischen Gesellschaft in Wien* 51: 593–614. <https://doi.org/10.5962/bhl.part.4586>

Appendix I

Table A1. GenBank accession numbers for loci and terminals of taxa and outgroups sampled in this study. Novel sequence data produced in this study are marked with an asterisk (*).

Species	Voucher	16S	CYTB	ND4	CMOS	NT3	RAG1
<i>A. arangoi</i>	DHMECN 8343	KY610059	–	KY610105	–	–	–
<i>A. arangoi</i>	ZSFQ 4947	ON907812*	ON925021*	ON925012*	–	–	–
<i>A. arangoi</i>	ZSFQ 4948	ON907811*	ON925020*	ON925011*	–	–	–
<i>A. atlas</i>	QCAZ 14946	MH790470	MN887669	MN887691	MN887640	MN887715	MN887745
<i>A. badius</i>	MNRJ 26717	MH790476	MK835891	–	MK835864	MK835980	MK835948
<i>A. boimirim</i>	MPEG 21233	MH790478	–	–	MK835866	MK835982	MK835951
<i>A. carrioni</i>	MZUTI 4195	KY610046	–	KY610094	–	–	–
<i>A. carrioni</i>	QCAZ 6446	MT507867	–	MT511983	–	–	–
<i>A. carrioni</i>	QCAZ 6533	MT507868	–	MT511984	–	–	–
<i>A. carrioni</i>	QCAZ 6534	MT507869	–	MT511985	–	–	–
<i>A. carrioni</i>	QCAZ 10038	MT507864	MT511977	MT511982	–	–	–
<i>A. carrioni</i>	QCAZ 13094	MT507865	MT511978	–	–	–	–
<i>A. cerberus</i>	MZUTI 4330	KY610047	KY610073	KY610095	–	–	–
<i>A. dapsilis</i>	MNRJ 16796	MH790480	MK835894	MK835926	MN887642	MN887716	MK835951
<i>A. discovery</i> sp. nov.	MZUA.Re.466	OP225330*	OP244686*	OP225393*	–	–	–
<i>A. duboisi</i>	MZUTI 62	KT944041	–	KT944059	–	–	–
<i>A. dunni</i>	MZUTI 2189	KY610048	–	KY610096	–	–	–
<i>A. dunni</i>	MZUTI 3031	KY610049	–	KY610097	–	–	–
<i>A. dunni</i>	MZUTI 4318	KY610050	KY610074	KY610098	–	–	–
<i>A. dunni</i>	MZUTI 4319	KY610051	KY610075	KY610099	–	–	–
<i>A. ecuadorensis</i>	DHMECN 5105	–	–	KY610100	–	–	–
<i>A. elaps</i>	QCAZ 5574	MN855378	MK835896	MN887692	MK835867	MN887717	MK835954
<i>A. esepe</i>	MZUTI 3758	KY610053	KT944052	KY610102	–	–	–
<i>A. esepe</i>	MZUTI 3759	KT944039	KT944051	KT944058	–	–	–
<i>A. favae</i>	MZUSP 20211	MN855380	MN887670	–	–	–	–
<i>A. flammigerus</i>	MNRJ 26720	MH790488	MK835903	MK835932	MK835873	MK835994	–
<i>A. gigas</i>	MZUTI 3286	KT944043	KT944053	MN891764	–	–	–
<i>A. iridescens</i>	DHMECN 9633	KY610054	KY610077	–	–	–	–

Species	Voucher	16S	CYTB	ND4	CMOS	NT3	RAG1
<i>A. iridescens</i>	MZUTI 3548	KY610055	KY610078	–	–	–	–
<i>A. iridescens</i>	MZUTI 3680	KY610056	KY610079	–	–	–	–
<i>A. iridescens</i>	MZUTI 4178	KT944040	KY610080	–	MH374931	–	–
<i>A. iridescens</i>	MZUTI 4697	KY610057	KY610081	–	–	–	–
<i>A. lasallei</i>	MHUA 14368	–	GQ334480	GQ334581	–	–	–
<i>A. latifrons</i>	MPEG 22630	MH790493	MK835908	MN887694	MK835875	–	–
<i>A. major</i>	ANF 1545	KT944045	–	KY610104	–	–	–
<i>A. major</i>	CORBIDI 223	MH790497	–	–	–	–	–
<i>A. major</i>	MNRJ 26126	MH790498	MK835911	–	–	–	MK835958
<i>A. major</i>	MZUSP 20868	MH790499	–	–	–	–	–
<i>A. major</i>	MZUSP 20887	MH790500	–	–	–	–	–
<i>A. major</i>	QCAZ 4691	MH790506	MK835912	MK835934	MN887643	MK836002	MN887747
<i>A. major</i>	QCAZ 4993	MH790507	–	MK835935	–	–	–
<i>A. major</i>	QCAZ 5891	MH790508	MK835913	MK835936	MK835878	MK836003	MK835962
<i>A. major</i>	QCAZ 7881	MH790509	MK835914	MK835937	–	MK836004	MK835963
<i>A. major</i>	QCAZ 13819	MH790504	–	MK835933	–	MK836000	MK835960
<i>A. major</i>	UFACRB 532	MH790511	MK835915	–	MK835879	MK836005	–
<i>A. michaelsabini</i> sp. nov.	AMARU 002	ON907809*	ON925018*	ON925009*	–	–	–
<i>A. michaelsabini</i> sp. nov.	MZUTI 5289	ON907810*	ON925019*	ON925010*	–	–	–
<i>A. michaelsabini</i> sp. nov.	DHMECN 7644	KY610058	KY610082	KY610103	–	–	–
<i>A. michaelsabini</i> sp. nov.	QCAZ 7887	MT507872	–	MT511989	–	–	–
<i>A. michaelsabini</i> sp. nov.	QCAZ 7889	MT507874	–	MT511990	–	–	–
<i>A. michaelsabini</i> sp. nov.	QCAZ 9643	MT507875	MT511981	MT511991	–	–	–
<i>A. michaelsabini</i> sp. nov.	QCAZ 9652	MT507876	–	MT511992	–	–	–
<i>A. michaelsabini</i> sp. nov.	ZSFQ 4939	ON907808*	ON925017*	ON925008*	–	–	–
<i>A. microrhynchus</i>	MZUTI 1385	KY610063	KY610086	KY610109	–	–	–
<i>A. microrhynchus</i>	MZUTI 2649	KY610064	KY610087	KY610110	–	–	–
<i>A. microrhynchus</i>	MZUTI 2650	KT944038	KT944050	KT944057	–	–	–
<i>A. microrhynchus</i>	MZUTI 3323	KY610065	KY610088	KY610111	–	–	–
<i>A. microrhynchus</i>	MZUTI 4122	KT944037	KT944049	KT944056	–	–	–
<i>A. microrhynchus</i>	MZUTI 5109	KY610060	KY610083	KY610106	–	–	–
<i>A. modestus</i>	MZUTI 4760	KY610061	KY610084	KY610107	–	–	–
<i>A. multicoloratus</i>	MZUTI 5106	KY610062	KY610085	KY610108	–	–	–
<i>A. orcesi</i>	ZSFQ 2222	ON907807*	–	ON925007*	–	–	–
<i>A. orcesi</i>	ZSFQ 2237	ON907806*	ON925016*	ON925006*	–	–	–
<i>A. pachacamac</i>	QCAZ 12630	MH790524	MN887672	MN887697	MN887647	MN887723	MN887751
<i>A. paucidens</i>	MZUTI 5102	KY610066	ON925015*	KY610112	–	–	–
<i>A. resplendens</i>	MZUTI 3996	KT944042	KT944055	KT944060	–	–	–
<i>A. riveroi</i>	MNRJ 26087	MH790526	MK835916	–	–	MK836006	MK835964
<i>A. roulei</i>	MZUTI 4503	KY610069	KY610090	KY610116	–	–	–
<i>A. roulei</i>	MZUTI 4544	KY610069	KY610091	KY610117	–	–	–
<i>A. roulei</i>	MZUTI 5107	KY610068	KY610089	KY610115	–	–	–
<i>A. roulei</i>	QCAZ 6256	–	MT511980	MT511988	–	–	–
<i>A. roulei</i>	QCAZ 7192	MT507871	MT511980	–	–	–	–
<i>A. roulei</i>	ZSFQ 4945	ON907805*	ON925014*	ON925005*	–	–	–
<i>A. savagei</i>	MZUTI 4916	KY610070	KY610092	KY610118	–	–	–
<i>A. schach</i>	AF 1716	MH790527	MK835917	–	MK835880	MK836007	–
<i>A. snethlageae</i>	MPEG 20605	MH790513	MN887678	MN887705	MN887655	MN887731	MN887759
<i>A. tartarus</i>	MPEG 23931	MH790529	MK835919	MK835938	–	MK836009	MK835965
<i>A. torquatus</i>	MPEG 23686	MH790532	MK835921	MK835941	–	MK836012	MK835968
<i>A. touzeti</i>	ZSFQ 4949	ON907804*	ON925013*	ON925004*	–	–	–
<i>A. trefauti</i>	MNRJ 26709	MH790536	MK835923	MK835942	MK835883	MK836015	MK835971
<i>A. trilineatus</i>	CAS 257740	MK648018	MK648027	MK648035	MK648043	–	–
<i>A. trilineatus</i>	UWISM 2015.18.2	MK648014	MK648022	MK648031	MK648039	–	–
<i>A. typhon</i>	MZUTI 3284	KT944044	KT944054	KT944062	–	–	–

Species	Voucher	16S	CYTB	ND4	CMOS	NT3	RAG1
<i>A. ukupacha</i>	QCAZ 4944	MH790540	MN887689	MN887714	MN887668	MN887744	MN887774
<i>A. zgap</i> sp. nov.	MZUTI 5311	ON907803*	–	ON925003*	–	–	–
<i>A. zidoki</i>	MNHN 1997.2046	AF158487	–	–	–	–	–
<i>G. godmani</i>	MVZ 233298	JQ598877	JQ598932	–	–	–	–
<i>S. nebulatus</i>	MVZ 233298	EU728583	EU728583	EU728583	–	–	–

Appendix II

Table A2. List of PCR and sequencing primers and their respective PCR conditions (denaturation, annealing, extension, and number of corresponding cycles) used in this study. All PCR protocols included an initial 3-min step at 94 °C and a final extension of 10 min at 72 °C.

Locus	Primer	Sequence (5'-3')	Reference	PCR profile
16S	16Sar-L	CGCCTGTTTATCAAAAACAT	Palumbi et al. (1991)	30 cycles of 94 °C (45 sec), 53 °C (45 sec), 72 °C (1 min)
	16Sbr-H-R	CCGGTCTGAACCTCAGATCACGT		
Cytb	L14910	GACCTGTGATMTGAAAACCAYCGTTGT	Burbrink et al. (2000)	94 °C (1 min), 58 °C (1 min), 72 °C (2 min) [x30–36]
	H16064	CTTTGGTTTACAAGAACAATGCTTTA		
ND4	ND4	CACCTATGACTACCAAAGCTCATGTAGAAGC	Arévalo et al. (1994)	94 °C (25 sec), 56 or 60 °C (1 min), 72 °C (2 min) [x25–30]
	Leu	CATTACTTTTACTTGGATTTGCACCA		
	S78	CCTTGGGTGTGATTTTCTCACCT		

Supplementary material I

Table S1

Authors: Alejandro Arteaga, Amanda Quezada, Jose Vieira, Juan M. Guayasamin

Data type: excel file.

Explanation note: Locality data for species included in Fig. 2.

Copyright notice: This dataset is made available under the Open Database License (<http://opendatacommons.org/licenses/odbl/1.0/>). The Open Database License (ODbL) is a license agreement intended to allow users to freely share, modify, and use this Dataset while maintaining this same freedom for others, provided that the original source and author(s) are credited.

Link: <https://doi.org/10.3897/zookeys.1121.86539.suppl1>

Supplementary material 2

Figure S1

Authors: Alejandro Arteaga, Amanda Quezada, Jose Vieira, Juan M. Guayasamin

Data type: Image.

Explanation note: Phylogenetic relationships within *Atractus* inferred using a maximum-likelihood approach and derived from analysis of 3,985 bp of DNA (gene fragments 16S, cytb, ND4, c-mos, NT3, and RAG1). Support values on intra-specific branches are not shown for clarity. Voucher numbers for sequences are indicated for each terminal. Black dots indicate clades with bootstrap values from 90–100%. Grey dots indicate values from 70–89%. White dots indicate values from 50–69% (values < 50% not shown). Colored clades correspond to the species' distribution presented in the map of Fig. 2. New or resurrected species are indicated in bold type.

Copyright notice: This dataset is made available under the Open Database License (<http://opendatacommons.org/licenses/odbl/1.0/>). The Open Database License (ODbL) is a license agreement intended to allow users to freely share, modify, and use this Dataset while maintaining this same freedom for others, provided that the original source and author(s) are credited.

Link: <https://doi.org/10.3897/zookeys.1121.86539.suppl2>